2007

Enantiomeric separations on cyclodextrin-based and synthetic polymeric chiral stationary phases by high performance liquid chromatography and supercritical fluid chromatography

Xinxin Han
Iowa State University

Enantiomeric separations on cyclodextrin-based and synthetic polymeric chiral stationary phases by high performance liquid chromatography and supercritical fluid chromatography

by

Xinxin Han

A dissertation submitted to the graduate faculty

in partial fulfillment of the requirements for the degree of

DOCTOR OF PHILOSOPHY

Major: Analytical Chemistry

Program of Study Committee:
Daniel W. Armstrong, Co-major Professor
Robert S. Houk, Co-major Professor
Jacob W. Petrich
Klaus Schmidt-Rohr
George A. Kraus

Iowa State University

Ames, Iowa

2007

UMI Number: 3289401

UMI Microform 3289401

ProQuest Information and Learning Company
300 North Zeeb Road
P.O. Box 1346
Ann Arbor, MI 48106-1346

Table of Contents

Abstract

High performance liquid chromatography (HPLC) employing chiral stationary phases (CSPs) is the most popular and effective method for the separation of enantiomers. In this dissertation, the first chapter is an overview of chiral stationary phases for HPLC, which includes the structures, separation mechanisms, and applications of a variety of chiral stationary phases. The use of some chiral stationary phases in SFC also is discussed.

The next three chapters present the enantiomeric separations of chiral furans, isochromenes, and polycycles on cyclodextrin-based chiral stationary phases. The performance of chiral stationary phases for the separation of these analytes was compared. The effect of the mobile phase compositions and structures of the analytes on the chiral recognitions were discussed.

Chapter 5 through chapter 7 focuses mainly on the development and evaluation of new synthetic polymeric chiral stationary phases. First, the enantiomeric separation abilities of a new polymeric chiral stationary phase based on the monomer *N,N'*-(1S,2S)-1,2-cyclohexanediyl-bis-2-propenamide was screened with 200 racemic samples. The enantiomeric separations obtained were optimized. The mobile phase compositions and a mobile phase additive (trifluoroacetic acid) were evaluated and the chiral recognition mechanism was discussed. The new CSP showed high sample loading capacity. Then, we developed two new synthetic polymeric CSPs with two other monomers, which are polymerible derivatives of *trans*-1,2-diphenylethylenediamine and *trans*-9,10-dihydro-9,10-ethanoanthracene-(11S,12S)-11,12-dicarboxylic acid. The two new CSPs also showed enantiomeric selectivities for a variety of chiral compounds and high sample loading capacity. The three new synthetic polymeric CSPs are complementary to each other.

Chapter 8 is a study on the use of the new synthetic polymeric CSPs with supercritical fluid eluents. The new CSPs also can separate many compounds using supercritical fluid chromatography (SFC). They showed high stabilities under SFC conditions. Compared with HPLC, SFC provides much faster separations due to the high flow rates. For some analytes, better enantiomeric separations were observed with SFC due to the better separation efficiencies.

Chapter 1. General introduction

1.1. Introduction

A molecule is chiral if it differs from its mirror image. Two molecules which are nonsuperimposable mirror images of one another are enantiomers. Chirality is important in most aspects of life. Biological systems consist of mainly of L-amino acids and D-sugars. Therefore, it is not unusual for there to be different biological responses to enantiomers. A much publicized example is the thalidomide tragedy in the last century [1]. The guidelines for the development of stereisomeric drugs issued by the Food and Drug Administration (FDA) in 1992 were due to the advent of facile methods for enantiomeric analysis, especially HPLC [2]. The pharmacological effect of both enantiomers of chiral drugs must be evaluated and the development of enantiomerically pure drugs can simplify the regulatory process. In 2004, all the top four best-selling drugs (Lipitor, Zocor, Plavix, and Nexium) are in single enantiomeric forms [3]. Therefore, analysis of enantiomeric impurities and obtaining pure enantiomers are important for drug development and production.

A variety of analytical technologies such as gas chromatography (GC), HPLC, supercritical fluid chromatography (SFC), and capillary electrophoresis (CE), have been used for analytical or preparative scale enantiomeric separations [4-5]. Enantioselective HPLC is the most popular method for enantiomeric separations in industry because of its robustness, reproducibility, and capability for both analytical and preparative scale chiral separations. Preparative scale HPLC separations are widely used for the separations of enantiomers in industry, particularly when other ways to obtain these species (such as asymmetric synthesis, fractional recrystallization of diastereomers, and enzymatic resolution) are limited [4-5]. Till now, more than one hundred chiral stationary phases for HPLC have been commercialized. The most important CSPs can be classified as three types based on their structures. They are macrocyclic, π-π association, and polymeric CSPs [6].

1.2. Macrocyclic CSPs

Macrocyclic CSPs includes three groups of chiral selectors. They are chiral crown ethers, cyclodextrin derivatives, and macrocyclic glycopeptides. Macrocyclic CSPs, particularly cyclodextrin-based CSPs, dominate enantiomeric separations in CE and GC [4-5]. They also are important HPLC chiral stationary phases, particularly in the reverse phase and polar

organic modes [4-5].

1.2.1. Chiral crown ether based CSPs

Chiral crown ether based CSPs for HPLC were first introduced by Cram and co-workers [7-9]. Crown ether (18-crown-6 ether) modified with an optically-active binaphthyl unit was used as the chiral selector (Fig. 1) [10]. The cavity of 18-crown-6 ether is an optimum size for complexation of potassium and ammonium ions. This inclusion complexation was key for the retention and separation of analytes on this CSP. Therefore, this kind of CSP exclusively separates analytes with primary amine functional groups. Acidic mobile phase additives such as perchloric acid are needed for complete protonation of the primary amine analytes [11-12]. Competing ions for complexation with crown ethers such as potassium ions need to be excluded from the mobile phase. Crown ether based CSPs are used in the reverse phase mode. This type of CSPs is not generally used for preparative separations due to the formation of potentially explosive organic-perchloric acid mixtures in the solvent removing process [13].

1.2.2. Cyclodextrin based CSPs

Cyclodextrins are cyclic oligomers of α-1,4-linked D-glucose units [14]. They can be prepared by the treatment of starch with cyclodextrin glycosyltransferase. The cyclodextrins used for chiral selectors are α-,β-, and γ-cyclodextrins, which contains 6, 7, and 8 glucose units respectively. The shape of cyclodextrin is like a hollow, truncated cone (Fig. 2) [4]. The cavity is hydrophobic and the exterior rims are hydrophilic. Therefore, nonpolar molecules or parts of the molecules will form inclusion complexes with the hydrophobic cavity in the aqueous or hydro-organic solutions [15-18].

The first successful cyclodextrin-based CSP was introduced by Armstrong in 1984 [15]. β-Cyclodextrin was bonded to silica gel via an ether linkage. This CSP can separate many compounds and is the first CSP used in the reverse phase mode [15]. Further research lead an understanding of the separation mechanism [19-20]. To achieve enantiomeric separations, two requirements must be met. First, a relatively “tight fit” inclusion complex must be formed between the hydrophobic part of the analyte and the cyclodextrin cavity. Second, the chiral center of the analyte must be close to the rim of the cyclodextrin and interactions (such as hydrogen bonding, dipolar, and steric) between the analyte functional groups near the

chiral center of the analyte and the "mouth" of the cyclodextrin molecule must be possible. At least one of the interactions should be different for the two enantiomers.

Cyclodextrins can be derivatized with various groups such as methyl, acetyl, 2-hydroxypropyl, etc. (Fig. 3) to broaden the enantioselectivity [17, 21-24]. Each modified cyclodextrin based CSPs can separate different types of chiral molecules. For example, the cyclodextrins functionalized with aromatic groups can separate compounds with π-acid groups in the normal phase mode. These CSPs also can separate compounds in the reverse phase mode via inclusion complex mechanism.

A new mobile phase mode, the polar organic mode, was developed by Armstrong for cyclodextrin based CSPs [25-30]. In the polar organic mode, acetonitrile is the major component of the mobile phase. Methanol is used to adjust the retention and small amounts of organic acids and bases are used to tune the enantioselectivity. Since the acetonitrile solvent molecules occupy the cavity of the cyclodextrin, the separation cannot be accomplished by an inclusion complexation mechanism. The analyte covers the large opening of the cyclodextrin toroid in a "lid" fashion (Fig. 4) [30]. The retention and separation are based mainly on hydrogen bonding, dipolar, and steric interactions. The enantiomers separated in this mode must contain two hydrogen bonding groups. Different types of molecules are separated in this mode as compared with the reverse phase mode. For analytes that can be separated in both modes, the separations in the polar organic mode are faster and more efficient. Subsequently, the polar organic mode has been found to be useful for other CSPs [31-34].

1.2.3. Macrocyclic glycopeptide based CSPs

A vancomycin (Fig. 5a) based CSP for HPLC was introduced by Armstrong in 1994 [35]. Following this, three other macrocyclic glycopeptides also were developed as CSPs [32, 36-38]. They are teicoplanin, teicoplanin aglycone and ristocetin A (Fig. 5b, 5c, and 5d). Today, the macrocyclic glycopeptide based CSPs are considered one of the most important tools in enantiomeric separations due to their broad enantioselectivities [32]. Particularly, the teicoplanin based CSPs can separate underivatized amino acids with high enantioselectivity in the reverse phase mode without any mobile phase additives. This means that it is suitable for preparative separations since the absence of additives in the mobile phase makes recovery

of the product much easier [38, 39-40]. The macrocyclic glycopeptides CSPs can be used in all mobile phase modes including normal phase, reverse phase and polar organic modes [32]. Different enantioselectivities are observed in the three different mobile phase modes. In addition, the four macrocyclic glycopeptides CSPs are complementary to each other. If a partial separation is observed for an analyte on one CSP, it can be baseline separated in one of the other related CSPs in most cases. This property simplifies method development [32, 41].

1.3. π-π association CSPs

The first commercialized π-π association CSP was (-)-3,5-dinitrobenzoylphenylglycine ionically bonded to a silica support [42]. As the name indicates, π-π interactions between the analytes and the CSP are required for enantiomeric separations. If the CSP has a π-acid moiety (i.e., a π-electron deficient group such as dinitro-, or trifluoromethyl-substituted phenyl moiety), the analytes separated on this CSP must have a complementary π-basic group (i.e., with π-electron rich groups such as alkyl-substituted phenyl or a naphthyl moiety) and vice versa [43-46]. For analytes without π-acid or π-base groups, derivatization is necessary. The combination type "π-acid plus π-base" CSPs were developed and showed broader enantioselectivities [47-48]. The most applicable CSP of this type is Whelk-O1 CSP [47]. (Fig. 6) Pi-pi interactions are very important for the enantiomeric recognition on these CSPs. Since this interaction is more prominent in non-polar solvents, π-π association CSPs are always used in the normal phase mode [6].

1.4. Polymeric CSPs

Polymeric chiral stationary phases play an important role in HPLC enantiomeric separations. Polymeric CSPs can be divided into two catagaries. One is based on natural polymers such as proteins and polysaccharides. Synthetic polymers constitute the other.

1.4.1. CSPs based on natural polymers

1.4.1.1. Protein based CSPs

Proteins are natural chiral polymers composed of L-amino acids. They were popular chiral selectors for HPLC in the 1980's due to their broad enantioselectivity [49-51]. This type of CSP is used in the reverse phase mode. Table 1 lists some important commercialized protein CSPs [4]. Protein based CSPs are not suitable for preparative separations due to two

reasons. First, the molar loading of the chiral selectors on the silica support is low because of the high molecular weight of proteins (40,000-70,000 Daltons). Secondly, just a small part of the protein is responsible for the enantiomeric separation. Therefore, protein CSPs are easily overloaded. In addition, protein-based CSPs are the most labile CSPs. Temperature, pH, and the composition of mobile phase can ruin the CSPs by causing irreversible changes in the secondary and/or tertiary structures of the proteins (which is important for enantioselectivity). With the development of new CSPs in the 1990s, the protein based CSPs decreased in importance since the enantiomeric separations achieved on these CSPs can also be obtained on the new CSPs.

1.4.1.2. Polysaccharide based CSPs

Polysaccharides such as cellulose and amylose are among the most abundant naturally occurring chiral polymers. Both of them are linear polymers composed of D-glucose moieties; however, they differ in the way the glucose units are linked. In cellulose, the glucose units are joined by β-1,4-glycosidic linkages, while they are connected via α-1,4-glycosidic linkages in amylose. Native cellulose and amylose are not very effective for the separation of enantiomers [6]. However, when the hydroxyl groups on these carbohydrates are derivatized with ester or carbamate groups, good enantioselectivities are observed for a wide variety of compounds [52-53].

In the 1970s, microcrystalline triacetylcellulose were used as CSP by German scientists [54]. Although this CSP showed enantioselectivity for many aromatic and aliphatic chiral molecules, the low mechanical strength and poor efficiency limited applications on this CSP [55-56]. In the 1980s, Okamoto et al. advanced the polysaccharide based CSPs by coating ester or carbamate derivatives of polysaccharides onto macroporous 3-aminopropyl silanized silica gel [57-59]. These CSPs showed high efficiency, high mechanical strength, and broad enantioselectivity. The most important commercialized polysaccharide based CSPs are listed in Table 2 [4]. The 3,5-dimethylphenylcarbamate derivative of cellulose and amylose (Chiralcel OD and Chiralpak AD) columns are the most widely used. These CSPs are also suitable for preparative separations due to their high sample loading capacity [60].

The polysaccharide based CSPs are mainly used in the normal phase mode. Since the chiral selectors are coated on the support and are soluble in some normal phase solvents such

as chloroform, acetonitrile etc., caution must be exercised when choosing a mobile phase and sample solvents. The polysaccharide based CSPs used in the reverse phase mode were also developed. However, the CSPs used in the reverse mode cannot be used in the normal phase mode [61]. The configuration (three-dimensional structure) of the chiral selectors, which is believed to be important for enantioselectivity, will be irreversibly changed in different mobile phase modes.

The stability and durability of the polysaccharide based CSPs can be improved by immobilization of the chiral selectors on the support. Attempts have been made in the last two decades by several groups [62-66]. None of them was successful due to the decrease of the enantioseparation ability or tedious polymerization process. Recently, the immobilized version of AD (IA) and OD (IB) columns were commercialized [60, 67-68]. The immobilized CSPs showed improved stability, durability, and solvent compatibility compared to the coated type CSPs. Although it was claimed that the new CSPs showed similar enantiomeric separation abilities to the coated types, recent research indicates that the enantioselectivity of the IA and IB columns are still not as broad as the coated type AD and OD CSPs [69].

1.4.2. CSPs based on synthetic polymers

Chiral synthetic polymeric CSPs have not been nearly as successful as polysaccharide based CSPs. However, recent research on these CSPs also is growing due to several of their attractive characteristics [70-74]. First, a variety of monomers are available and they can be polymerized via different methods to obtain different polymers. Hence the potential variety of polymeric CSPs is almost unlimited. Second, chemical modifications of the CSPs are easy. Third, chiral selectors with the opposite absolute configurations are possible. Finally, the synthetic polymeric CSPs almost always show high sample loading capacity [70-74]. Furthermore, the covalent bonding of chiral selectors results in high stability for these CSPs.

Four approaches have been reported for synthetic polymeric CSPs. The earliest report involved co-polymerization of a chiral monomer with an achiral cross-linking agent. The first polymeric CSPs of this type were prepared by Blaschke and coworkers [75-77]. Polymeric beads were prepared through copolymerization of chiral acrylamides or methacrylamides with ethylene diacrylate. The polymeric beads were used as CSPs and these CSPs showed

enantioselectivities for a few racemates. These CSPs cannot endure high pressure and were mainly used for preparative separations.

Polymeric chiral selectors also can be prepared through asymmetric catalyzed polymerization of prochiral monomers [52, 78]. Chiral polymers with a helical secondary structure were prepared via asymmetric catalyzed anionic polymerization of prochiral monomers such as triphenylmethyl methacrylate (TrMA) and diphenyl-2-pyridylmethyl methacrylate (D2PymA). These "one-handed" helical polymers were bonded or coated to silica gel to use as CSPs. These CSPs are specialized in the separation of relatively flat, planer, aromatic chiral molecules. The enantioselectivity of this CSP is dependant on its helical secondary structure, which could be irreversible changed with solvent composition and temperature.

The third approach was developed by Allenmark and coworkers. Chiral monomers with diallyl groups react with *tetrakis*(dialkylsiloxy) silane under catalysis by hydrogen hexachloroplatinate to form network polymeric chiral selectors. The polymeric chiral selectors were then covalently connected to the silical gel through the vinyl groups [79-81]. Two commercialized CSPs of this type are Kromasil CHI-TBB and Kromasil CHI-DMB CSPs [82]. The monomers of these two CSPs are based on derivatives of *N*, *N*'-diallyl-L-tartar-diamide. (Fig. 7)

In the last method, chiral linear homopolymers attached to the surface of silica gel were created through a free radical intiated polymeric reaction of a chiral acrylamide or methacrylamide. Poly-acrylamide and poly-methacrylamide CSPs with phenylalanine, 1-phenylethyl, 1-cyclohexylethyl [83], penicillin [84], and menthone or menthol [85] moieties were prepared. Enantiomeric separations of only a few chiral molecules were obtained on these CSPs. Recently, several new polymeric CSPs based on the last approach were prepared. The chiral monomers are based on derivatives of *trans*-1,2-diaminocyclohexane (commercial name: P-CAP) [70-72], *trans*-1,2-diphenylethylenediamine (commercial name: P-CAP-DP) [73], and *trans*-9,10-dihydro-9,10-ethanoanthracene-(11S,12S)-11,12-dicarboxylic acid [74] (Fig. 8.). All three of these CSPs show enantioselectivities for many chiral molecules and show high stability in the normal phase mode and polar organic mode. These CSPs showed high sample loading capacities and have the potential to be excellent preparative CSPs.

Finally, complementary enantioselectivities were observed on these three CSPs. Some analytes can only be separated on one of the columns, while for enantiomers that can be separated on all the three CSPs, different enantioselectivities were observed in most cases.

1.5. Applications of CSPs on packed column SFC

The CSPs for HPLC, particularly those CSPs that are used in the normal phase mode, can also be used for packed column supercritical fluid chromatography (SFC). SFC is a chromatographic mode, in which the mobile phase is a supercritical fluid. Carbon dioxide is the major mobile phase component for SFC. The polarity of supercritical CO_2 is similar to hexane. Polar organic modifiers such as methanol, ethanol, and etc. are added to adjust mobile phase strength. Packed column SFC shares similar theory and hardware to normal phase HPLC and is compatible with most of the LC detectors such as UV, mass, ELSD, etc. The first enantiomeric separation by packed column SFC was reported in 1985 [86]. Phosphine oxide enantiomers were resolved on (R)-*N*-(3,5-dinitrobenzoyl)phenylglycine CSP. Since then, more and more attention has been paid to SFC for both analytical and preparative scale enantiomeric separations. This is because of its advantages which include lower amount of toxic organic solvent consumption, high throughput, fast method development, and high efficiencies [87-90]. The substitution of normal phase HPLC by SFC is promising.

1.6. Summary

Due to the extensive development of chiral stationary phases in the last three decades, most known enantiomers can be separated on one or more commercialized CSP columns. Current research on enantiomeric separations is mainly in two areas. The first area involves separation of newly synthesized enantiomers with existing CSPs. The other is development of new CSPs with advantages over existing CSPs such as higher sample loading capacity, separation of analytes which currently remain are difficult to separate, compatibility with solvents, and etc. In this thesis, the first three chapters (chapters 2-4) involve the use of cyclodextrin based CSPs for the separation of three groups of recently synthesized chiral molecules (i.e., racemic furans, racemic isochromens, and racemic polycycles). Chapter 5 is an investigation of the enantiomeric separation abilities of a newly developed synthetic polymeric CSP (the P-CAP CSP). The following two chapters (chapters 6 & 7) describe the

development and evaluation of two new synthetic polymeric CSPs for LC. Chapter 8 focuses on the application of the new developed synthetic polymeric CSPs for SFC. The last chapter (chapter 9) gives general conclusions.

1.7 Dissertation Organization

This dissertation begins with the overview of the research background. The following chapters are the finished research projects which include seven published papers with cited references, tables, and figures. All these projects were designed by my major professor, Daniel W. Armstrong, and me. I am the primary researcher and author of these papers. The last chapter summarizes the research results.

References

1. Blaschke, G.; Kraft, H. P.; Markgraf, H. *Chem. Ber.* **1980**, *113*, 2318.

2. Food and Drug Administration *Chirality*, **1992**, *4*, 338.

3. Thayer, A. *Chem. Eng. News* **2005**, *83*, 49.

4. Liu, Y.; Lantz, A. W.; Armstrong, D. W. *J. Liq. Chromatogr. & Rel. Technol.* **2004**, *27*, 1121.

5. Armstrong, D. W. In A Century of Separation Science, Issaq, H. J., Ed.; Marcel Dekker: New York, 2002; pp 555-578.

6. Armstrong, D. W.; Zhang, B. *Anal. Chem.* **2001**, *73*, 557A.

7. Helgeson, R.; Timko, J.; Moreau, P.; Peacock, S.; Mayer, J.; Cram, D. J. *J. Am. Chem. Soc.* **1974**, *96*, 6762.

8. Sogah, G. D. Y.; Cram, D. J. *J. Am. Chem. Soc.* **1976**, *98*, 3038.

9. Newcomb, M.; Toner, J.; Helgeson, R.; Cram, D. J. *J. Am. Chem. Soc.* **1979**, *101*, 4941.

10. Armstrong, D. W. *LC-GC* **1997**, *59*(Supplemental issue), S20.

11. Shinbo, T.; Ysmsguchi, T.; Nishimura, K.; Sugiura, M *J. Chromatogr.* **1987**, *405*, 145.

12. Hilton, L.; Armstrong, D. W. *J. Liq. Chromatogr.* **1991**, *14*, 9.

13. Aboul-Enein, H. Y.; Ali, I. *Chiral Separations by liquid Chromatography and Related Technologies*, Marcel Dekker: New York, NY, **2003**; pp 281-300.

14. Cserháti, T.; Forgács, E. *Cyclodextrins in Chromatography*, Royal Society of Chemistry: Cambridge, UK, **2003**; pp 1-10.

15. Armstrong, D. W.; DeMond, W. *J. Chromatpgr. Sci.* **1984**, *22*, 411-415.

16. Bressolle, F.; Audran, M.; Pham, T. N.; Vallon, J. J. *J. Chromatogr. B* **1996**, *687*, 303.

17. Mitchell, C. R.; Armstrong, D. W. In *Chiral Separations: Methods and Protocols*, Gübitz, G.; Schmid, M. G., Eds.; Humana Press: Totowa, NJ, **2003**; pp 61-112.

18. Han, S. M.; Atkinson, W. M.; Purdie, N. *Anal. Chem.* **1984**, *56*, 2827.

19. Armstrong, D. W.; DeMond, W.; Czech, B. P. *Anal. Chem.* **1985**, *57*, 481.

20. Armstrong, D. W.; Ward, T. J.; Armstrong, R. D.; Beesley, T. E. *Science* **1986**, 232, 1131.

21. Armstrong, D. W.; Bertrand, G. L.; Ward, K. D.; Ward, T. J.; Secor, H. V.; Seeman, J. I. *Anal. Chem.* **1990**, *62*, 332.

22. Stalcup, A. M.; Chang, S. C.; Armstrong, D. W. *J. Chromatogr.* **1991**, *540*, 113.

23. Stalcup, A. M.; Chang, S. C.; Armstrong, D. W.; Pitha, J. *J. Chromatogr.* **1990**, *513*, 181.

24. Cyclobond Handbook: *A Guide to Using Cyclodextrin Bonded Phases for Chiral LC Separations*, 7th ed.; Advanced Separation Technologies Inc.: Whippany, NJ; **2005**.

25. Zukowski, J.; Pawlowska, M.; Armstrong, D. W. *J. Chromatogr.* **1992**, *623*, 33.

26. Armstrong, D. W.; Chen, S.; Chang, C.; Chang, S. *J. Liq. Chromatogr.* **1992**, *15*, 545.

27. Zukowski, J.; Pawlowska, M.; Nazatkina, M.; Armstrong, D. W. *J. Chromatogr.* **1993**, *629*, 169.

28. Pawlowska, M.; Chen, S.; Armstrong, D. W. *J. Chromatogr.* **1993**, *641*, 257.

29. Chang, S. C.; Reid, G. L., III; Chen, S.; Chang, C. D.; Armstrong, D. W. *Trends Anal. Chem.* **1993**, *12*, 144.

30. Armstrong, D. W.; Chang, L. W.; Chang, S. C.; Wang, X.; Ibrahim, H.; Reid, G. R., III; Beesley, T. E. *J. Liq. Chromatogr. & Rel. Technol.* **1997**, *20*, 3279.

31. Xiao, T. L.; Armstrong, D. W. In *Chiral Separations: Methods and Protocols*, Gübitz, G.; Schmid, M. G., Eds.; Humana Press: Totowa, NJ, **2003**; pp 113-171.

32. Chirobiotic Handbook: *A Guide to Using Macrocyclic Glycopeptide Bonded Phases for Chiral LC Separations*, 5th ed.; Advanced Separation Technologies Inc.: Whippany, NJ; **2004**.

33. Tang, Y.; Zielinski, W. L.; Bigott, H. M. *Chirality* **1998**, *10*, 364.

34. Armstrong, D. W.; Wang, X. D.; Ercal, N. *Chirality* **1998**, *10*, 587.

35. Armstrong, D. W.; Tang, Y.; Chen, S.; Zhou, Y.; Bagwill, C.; Chen, J. *Anal. Chem.* **1994**,

66, 1473.

36. Armstrong, D. W.; Liu, Y.; Ekborg-Ott, K. H. *Chirality* **1995**, *7*, 474.

37. Ekborg-Ott, K. H.; Liu, Y.; Armstrong, D. W. *Chirality* **1998**, *10*, 434.

38. Berthod, A.; Chen, X., Kullman, J. P.; Armstrong, D. W.; Gasparrini, F.; D'Acquarica, I.; Villani, C.; Carotti, A. *Anal. Chem.* **2000**, *72*, 1767.

39. Berthod, A.; Liu, Y.; Bagwill, C.; Armstrong, D. W. *J. Chromatogr. A* **1996**, *731*, 123.

40. Peter, A.; Torok, G.; Armstrong, D. W. *J. Chromatogr. A* **1998**, *793*, 283.

41. Chen, S.; Liu, Y.; Armstrong, D. W.; Borrell, J. I.; Martinez-Teipel, B.; Matallana, J. L. *J. Liq. Chromatogr.* **1995**, *18*, 1495.

42. Pirkle, W. H.; Finn, J. M.; Schreiner, J. L.; Hamper, B. C. *J. Am. Chem. Soc.* **1981**, *103*, 3964.

43. Welch, C. J. *J. Chromatogr. A* **1994**, *666*, 3.

44. Pirkle, W. H.; Murray, P. G.; Wilson, S. R. *J. Org. Chem.* **1996**, *61*, 4775.

45. Pirkle, W. H.; Liu, Y. *J. Chromatogr. A* **1996**, *749*, 19.

46. Lin, C.-E.; Li, F.-K. *J. Chromatogr. A* **1996**, *722*, 189.

47. Pirkle, W. H.; Welch, C. J. *J. Liq. Chromatogr.* **1992**, *15*, 1974.

48. Oi, N; Kitahara, J.; Doi, T. European patent: EP029793, **1998**.

49. Hermansson, J. *J. Chromatogr.* **1983**, *269*, 71.

50. Allenmark, S.; Bomgren, B.; Boren, H. *J. Chromatogr.* **1983**, *269*, 63.

51. Haginaka, J.; Seyama, C.; Kanasugi, N. *Anal. Chem.* **1995**, *67*, 2579.

52. Yamamoto, C.; Okamoto, Y. *Bull. Chem. Soc. Jpn*. **2004**, *77*, 227.

53. Okamoto, Y; Yashima, E. *Angew. Chem. Int. Ed.* **1998**, *37*, 1020.

54. Hesse, G.; Hagel, R. *Chromatographia*, **1973**, *6*, 277.

55. Linder, K. R.; Mannschreck, A. *J. Chromatogr.* **1980**, *193*, 308.

56. Blaschke, G. *J. Liq. Chromatogr.* **1986**, *9*, 341.

57. Okamoto, Y.; Kawashima, M.; Yamamoto, K.; Hatada, K. *Chem. Lett.* **1984**, *5*, 739.

58. Okamoto, Y.; Kawashima, M.; Hatada, K. *J. Am. Chem. Soc.* **1984**, *106*, 5357.

59. Ichida, A.; Shibata, T.; Okamoto, I.; Yuki, Y.; Namikoshi, N.; Toga, Y. *Chromatographia*, **1984**, *19*, 280.

60. http://www.chiraltech.com/index.html.

61. Tachibana, K.; Ohnishi, A. *J. Chromatogr. A* **2001**, *906*, 127.

62. Oliveros, L.; López, P.; Minguillón, C.; Franco, P. *J. Liq. Chromatogr.* **1995**, *18*, 1521.

63. Francotte, E. R. *J. Chromatogr. A* **2001**, *906*, 379.

64. Okamoto, Y.; Aburatani, R.; Miura, S.; Hatada, K. *J. Liq. Chromatogr.* **1987**, *10*, 1613.

65. Enomoto, N.; Furukawa, S.; Ogasawara, Y.; Akano, H.; Kawamura, Y.; Yashima, E.; Okamoto, Y. *Anal. Chem.* **1996**, *68*, 2798.

66. Ikai, T.; Yamamoto, C.; Kamigaito, M.; Okamoto, Y. *Chem. Rec.* **2007**, *7*, 91.

67. Zhang, T.; Kientzy, C.; Franco, P.; Ohnishi, A.; Kagamihara, Y.; Kurosawa, H. *J. Chromatogr. A* **2005**, *1075*, 65.

68. Zhang, T.; Nguyen, D.; Franco, P.; Murakami, T.; Ohnishi, A.; Kurosawa, H. *Anal. Chim. Acta* **2006** *557*, 221.

69. Xiao, T. L.; Han, X.; Murphy, J. B.; Gasper, M. P. unpublished results.

70. Gasparrini, F.; Misiti, D.; Villani, C. **2003** WO Patent 2003079002

71. Gasparrini, F.; Misiti, D.; Rompietti, R.; Villani, C. *J. Chromatog.r A.* **2005**, *1064*, 25.

72. Zhong, Q.; Han, X.; He, L.; Beesley T. E.; Trahanovsky, W. S.; Armstrong, D. W. *J. Chromatogr. A.* **2005**, *1066*, 55.

73. Han, X.; He, L.; Zhong, Q.; Beesley, T. E.; Armstrong D. W. *Chromatographia* **2006**, *63*,13.

74. Han, X.; Wang, C.; He, L.; Beesley, T. E.; Armstrong, D. W. *Anal. Bioanal. Chem.* **2007**, *387*, 2681.

75. Blaschke, G.; Donow, F. *Chem. Ber.* **1975**, *108*, 1188.

76. Blaschke, G.; Donow, F. *Chem. Ber.* **1975**, *108*, 2792.

77. Blaschke, G.; *Angew. Chem. Int. Ed.* **1980**, *19*, 13.

78. Okamoto, Y.; Honda, S.; Okamoto, I.; Yuki, H.; Murata, S.; Noyori, R.; Tanaka, H. *J. Am. Chem. Soc.* **1981**, *103*, 6971.

79. Allenmark, S. G.; Andersson, S.; Möller, P.; Sanchez, D. *Chirality* **1995**, *7*, 248.

80. Thunberg, L.; Allenmark, S.; Friberg, A. Ek F.; Frejd, T. *Chirality* **2004**, *16*, 614.

81. Thunberg, L.; Allenmark, S. *J. Chromatogr. A.* **2005**, *1026*, 65.

82. http://chromatographyshop.com/html/kromasil.html.

83. Blaschke, G.; Bröker, W.; Fraenkel, W. *Angew. Chem. Int. Ed.* **1980**, *25*, 830.

84. Saotome, Y.; Miyazawa, T.; Endo, T. *Chromatographia* **1989**, *28*, 505.

85. Arlt, D.; Bömer, B.; Grosser, R.; Lang, W. *Angew. Chem. Int. Ed.* **1991**, *30*, 1662.

86. Mourier, P. A.; Eliot, E.; Caude, M. H.; Rosset, R. H. *Anal. Chem.* **1985**, *57*, 2819.

87. Terfloth, G. *J. Chromatogr. A.* **2001**, *906*, 301.

88. Phinney, K. W. *Anal. Bioanal. Chem.* **2005**, *382*, 639.

89. Majewski, W; Valery, E; Ludemann-Hombourger, O. *J Liq Chromatogr Rel Technol* **2005**, *28*, 1233.

90. Han, X.; Berthod, A.; Wang, C.; Huang, K.; Armstrong, D. W. *Chromatographia* **2007**, *65*, 381.

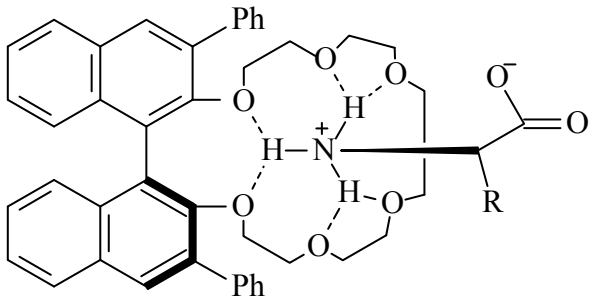

Fig. 1. Interactions between the primary amine analyte with crown ether CSP (from Ref. [10]).

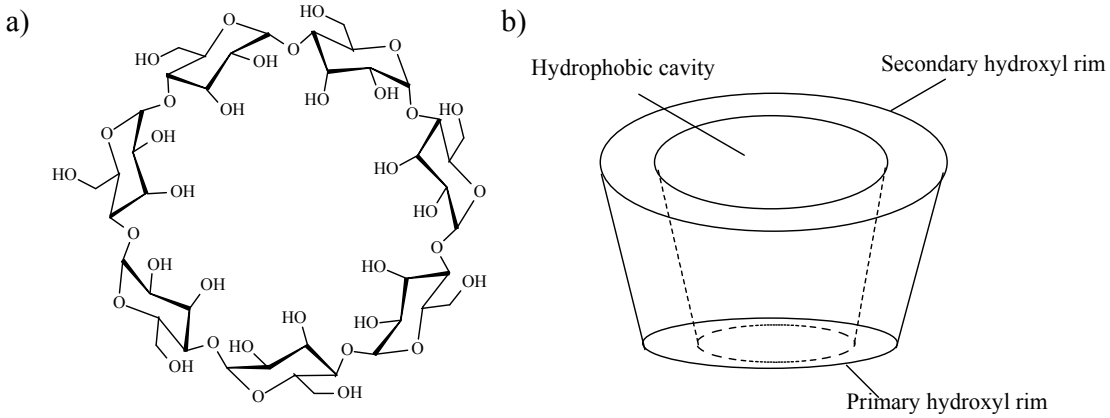

Fig. 2. Structure of β-cyclodextrin (a) and the toroidal shape of a cyclodextrin molecule (b) (from Ref. [4]).

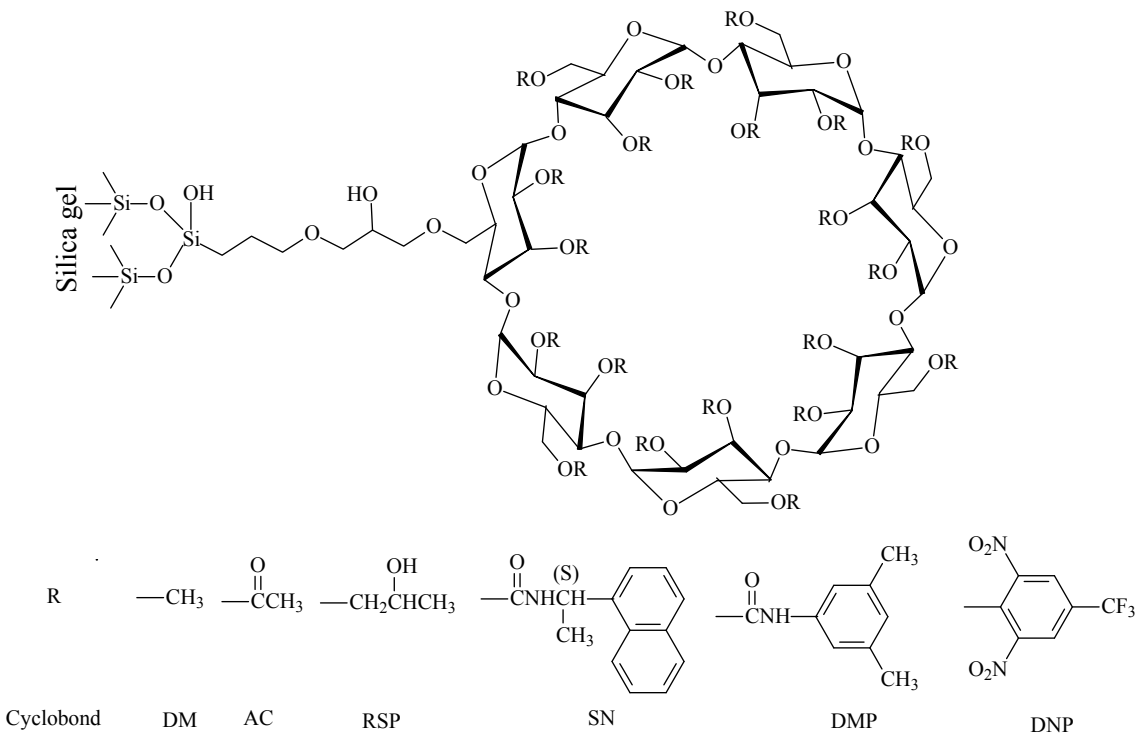

Fig. 3. Derivatized cyclodextrin CSPs (from Ref. [24]).

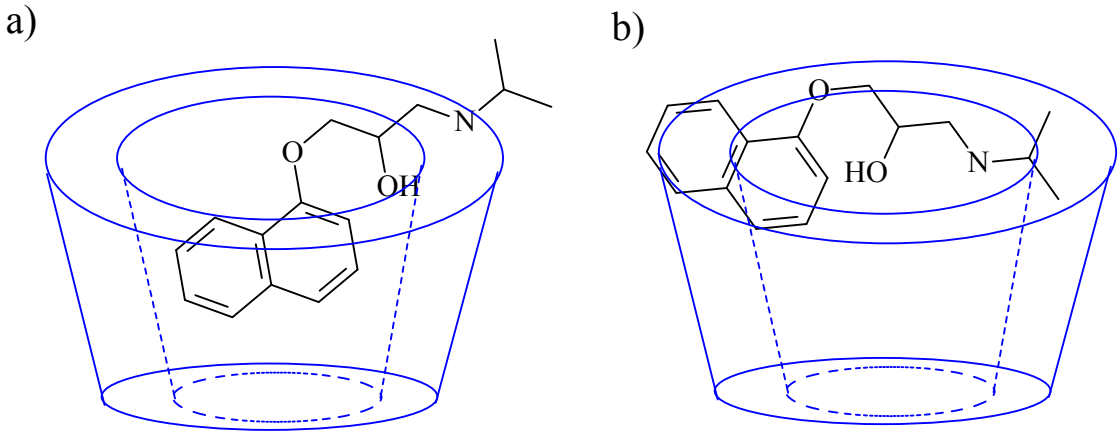

Fig. 4. The interactions between the analyte and cyclodextrin in (a) the reverse phase mode, and (b) the polar organic mode (from Ref. [30]).

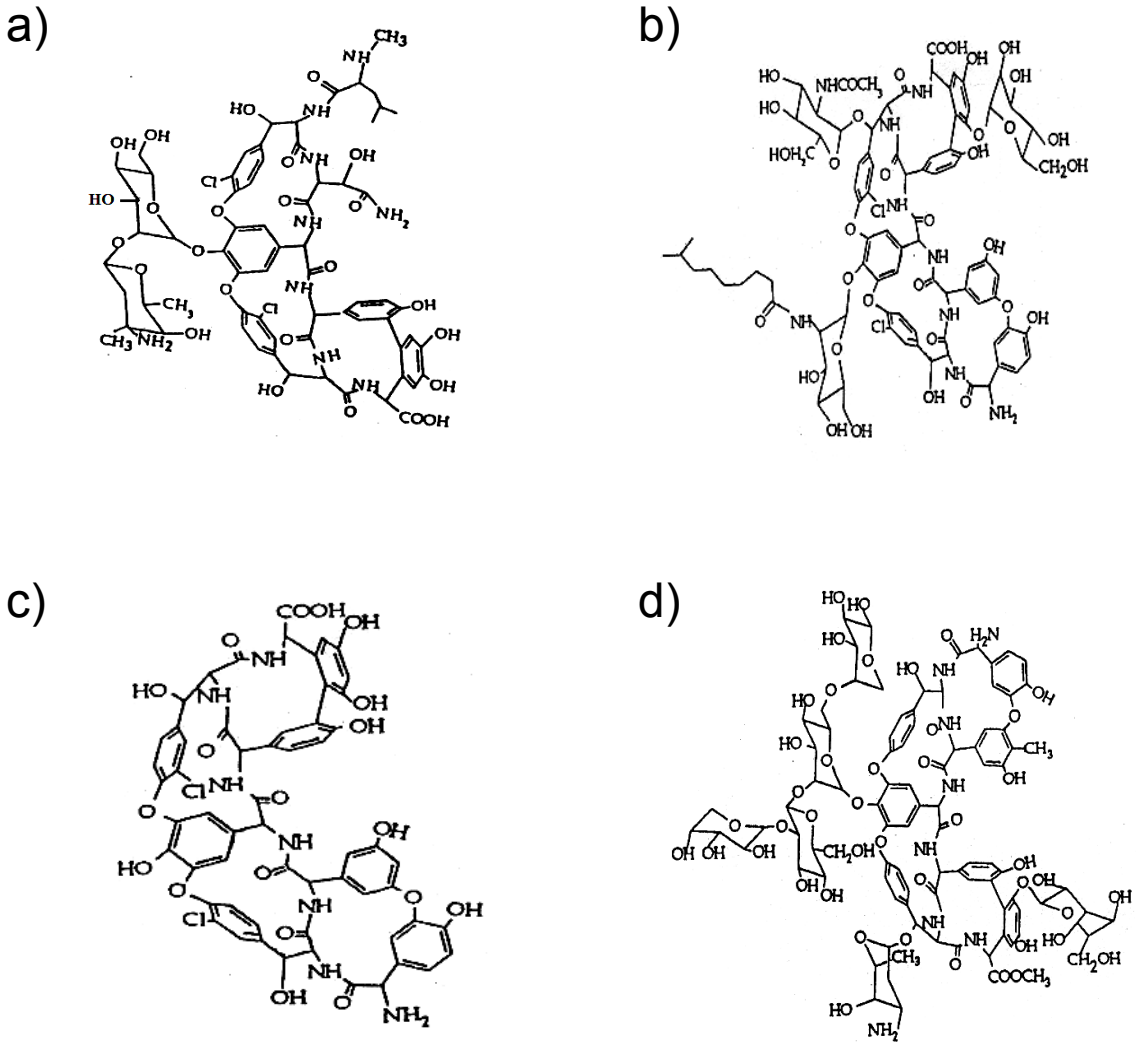

Fig. 5. Structures of the macrocyclic CSPs: a) vancomycin, b) teicoplanin, c) teicoplanin aglycon, and d) ristocetin A (from Ref. [5]).

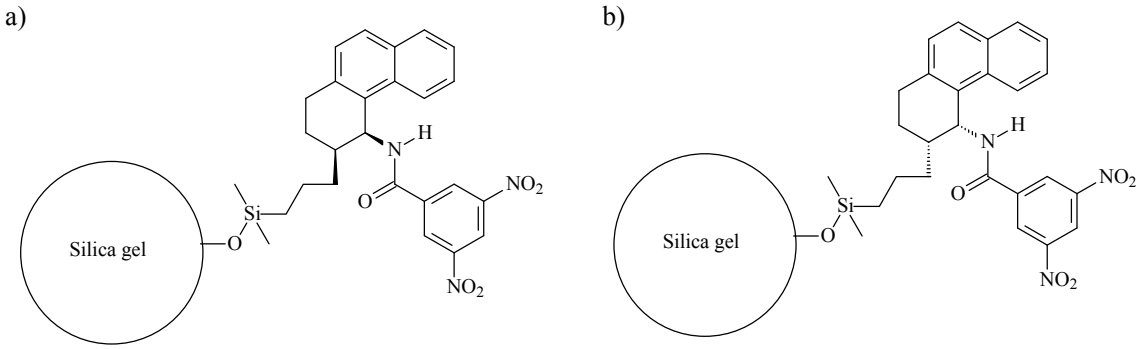

Fig. 6. Structure of (S,S)-Whelk-O1 CSP (a) and (R,R)-Whelk-O1 CSP (b) (from Ref. [47]).

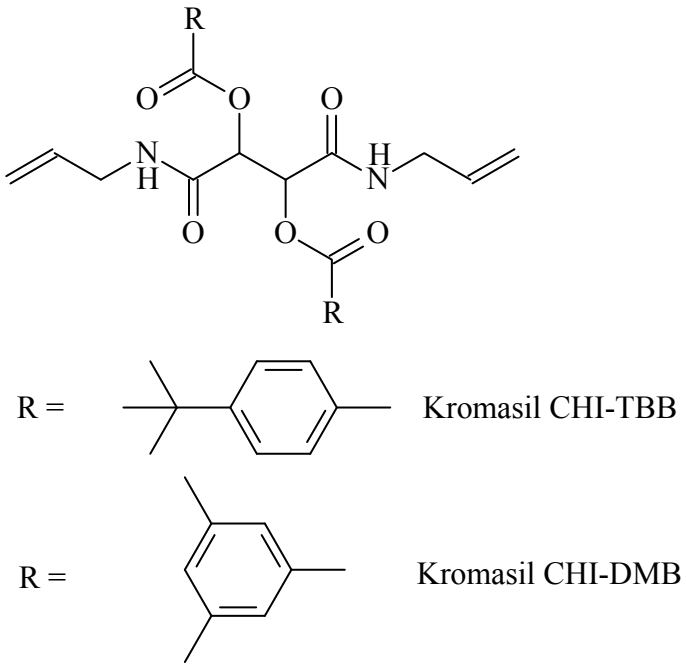

Fig. 7. Structures of monomers of Kromasil CHI-TBB and Kromasil CHI-DMB CSPs (from Ref. [83]).

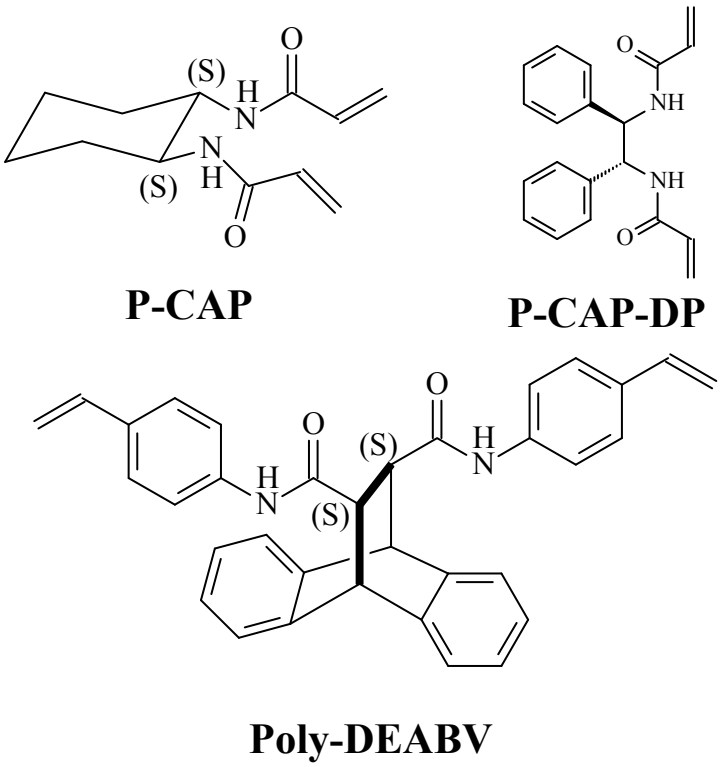

P-CAP **P-CAP-DP**

Poly-DEABV

Fig. 8. Structures of the recent developed syhthetic polymeric CSPs.

Table 1. Proteins used as chiral selectors in HPLC Chiral Stationary Phases (Abbreviated from Ref. [4])

Proteins	Molecular Weight	Isoelectric point	Trade Name
BSA	66,000	4.7	CHIRAL BSA; RESOLVOSIL BSA-7, BSA-7PX; USTRON ES-BSA
HSA	69,000	4.8	CHIRAL HSA; CHIRAL -HSA
α_1-Acid glycoprotein (AGP)	41,000	2.7	CHIRAL-AGP
Ovomucoid (OMCHI)	55,000	4.1	ULTRON ES-OVM
Avidin (AVI)	66,000	1.0	Bioptic AV-1
Cellobiohydrolase 1 (CBH I)	64,000	3.9	CHIRAL-CBH
Pepsin	34,600	< 1.0	ULTRON ES-PEPSIN

Table 2. Important commercialized chiral stationary phases based on derivatives of cellulose and amylase (Abbreviated from Ref. [4])

Type of derivatives	Derivative	Trademark
Amylose Derivatives		
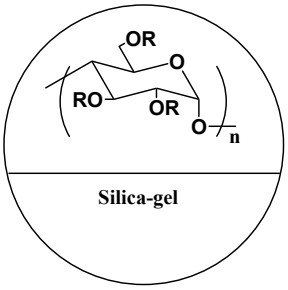	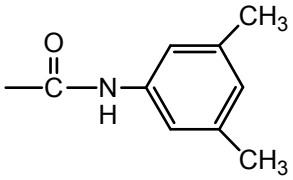 tris(3,5-dimethylphenyl carbamate)	AD
	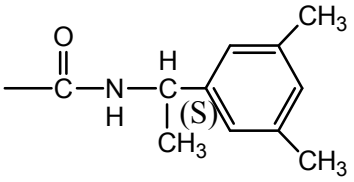 Tris(S)-α-methylbenzyl carbamate	AS
Cellulose Derivatives		
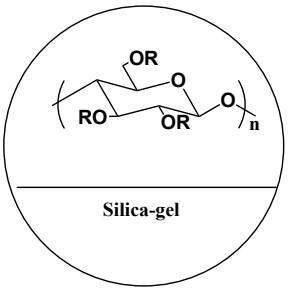	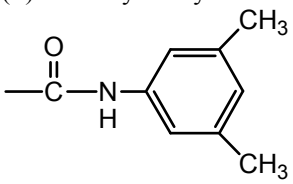 Tris (3,5-dimethylphenyl carbamate)	OD
	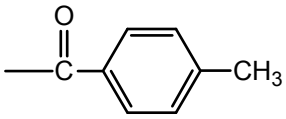 Tris (4-methylbenzoate)	OJ

Chapter 2. Separation of chiral furan derivatives by liquid chromatography using cyclodextrin-based chiral stationary phases

A paper published in *Journal of Chromatography A*[1]

Xinxin Han, Tuanli Yao, Ying Liu, Richard C. Larock, and Daniel W. Armstrong

Abstract

The enantiomeric separation of a set of 30 new chiral furan derivatives has been achieved on native and derivatized β-cyclodextrin stationary phases using high performance liquid chromatography (HPLC). The hydroxypropyl-β-cyclodextrin (Cyclobond RSP), the 2,3-dimethyl-β-cyclodextrin (Cyclobond DM), and the acetyl-β-cyclodextrin (Cyclobond AC) stationary phases are the most effective chiral stationary phases (CSPs) for the separation of these racemates in the reverse phase mode. No enantioseparations have been observed on the native β-cyclodextrin chiral stationary phase (Cyclobond I 2000) and only a few separations have been attained on the S-naphthylethyl carbamate β-cyclodextrin (Cyclobond SN) and 3,5-dimethylphenyl carbamate β-cyclodextrin (Cyclobond DMP) chiral stationary phases in the reverse phase mode. The polar organic and the normal phase mode on these CSPs are not effective for separation of these compounds. The characteristics of the analytes, including steric bulk, hydrogen bonding ability, and geometry, play an important role in the chiral recognition process. The pH affects the enantioseparation of compounds with ionizable groups and the addition of 0.5% methyl *tert*-butyl ether to the mobile phase significantly enhances the separation efficiency for some highly retained compounds.

Keywords: Chiral separation; Enantioseparation; Chiral stationary phase; Cyclodextrin; Derivatized cyclodextrins; Chiral furan derivatives

2.1. Introduction

Furan derivatives are important structure units in a variety of natural products and pharmaceuticals [1-3]. Furanosesquiterpenes [4] are metabolites found in many marine invertebrates. Richardianidins [5] are isolated from the leaves of the plant *Cluytia*

richardiana and the melatonin receptor agonist drug candidate TAK-375 [6] has a chiral substituted furan structure. Furthermore, chiral furan derivatives are important building blocks in synthetic organic chemistry [7-11]. Oxidative cleavage of the furan ring under mild conditions allows certain furans to be converted to amino acids [12-14]. Piperidines and aza sugars can be obtained by the aza-*Achmatowicz* reaction from furan derivatives [15-17]. Furans also can act as dienes, and participate in [4+2] cycloaddition reactions with alkenes, alkynes or allenes, to form many important compounds [18-21].

Recently, Yao and Larock have synthesized a series of new chiral furans through the cyclization-cross-coupling of 2-(1-alkynyl)-2-alken-1-ones with various nucleophiles using auric chloride catalysis (Fig. 1) [22]. Alternatively, one can employ I_2, rather than $AuCl_3$, to form iodofurans [23]. The stereogenic center adjacent to the furan ring is generated by the attack of nucleophile on the alkene portion of the starting material. The potential of these compounds as drug candidates and/or useful synthetic intermediates is promising. It is well known that different enantiomers of a chiral compound show different biological activities [24]. Therefore, separation and assessment of the properties of these new chiral furans are necessary.

Cyclodextrin-based chiral stationary phases (Fig. 2), due to their ability to separate enantiomers of many chiral compounds [25-28] and especially neutral chiral molecules with aromatic units [29-34], are a natural choice for the separation of these new chiral furan derivatives. One previous publication has described the separation of two chiral substituted furans (racemic 1-(2-furylethyl) prenyl ether and racemic *anti*-3-isopropenyl-12-methyl-13-oxabicyclo[8.2.1]trideca-1(12), 10-dien-2-ol) using GC with a heptakis(2,3,6-tri-*O*-methyl)-β-cyclodextrin column, and also by SFC and LC with a carbamoylated cellulose and amylose chiral stationary phases [35]. To our knowledge, no other systematic or individual enantioseparations of chiral furans have been reported. In this work, the enantioselectivity of native and derivatized cyclodextrin based chiral stationary phases for 30 new chiral substituted furans was evaluated in different chromatographic modes. The cyclodextrin-based CSPs show enantioselectivity for 28 compounds and baseline separated 16 of them. The effects of analyte structure and the composition of the mobile phase on the enantioseparations are discussed.

2.2. Experimental

2.2.1. Materials

Cyclobond I 2000, DM, AC, RSP, DMP, and SN CSPs were obtained from Advanced Separation Technologies (Whippany, NJ, USA). All stationary phases used consisted of the chiral selector bonded to 5 μm spherical silica gel [27, 28]. The chiral selectors used are the native β-cyclodextrin and its derivatives, which are shown in Figure 2. The dimensions of the columns are 250 x 4.6 mm. Methanol, acetonitrile, 2-propanol, heptane, and methyl *tert*-butyl ether were HPLC grade from Fisher (Fairlawn, NJ, USA). Triethylamine, and acetic acid were ACS certified grade from Fisher. Water was deionized and filtered through active charcoal and a 5 μm filter.

2.2.2. Preparation of chiral furan derivatives

All chiral furan derivatives were prepared as previously reported via cyclization of 2-(1-alkynyl)-2-alken-1-ones with various nucleophiles using auric chloride catalysis [22] or iodine [23]. The general procedure is as below:

A solution of $AuCl_3$ (30.3 mg) in acetonotrile (970mg) was prepared. To the appropriate 2-(1-alkynyl)-2-alken-1-one (0.2 mmol) and nucleophile (1.5 equiv) in dichloromethane (1 ml), was added the above $AuCl_3$ solution (20mg, 1 mol %). The mixture was stirred at room temperature for 1 h unless otherwise specified. The solvent was removed under vacuum and the residue was purified by flash chromatography on silica gel.

2.2.3. Equipment

Chromatographic separations were carried out using a HP 1050 HPLC system with a UV VWD detector, an auto sampler, and computer controlled Chem-station data processing software. The mobile phases were degassed by ultra-sonication under vacuum for 10 minutes. UV detection was carried out at 300 nm for most of the compounds, except compound **18**, which was detected at 254 nm. All separations were carried out at room temperature (~ 23˚C).

2.2.4. Column Evaluation

The performance of each stationary phase was evaluated in the reverse phase mode using acetonitrile-water and methanol-water mobile phases. Cyclobond I 2000, AC, RSP, SN, and DMP CSPs were evaluated in the polar organic mode using acetonitrile and the

Cyclobond SN and DMP CSPs were evaluated in the normal phase mode using isopropanol-heptane. The flow rate of the mobile phase optimized for resolving the enantiomers of each compound was 1.0 mL/min.

2.2.5. Calculations

The dead time (t_0) was estimated using the peak resulting from the change in refractive index from the injection solvent on each CSP. The retention factor (k) was calculated using the equation $k = (t_r-t_0) / t_0$. The enantioselectivity (α) was calculated using $\alpha = k_2 / k_1$. The resolution factor (R_S) was calculated using the equation $R_S = 2 \times (t_{r2}-t_{r1}) / (w_1+w_2)$, where t_{r2} and t_{r1} are the retention times of the second and first enantiomers, respectively, and w_1 and w_2 are the corresponding base peak widths. The efficiency (number of theoretical plates, N) was calculated using $N = 16(t_r/w)^2$.

2.3. Results and discussion

2.3.1. Performance of the CSPs

All of the 30 substituted chiral furans, including 22 tetrahydrobenzofuran derivatives, 4 furochromene derivatives, and 4 simple, multiply-substituted furans have been assessed on six different cyclodextrin-based CSPs in the reverse phase mode. The polar organic mode and normal phase mode have been utilized with five CSPs (except the Cyclobond DM CSP) and two aromatically derivatized cyclodextrin CSPs, respectively. The chromatographic data for all successful and several unsuccessful separations are given in Tables 1 and 2. Most compounds were eluted at the dead volume of the column in the polar organic mode under the weakest solvent condition (100% acetonitrile) for this separation mode and no enantioseparation was observed for the compounds that were retained. All analytes were retained in the normal phase mode with a 1:99 isopropanol-heptane mobile phase, but only one partial diastereomeric separation was observed for compound **5** on the Cyclobond SN CSP. For reverse phase LC, enantioseparations ($\alpha > 1.02$) were observed for 28 compounds and 16 baseline separations ($R_S > 1.5$) were achieved. The performance of each CSP in the reverse phase mode is summarized in Fig. 3 and Table 1. Obviously, the most effective CSPs for resolving these chiral substituted furans are Cyclobond DM, RSP, and AC CSPs. The Cyclobond DM CSP was able to separate 19 of the enantiomers with 10 baseline separations. Eighteen enantioselective and 5 baseline separations were observed on the Cyclobond RSP

column. The Cyclobond AC column also showed enantioseparations of 11 analytes and baseline separation of 5 of them. The remaining CSPs, Cyclobond I 2000 and the aromatic derivatized Cyclobond SN and DMP CSPs were either ineffective or showed enantioseparation for only a few of the examined chiral furans in the reverse phase mode. The separation data for these CSPs are summarized in Table 2.

2.3.2. Effect of mobile phase composition

For separations in the reverse phase mode, two organic modifiers, acetonitrile and methanol, were examined. In general, similar enantioseparations were observed with both organic modifiers. Compared to methanol, acetonitrile has greater solvent strength in the reverse phase mode and a higher affinity for the cyclodextrin cavity; therefore, less retention and enantioselectivity were found when using acetonitrile as opposed to methanol at equivalent volume-based mobile phase compositions.

The effect of the pH of the buffer was also assessed. All 30 compounds were investigated on all of the examined CSPs with 0.1% TEAA (triethylamine/acetic acid) buffer solution from pH = 4 to pH = 8. No appreciable difference in selectivity or resolution was observed for the neutral compounds. However, a mobile phase pH effect on the enantioseparation of compounds **3**, **7** and **14**, which contain ionizable groups, was observed. Table 3 shows the separation data for these three compounds at different pH values. For example, compound **7**, which has a weakly basic indole group, shows an appreciable decrease in retention at pH 4 on the Cyclobond DM CSP. At other pHs, the retention, selectivity, and resolution were similar. For compound **14** with a dimethyl aniline group, the reduction in retention at pH 4 was observed with both the Cyclobond RSP and AC CSPs. The separation data at all other pHs from 5 to 8 are quite similar. Compared to the separation achieved in a water/methanol mobile phase, the retention decreased, while the resolution increased, at all pHs. Since the enantioselectivity (α-value) is similar, the increase in resolution is due to the increase in efficiency. The greatest effect of pH on retention, selectivity, and resolution was found for compound **3**, which has a carboxylic acid group (Fig. 4). Although good enantioselectivity was achieved with a methanol/water mobile phase, the efficiency was so poor that the resolution was only 0.8. When using methanol/buffer as the mobile phase, the retention decreased and sharper peaks with better resolution were

achieved. The best separation was attained at pH 5 (Fig. 4). With an increase in the pH of the buffer, the analyte is ionized and more hydrophilic. Thus, both the retention and resolution decrease.

It has been reported that the addition of a small amount of methyl *tert*-butyl ether in the mobile phase can improve the peak shape and efficiency for some analytes with high enantioselectivity, but very poor efficiency, due to stationary phase mass transfer effects (often due to very strong inclusion in the cyclodextrin cavity) [31]. In this work, there appear to be two such cases. They involve the separations of compounds **14** and **15** on the Cyclobond DM and Cyclobond AC CSPs, respectively. These separations afforded broad, asymmetric peak shapes, but they retained significant peak-to-peak separations (Figs. 5a and 5c). An appreciable decrease in retention and great increase in efficiency were observed for both compounds with the addition of a small amount of methyl *tert*-butyl ether (Figs. 5b and 5d). For compound **14**, the efficiencies (number of theoretical plates, N) for peak 1 are 1200 and 500 using methyl *tert*-butyl ether as an additive versus no additive, respectively. For compound **15**, the efficiency of peak 1 increased from 660 to 3300 with the additive in the mobile phase. Therefore, better efficiency and shorter separation times were achieved, although the enantioselectivity was similar. The methyl *tert*-butyl ether serves as a competitive binding agent for the cyclodextrin cavity, thereby displacing the analyte more readily and effectively than other mobile phase components.

2.3.3. Effects due to the structure of the individual analyte

The differences in the structures of the compounds greatly affect the enantioseparations of the three groups of analytes listed in Table 1 and Fig. 1. The chiral tetrahydrobenzofurans are the easiest to separate. The Cyclobond CSPs showed enantioselectivity for all 22 of these compounds and baseline separated 15 of them. These same CSPs showed moderate selectivity for the four furochromenes. All four compounds were separated with one providing a baseline separation. The four simple, multiply-substituted furans were the most difficult to separate with the Cyclobond CSPs. Only partial separations of two of these compounds were observed.

2.3.3.1. Effect of an iodide group

It is well known that halogen substituents have a strong affinity for the cyclodextrin

cavity. Therefore, an iodide substituent in the analyte may play an important role in the enantioseparation. For example, the separations of compounds **27** and **30** clearly show the effect of an iodide group in the β-position of the furan ring on the enantioseparation. Compound **27** cannot be separated on any Cyclobond column, but a partial separation of compound **30** was observed on the Cyclobond AC, RSP, and DM CSPs. A comparison of compounds **23** and **25** is more interesting (Fig. 6). The Cyclobond RSP column showed a baseline separation for compound **23**, which has an iodide substituent in the β-position of the furan ring, while no enantioselectivity was observed on the Cyclobond DM and AC columns. Compound **25**, which has no iodide substituent, could be only partial separated on the Cyclobond DM, RSP, and AC CSPs. For compounds **17** and **19**, the iodide group in compound **19** enhanced the enantioselectivity on the Cyclobond RSP, DM and AC CSPs. However, for compounds **18** and **20**, the enantioselectivity for compound **18** was much better on the Cyclobond DM CSP compared to that of compound **20**. Clearly, the presence of a halogen substituent can either help or hurt an enantiomeric separation depending on its exact location. If the halogen moiety redirects inclusion complexation (by offering a more favorable complexation site) away from the stereogenic center and/or its substituents, it can hurt an enantioselective separation. Conversely, if the presence of a halogen moiety redirects inclusion complexation in such a way that there is enhanced interaction with the substituents from the stereogenic center, the enantioselective separation can be improved.

2.3.3.2. Steric effects

Steric repulsion plays an important role in chiral recognition for the Cyclobond DM CSP. The separations of compounds **6** and **15** show that an increase in steric bulk near their stereogenic centers improves the separation on the Cyclobond DM CSP. These two compounds have similar structures. The only difference is that compound **15** has a six-membered ring fused to the furan moiety, while compound **6** has a seven-membered ring. The bigger ring in compound **6** produces less retention, but higher enantioselectivity (Fig. 7). A similar trend can be found for compounds **15**, **10**, and **12**. With an increase in the size of the substitutent connected to the chiral center (from a methoxy group, to an allyloxy group to an isopropoxy group), a decrease in retention coupled with an enhancement in the enantioresolution was observed. However, too large an increase in the steric bulk around the

chiral center of the analyte can hinder the separation on the Cyclobond DM CSP. For example, compounds **13** and **5**, which have much more bulky substituents attached to the chiral center, could not be resolved on the Cyclobond DM CSP, while they can be separated on the Cyclobond AC and SN CSPs, respectively.

2.3.3.3. Effect of hydrogen bonding groups

Hydrogen bonding interactions greatly affect separations on Cyclobond RSP and AC CSPs. For example, compound **3**, which has a carboxylic acid group (a hydrogen bond donor and acceptor), shows satisfactory enantioseparation on the Cyclobond AC CSP with the methanol/buffer mobile phase. While compound **15**, which has no carboxylic acid group, showed no enantioselectivity on this CSP. Another example is the separation of compounds **14** and **11**. The presence of a tertiary amine group, a much better hydrogen bond acceptor compared to iodine, results in compound **14** being baseline separated on the Cyclobond RSP and AC columns, while no enantioselectivity was observed for compound **11** on these CSPs. Some other compounds with hydrogen bond donor or acceptor groups, such as compounds **2**, **7**, and **13**, also show acceptable enantioseparation on the Cyclobond RSP or AC CSPs.

2.3.3.4. Effect of substituent geometry

The separations of two pairs of compounds **17**, **18** and **19**, **20** are also interesting. Each pair has similar structures. Both of them have two chiral centers, one of which is the *trans* configuration and the other is the *cis* configuration. The two compounds showed different selectivity on different cyclodextrin CSPs. For the first group, compounds **17** and **18**, Cyclobond RSP and AC CSPs showed better selectivity for the analyte with the *trans* configuration, but the compound with the *cis* configuration was separated better on the Cyclobond DM CSP. For the second group, compounds **19** and **20**, all three non-aromatic derivatized Cyclobond CSPs produced better enantioseparations for the compound with the *trans* configuration than the one with the *cis* configuration. Another interesting example of the effect of geometry is compound **21**. It can be baseline separated on any non-aromatic derivatized Cyclobond CSPs due to its highly rigid fused tricyclic structure.

2.4. Conclusions

The Cyclobond DM, RSP, and AC CSPs have been shown to be very effective for the enantioselective separation of many chiral, substituted furan derivatives in the reverse phase

mode. The nature of the organic modifier has little effect on the enantioseparation. The pH of the mobile phase only affects the separation of the compounds with ionizable groups. The addition of 0.5 % methyl *tert*-butyl ether to the mobile phase enhanced the separation for some compounds, which had high α-values, but very poor efficiencies. The nature of the compounds, including the steric bulk, hydrogen bonding ability, and geometry, greatly affects the chiral recognition. In general, the tetrahydrobenzofurans and furochromenes are better separated than simple substituted furans. The normal phase and polar organic phase are not as effective as the reverse phase mode for the separation of these compounds.

Acknowledgements

We gratefully acknowledge the support of this work by the National Institutes of Health, NIH RO1 GM53825-08.

References

[1] M. F. Dean, in: R. A. Kartritzky, (Eds.), In Advances in Heterocyclic Chemistry, Academic, New York, 1983, Vol. 31, p. 237.

[2] B. H. Lipshutz, Chem. Rev. 86 (1986) 795.

[3] B. M. Fraga, Nat. Prod. Rep. 12 (1995) 303.

[4] V. Vaillancourt, M. R. Agharahimi, U. N. Sundram, O. Richou, D. J. Faulkner, K. F. Albizati, J. Org. Chem. 56 (1991) 378.

[5] A. Soriente, M. De Rosa, P. Dovinola, G. Sodano, A. Scettri, Tetrahedron: Assymmetry 9 (1998) 2197.

[6] N. Tarui, Y. Nagano, T. Sakane, K. Matsumoto, M. Kawada, O. Uchikawa, S. Ohkawa, K. Nakahama, J. Biosci. Bioeng. 93 (2002) 44.

[7] M. Cinfolini, C. Y. W. Hermann, Q. Dong, T. Shimizu, S. Swaminathan, N. Yi, Synlett (1998) 105.

[8] W. P. Chen, S. M. Roberts, J. Chem. Soc., Perkin Trans. I (1999) 103.

[9] W. S. Zhou, Z. H. Lu, Y. M. Xu, L. Y. Liao, Z. M. Wang, Tetrahedron 55 (1999) 11959.

[10] R. Hodgson, T. Majid, A. Nelson, J. Chem. Soc., Perkin Trans. I (2002) 1631.

[11] A. S. Demir, Ö. Sesenoglu, D. Ülkü, C. Arıcı, Helv. Chim. Acta 86 (2003) 91.

[12] T. Shono, Y. Matsumura, J. Tsubata, Chem. Lett. (1981) 1121.

[13] P. S. Bailey, Ozonation in Organic Chemistry, Academic, New York, 1982, Vol. 2,

Chapt. 6.

[14] M. Kasai, H. Ziffer, J. Org. Chem. 48 (1983) 2346.

[15] O. Achmatowicz, P. Bukowski, B. Szechnev, Z. Zwierzchowska, A. Zamojski, Tetrahedron 27 (1971) 1973.

[16] N. Yi, M. A. Cinfolini, Tetrahedron Lett. 36 (1995) 6595.

[17] C. F. Yana, Y. M. Xu, L. X. Liao, W. S. Zhou, Tetrahedron Lett. 39 (1998) 9227.

[18] W. A. Rendall, M. Torres, O. P. Strausz, J. Org. Chem. 50 (1985) 3034.

[19] K. H. Dötz, R. Noack, K. Harms, G. Müller, Tetrahedron 46 (1990) 1235.

[20] C. O. Kappe, S. S. Murphree, A. Padwa, Tetrahedron 53 (1997) 14179.

[21] R. T. Brown, S. B. Jameson, D. Ouali, P. I. Tattersall, J. Chem. Res. (2000) 176.

[22] T. Yao, X. Zhang, R. C. Larock, J. Am. Chem. Soc. 126 (2004) 11164.

[23] T. Yao, R. C. Larock, Work in progress (2004).

[24] United States Food and Drug Administration, Chirality 4 (1992) 338.

[25] D. W. Armstrong, W. DeMond, J. Chromatogr. Sci. 22 (1984) 411.

[26] D. W. Armstrong, T. J. Ward, R. D. Armstrong, T. E. Beesley, Science 232 (1986) 1132.

[27] A. M. Stalcup, S.-C. Chang, D. W. Armstrong, J. Chromatogr. 513 (1990) 181.

[28] D. W. Armstrong, A. M. Stalcup, M. L. Hilton, J. D. Duncan, J. R. Faulkner, Jr., S.-C. Chang, Anal. Chem. 62 (1990) 1610.

[29] D. W. Armstrong, W. DeMond, B. P. Czech, Anal. Chem. 57 (1985) 481.

[30] D. W. Armstrong, T. J. Ward, A. Czech, B. P. Czech, R. A. Bartsch, J. Org. Chem. 50 (1985) 5556.

[31] D. W. Armstrong, J. Zukowski, J. Chromatogr. A 666 (1994) 445.

[32] D. W. Armstrong, L. W. Chang, S. C. Chang, X. Wang, H. Ibrahim, G. R. Reid, T. E. Beesley, J. Liq. Chromatogr. Rel. Technol. 20 (1997) 3279.

[33] C. R. Mitchell, M. Desai, R. McCulla, W. Jenks, D. W. Armstrong, Chromatographia 56 (2002) 127.

[34] D. D. Schumacher, C. R. Mitchell, T. L. Xiao, R. V. Rozhkov, R. C. Larock, D. W. Armstrong, J. Chromatogr. A 1011 (2003) 37.

[35] H. F. Kasai, M. Tsubuki, K. Takahashi, M. Shirao, Y. Matsumoto, T. Honda, Y. Seyama, J. Chromatogr. A 977 (2002) 125.

Table 1. Retention factor of the first peak (k_1), enantioselectivity (α), and enantioresolution (R_S) of all chiral furans on the Cyclobond RSP, DM, and AC CSP

#	Structure	CSP	k_1	α	R_S	Mobile Phase (v / v)
1	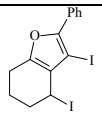	RSP	8.52	1.05	0.3	CH_3OH/H_2O = 50/50
		DM	7.59			CH_3OH/H_2O = 50/50
		AC	8.38			CH_3OH/H_2O = 50/50
2	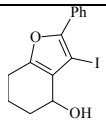	RSP	8.58	1.10	1.2	CH_3OH/H_2O = 45/55
		DM	7.46	1.23	1.9	CH_3OH/H_2O = 25/75
		AC	4.57			CH_3OH/H_2O = 40/60
3	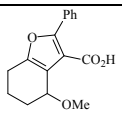	RSP	3.48			CH_3OH/H_2O = 40/60
		DM	2.03			CH_3OH/H_2O = 40/60
		AC	8.15	1.30	0.8	CH_3OH/H_2O = 60/40
4	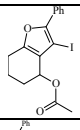	RSP	10.38	1.05	0.5	CH_3OH/H_2O = 45/55
		DM	5.13	1.13	1.2	CH_3OH/H_2O = 40/60
		AC	5.04	1.13	0.8	CH_3OH/H_2O = 40/60
5[a]	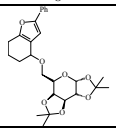	RSP	8.89			CH_3OH/H_2O = 50/50
		DM	2.12			CH_3OH/H_2O = 40/60
		AC	2.55			CH_3OH/H_2O = 50/50
6	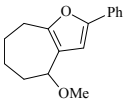	RSP	3.35			CH_3OH/H_2O = 60/40
		DM	2.72	1.48	2.6	CH_3OH/H_2O = 40/60
		AC	2.79			CH_3OH/H_2O = 50/50
7	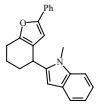	RSP	5.43	1.17	1.7	CH_3OH/H_2O = 60/40
		DM	3.94	1.35	1.6	CH_3OH/H_2O = 50/50
		AC	5.52			CH_3OH/H_2O = 50/50
8	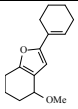	RSP	7.14			CH_3OH/H_2O = 60/40
		DM	4.08	1.29	1.9	CH_3OH/H_2O = 40/60
		AC	3.69			CH_3OH/H_2O = 50/50
9	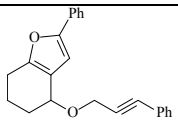	RSP	4.31	1.06	0.6	CH_3OH/H_2O = 60/40
		DM	8.75	1.10	0.4	CH_3OH/H_2O = 40/60
		AC	9.33			CH_3OH/H_2O = 50/50
10	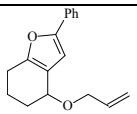	RSP	2.24			CH_3OH/H_2O = 60/40
		DM	2.52	1.32	2.0	CH_3OH/H_2O = 40/60
		AC	2.57			CH_3OH/H_2O = 50/50
11	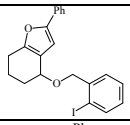	RSP	12.79			CH_3OH/H_2O = 50/50
		DM	6.96	1.26	1.0	CH_3OH/H_2O = 40/60
		AC	5.98			CH_3OH/H_2O = 50/50
12	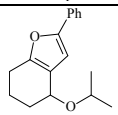	RSP	4.76	1.03	0.3	CH_3OH/H_2O = 50/50
		DM	1.57	1.34	1.7	CH_3OH/H_2O = 40/60
		AC	4.95	1.08	0.8	CH_3OH/H_2O = 40/60
13	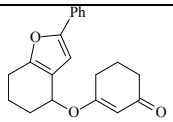	RSP	2.77			CH_3OH/H_2O = 60/40
		DM	4.06			CH_3OH/H_2O = 40/60
		AC	7.81	1.13	1.4	CH_3OH/H_2O = 40/60

Table 1. (continued)

#	Structure	CSP	k_1	α	R_S	Mobile Phase (v / v)
14	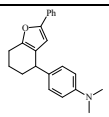	RSP	8.97	1.37	2.9	CH_3OH/H_2O = 60/40
		DM	6.28			CH_3OH/H_2O = 50/50
		AC	6.94	1.36	2.4	CH_3OH/H_2O = 50/50
15	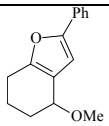	RSP	4.40	1.03	0.3	CH_3OH/H_2O = 50/50
		DM	9.57	1.28	1.7	CH_3OH/H_2O = 40/60
		AC	5.76			CH_3OH/H_2O = 40/60
16	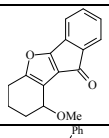	RSP	7.64	1.13	1.2	CH_3OH/H_2O = 40/60
		DM	1.66			CH_3OH/H_2O = 40/60
		AC	3.32			CH_3OH/H_2O = 40/60
17	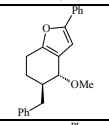	RSP	8.69	1.11	1.2	CH_3OH/H_2O = 60/40
		DM	12.60	1.10	0.6	CH_3OH/H_2O = 40/60
		AC	11.40	1.17	1.6	CH_3OH/H_2O = 40/60
18	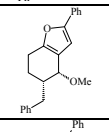	RSP	7.00			CH_3OH/H_2O = 60/40
		DM	6.95	1.55	3.1	CH_3OH/H_2O = 40/60
		AC	10.83	1.09	0.9	CH_3OH/H_2O = 40/60
19	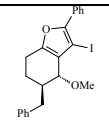	RSP	6.02	1.15	1.5	CH_3OH/H_2O = 60/40
		DM	4.50	1.27	1.2	CH_3OH/H_2O = 50/50
		AC	9.88	1.31	1.6	CH_3OH/H_2O = 40/60
20	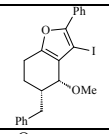	RSP	4.00			CH_3OH/H_2O = 60/40
		DM	7.37	1.22	1.0	CH_3OH/H_2O = 40/60
		AC	7.75			CH_3OH/H_2O = 40/60
21	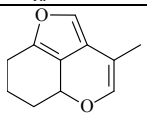	RSP	3.13	1.17	1.5	CH_3OH/H_2O = 60/40
		DM	4.64	1.34	2.8	CH_3OH/H_2O = 40/60
		AC	5.33	1.23	2.2	CH_3OH/H_2O = 40/60
22	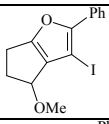	RSP	10.99	1.09	1.1	CH_3OH/H_2O = 45/55
		DM	4.09	1.28	1.7	CH_3OH/H_2O = 40/60
		AC	6.59			CH_3OH/H_2O = 40/60
23	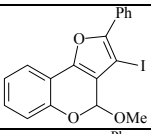	RSP	14.24	1.12	1.5	CH_3OH/H_2O = 45/55
		DM	9.57			CH_3OH/H_2O = 35/65
		AC	6.28			CH_3OH/H_2O = 40/60
24	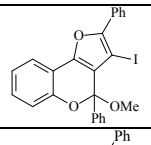	RSP	7.52			CH_3OH/H_2O = 50/50
		DM	8.26	1.11	0.6	CH_3OH/H_2O = 40/60
		AC	5.25			CH_3OH/H_2O = 50/50
25	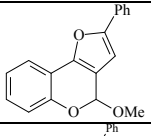	RSP	5.43	1.06	0.6	CH_3OH/H_2O = 50/50
		DM	6.99	1.15	1.2	CH_3OH/H_2O = 35/65
		AC	5.59	1.04	0.3	CH_3OH/H_2O = 40/60
26	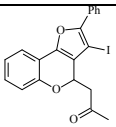	RSP	9.05	1.11	1.1	CH_3OH/H_2O = 45/55
		DM	3.71			CH_3OH/H_2O = 40/60
		AC	3.04			CH_3OH/H_2O = 50/50

Table 1. (continued)

#	Structure	CSP	k_1	α	R_S	Mobile Phase (v / v)
27	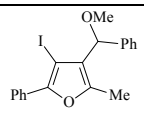	RSP	7.34			CH_3OH/H_2O = 50/50
		DM	4.83			CH_3OH/H_2O = 40/60
		AC	5.84			CH_3OH/H_2O = 40/60
28	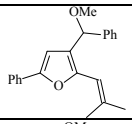	RSP	3.43			CH_3OH/H_2O = 50/50
		DM	2.28			CH_3OH/H_2O = 50/50
		AC	2.88			CH_3OH/H_2O = 50/50
29	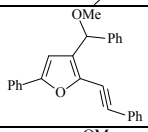	RSP	4.24	1.08	0.7	CH_3OH/H_2O = 60/40
		DM	3.86			CH_3OH/H_2O = 50/50
		AC	8.97			CH_3OH/H_2O = 50/50
30	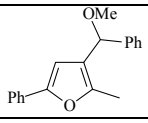	RSP	4.95	1.05	0.6	CH_3OH/H_2O = 50/50
		DM	5.78	1.10	0.8	CH_3OH/H_2O = 40/60
		AC	5.71	1.11	0.7	CH_3OH/H_2O = 40/60

[a] Separation of diastereomers

Table 2. Retention factor of the first peak (k_1), enantioselectivity (α), and enantioresolution (R_S) of chiral furans separated on the Cyclobond SN and DMP CSPs

Compound #	k_1	α	R_S	Mobile Phase (v / v)
Cyclobond SN CSP				
5[a]	2.11	1.26	1.7	CH_3OH/H_2O = 60/40
9	5.94	1.08	0.6	CH_3OH/H_2O = 60/40
12	1.00	1.06	0.3	CH_3OH/H_2O = 60/40
14	7.55	1.07	0.6	CH_3OH/H_2O = 60/40
21	1.40	1.08	0.6	CH_3OH/H_2O = 60/40
Cyclobond DMP CSP				
5[a]	12.54	1.02	0.3	CH_3OH/H_2O = 60/40
8	3.98	1.06	0.5	CH_3OH/H_2O = 70/30
14	14.36	1.03	0.4	CH_3OH/H_2O = 60/40
17	10.36	1.11	1.5	CH_3OH/H_2O = 70/30

[a] Separation of diastereomers

Table 3. Retention factor of the first peak (k_1), enantioselectivity (α), and enantioresolution (R_S) of compounds **3**, **7**, and **14** at different pHs of the mobile phase (0.1% triethylamine with pH adjusted by acetic acid).

pH		4			5			6			7			8		
#	CSP	k_1	α	R_S	k_1	α	R_S	k_1	α	R_S	k_1	α	R_S	k_1	α	R_S
3	AC	1.74	1.14	1.6	2.53	1.15	2.1	1.04	1.19	1.6	0.26	1.35	1.1	0.18	1.50	1.1
7	DM	3.16	1.35	2.0	3.73	1.35	2.1	3.91	1.35	2.0	3.59	1.35	2.1	3.57	1.35	2.1
	RSP	4.14	1.17	1.6	4.19	1.18	1.8	4.20	1.17	1.8	3.93	1.17	1.8	4.02	1.17	1.8
14	RSP	5.95	1.37	3.4	6.92	1.37	3.5	7.23	1.37	3.7	6.74	1.37	3.7	6.88	1.37	3.6
	AC	3.50	1.36	2.4	5.00	1.36	2.7	5.64	1.36	2.8	5.81	1.36	3.1	5.67	1.36	3.0

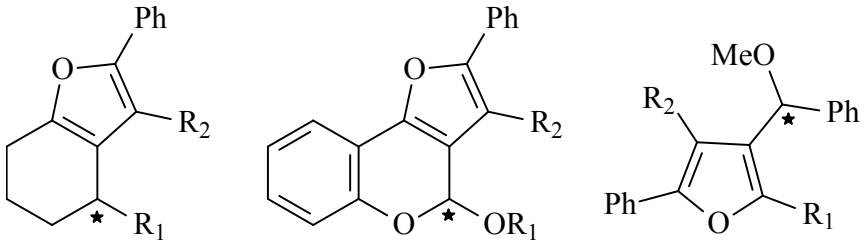

1 **2** **3**

Fig. 1. Structure **1** is a tetrahydrobenzofuran derivative. Structure **2** is a furochromene derivative. Structure **3** is a simple multiply-substituted furan. R_1 can be various types of aliphatic or aromatic substituents. R_2 can be an iodine or a hydrogen atom. The carbon marked with an asterisk is the stereogenic center.

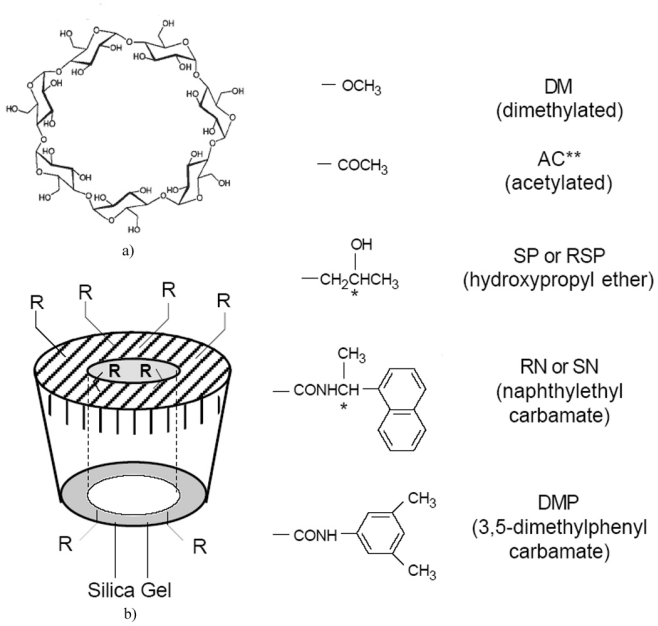

Fig. 2. (a) Native β-cyclodextrin (Cyclobond I 2000). (b) Types of derivatized β-cyclodextrins. An asterisk denotes the chiral center. Taken form Cyclobond Handbook, 6th Edition, 2002 with permission.

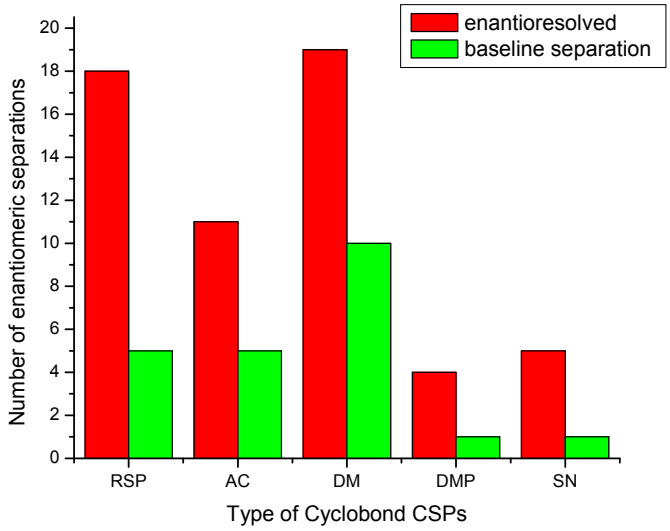

Fig. 3. Summary of the number of baseline and partial separations obtained on different CSPs.

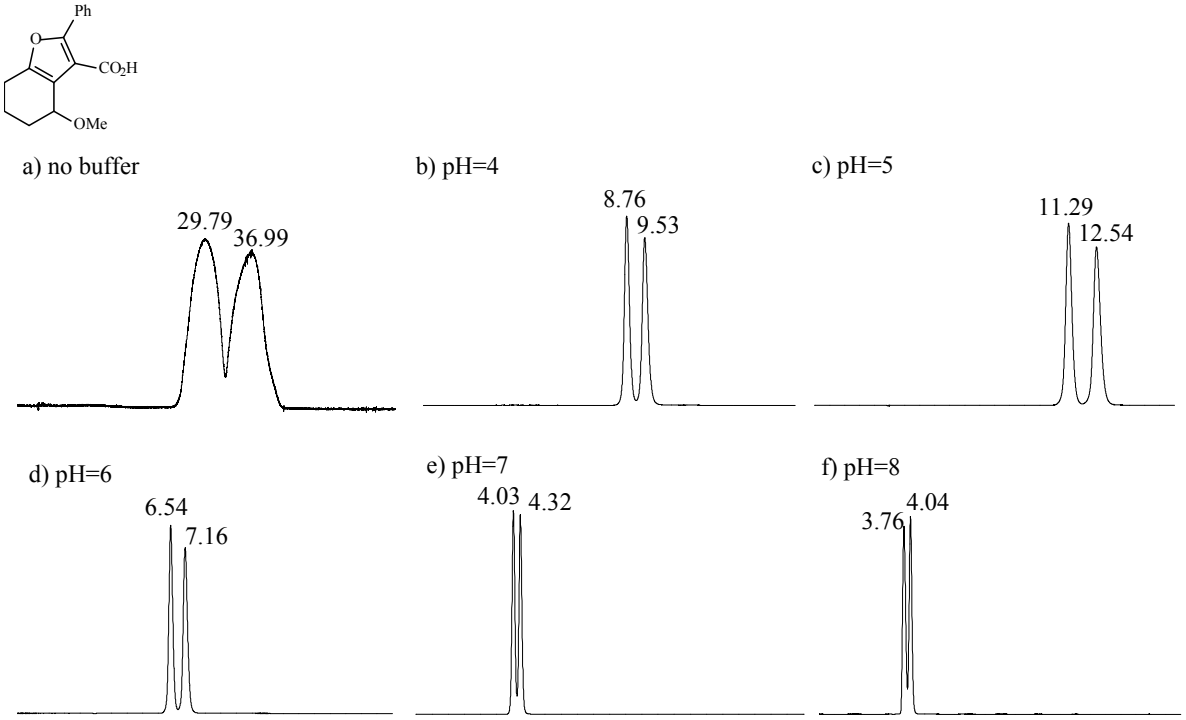

Fig. 4. The pH effect for the enantioseparation of compound **3** on the Cyclobond AC CSP. Mobile phase: a) CH_3OH/H_2O = 60/40, b) through f) were used a mobile phase of CH_3OH/buffer = 60/40 where the buffer was 0.1% triethylamine with different concentrations of acetic acid to adjust the pH values indicated above.

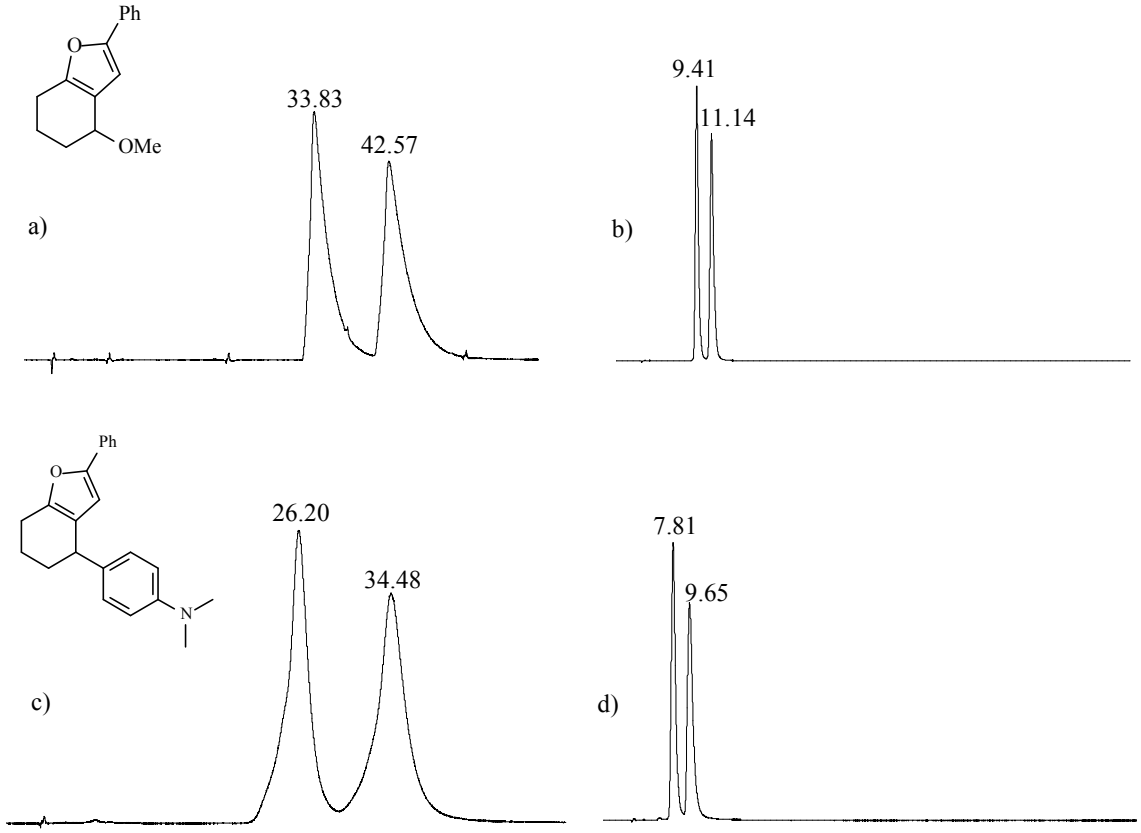

Fig. 5. The effect of 0.5% methyl *tert*-butyl ether in the mobile phase for the separation of compounds **14** and **15**. Chromatograms a) and b) were done using the Cyclobond DM CSP. Chromatograms c) and d) were done using the Cyclobond AC CSP. The mobile phase composition in each case was as follows: a) CH_3OH/H_2O = 40/60, b) CH_3OH/H_2O/methyl *tert*-butyl ether = 40/60/0.5, c) CH_3OH/H_2O = 50/50, d) CH_3OH/H_2O/methyl *tert*-butyl ether = 50/50/0.5. Enantioselectivity α: a) α = 1.28, b) α = 1.28, c) α = 1.36, d) α = 1.40. Number of theoretical plates of the first peak N_1: a) N_1 = 660, b) N_1 = 3300, c) N_1 = 500, d) N_1 = 1200.

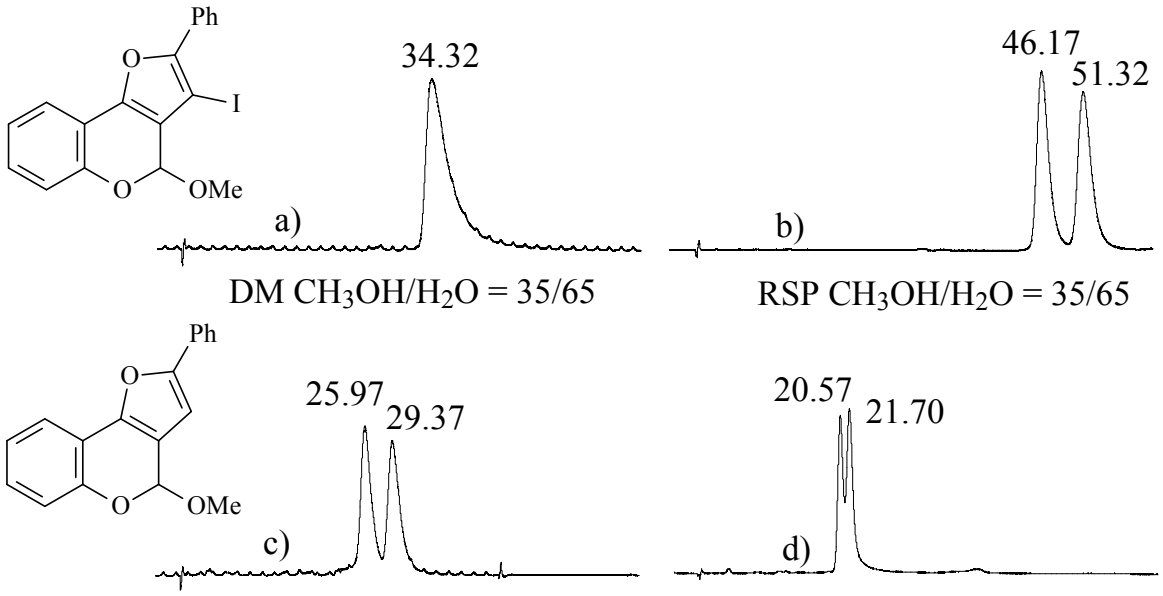

Fig. 6. The iodide effect on the separation for compounds **23** and **25**. Chromatograms a) and c) were done using the Cyclobond DM CSP. Chromatograms b) and d) were done using the Cyclobond RSP CSP. The mobile phase composition in each chromatogram was as follows: a), c) CH_3OH/H_2O = 35/65, b) CH_3OH/H_2O = 45/55, d) CH_3OH/H_2O = 50/50.

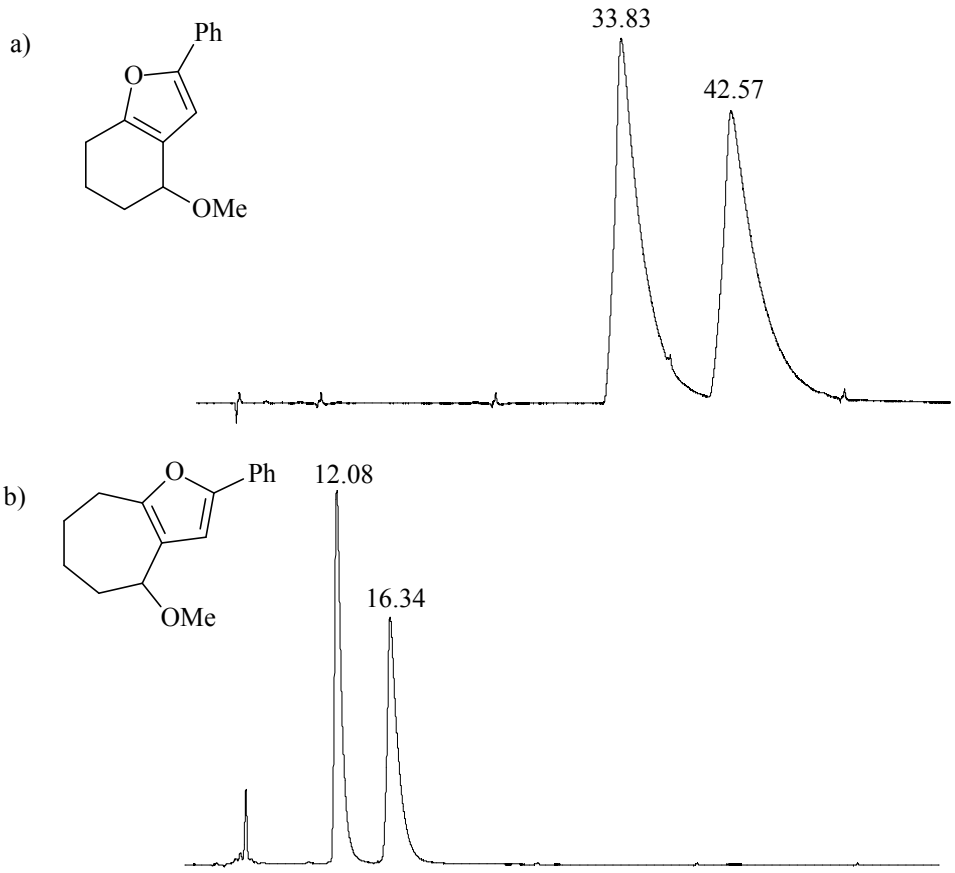

Fig. 7. Steric effect on the separation of compounds **15** and **6** on Cyclobond DM CSP. Mobile phase: CH_3OH/H_2O = 40/60. Enantioselectivity α: a) α = 1.28, b) α = 1.48.

Chapter 3. Separation of enantiomers of isochromene derivatives by HPLC using cyclodextrin-based stationary phases

A paper published in *Chromatographia*[1]

X. Han, Q. Zhong, D. Yue, N. Della Cà, R. C. Larock, D. W. Armstrong

Abstract

Twenty chiral isochromene derivatives have been chromatographed on native and derivatized cyclodextrin stationary phases using HPLC. The most effective CSPs for the enantioresolution of these analytes in the reverse phase mode are the hydroxypropyl-*β*-cyclodextrin (Cyclobond RSP), the 2,3-dimethyl-*β*-cyclodextrin (Cyclobond DM), and the *γ*-cyclodextrin (Cyclobond II) stationary phases. The α-cyclodextrin (Cyclobond III), *β*-cyclodextrin (Cyclobond I), acetyl-*β*-cyclodextrin (Cyclobond AC), *S*-1-naphthylethyl carbamate-β-cyclodextrin (Cyclobond SN), and 3,5-dimethylphenyl carbamate-*β*-cyclodextrin (Cyclobond DMP) stationary phases also show enantioselectivities for some analytes. No enantioresolution has been observed in the polar organic mode and only a few separations were found in the normal phase mode. The Cyclobond RSP CSP shows the highest efficiency of separation for these analytes in the reverse phase mode. The pH of the mobile phase and the nature of organic modifiers have little effect on the enantioresolution. The substituents in the isochromene ring greatly affect the chiral recognitions.

Keywords**:** Column liquid chromatography, Enantioresolution, CSP, Isochromene derivatives, Cyclodextrin

3.1. Introduction

Derivatives of isochromene are found throughout in nature, particularly in fungi. A variety of isochromene derivatives have been isolated from *Phellinus igniarius* [1], *Monascus purpureus* Wentii, *Penicillium sclerotiorum* van Beyma, *Daldinia concentrica* [2], insect pathogenic fungus *Cordyceps pseudomilitaris* BCC 1620 [3], *Streptomyces exfoliatus* [4], and marine fungus *Leptosphaeria obiones* [5]. In addition, isochromene derivatives have also been found in the root bark of *Fijian Ventilago vitiensis* [6], and *Pentas longiflora* [7].

Isochromene analogues also possess a broad range of useful biological properties. Most important are their antitumor properties. Isochromene carboxamides show activity against the human ovarian cancer cell line SKOV3 through its interaction with DNA [8, 9]. Two isochromene derivatives, phelligridins C and D, display *in vitro* cytotoxicity against the A549 human lung cancer cell line, and a liver cancer line, Bel7402 [1]. In addition, exfoliamycin, an isochromene derivative, is a bactericide against gram-positive organisms [4]. Another isochromene analogue, trichoflectin, inhibits the biosynthesis of dihydroxynaphthalene melanin in fungi [10].

Recently, Yue, Della Cà, and Larock have synthesized a series of substituted chiral isochromenes by electrophilic cyclization of acetylenic aldehydes and ketones with a variety of electrophiles and nucleophiles (Fig. 1) [11]. The stereogenic center is produced by the attack of a nucleophile on the carbonyl group of the starting material. Clearly, the potential of pharmaceutical and/or synthetic applications of these compounds is promising. In most cases, the enantiomers of chiral compounds have different pharmacological properties [12]. Therefore, the separation and evaluation of the properties of the enantiomers of these compounds are necessary.

Cyclodextrin-based chiral stationary phases (Fig. 2), due to their high enantiomeric selectivities for many chiral compounds [13-19], and especially for neutral chiral molecules with aromatic portions [20-25], are a natural choice for the separation of chiral substituted isochromenes. To our knowledge, no systematic chiral separations of isochromene derivatives have been reported previously. In this paper, the enantioselectivity of 3 native and 5 derivatized cyclodextrin based chiral stationary phases for 20 chiral isochromenes are assessed in different chromatographic modes. The effects of the structure of the analytes and the composition of the mobile phase on enantiomeric separation are discussed.

3.2. Experimental

3.2.1. Materials

Cyclobond I, II, III, DM, AC, RSP, DMP, and SN CSPs (Fig. 2) were obtained from Advanced Separation Technologies (Whippany, NJ, USA) [26]. All stationary phases used consist of the chiral selector bonded to 5 μm spherical silica gel. The chiral selectors used are the native α, β, and γ-cyclodextrins and derivatives of β-cyclodextrin. The dimensions of the

columns are 250 x 4.6 mm. Methanol, acetonitrile, 2-propanol, ethanol, and heptane were HPLC grade from Fisher (Fairlawn, NJ, USA). Triethylamine and acetic acid were ACS certified grade from Fisher. Water was deionized and filtered through active charcoal and a 5 μm filter. All chiral isochromene derivatives were prepared as previously reported via electrophilic cyclization of acetylenic aldehydes and ketones with a variety of electrophiles and nucleophiles [11].

3.2.2. Equipment

Chromatographic separations were carried out using a HP 1050 HPLC system with a UV VWD detector, an auto sampler, and computer controlled Chem-station data processing software (Agilent Technologies, Palo Alto, CA, USA). The mobile phases were degassed by ultra-sonication under vacuum for 10 min. UV detection was carried out at 300 nm for most of the compounds, except compounds **5** and **13**, which were detected at 254 nm. All separations were carried out at room temperature (~ 23˚C). The flow rate of the mobile phase for all separations was 1.0 mL min^{-1}.

3.2.3. Column Evaluation

The performance of each stationary phase was evaluated in the reverse phase mode using acetonitrile-water and methanol-water mobile phases. Cyclobond I, II, III, AC, RSP, SN, and DMP were evaluated in the polar organic mode using acetonitrile and the Cyclobond SN and DMP were evaluated in the normal phase mode using ethanol-heptane. Over the amount of 600 injections, no change in the performance of these columns was observed. When using a new mobile phase, ten column volumes of solution were pumped through the column prior to injections of the analyte.

3.2.4.Calculations

The dead time (t_0) was estimated using the peak resulting from the change in refractive index from the injection solvent on each CSP. The retention factor (k) was calculated using the equation $k = (t_r\text{-}t_0) / t_0$. The enantioselectivity (α) was calculated using $\alpha = k_2 / k_1$. The resolution factor (R_S) was calculated using the equation $R_S = 2$ x $(t_{r2}\text{-}t_{r1}) / (w_1+w_2)$, where t_{r2} and t_{r1} are the retention times of the second and first enantiomers, respectively, and w_1 and w_2 are the corresponding base peak widths. The efficiency (number of theoretical plates, N) was calculated using $N = 16(t_r/w)^2$.

3.3. Results and Discussion

3.3.1. Performance of the 8 CSPs in the 3 Separation Modes

The separations of 20 chiral isochromene derivatives were evaluated on the Cyclobond I, II, III, DM, AC, RSP, DMP, and SN columns in the reverse phase mode. The polar organic mode was utilized with all Cyclobond columns except Cyclobond DM. The normal phase mode was used with two aromatically derivatized cyclodextrin CSPs (Cyclobond SN, and DMP). In the polar organic mode, most compounds were eluted at the dead volume of the column even with the weakest mobile phase (100% acetonitrile) for this separation mode. As expected, no enantiomeric separations were observed for the weakly retained compounds. In the reverse phase mode, observable enantioresolutions ($Rs \geq 0.3$) were attained for 17 chiral isochromenes and 15 baseline separations ($Rs \geq 1.5$) were achieved. The chromatographic data for the successful and unsuccessful separations in the reverse phase mode are listed in Tables 1 and 2. The normal phase mode did not produce as many enantiomeric separations as the reverse phase mode. However, the partial separation of 5 compounds and one baseline separation are observed with a 1:99 ethanol-heptane or 100% heptane mobile phase (Table 3).

The various Cyclobond columns showed widely varying selectivities for the separation of these chiral substituted isochromenes. The overall number of observable and baseline separations obtained on each CSP in the reverse phase mode is summarized in Fig. 3. Clearly, the most effective columns for the enantioresolution of these compounds are Cyclobond RSP, DM, and II (Table 1). The Cyclobond RSP was able to separate enantiomers of 12 isochromenes and 10 of these were baseline separations. The Cyclobond DM also showed enantioselectivity for 12 compounds, but only 3 baseline separations were achieved. Thirteen separations with 5 baseline were observed on the γ-cyclodextrin column. The other five CSPs, Cyclobond I, III, AC, SN, and DMP, were not as effective as the former 3 CSPs, but they also showed enantioselectivities for quite a few examined compounds and some baseline separations were obtained on these CSPs (See Table 2).

The difference in efficiencies of the three most effective CSPs is also interesting. The chiral separation of compound **1** is a good example (Fig. 4). The enantioselectivity of this analyte is higher on the Cyclobond DM than on the Cyclobond RSP. However, the

enantiomeric resolution of this compound on the Cyclobond DM is not as good as on the Cyclobond RSP due to the poor separation efficiency (the number of theoretical plates for the first peak, N_1, for the Cyclobond DM is 530 and 1900 for the Cyclobond RSP column). Although the Cyclobond RSP and II show similar enantioselectivities for compound **1**, the resolution is much worse on the Cyclobond II, which means that the Cyclobond RSP produces better mass transfer and higher efficiency separations (N_1 for the Cyclobond II is 630). The enantioresolutions for compounds **2**, **8**, **14**, **17**, and **18** showed the same trends. Most of the time, the Cyclobond RSP produced higher efficiencies in the reverse phase mode than all other native or derivatized cyclodextrin-based CSPs.

3.3.2. Effect of Mobile Phase Composition in the Reverse Phase Mode

Two organic modifiers, acetonitrile and methanol, were examined for the separations in the reverse phase mode. Similar enantioselectivities, and resolutions were observed in most cases with the two organic modifiers. Since acetonitrile has greater solvent strength in the reverse phase mode and a higher affinity for the cyclodextrin cavity, less retention and enantiomeric resolution were observed when using acetonitrile compared to methanol at equivalent volume-based mobile phase compositions.

According to our previous publications [24-25], the pH value of the mobile phase only influences the enantiomeric separation of compounds with ionizable groups when using Cyclobond columns. Therefore, in this work, the pH effect on the enantioresolutions of compounds **11**, **12**, **17**, and **20**, which have amine or pyridine groups, were investigated on all of the examined CSPs with 0.1% TEAA (triethylamine/acetic acid) buffer solution from pH = 4 to pH = 8. For the compounds **12** and **20** with pyridine moieties, the retention, enantioselectivity, efficiency, and resolution observed were almost the same as when using a methanol/buffer mobile phase, as opposed to using a methanol/water mobile phase. For compounds **11** and **17** with a dimethylaniline moiety, a decrease in retention was observed at pH 4, but the enantioselectivity, and efficiency were similar to those obtained with the methanol/water mobile phase.

3.3.3. Effects of Substituents on the Isochromene Ring

Steric repulsion plays an important role in chiral recognition for the Cyclobond columns, particularly when bulky substituents are close to the stereogenic center. A comparison of the

enantioresolutions of compounds **2** and **19** clearly shows that an increase in the size of the substituent near the stereogenic center destroys the enantioseparation. Both compounds have similar structures, except for the *n*-butyl group versus the *t*-butyl group connected to the stereogenic center. Enantiomers of compound **2** were baseline separated on the Cyclobond RSP and a satisfactory separation was obtained on the Cyclobond DM. However, no Cyclobond CSP showed any enantioselectivity for compound **19**, which has a bulky *t*-butyl group. Another example of the steric effect is the separations of compounds **2** and **4**. The larger aromatic substituent close to the chiral center resulted in compound **4** exhibiting worse enantioresolutions on the Cyclobond RSP and DM than compound **2**. However, the Cyclobond II showed chiral recognition for compound **4** and showed no enantioselectivity for compound **2**, because γ-cyclodextrin prefers to form inclusion complexes with multi-ring molecules.

Substituents further removed from the stereogenic center can also affect the enantioresolution. For example, compounds **1** and **9** have similar structures except for the substituents at the 3 position of the isochromene ring. Simply changing the phenyl group to an *n*-butyl group caused compound **9** to lose enantioselectivity on all cyclodextrin-based CSPs. For compounds **11** and **17**, the compound with a cyclohexenyl group at the 3 position of the isochromene ring can be baseline separated on the Cyclobond RSP and partially separated only on the Cyclobond DM, AC, and II. Conversely, compound **11**, which has a *n*-butyl substituent at the 3 position of the isochromene ring can be baseline separated only on the Cyclobond II and slightly separated on the Cyclobond I. Therefore, if the 3 position of the isochromene ring is occupied by a phenyl or cyclohexenyl substituent, the enantioseparation on Cyclobond CSPs is improved.

A comparison of the separations of compounds **1** and **18** is also interesting. The two methoxy groups at the 6 and 7 positions of the isochromene in compound **18** increase the enantioselectivity on the Cyclobond RSP, maintain similar enantioselectivity on the Cyclobond DM, and decrease the enantioselectivity on the Cyclobond II as opposed to compound **1**. Almost all of the Cyclobond CSPs showed enantioselectivity for compounds **12** and **20** due to the pyridine moiety. The only difference in these two compounds is that compound **12** contains a phenyl group at the 3 position of the isochromene ring, while

compound **20** has a 4-methoxyphenyl group at the same position. The separations of these two compounds are similar for all cyclodextrin CSPs, except for the Cyclobond SN (which contains aromatic substituents). However, much better enantioresolution for compound **12** on the Cyclobond SN was observed. This means that π-π interaction may play a role in the chiral recognition for the Cyclobond SN. The electron-donating methoxy group can change the electron density in the phenyl ring and thus change the strength of the π-π interaction.

The effect of a substituent in the 4 position of the isochromene ring can be observed for compounds **8** and **14**. The iodine-substituted compound **14** shows better enantioresolution than compound **8** with a thiophenyl group at the same position on all Cyclobond CSPs.

3.4. Conclusions

Cyclodextrin-based CSPs show enantioselectivity for 17 of the 20 substituted isochromene compounds and baseline separate 15 of them. The Cyclobond RSP, DM, and II columns were most effective for the enantioresolution of the chiral isochromene derivatives in the reverse phase mode. The other CSPs, such as the Cyclobond AC, SN, DMP, I, and III, also show enantioselectivities for a few of the analytes. Weak chiral recognition was observed in the normal phase mode with the aromatic functionalized Cyclobond SN, and DMP CSPs. No enantiomeric separations were found in the polar organic mode for all the Cyclobond CSPs. The Cyclobond RSP CSP showed the highest efficiencies for the enantioresolutions of most analytes. The nature of the organic modifiers and mobile phase pH produce only minor effects in these enantioseparations. The substituents on the isochromene ring greatly affect the enantiomeric separations.

Acknowledgements

We gratefully acknowledge the support of this work by the National Institutes of Health, NIH RO1 GM53825-08.

References

1. Mo S, Wang S, Zhou G, Yang Y, Li Y, Chen X, Shi J (2004) J Nat Prod 67: 823-828

2. Suzuki T, Okada C, Arai K, Awaji A, Shimizu T, Tanemura K, Horaguchi T (2001) J Heterocyc Chem 38: 1409-1418

3. Isaka M, Kongsaeree P, Thebtaranonth Y (2001) J Antibiot 54: 36-43

4. Potterat O, Zahner H, Volkmann C, Zeeck A (1993) J Antibiot 46: 346-349

5. Poch GK, Gloer JB (1989), Tetrahedron Lett 30: 3483-3486

6. Ali S, Read RW, Sotheeswaran S (1994) Phytochemistry 35: 1029-1032

7. Hari L, De Buyck LF, De Pooter HL (1991) Phytochemistry 30: 1726-1727

8. Mondal S, Nogami T, Asao N, Yamamoto Y (2003) J Org Chem 68: 9496-9498

9. Wang W, Li T, Milburn R, Yates J, Hinnant E, Luzzio MJ, Noble SA, Attardo G (1998) Bioorg Med Chem Lett 8: 1579-1584

10. Thines E, Anke H, Sterner O (1998) J Nat Prod 61: 306-308

11. Yue D, Della Cà N, Larock RC (2004) Org Lett 6: 1581-1584

12. United States Food and Drug Administration, (1992) Chirality 4: 338-340.

13. Armstrong DW, DeMond W (1984) J Chromatogr Sci 22: 411-415

14. Armstrong DW, Ward TJ, Armstrong RD, Beesley TE (1986) Science 232: 1132-1135

15. Stalcup AM, Williams KL (1992) J Liq Chromatogr 15: 29-37

16. Camilleri P, Reid CA, Manallack DT (1994) Chromatographia 38: 771-775

17. Risley DS, Strege MA (2000) Anal Chem 72: 1736-1739

18. Armstrong DW US Patent (1985) 4539399

19. Mitchell CR, Armstrong DW (2004) In: Methods in Molecular Biology, Gübitz G, Schmid MG (Ed) Humana Press Inc., Totowa, NJ, USA, Vol. 243, pp. 61-112

20. Armstrong DW, DeMond W, Czech BP (1985) Anal Chem 57: 481-484

21. Armstrong DW, Ward TJ, Czech A, Czech BP, Bartsch RA (1985) J Org Chem 50: 5556-5559

22. Armstrong. DW, Zukowski J (1994) J Chromatogr A 666: 445-448

23. Armstrong DW, Chang LW, Chang SC, Wang X, Ibrahim H, Reid GR, Beesley TE (1997) J Liq Chromatogr Rel Technol 20: 3279-3295

24. Mitchell CR, Desai M, McCulla R, Jenks W, Armstrong DW (2002) Chromatographia 56: 127-135

25. Schumacher DD, Mitchell CR, Xiao TL, Rozhkov RV, Larock RC, Armstrong DW (2003) J Chromatogr A 1011: 37-47

26. Cyclobond Handbook, Advanced Separation Technologies Inc, Whippany, NJ, USA, 2002

Table 1. Retention factor of the first peak (k_1), enantioselectivity (α), and enantioresolution (R_S) of all chiral isochromenes on the Cyclobond RSP, DM, and II CSPs in the reverse phase mode.

#	Structure	CSP	k_1	α	R_S	Mobile Phase: CH_3OH/H_2O (v / v)
1	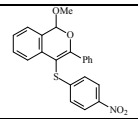	RSP	3.93	1.25	2.1	50/50
		DM	3.69	1.40	1.6	40/60
		II	3.40	1.22	1.0	40/60
2	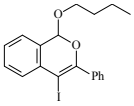	RSP	2.48	1.40	2.5	50/50
		DM	1.93	1.43	1.1	40/60
		II	3.70			40/60
3	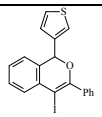	RSP	7.89	1.09	1.0	50/50
		DM	4.46	1.38	1.7	40/60
		II	5.59	1.13	0.9	45/55
4	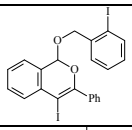	RSP	4.91	1.32	1.5	50/50
		DM	3.26	1.24	0.3	45/55
		II	3.83	1.19	0.8	45/55
5	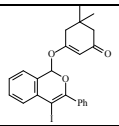	RSP	2.42			45/55
		DM	2.06			40/60
		II	7.03	1.12	1.0	30/70
6	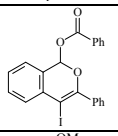	RSP	7.50	1.17	1.5	45/55
		DM	5.13	1.09	0.3	40/60
		II	3.34	1.19	1.0	45/55
7	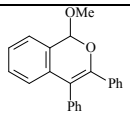	RSP	4.22			40/60
		DM	1.94			35/65
		II	2.77			35/65
8	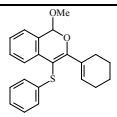	RSP	10.9	1.24	1.9	50/50
		DM	3.34	1.21	0.8	40/60
		II	6.18	1.10	0.3	35/65
9	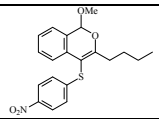	RSP	4.23			50/50
		DM	3.31			40/60
		II	3.62			35/65
10	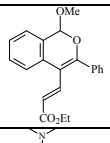	RSP	2.62			40/60
		DM	2.21			30/70
		II	2.52	1.33	1.8	25/75
11	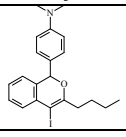	RSP	10.3			50/50
		DM	5.05			45/55
		II	2.32	1.33	2.7	40/60
12	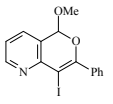	RSP	1.49	1.36	2.0	50/50
		DM	3.55	1.12	1.0	25/75
		II	2.80	1.24	1.6	30/70

Table 1. (continued)

#	Structure	CSP	k_1	α	R_S	Mobile Phase: CH_3OH/H_2O (v / v)
13	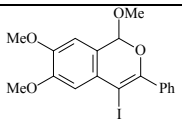	RSP	5.11			45/55
		DM	2.12			35/65
		II	4.58			40/60
14	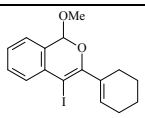	RSP	2.64	1.31	2.3	50/50
		DM	4.54	1.35	1.3	40/60
		II	5.79	1.14	1.0	45/55
15	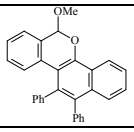	RSP	6.33	1.08	0.3	40/60
		DM	4.21	1.09	0.3	40/60
		II	3.00	1.31	2.4	35/65
16	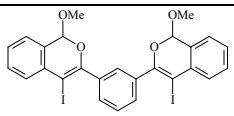	RSP	7.53			45/55
		DM	5.80			35/65
		II	2.30			50/50
17	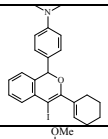	RSP	6.36	1.18	1.5	55/45
		DM	5.16	1.24	0.7	45/55
		II	12.4	1.21	0.8	40/60
18	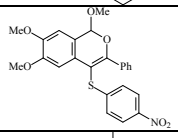	RSP	4.10	1.46	3.5	45/55
		DM	1.92	1.42	1.1	40/60
		II	3.94			40/60
19	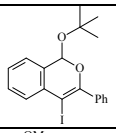	RSP	6.26			45/55
		DM	3.41			40/60
		II	6.25			30/70
20	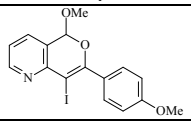	RSP	2.18	1.32	2.0	50/50
		DM	3.08	1.18	1.5	30/70
		II	5.31	1.22	2.0	25/75

Table 2. Retention factor of the first peak (k_1), enantioselectivity (α), and enantioresolution (R_S) of chiral isochromenes separated on the Cyclobond AC, SN, DMP, III and I CSPs in the reverse phase mode.

Compound #	k_1	α	R_S	Mobile Phase: CH_3OH/H_2O (v / v)
Cyclobond AC CSP				
1	4.94	1.16	0.9	40/60
3	5.92	1.14	0.8	40/60
5	5.24	1.15	1.2	40/60
8	4.56	1.08	0.3	40/60
12	1.30	1.22	1.6	40/60
14	5.91	1.14	0.7	40/60
17	12.8	1.32	1.1	40/60
20	1.74	1.30	1.7	40/60
Cyclobond SN CSP				
1	6.50	1.04	0.3	50/50
3	5.78	1.08	0.7	50/50
5	4.12	1.26	2.0	50/50
12	2.90	1.15	1.3	40/60
14	5.58	1.08	0.7	50/50
17	3.63	1.18	1.5	60/40
20	6.98	1.08	0.8	40/60
Cyclobond DMP CSP				
6	6.52	1.03	0.4	70/30
7	6.56	1.04	0.6	60/40
10	6.67	1.02	0.3	60/40
15	7.24	1.10	1.6	70/30
16	9.36	1.04	0.5	70/30
Cyclobond III CSP				
10	3.19	1.14	0.5	20/80
Cyclobond I CSP				
1	2.63	1.27	0.5	35/65
5	4.41	1.56	2.8	35/65
11	2.55	1.08	0.3	20/80

Table 2. (continued)

Compound #	k_1	α	R_S	Mobile Phase: CH_3OH/H_2O (v / v)
12	4.19	1.25	1.5	20/80
15	2.70	1.04	0.3	20/80
20	7.06	1.23	1.5	20/80

Table 3. Retention factor of the first peak (k_1), enantioselectivity (α), and enantioresolution (R_S) of chiral isochromenes separated on the Cyclobond SN and DMP CSPs in the normal phase mode.

Compound #	k_1	α	R_S	Mobile Phase (v / v)
Cyclobond SN CSP				
12	3.86	1.04	0.3	Heptane/Ethanol = 99/1
Cyclobond DMP CSP				
7	1.63	1.13	1.0	Heptane
10	2.00	1.04	0.3	Heptane/Ethanol = 99/1
12	5.99	1.04	0.5	Heptane/Ethanol = 99/1
15	0.66	1.24	1.6	Heptane/Ethanol = 99/1
20	6.37	1.03	0.3	Heptane/Ethanol = 98/2

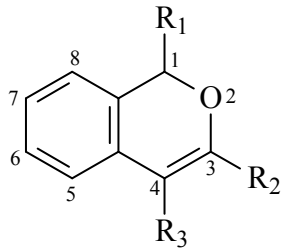

Fig. 1. General structure and ring numbering conventions for substituted isochromene. R_1 and R_2 can be various types of aliphatic or aromatic substituents. R_3 can be an iodine, a sulfur group or other aliphatic or aromatic groups. Position 1 is the stereogenic center.

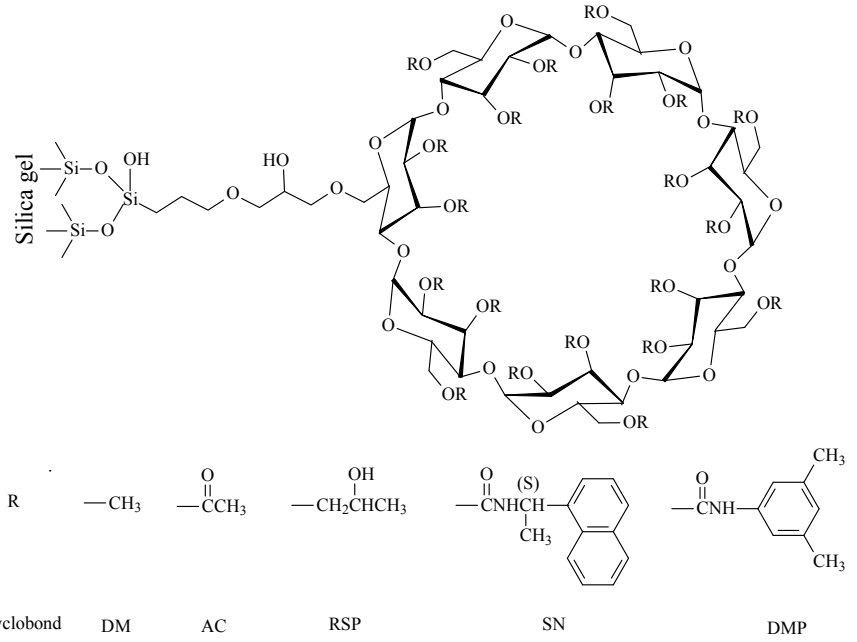

Fig. 2. General structure of the Cyclobond CSPs (can have 1-3 linkages for each cyclodextrin molecule). R=H, Cyclobond I (β-cyclodextrin), II (γ-cyclodextrin), III (α-cyclodextrin). All derivatized cyclodextrin CSPs are made from β-cyclodextrin.

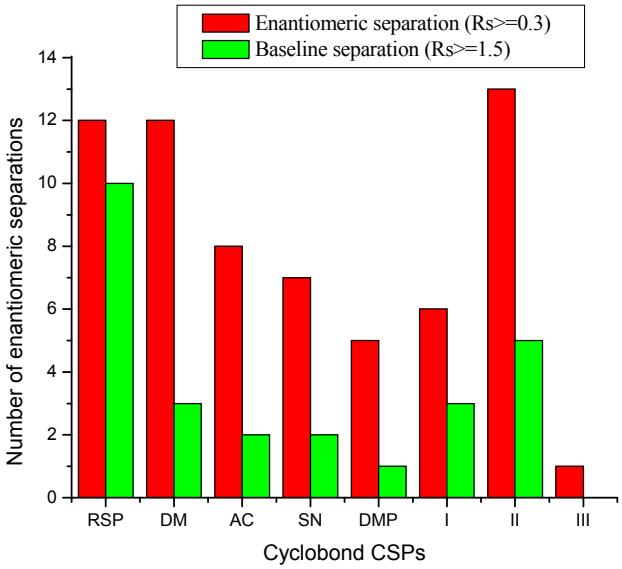

Fig. 3. Summary of the number of baseline and partial separations obtained on different CSPs in the reverse phase mode.

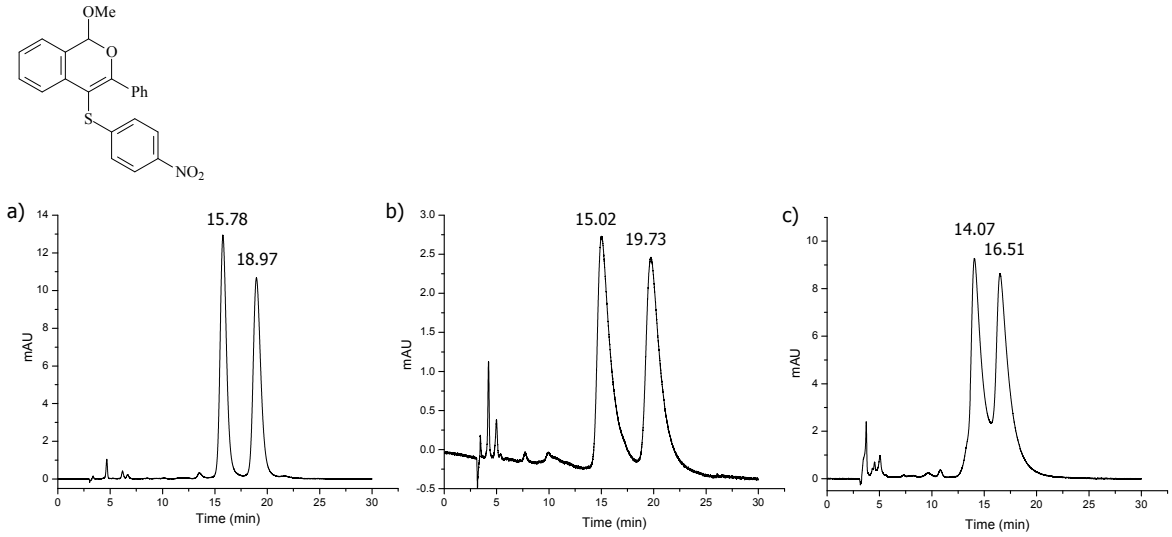

Fig. 4. Comparison of the efficiencies of the Cyclobond RSP (a), DM (b), and II (c) CSPs. The mobile phase composition in each case was as follows: a) CH_3OH/H_2O = 50/50, b) CH_3OH/H_2O = 40/60, c) CH_3OH/H_2O = 40/60. Enantioselectivity α: a) α = 1.25, b) α = 1.40, c) α = 1.22. Number of theoretical plates of the first peak N_1: a) N_1 = 1900, b) N_1 = 530, c) N_1 = 630.

Chapter 4. Enantiomeric separation of fused polycycles by HPLC with cyclodextrin and macrocyclic glycopeptide chiral stationary phases

A paper published in *Separation Science & Technology*[1]

Xinxin Han, Qinhua Huang, Jie Ding, Richard C. Larock, and Daniel W. Armstrong

Abstract

The enantiomeric separation of a series of 13 new chiral polycycles have been examined on both cyclodextrin-based and macrocyclic glycopeptide chiral stationary phases (CSPs) using HPLC in the normal phase, reversed phase, and polar organic modes. The most effective chiral selectors for the enantiomeric separation of these analytes are the 2,3-dimethyl-*β*-cyclodextrin (Cyclobond I-2000 DM) and hydroxypropyl-*β*-cyclodextrin (Cyclobond I-2000 RSP). The other Cyclobond-type and Chirobiotic (macrocyclic glycopeptide) CSPs only show enantioselectivity for a few of the racemic polycycles. The effects of mobile phase composition and analyte structure on chiral recognition and separation are considered.

Keywords: Fused polycycles, Enantiomeric separation, Chiral stationary phase, Cyclodextrin, Macrocyclic glycopeptides

4.1. Introduction

Fused polycycles exist widely in the natural world. Two pentacyclic proaporphine alkaloids, (-)-misramine[1] and (-)-labrandine[2], have been found in the Egyptian and Turkish flowering plant, *Roemeria hybrida*, respectively. A complex fused polycycle, dipuupehetriol[3], has been isolated from a Verongid sponge. From the Caribbean sponge *Smenospongia aurea*, aureol and its derivatives have been obtained[4]. Esmeraldin A and B, derivatives of diphenazine, have been found in *Streptomyces antibioticus*, strain Tü 2706[5].

Many fused polycycles are known to possess beneficial therapeutic activities. Dipuupehetriol has shown selectivity against the human lung cancer cell line A549 and the CV-1 cell line[3]. Two analogues of aureol inhibit the growth of some gram-positive and gram-negative bacteria[4]. Strong antitumor activities of hexacyclic derivatives of

camptothecin have been reported[6]. Some other tetracyclic compounds are inhibitors of kynurenine-3-hydroxylase[7] and poly(ADP-ribose)polymerase[8,9].

Huang, Larock, and co-workers have recently prepared a set of new chiral fused polycycles (Fig. 1)[10], which includes 8 chromene derivatives, 2 quinoline derivatives, 2 isochromene derivatives, and 1 polycyclic diester. These compounds are obtained through palladium-catalyzed alkyl to aryl palladium migration, followed by intramolecular arylation. Since different enantiomers of a chiral compound can have different biological properties[11], separation of these new chiral polycycles and evaluation of their properties are desirable.

Cyclodextrin-based[12-23] and macrocyclic glycopeptide[24-35] chiral stationary phases (Fig. 2) are well known for their high enantioselectivities for separation of a variety of different chiral molecules. In this work, the enantiomeric selectivity of 8 cyclodextrin and 4 macrocyclic glycopeptide chiral stationary phases for 13 recently synthesized racemic fused polycycles have been investigated in the reversed phase, polar organic and normal phase modes.

4.2. Experimental

4.2.1. Materials

Cyclobond I, II, III, DM, AC, RSP, DMP, SN; as well as the Chirobiotic V, R, T, and TAG CSPs (Fig. 2) were obtained from Advanced Separation Technologies (Whippany, NJ, USA). All the stationary phases consist of chiral selectors bonded to 5 μm spherical porous silica gel[14,15,24]. The chiral selectors are the native *α*-, *β*-, and *γ*-cyclodextrins, various derivatives of *β*-cyclodextrin, vancomycin, ristocetin A, teicoplanin, and teicoplanin aglycone (Fig. 2). The dimensions of the columns are 250 x 4.6 mm. HPLC grade methanol, acetonitrile, ethanol, and heptane were obtained from Fisher (Fairlawn, NJ, USA). The triethylamine and acetic acid used were ACS certified grade from Fisher. Water was deionized and filtered through active charcoal and a 5 μm filter. All chiral polycycles were prepared as previously reported via palladium-catalyzed alkyl to aryl migrations and cyclization [10].

4.2.2. Equipment

Chromatographic separations were carried out using an HP 1050 HPLC system with a UV VWD detector, an auto sampler, and computer-controlled Chem-station data processing

software (Agilent Technologies, Palo Alto, CA, USA). The mobile phases were degassed by ultra-sonication under vacuum. UV detection was carried out at 254 nm for all of the compounds. All separations were carried out at room temperature (~ 23˚C) and the flow rate of the mobile phase was 1.0 mL min^{-1}.

4.2.3. Column evaluation

The performance of all stationary phases was evaluated in the reversed phase mode using acetonitrile/water and methanol/water mobile phases. Cyclobond I, II, III, AC, RSP, SN, and DMP and all Chirobiotic CSPs were evaluated in the polar organic mode using acetonitrile as mobile phase. All Chirobiotic CSPs also were evaluated in the polar organic mode using ethanol as mobile phase. Cyclobond SN and DMP and all Chirobiotic CSPs were evaluated in the normal phase mode using an ethanol/heptane mobile phase. Over the course of 1000 injections, no degradation of these columns was observed. When using a new mobile phase, ten column volumes of solution were pumped through the column prior to injection of the analytes.

4.2.4. Calculations

The dead time (t_0) was estimated using the peak resulting from the change in refractive index from the injection solvent on each chiral stationary phase. The retention factor (k) was calculated using the equation $k = (t_r-t_0) / t_0$. The enantioselectivity (α) was calculated using $\alpha = k_2 / k_1$. The resolution factor (R_S) was calculated using the equation $R_S = 2 \times (t_{r2}-t_{r1}) / (w_1+w_2)$, where t_{r2} and t_{r1} are the retention times of the second and first enantiomers, respectively, and w_1 and w_2 are the corresponding base peak widths. The efficiency (number of theoretical plates, N) was calculated using $N = 16(t_r/w)^2$.

4.3. Results and Discussion

4.3.1. Performance of the chiral stationary phases

The chromatographic parameters for successful and unsuccessful separations are given in Tables 1-4. For the Cyclobond CSPs, enantiomeric separations were only observed in the reversed phase mode. No enantiomeric separations were achieved on these CSPs in the normal phase mode or the polar organic mode. Chirobiotic CSPs showed enantioselectivities for several of these compounds in the reversed phase mode, but no enantiomeric separations were observed in the polar organic mode. Only separations for compounds **3** and **4** were

observed for Chirobiotic CSPs in the normal phase mode. For all of the CSPs, enantiomeric separations (*Rs* > 0.3) of all the 13 analytes and baseline separations for 11 of them were achieved. The performance of all of the CSPs is summarized in Fig. 3. Obviously, the Cyclobond I-2000 RSP and DM CSPs are the most effective for the enantiomeric separation of these chiral polycycles. Eleven enantiomeric and 8 baseline separations were obtained with the Cyclobond I-2000 RSP CSP alone. The Cyclobond I-2000 DM CSP was able to separate 12 analytes, with 5 baseline separations. The other Cyclobond and Chirobiotic CSPs were not as effective as the former two CSPs. Only a few analytes were resolved on these other CSPs. For the separation of these neutral chiral fused-ring polycycles, the Cyclobond CSPs are superior to the Chirobiotic CSPs. However, for compounds **3** and **4**, high enantioselectivities and resolutions were observed on Chirobiotic T and Tag columns.

4.3.2. Effect of mobile phase composition

Based on studies reported in our previous publications, the pH of the reversed phase mobile phase has little effect on the enantiomeric separation of hydrophobic compounds that lack ionizable groups[21-23,35]. Two organic modifiers, acetonitrile and methanol were examined for separation of all of the analytes on all CSPs. In most cases, the organic modifiers have only small effects on the enantioselectivity, but they do affect resolution to some extent (Table 1). For example, Cyclobond I-2000 RSP and DM CSPs showed similar enantioselectivities for compound **1** when using a methanol/water or acetonitrile/water mobile phase. However, the enantiomeric resolution was better when using an acetonitrile/water mobile phase due to an increase in the efficiency (Fig. 4a and 4b). The theoretical plate number of the first peak, N_1, is 3200, when methanol was used as the organic modifier, while N_1 is 4300, when acetonitrile was used. Similar trends were observed for the separation of compounds **3-5**, **7**, and **9-12** on the Cyclobond I-2000 RSP column and compounds **4-7** on the Cyclobond I-2000 DM column. The resolution usually increases when using acetonitrile as the organic modifier due to an increase in the efficiency of the column. However, it should be noted that in a few special cases, better resolution was observed when methanol was used as the organic modifier, because of higher enantioselectivity. One typical example is the separation of compound **13** on the Cyclobond I-2000 DM CSP. Higher enantioselectivity, which resulted in better resolution, was observed when using a

methanol/water mobile phase as opposed to an acetonitrile/water mobile phase (Fig. 4c and 4d).

4.3.3. Effects of the structure of the analyte

Although all analytes have similar molecular skeletons, as well as stereogenic centers, a small difference in the structure of these analytes away from the stereogenic center produces large effects on these enantiomeric separations. These effects are illustrated using the following examples.

Both the Cyclobond I-2000 RSP and DM columns displayed higher enantioselectivities for compound **2**, which has a methyl ester substituent at the 6 position, than compound **1** without such a group, when a methanol/water mobile phase was used. Therefore, the resolution for compound **2** is higher than compound **1** on these two columns. Compound **2** also can be easily separated on the Cyclobond I-2000 AC, I, Chirobiotic V, and R Columns, while no enantioselectivity was observed for compound **1** on these CSPs. Another example is the separation of compounds **11** and **12**. The methylenedioxy group at the 4 and 5 positions of the polycycle enhanced the enantiomeric resolution. Baseline separation of compound **12** was achieved on the Cyclobond DM CSP, while no selectivity for compound **11** was found on this column due to the lack of substituents. In general, Cyclobond CSPs showed higher enantioselectivities for the racemic polycycles with substituents than the analogous compounds without substituents. A substituent on any chiral compound can provide steric interactions that adjust the geometry of the inclusion complexation, thereby providing a more or less favorable enantioselective binding site. Obviously, in these specific cases, the substituent on the polycycle resulted in an inclusion complex that enhanced the enantiomeric recognition between the racemic analytes and the derivatized cyclodextrin, thereby improving the separations.

Another interesting example is the separation of chromene derivatives **5-7**. These three compounds have similar structures, except for differing substituents in the 5 position of the polycycle. Compound **5** has a proton, while compounds **6** and **7** have nitro and methoxy groups, respectively. The methoxy group has a small effect on the enantiomeric separation on the Cyclobond I-2000 RSP and DM CSPs. Both CSPs showed similar enantioselectivities for compounds **5** and **7** (Fig. 5). Conversely, the nitro group affects enantiomeric separation

greatly. Although Cyclobond I-2000 RSP CSP was not able to separate the enantiomers of compound **6**, the enantiomeric separation was improved for this compound on Cyclobond I-2000 DM CSP compared with compounds **5** and **7** (Fig. 5).

A comparison of the separation of the structural isomers **8** and **9** is also interesting. A change in the position of the methylenedioxy substituent resulted in different enantioselectivities for these two compounds on the Cyclobond I-2000 RSP column. Using the same mobile phase on the Cyclobond I-2000 RSP CSP, compound **8** (with the methylenedioxy substituent at the 7 and 8 positions) showed lower retention, but higher enantioselectivity, than compound **9** (with the same group at the 8 and 9 positions). Clearly, the location of the same substituents on the polycycles also affected the enantiomeric separations of these compounds.

Although there is no significant difference for the separations of two somewhat similar quinoline derivatives **3** and **4** on the Cyclobond DM and RSP CSPs, the Chirobiotic T and TAG CSPs showed different enantioselectivity for these two analytes. In the reversed phase mode, the Chirobiotic T column showed much higher enantioselectivity for compound **3** than compound **4** and the enantiomeric resolution of compound **3** is about 3.5 times that of compound **4**. However, on Chirobiotic TAG column, the enantioselectivity of both compounds **3** and **4** increased (Fig. 6). Although higher enantioselectivity was observed for compound **3** on the Chirobiotic TAG than the Chirobiotic T column, the resolution was worse on the Chirobiotic TAG column due to the low efficiency (N_1 is 1400 on Chirobiotic TAG CSP and 2600 on Chirobiotic T CSP). The enantiomeric resolution for compound **4** was significantly greater on the Chirobiotic TAG column than on the Chirobiotic T column, because of the increase in the enantiomeric selectivity. In the normal phase mode, high enantiomeric resolutions of compounds **3** and **4** were observed on both Chirobiotic T and TAG CSPs. The Chirobiotic TAG column showed much higher enantioselectivities (more than twice) for these two compounds compared to the Chirobiotic T column. However, no great increase in separation was observed due to the poor efficiency of the Chirobiotic TAG column. The results in the normal phase (Table 4) indicated that the steric effect of the bulky sugar groups on the teicoplanin decreased the chiral recognition of these two compounds. On the contrary, these repulsive steric interactions of the Chirobiotic T column decreased the

retention and increased the efficiency greatly compared with the Chirobiotic TAG column. In addition, compounds **3** and **4** are the only compounds, which can be separated in normal phase mode on all Chirobiotic CSPs.

4.4. Conclusions

All of the 13 chiral fused polycycles examined were separated on Cyclobond and Chirobiotic CSPs and 11 of them were baseline separations. Cyclobond I-2000 DM and RSP CSPs are the most broadly applicable CSPs for the separation of these chiral compounds. Although Chirobiotic CSPs are not as effective as Cyclobond CSPs for these analytes, high enantioselectivities and resolutions for two analytes were observed on the Chirobiotic T and TAG columns in the reversed phase and normal phase modes. The reversed phase mode is the best mobile phase for these separations. Enantiomeric separations of only two analytes were observed in the normal phase mode on Chirobiotic CSPs and no enantioselectivity was found in the polar organic mode on any CSP. Similar enantioselectivities were found for analytes when either acetonitrile or methanol was used in the reversed phase mode. Generally, the acetonitrile/water mobile phases showed higher efficiencies than methanol/water mobile phases. For some special cases, the enantioselectivity in the methanol/water mobile phase was higher than with the acetonitrile/water mobile phase. The structure of the individual analytes greatly affected the enantiomeric separation. Chiral analytes with substituents generally were better separated than their unsubstituted parent compounds.

Acknowledgements

We gratefully acknowledge the support of this work by the National Institutes of Health, NIH RO1 GM53825-08.

References

[1] Kende, A. S.; Johnson, S. (-)-Misramine: an unusual proaporphine alkaloid. J. Org. Chem. **1985**, 50 (5), 729-730.

[2] Gözler, B. Labrandine: a new pentacyclic proaporphine alkaloid from *roemeria hybrida*. Heterocycles **1990**, 31 (1), 149-152.

[3] Hamann, M. T.; Scheuer, P. J. Biogenetically diverse, bioactive constituents of a sponge, order verongida: bromotyramines and sesquiterpene-shikimate derived metabolites. J. Org.

Chem. **1993**, 58 (24), 6565-6569.

[4] Aiello, A.; Fattorusso, E.; Menna, M. A new antibiotic chloro-sesquiterpene from the Caribbean sponge *smenospongia aurea*. Z. Naturforsch. **1993**, 48b (2), 209-212.

[5] Van't Land, C. W.; Mocek, U.; Floss, H. G. Biosynthesis of the phenazine antibiotics, the saphenamycins and esmeraldins, in *streptomyces antibioticus*. J. Org. Chem. **1993**, 58 (24), 6576-6582.

[6] Sugimori, M.; Ejima, A.; Ohsuki, S.; Uoto, K.; Mitsui, I.; Matsumoto, K.; Kawato, Y., Yasuoka, M.; Sato, K.; Tagawa, H.; Terasawa, H. Antitumor agents. 7. synthesis and antitumor activity of novel hexacyclic camptothecin analogues. J. Med. Chem. **1994**, 37 (19), 3033-3039.

[7] Varasi, M.; Pevarello, P.; Heidempergher, F.; Toma, S.; Speciale, C. Preparation of condensed pyrazole compounds as a kynurenine-3-hydroxylase inhibitors. WO Patent 9906374, 1999.

[8] Li, J.-H.; Zhang, J.; Kalish, V. J. Preparation of substituted 4, 9-dihydrocyclopenta[*lmn*] phenanthridine-5-ones and derivatives thereof as PARP inhibitors. WO Patent 2002006240, 2002.

[9] Li, J.-H.; Zhang, J.; Kalish, V. Preparation of substituted 4, 9-dihydrocyclopenta[*lmn*] phenanthridine-5-ones as PARP inhibitors. WO Patent 2003057145, 2003.

[10] Huang, Q.; Fazio, A.; Dai, G.; Campo, M. A.; Larock, R. C. Pd-Catalyzed alkyl to aryl migration and cyclization: an efficient synthesis of fused polycycles via multiple C-H activation. J. Am. Chem. Soc. **2004**, 126 (24), 7460-7461.

[11] FDA's policy statement for the development of new stereoisomeric drugs. Chirality **1992**, 4, 338-340.

[12] Armstrong, D. W.; DeMond, W. Cyclodextrin bonded phases for the liquid chromatographic separation of optical, geometrical, and structural isomers. J. Chromatogr. Sci. **1984**, 22 (9), 411-415.

[13] Armstrong, D. W.; Ward, T. J.; Armstrong, R. D.; Beesley, T. E. Separation of drug stereoisomers by the formation of β-cyclodextrin inclusion complexes. Science **1986**, 232, 1132-1135.

[14] Stalcup, A. M.; Chang, S.-C.; Armstrong, D. W. (S)-2-Hydroxypropyl-β-cyclodextrin, a

new chiral stationary phase for reversed-phase liquid chromatography. J. Chromatogr. **1990**, 513, 181-194.

[15] Armstrong, D. W.; Stalcup, A. M.; Hilton, A. M.; Duncan, J. D.; Faulkner, J. R. Jr., Chang, J. R. Derivatized cyclodextrins for normal-phase liquid chromatographic separation of enantiomers. Anal. Chem. **1990**, 62 (15), 1610-1615.

[16] Armstrong, D. W.; DeMond, W.; Czech, B. P. Separation of metallocene enantiomers by liquid chromatography: chiral recognition via cyclodextrin bonded phases. Anal. Chem. **1985**, 57 (2), 481-484.

[17] Armstrong, D. W.; Ward, T. J.; Czech, A.; Czech, B. P.; Bartsch, R. A. Synthesis, rapid resolution, and determination of absolute configuration of racemic 2,2'-binaphthyldiyl crown ethers and analogs via β-cyclodextrin complexation. J. Org. Chem. **1985**, 50 (26), 5556-5559.

[18] Camilleri, P.; Reid, C. A.; Manallack, D. T. Chiral recognition of structurally related aminoalkylphosphonic acid derivatives on an acetylated beta-cyclodextrin bonded phase. Chromatographia **1994**, 38 (11-12), 771-775.

[19] Armstrong, D. W.; Chang, L. W.; Chang, S. C.; Wang, X.; Ibrahim, H.; Reid, G. R. III; Beesley, T. E. Comparison of the enantioselectivity of β-cyclodextrin vs. heptakis-2,3-O-dimethyl-β-cyclodextrin LC stationary phases. J. Liq. Chromatogr. Rel. Technol. **1997**, 20 (20), 3279-3295.

[20] Risley, D. S.; Strege, M. A. Chiral separations of polar compounds by hydrophilic interaction chromatography with evaporative light scattering detection. Anal. Chem. **2000**, 72 (8), 1736-1739.

[21] Mitchell, C.; Desai, M.; McCulla, R.; Jenks, W.; Armstrong, D. Use of native and derivatized cyclodextrin chiral stationary phases for the enantioseparation of aromatic and aliphatic sulfoxides by high performance liquid chromatography. Chromatographia **2002**, 56 (3/4), 127-135.

[22] Schumacher, D. D.; Mitchell, C. R.; Xiao, T. L.; Rozhkov, R. V.; Larock, R. C.; Armstrong, D. W. Cyclodextrin-based liquid chromatographic enantiomeric separation of chiral dihydrofurocoumarins, an emerging class of medicinal compounds. J. Chromatogr. A **2003**, 1011 (1-2), 37-47.

[23] Han, X.; Yao, T.; Liu, Y.; Larock, R. C.; Armstrong, D. W. Separation of chiral furan

derivatives by liquid chromatography using cyclodextrin-based chiral stationary phases. J. Chromatogr. A **2005**, 1063 (1-2), 111-120.

[24] Armstrong, D. W.; Tang, Y.; Chen, S.; Zhou, Y.; Bagwill, C.; Chen, J.-R. Macrocyclic antibiotics as a new class of chiral selectors for liquid chromatography. Anal. Chem. **1994**, 66 (9), 1473-1484.

[25] Armstrong, D. W.; Zhou, Y. Use of a macrocyclic antibiotic as the chiral selector for enantiomeric separations by TLC. J. Liq. Chromatogr. **1994**, 17 (8), 1695-1707.

[26] Ward, T. J.; Dann, C. I.; Blaylock, A. Enantiomeric resolution using the macrocyclic antibiotics rifamycin B and rifamycin SV as chiral selectors for capillary electrophoresis. J. Chromatogr. A **1995**, 715 (2), 337-344.

[27] Gasper, M. P.; Berthod, A.; Nair, U. B.; Armstrong, D. W. Comparison and Modeling Study of Vancomycin, Ristocetin A, and Teicoplanin for CE Enantioseparations. Anal. Chem. **1996**, 68 (15), 2501-2514.

[28] Berthod, A.; Liu, Y.; Bagwill, C.; Armstrong, D. W. Facile LC enantioresolution of native amino acids and peptides using a teicoplanin chiral stationary phase. J. Chromatogr. A **1996**, 731 (1/2), 123-137.

[29] Peter, A.; Torok, G.; Toth, G.; Van den Nest, W.; Tourwe, D.; Armstrong, D. W. Enantiomeric separation of unusual secondary aromatic amino acids. Chromatographia **1998**, 48 (1-2), 53-58.

[30] Aboul-Enein, H. Y.; Serignese, V. Enantiomeric separation of several cyclic imides on a macrocyclic antibiotic (vancomycin) chiral stationary phase under normal and reversed phase conditions. Chirality **1998**, 10 (4), 358-361.

[31] Berthod, A.; Chen, X.; Kullman, J. P.; Armstrong, D. W.; Gasparrini, F.; D'Acquarica, I., Villani, C.; Carotti, A. Role of the carbohydrate moieties in chiral recognition on teicoplanin-based LC stationary phases. Anal. Chem. **2000**, 72 (8), 1767-1780.

[32] Karlsson, C.; Karlsson, L.; Armstrong, D. W.; Owens, P. K. Evaluation of a vancomycin chiral stationary phase in capillary electrochromatography using polar organic and reversed-phase modes. Anal. Chem. **2000**, 72 (18), 4394-4401.

[33] Xiao, T. L.; Zhang, B.; Lee, J. T.; Hui, F.; Armstrong, D. W. Reversal of enantiomeric elution order on macrocyclic glycopeptide chiral stationary phases. J. Liq. Chromatogr. Rel.

Technol. **2001**, 24 (17), 2673-2684.

[34] Berthod, A.; Xiao, T. L.; Liu, Y.; Jenks, W. S., Armstrong, D. W. Separation of chiral sulfoxides by liquid chromatography using macrocyclic glycopeptide chiral stationary phases. J. Chromatogr. A **2002**, 955 (1), 53-69.

[35] Xiao, T. L.; Rozhkov, R. V.; Larock, R. C.; Armstrong, D. W. Separation of the enantiomers of substituted dihydrofurocoumarins by HPLC using macrocyclic glycopeptide chiral stationary phases. Anal. Bioanal. Chem. **2003**, 377 (4), 639-654.

Table 1. Retention factor of the first peak (k_1), enantioselectivity (α), and enantiomeric resolution (R_S) of all chiral polycycles on the Cyclobond RSP and DM CSPs in the reversed phase mode.

#	Structure	CSP	k_1	α	R_S	Mobile Phase (v / v)
1	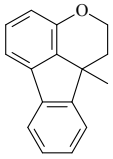	RSP	7.34	1.09	1.0	CH_3OH/H_2O = 35/65
			5.43	1.10	1.4	CH_3CN/H_2O = 20/80
		DM	10.5	1.04	0.4	CH_3OH/H_2O = 30/70
			9.45	1.05	0.7	CH_3CN/H_2O = 15/85
2	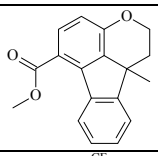	RSP	5.59	1.17	1.8	CH_3OH/H_2O = 40/60
			6.02	1.11	1.5	CH_3CN/H_2O = 20/80
		DM	6.95	1.14	1.4	CH_3OH/H_2O = 30/70
			5.95	1.09	1.0	CH_3CN/H_2O = 15/85
3	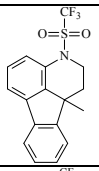	RSP	6.34	1.12	1.5	CH_3OH/H_2O = 40/60
			7.03	1.14	1.8	CH_3CN/H_2O = 20/80
		DM	9.30	1.10	1.2	CH_3OH/H_2O = 30/70
			9.65	1.07	0.9	CH_3CN/H_2O = 15/85
4	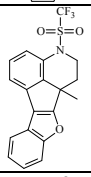	RSP	4.76	1.17	1.7	CH_3OH/H_2O = 50/50
			4.97	1.15	2.1	CH_3CN/H_2O = 25/75
		DM	4.95	1.18	1.2	CH_3OH/H_2O = 35/65
			13.7	1.13	1.4	CH_3CN/H_2O = 20/80
5	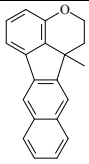	RSP	6.55	1.10	1.3	CH_3OH/H_2O = 50/50
			7.46	1.10	1.5	CH_3CN/H_2O = 25/75
		DM	7.70	1.08	0.5	CH_3OH/H_2O = 35/65
			8.24	1.06	0.8	CH_3CN/H_2O = 25/75
6	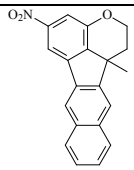	RSP	10.3	1	0	CH_3OH/H_2O = 50/50
			9.34	1	0	CH_3CN/H_2O = 25/75
		DM	7.12	1.32	3.4	CH_3OH/H_2O = 50/50
			11.6	1.37	4.2	CH_3CN/H_2O = 25/75
7	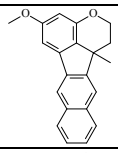	RSP	7.57	1.11	1.3	CH_3OH/H_2O = 50/50
			7.21	1.12	1.5	CH_3CN/H_2O = 25/75
		DM	8.53	1.10	0.6	CH_3OH/H_2O = 35/65
			8.29	1.10	1.3	CH_3CN/H_2O = 25/75
8	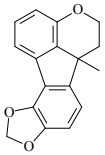	RSP	5.48	1.23	2.5	CH_3OH/H_2O = 40/60
			5.00	1.24	2.6	CH_3CN/H_2O = 20/80
		DM	8.81	1.18	1.8	CH_3OH/H_2O = 35/65
			5.82	1.13	1.5	CH_3CN/H_2O = 20/80
9	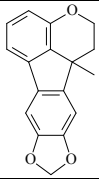	RSP	12.8	1.03	0.3	CH_3OH/H_2O = 40/60
			9.80	1.05	0.6	CH_3CN/H_2O = 20/80
		DM	3.82	1.18	1.9	CH_3OH/H_2O = 50/50
			4.96	1.12	1.5	CH_3CN/H_2O = 25/75

Table 1. (continued)

#	Structure	CSP	k_1	α	R_S	Mobile Phase (v / v)
10	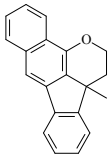	RSP	11.6	1.13	1.5	CH_3OH/H_2O = 50/50
			11.6	1.14	1.8	CH_3CN/H_2O = 25/75
		DM	9.04	1	0	CH_3OH/H_2O = 35/65
			9.52	1.03	0.3	CH_3CN/H_2O = 25/75
11	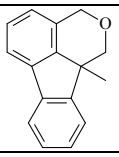	RSP	5.23	1.07	0.8	CH_3OH/H_2O = 35/65
			3.68	1.07	1.0	CH_3CN/H_2O = 20/80
		DM	5.18	1	0	CH_3OH/H_2O = 35/65
			7.34	1	0	CH_3CN/H_2O = 15/85
12	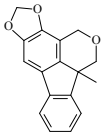	RSP	5.12	1.10	1.3	CH_3OH/H_2O = 40/60
			5.06	1.11	1.5	CH_3CN/H_2O = 20/80
		DM	7.78	1.17	2.0	CH_3OH/H_2O = 35/65
			5.04	1.12	1.6	CH_3CN/H_2O = 20/80
13	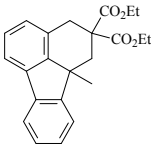	RSP	2.28	1	0	CH_3OH/H_2O = 40/60
			3.17	1	0	CH_3CN/H_2O = 20/80
		DM	5.48	1.46	4.0	CH_3OH/H_2O = 35/65
			6.16	1.26	2.5	CH_3CN/H_2O = 20/80

Table 2. Retention factor of the first peak (k_1), enantioselectivity (α), and enantiomeric resolution (R_S) of chiral polycycles separated on the Cyclobond AC, I, DMP, and II CSPs in the reversed phase mode.

Compound #	CSP	k_1	α	R_S	Mobile Phase (v / v)
2	AC	2.52	1.30	2.0	CH_3OH/H_2O = 40/60
8	AC	5.15	1.07	0.6	CH_3OH/H_2O = 30/70
10	AC	8.27	1.11	1.1	CH_3OH/H_2O = 40/60
2	I	1.95	1.35	1.1	CH_3OH/H_2O = 30/70
4	I	2.10	1.40	0.7	CH_3OH/H_2O = 40/60
1	DMP	3.74	1.04	0.6	CH_3OH/H_2O = 60/40
2	DMP	4.81	1.04	0.4	CH_3OH/H_2O = 60/40
4	DMP	8.66	1.04	0.4	CH_3OH/H_2O = 60/40
5	DMP	11.25	1.02	0.3	CH_3OH/H_2O = 60/40
6	DMP	9.81	1.10	1.5	CH_3OH/H_2O = 70/30
9	DMP	5.89	1.13	1.8	CH_3OH/H_2O = 60/40
3	II	2.16	1.08	0.8	CH_3OH/H_2O = 30/70
13	II	4.35	1.42	2.1	CH_3OH/H_2O = 30/70

Table 3. Retention factor of the first peak (k_1), enantioselectivity (α), and enantioresolution (R_S) of chiral polycycles separated on the Chirobiotic V, R, T, and Tag CSPs in the reversed phase mode.

Compound #	CSP	k_1	α	R_S	Mobile Phase (v / v)
2	V	3.04	1.20	1.7	CH_3OH/H_2O = 30/70
4	V	6.62	1.03	0.3	CH_3OH/H_2O = 30/70
13	V	3.42	1.08	0.5	CH_3OH/H_2O = 30/70
2	R	6.89	1.22	1.3	CH_3OH/H_2O = 20/80
9	R	3.81	1.14	0.9	CH_3OH/H_2O = 30/70
11	R	2.59	1.09	0.4	CH_3OH/H_2O = 30/70
12	R	3.40	1.08	0.5	CH_3OH/H_2O = 30/70
3	T	6.58	1.66	4.9	CH_3OH/H_2O = 40/60
4	T	11.9	1.13	1.4	CH_3OH/H_2O = 40/60
3	Tag	6.39	1.86	3.6	CH_3OH/H_2O = 50/50
4	Tag	3.44	1.87	3.4	CH_3OH/H_2O = 60/40

Table 4. Retention factor of the first peak (k_1), enantioselectivity (α), and enantiomeric resolution (R_S) of chiral polycycles separated on the Chirobiotic V, R, T, and Tag CSPs in the normal phase mode.

Compound #	CSP	k_1	α	R_S	Mobile Phase (v / v)
3	V	8.00	1.04	0.8	HEP/EtOH = 99/1
4	V	8.32	1.06	0.9	HEP/EtOH = 99/1
3	R	7.40	1.04	0.6	HEP/EtOH = 99/1
4	R	7.99	1.04	0.4	HEP/EtOH = 99/1
3	T	4.94	1.44	3.2	HEP/EtOH = 98/2
4	T	5.14	1.30	2.3	HEP/EtOH = 98/2
3	Tag	2.08	3.29	3.1	HEP/EtOH = 80/20
4	Tag	1.61	3.50	2.7	HEP/EtOH = 80/20

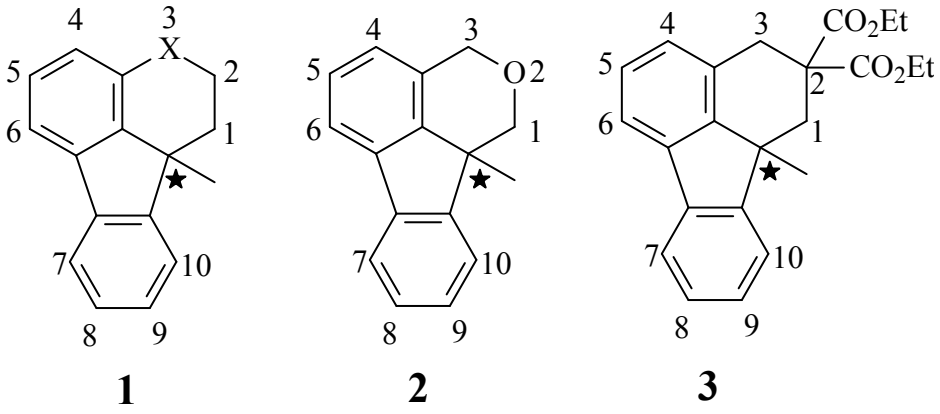

Fig. 1. General structure and ring numbering conventions for the chiral polycycles. Structure **1** is a chromene (X = O) or quinoline (X = NSO_2CF_3) derivative. Structure **2** is an isochromene derivative. Structure **3** is a polycyclic diester. The carbon marked with an asterisk is the stereogenic center.

a)

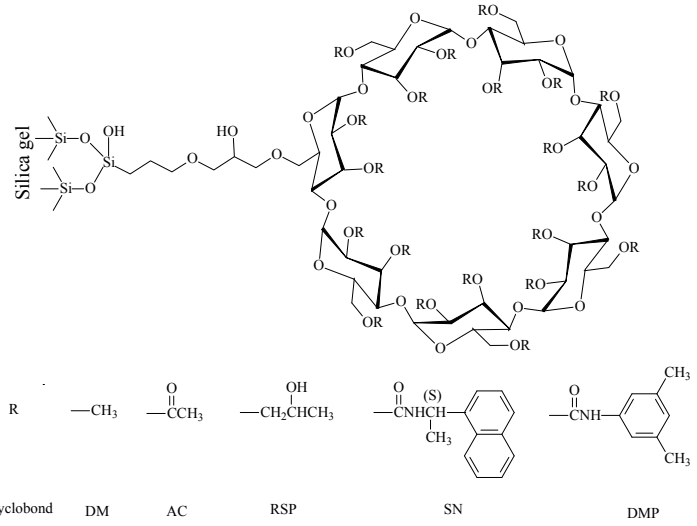

b)

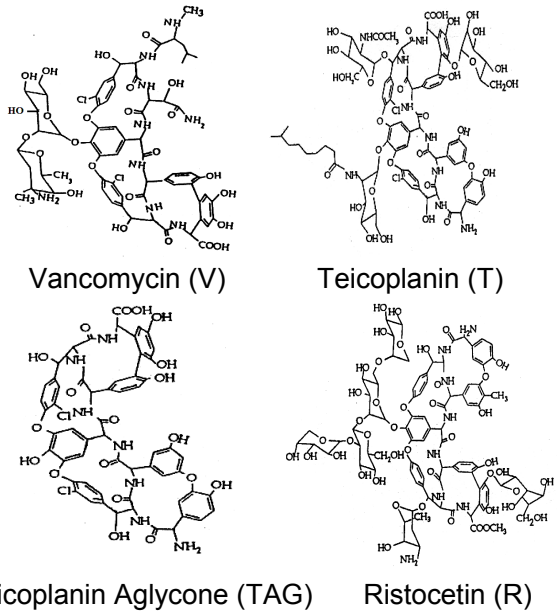

Fig. 2. General structure of the (a) Cyclobond and (b) Chirobiotic CSPs (there can be 1-3 linkages for each cyclodextrin or macrocyclic glycopeptide molecule). R = H for Cyclobond I (β-cyclodextrin), II (γ-cyclodextrin), III (α-cyclodextrin). All derivatized cyclodextrin CSPs are made from β-cyclodextrin.

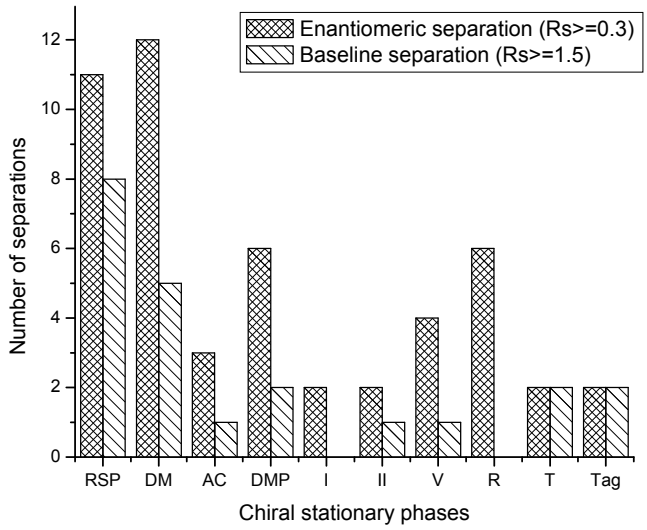

Fig. 3. Summary of the number of baseline and partial separations obtained on different Cyclobond and Chirobiotic CSPs.

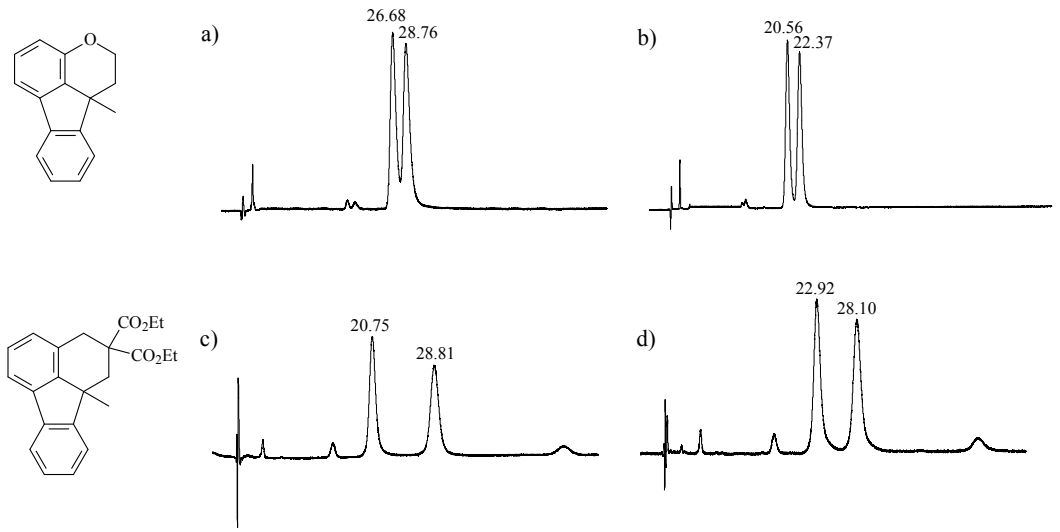

Fig. 4. Chromatograms showing the difference in the separation when using two different organic modifiers in the reversed phase mode. Chromatograms a) and b) were obtained using the Cyclobond I-2000 RSP CSP. Chromatograms c) and d) were obtained using the Cyclobond I-2000 DM CSP. The mobile phase composition (volume ratio) in each case was as follows: a) and c) CH_3OH/H_2O = 35/65, b) and d) CH_3CN/H_2O = 20/80. Enantioselectivity: a) α = 1.09, b) α = 1.10, c) α = 1.46, d) α = 1.26. Number of theoretical plates of the first peak: a) N_1 = 3200, b) N_1 = 4300.

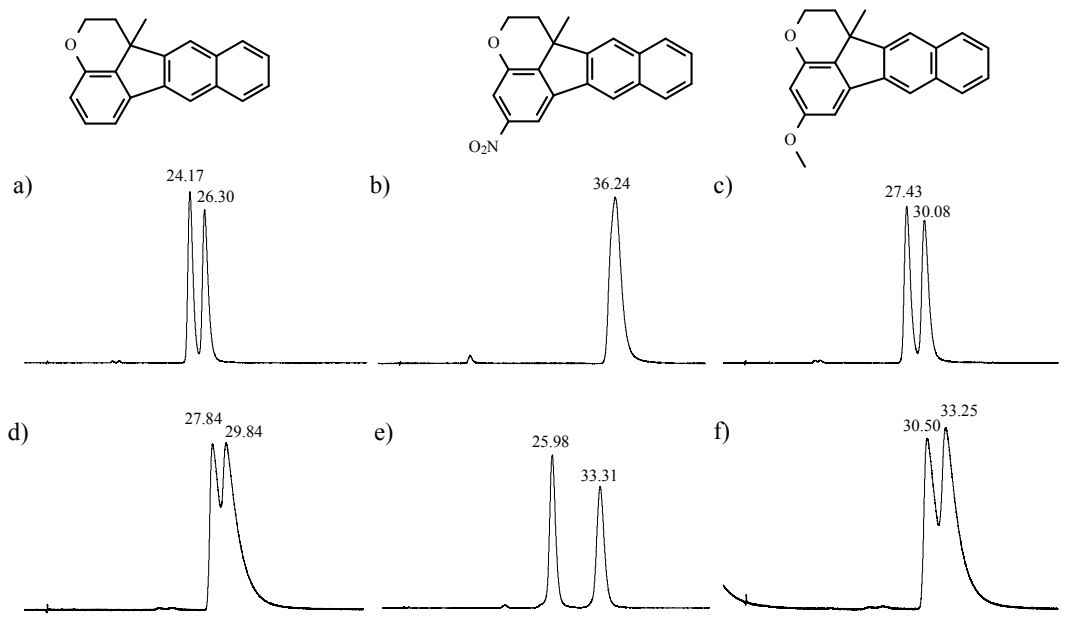

Fig. 5. The effects of different analyte substituents on the enantiomeric separation. Chromatograms a), b), and c) were obtained using the Cyclobond I-2000 RSP CSP. Chromatograms d), e), and f) were obtained using the Cyclobond I-2000 DM CSP. The mobile phase composition (volume ratio) in each case was as follows: a), b), c), and e) CH_3OH/H_2O = 50/50, d), f) CH_3OH/H_2O = 35/65. Enantioselectivity α: a) α = 1.10, c) α = 1.11, d) α = 1.08, e) α = 1.32, f) α = 1.10.

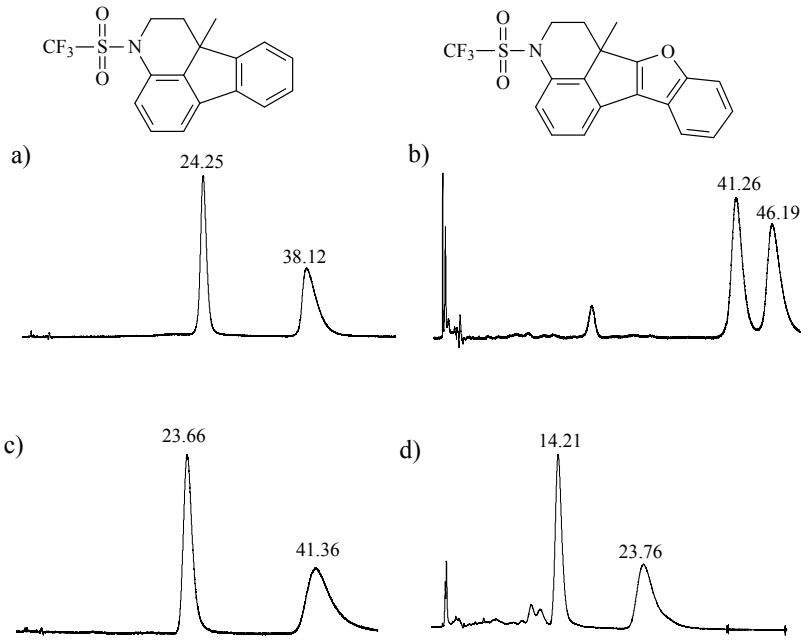

Fig. 6. Comparison of the separations of compounds **3** and **4** on Chirobiotic T and TAG CSPs in reversed phase mode. Chromatograms a) and b) were obtained using the Chirobiotic T CSP. Chromatograms c) and d) were obtained using the Chirobiotic TAG CSP. The mobile phase composition (volume ratio) in each case was as follows: a) and b) CH_3OH/H_2O = 40/60, c) CH_3OH/H_2O = 50/50, d) CH_3OH/H_2O = 60/40. Enantioselectivity α: a) α = 1.66, b) α = 1.13, c) α = 1.86, d) α = 1.87. Number of theoretical plates of the first peak N_1: a) N_1 = 2600, c) N_1 = 1400.

Chapter 5. Chromatographic evaluation of the poly(trans-1,2-cyclohexanediamine acrylamide) as a chiral sationary phase for HPLC

A paper published in *Journal of Chromatography A*[1]

Qiqing Zhong, Xinxin Han, Lingfeng He, Thomas E. Beesley, Walter S. Trahanovsky, and Daniel W. Armstrong

Abstract

Chiral stationary phases (CSPs) based on polymeric (*R*,*R*)- or (*S*,*S*)-1,2-diaminocyclohexane derivatives are synthesized. When bonded to 5-μm porous spherical silica gel, the poly (*trans*-1,2-cyclohexanediamine acrylamide) stationary phases (P-CAP) proved to be effective chiral stationary phases that could be used in the normal phase mode, polar organic mode and with halogenated solvent mobile phases, if desired. Since these are entirely synthetic CSPs, the elution order of all enantiomers can be reversed between the (*R*,*R*)-P-CAP and (*S*,*S*)-P-CAP columns. Because of the high loading of chiral selectors, the columns exhibit very high sample capacities. Thus, P-CAP columns are useful for preparative and semi-preparative enantiomeric separations. The application of these CSPs and optimization of their separations are discussed.

Keywords: P-CAP; Synthetic polymeric chiral stationary phases; Enantiomeric separations; Poly (*trans*-1,2-cyclohexanediyl-bis acrylamide); Preparative enantiomeric separation

5.1. Introduction

Enantiomeric separations were thought to be difficult or impossible prior to the early 1980s with only a few enantiomeric resolutions reported [1-4]. By the late 1990s, advances in the field of analytical chiral separations have made the separation of enantiomers practical and even routine [1,5]. Over 100 chiral stationary phases (CSPs) were commercialized through the 1980s and 1990s [6-8]. Based on their structure, chiral selectors can be classified as macrocyclic, polymeric, π–π association, ligand exchange, miscellaneous and hybrid CSPs [6]. Generally, polymeric CSPs, with the exception of proteins, have a high loading of chiral

selector on the surface of silica gel, thus they have the potential of high sample loading capacity. This feature makes them suitable for preparative purposes

Enantiomeric separations were thought to be difficult or impossible prior to the early 1980s with only a few enantiomeric resolutions reported [1-4]. By the late 1990s, advances in the field of analytical chiral separations have made the separation of enantiomers practical and even routine [1,5]. Over 100 chiral stationary phases (CSPs) were commercialized through the 1980s and 1990s [6-8]. Based on their structure, chiral selectors can be classified as macrocyclic, polymeric, π–π association, ligand exchange, miscellaneous and hybrid CSPs [6]. Generally, polymeric CSPs, with the exception of proteins, have a high loading of chiral selector on the surface of silica gel, thus they have the potential of high sample loading capacity. This feature makes them suitable for preparative purposes

In 1926, Wieland et al. reported the synthesis of *trans*-1,2-diaminocyclohexane (DACH) for the first time [9]. This diamine has C_2 symmetry and its enantiomers can be resolved by recrystallization with *d*- or *l*-tartaric acid to give enantiomerically pure (1*R*,2*R*)- or (1*S*,2*S*)-DACH [10-11]. In industry, *trans*-1,2-diaminocyclohexane can be obtained as a byproduct from purification of 1,6-diaminohexane, which is a starting material for the manufacture of Nylon 66. Thus, enantiomerically pure DACH is commercially available at relatively low prices. Both the pure enantiomers and derivatives of *trans*-DACH can serve as powerful stereogenic ligands in asymmetric synthesis [12-16] or as components of chiral stationary phases in chiral chromatographic separations [17-26].

Polymeric CSPs have been used extensively for enantiomeric HPLC separations. Two types of chiral polymers are used as CSPs. They can be classified by their origin. One group consists of naturally occurring polymers (such as proteins and linear carbohydrates) and their derivatives; the other is composed of purely synthetic polymers [27-29]. Unlike small molecule chiral selectors, which are usually bonded on to the surface of silica gel, chiral polymers can be bonded or coated on the surface of a silica gel support. Moreover, chiral polymers can also be crosslinked as a monolithic gel. The ability of chiral recognition by small molecular CSPs depends mainly on the structure of the small molecules. However, the mechanism of enantiomeric separation by polymeric CSPs is more complicated than that by small molecule CSPs because of the secondary structure of the polymers which may be

critical for chiral recognition [7]. Generally, it is easier to increase the loading of polymeric chiral selectors onto the surface of a silica gel support than it is for small molecule-based covalently bonded CSPs. Therefore, synthetic or semi-synthetic polymeric CSPs may have a greater potential for high sample loading capacity.

The poly (*trans*-1,2-cyclohexanediyl-bis acrylamide) based stationary phases has been commercialized by Advanced Separation Technologies Inc. (Astec, Whippany, NJ) with the commercial name of poly-cyclic amine polymer (P-CAP). P-CAP CSP can be prepared from either (1*R*,2*R*)-DACH or (1*S*,2*S*)-DACH and thus (*R*,*R*)-P-CAP or (*S*,*S*)-P-CAP, respectively. These two chiral selectors are enantiomers. Thus, unlike most naturally occurring polymeric CSPs such as derivatized linear or branched carbohydrates and proteins, it is easy to obtain opposite selectivity CSPs using these synthetic polymeric chiral selectors.

5.2. Experimental

5.2.1. Materials

Porous spherical silica gel (diameter: 5 μm; pore size: 200 Å; pore volume: 0.9 ml/g; specific surface area: 213 m^2/g) was from Akzo Nobel, EKA Chemicals AB, Sweden. Acryloyl chloride and 1-methoxy-2-methyl-1-trimethylsyliloxy-1-propene were from Lancaster Synthesis, Inc, Pelham, NH. 3-Aminopropyltrimehoxysilane was from SILAR Lab, Scotia, NY. Anhydrous toluene, methylene chloride and chloroform were from Sigma-Aldrich. 4,4′-Azo-bis-4-cyanovaleric acid was from Fluka. Phosphorus pentachloride (*R*,*R*)- and (*S*,*S*)-diaminocyclohexane, and diisopropylethylamine were from Alfa Aesar, Ward Hill, MA. Absolute ethanol was obtained from AAPER Alcohol and Chemical Co., Shelbyville, KY, USA. Acetonitrile, 2-propanol, *n*-heptane, and methylene chloride were HPLC grade from Fischer, Fairlawn, NJ. Triethylamine, trifluoroacetic acid and acetic acid were ACS certified grade from Fisher Scientific. Water was deionized and filtered through activated charcoal and a 5 μm filter. Most analytes used in this study were from Sigma-Aldrich.

5.2.2. Synthetic procedure

The (*R*,*R*)-P-CAP and (*S*,*S*)-P-CAP columns were prepared as previously reported [30]. The stationary phases consisted of the chiral selector were covalently bonded to 5 μm porous spherical silica gel. The dimensions of the columns are 250 mm × 4.6 mm. The synthetic procedure is summarized below.

5.2.2.1. Preparation of (1*R*,2*R*)-cyclohexanediyl-bis acrylamide (DACH-ACR)

(1*R*,2*R*)-Diaminocyclohexane (12.1 g, 105.96 mmol) and diisopropylethylamine (36.3 ml, 210.18 mmol) were dissolved in 160 mL mixed anhydrous solvent (chloroform:toluene = 3:1 (v/v)). Acryloyl chloride (17.3 ml, 210.18 mmol) was added dropwise into the solution at 0 °C under nitrogen protection with stirring. The reaction was warmed up to room temperature for 2 h. The product was collected by filtration, washed with toluene and hexane, and dried at reduced pressure (0.1 mbar, 25 °C) over night to obtain 19.08 g white solid (yield: 81.6%).

TLC: Merck Kieselgel 60-F254; Eluent: CH_2Cl_2/MeOH 90/10, $R_f = 0.56$. Elemental analysis found: C 61.78%; H 8.41%; N 12.81%. Calculated for $C_{12}H_{18}N_2O_2$: C 64.83%; H 8.16%; N 12.61%. ^{1}H NMR (400 MHz, methanol-*d*4): δ 8.00 (s, 2H), 6.17–6.15 (m, 4H), 5.60 (dd, J =6.8 Hz, 5.2 Hz, 2H), 3.80–3.70 (m, 2H), 2.00–1.95 (m, 2H), 1.80–1.70 (m, 2H), 1.40–1.30 (m, 4H). ^{13}C NMR (methanol-*d*4): δ 166.7, 130.8, 125.3, 52.8, 31.9, 24.5.

5.2.2.2. Preparation of the dichloride of 4,4'-azo-bis-4-cyanovaleric acid

To a suspension of phosphorous pentachloride (115.1 g, 552.48 mmol) in 576 ml of anhydrous methylene chloride is added a suspension of 4,4′-azo-bis-4-cyanovaleric acid (28.8 g, 138.24 mol) in 900 ml of anhydrous methylene chloride at −5 °C under nitrogen protection with continuous stirring. After 1 h, the reaction mixture was warmed up to room temperature and kept over night, and then filtered. The precipitate was dried under reduced pressure (0.1 mbar, 25 °C) to obtain 24.8 g of the title compound (yield: 73.7%).

5.2.2.3. Preparation of 3-aminopropyl silica gel (3-APSG-200)

To anhydrous slurry of 5 μm silica gel (85.7 g) dispersed in 850 ml of anhydrous toluene is added 3-aminopropyltrimethoxysilane (42 ml, 180.6 mmol) at room temperature. The mixture was heated to reflux for 5 h and filtered afterwards. The silica gel was dried at 105 °C over night to obtain 91.97 g 3-APSG-200 (weight gain: 7.4%). Elemental analysis found: C 3.22%, H 0.88%, N 0.88%.

5.2.2.4. Functionalization of 3-aminopropyl silica gel with the dichloride of 4,4'-azo-bis-cyanovaleric acid

To anhydrous slurry of 3-APSG-200 (88.5 g) dispersed in 742 ml anhydrous toluene is added a solution of 1-methoxy-2-methyl-1-(trimethylsyliloxy)-1-propene (MMTP) (14.8 ml,

72.52 mmol) at −5 °C, followed by adding the solution of dichloride of 4,4′-azo-bis-4-cyanovaleric acid (9.98 g, 36.24 mmol) in 297 ml anhydrous toluene under nitrogen protection with mechanical stirring. The mixture was warmed up to room temperature (25 °C) for 5 h. The modified silica gel was filtered, and dried at reduced pressure (0.1 mbar, 25 °C) to obtain 95.9 g functionalized silica gel (3-APSG-AZO-200). The percentage of weight gain was 8.4%. Elemental analysis found: C 7.00%, H 1.10%, N 2.26%.

5.2.2.4. Preparation of (*R*,*R*)-P-CAP CSP

To a solution of (1*R*,2*R*)-DACH-ACR (14.0 g) in 1380 ml anhydrous, degassed chloroform, is added 3-APSG-AZO-200 (82.4 g) under nitrogen protection. The mixture was heated at 61 °C for 5 h and then heated to reflux for 1 h. After cooling down to room temperature, the reaction mixture was filtered, washed with methanol and acetone, and dried under vacuum (0.1 mbar, 60 °C) for 4 h to obtain 91.5 g (*R*,*R*) P-CAP bonded silica gel (weight gain: 11.1%). Elemental analysis found: C 12.83%, H 1.98%, N 2.69%.

5.2.3 Equipment

Chromatographic separations were carried out using an HP 1050 HPLC system with a UV VWD detector, an auto sampler, and computer-controlled HP ChemStation for LC data processing software. The mobile phases were degassed by purging compressed pure helium gas for 10 min. UV detection was carried out at 210, 254 or 264 nm for most of the probe compounds. All separations were carried out at room temperature (~ 23˚C).

5.2.4. Column Evaluation

The performance of (R,R)-P-CAP and (S,S)-P-CAP CSPs was evaluated in the normal phase mode using n-heptane/ethanol, n-heptane/2-propanol and methylene chloride/methanol mobile phases; in polar organic phase mode using acetonitrile/methanol mobile phase.

5.2.5. Calculations

The chiral separation ability of CSPs can be quantitatively evaluated by retention factors (*k'*), selectivity factor (α), and resolution factor (R_S). Those parameters are defined as follows:

$$k_1^{'} = \frac{(t_1 - t_0)}{t_0} \qquad (1)$$

$$k_2^{'} = \frac{(t_2 - t_0)}{t_0} \quad (2)$$

$$\alpha = \frac{t_2 - t_0}{t_1 - t_0} = \frac{k_2^{'}}{k_1^{'}} \quad (3)$$

$$R_S = \frac{2(t_2 - t_1)}{W_1 + W_2} \quad (4)$$

in which, t_1 and t_2 are the retention times of enantiomers; t_0 is the dead time and was estimated by using the peak resulting from the change in refractive index from the injection solvent on columns; W_1 and W_2 are the peak widths. To evaluate the efficiency of separation, the number of theoretical plates (N) is also used

$$N = 16\left(\frac{t_R}{W}\right)^2 \quad (5)$$

where t_R is the retention time of the peak and W is the peak width.

5.3. Results and discussion

5.3.1 The structure of P-CAP chiral selectors

Gasparrini and co-workers [19-20, 31] used *trans*-1,2-cyclohexanediamine acrylamide as monomer to synthesize poly-DACH-ACR, which forms a crosslinked structure. In synthesizing the related P-CAP chiral stationary phase, the free radical initiator was immobilized on the surface of silica gel before the free radical polymerization process was carried out [30,32]. Therefore, P-CAP is basically a linear brush-type polymer with the DACH-ACR units as the branches. The idealized structure of (*R*,*R*)-P-CAP CSP is shown in Fig. 1. The structure of (*S*,*S*)-P-CAP CSP has the opposite configuration of each stereogenic center of the cyclohexyl units on (*R*,*R*)-P-CAP CSP.

5.3.2. Column performance

A total of 62 chiral compounds were separated on the P-CAP CSPs in the normal-phase mode (including two different solvent systems: traditional normal phase and halogenated solvent mobile phase) and polar organic mode combined. The majority of compounds were separated in the traditional normal-phase mode (heptane/ethanol). Table 1 shows the chromatographic data for 43 racemic compounds separated in the traditional normal-phase

mode. Of these compounds, 23 were not separated in the polar organic mode. Sixteen out of 43 compounds were baseline separated.

Table 2 lists the enantioseparation data obtained for the polar organic mobile phase mode (34 compounds). The polar organic mode is similar to the normal-phase mode. The difference of mobile phase composition is the normal phase contains *n*-heptane while the polar-organic phase does not. Instead, the polar-organic phase has acetonitrile as its main solvent. There are 16 compounds separated in polar organic phase mode only but not in the normal-phase mode. Twelve baseline separations were achieved in polar organic mode.

Table 3 shows the enantioseparation data in the normal phase mode with a halogenated solvent (methylene chloride) and other mobile phases (10 compounds). Methanol was used as a modifier for these separations. For all 10 compounds separated using a methylene chloride based mobile phase can also be separated in either the normal phase mode (8 compounds) or polar organic mode (5 compounds). Three compounds were enantioseparated in all three solvent systems (i.e. the traditional normal-phase mode, polar organic mode, and the normal phase mode with halogenated solvent). One baseline enantiomeric resolution of 1,1'-bi-2-naphthol was achieved using a neat acetone mobile phase.

Because of the covalent linkage between the polymeric chiral selector and their solid support (5 μm porous silica gel), no degradation in column performance was observed even after more than 1000 injections in each mobile phase mode.

5.3.2.1 Retention behavior

Typical normal-phase retention (k') behavior of two analytes, (A) 1,1'-bi-2-naphthol and (B) fipronil is shown in Fig. 2. The diagrams show that the first and second eluting enantiomers of each analyte as plotted as the function of mobile phase composition with different ratio of ethanol and *n*-heptane. In both cases, the retention and selectivity are greatest when using ethanol/heptane 10/90 (v/v) as the mobile phase. No data were available at 100% n-heptane because the elution times are extremely long. As can be seen, retention decreases with increasing the concentration of ethanol. Retention of all analytes tends to be minimal at ethanol concentration of ≥ 50% (by volume). However, it is interesting that even at 100% ethanol, the P-CAP column still gives an enantioselectivity (α) of 1.23 and resolution (*Rs*) of 1.15 for 1,1'-bi-2-naphthol.

Figure 3 contains plot for the retention factor k_1' of the first eluted enantiomer, selectivity factor α, and resolution *Rs* of 1,1'-bi-2-naphthol as a function of polar organic mode mobile phase composition. The resolution (*Rs*) curve has a minimum at a mobile phase composition of acetonitrile/methanol 30/70 (v/v). The maximum of retention factor k_1' of the first eluted enantiomer, selectivity factor α, and resolution *Rs* are all at 100% acetonitrile.

5.3.2.2. Effects of mobile phase additives

Additives to the mobile phase can usually improve chromatographic efficiency. Trifluoroacetic acid (TFA) is the most effective additive for both normal-phase mode and polar organic mode. Ammonium acetate sometimes can also be used in the polar organic mode as an additive. These additives usually shorten the retention time, decrease tailing and sharpen the peaks. Figure 4 shows the enantiomeric separation of (*R*,*R*)- and (*S*,*S*)-hydrobenzoin on the (*R*,*R*)-P-CAP column with different composition of normal-phase solvents. The best separation (Chromatogram A) was achieved when heptane/2-propanol/TFA 80/20/0.1 was used as the mobile phase. Without the TFA additive (Chromatogram B), only a partial separation can be achieved and the peaks become broader.

Three probe molecules, including chlorthalidone, sulindac, and (±)-2,3-dibenzoyl-*dl*-tartaric acid, were chosen to investigate the influence of acid additives in polar organic mode. The results are summarized in Table 4. Chlorthalidone ($pK_a = 9.4$) is a weak base. The acid additives, acetic acid and TFA, have almost no influence on separation factor α, and a minor influence on the resolution (R_s). Under the same solvent system with the same volume ratio of acid additives, TFA increases the R_s more than acetic acid does. Sulindac ($pK_a = 4.7$) has one carboxylic acid group. It could not be eluted with a mobile phase of $CH_3CN/CH_3OH = 95/5$, without acid additives. The compound (±)-2,3-dibenzoyl-*dl*-tartaric acid has two carboxylic acid groups. It is the strongest acid among three analytes. With the mobile phase of $CH_3CN/CH_3OH = 95/5$, it can only be eluted with the addition of 0.1% trifluoroacetic acid. The acid additives protonate acidic analytes as well as any residual amine groups on the stationary phase (e.g. from the 3-aminopropylsilanized silica gel). This minimizes a source of strong non-enantioselective association between acidic analytes and the CSP. The additives therefore improve the mass transfer and thus improve the efficiency.

Compared to acetic acid, TFA is a stronger acid and produces better separations.

5.3.2.3. Normal phase modifier

The choice of organic modifier in the normal phase mode (i.e. ethanol, 2-propanol, etc. in *n*-heptane) affects the efficiency, retention, and the resolution of enantiomers. In Fig. 4, 2-propanol is used as normal-phase modifier for Chromatogram A. While for Chromatogram C, ethanol is used instead of 2-propanol. A baseline separation was achieved within 15 minutes with the mobile phase of heptane/2-propanol/TFA 80/20/0.1. But for ethanol, with the same mobile phase ratio (heptane/ethanol/TFA 80/20/0.1), only a partial separation (R_s = 0.8) was achieved. When decreasing the ratio of ethanol to 10% (Chromatogram D in Fig. 4. Mobile phase: Heptane/ethanol/TFA 90/10/0.1), the retention time is comparable to that of Chromatogram A, but the separation still wasn't baseline even with a longer retention time. In both cases, a TFA additive was used. Separations of some other compounds in the normal-phase mode, such as fipronil, produced the same general trend. For these chiral stationary phases, 2-propanol was a better normal mobile phase modifier than ethanol.

5.3.2.4 Effect of mobile phase flow rate

The effect of mobile phase flow rate on enantiomeric selectivity and resolution in the normal-phase mode also was evaluated. Table 4 shows the chromatographic data of the normal-phase enantiomeric separations of fipronil on the (*R*,*R*)-P-CAP column at flow rates of 0.5 ml/min, 1.0 ml/min, 1.5 ml/min and 2.0 ml/min. As can be seen, flow rate has little or no effect on enantioselectivity, while resolution is affected. The resolution is improved from 1.40 to 1.71 if the flow rate is dropped from 2.0 to 0.5ml/min. This is because of the mass transfer in the stationary phase affects efficiency at higher flow rates [33]. This is a common phenomenon for other CSPs. For high throughput screening, one can use higher flow rates, like 2.0 ml/min, and still gets reasonable resolution.

5.3.2.5 Column efficiency in different mobile phase modes

The normal-phase mode with two different solvent systems (heptane/IPA and methylene chloride/methanol) and the polar organic mode can be used on P-CAP columns. Table 5 shows the chromatographic data for the enantiomeric separation of 1,1'-bi-2-naphthol in different mobile phases. As can be seen in Table 5, the halogenated mobile phase gives the highest efficiency (greatest *N*). The polar organic mode produces intermediate efficiency and

the traditional normal-phase separations are the least efficient among three mobile phase systems.

5.3.2.6 Sample loading capacity

P-CAP columns are polymeric CSPs. The high loading of the chiral selector on the silica gel provides the potential of having a high sample loading capacity. Figure 5 shows the chromatogram of the separation of 1,1'-bi-2-naphthol when 1μg and 1000μg racemic sample was injected sequentially. As can be seen, the resolution is still nearly 1.5 even given the heavy sample load on an analytical column. Clearly, the P-CAP CSPs are suitable for large-scale enantiomeric separations.

5.3.3. Reversal of elution order

The totally synthetic chiral selectors of the (*R*,*R*)-P-CAP column and the (*S*,*S*)-P-CAP column have the opposite absolute configuration. Therefore, the elution order of all separable enantiomers will be inverted on these two columns. Figure 6 shows the inversion of elution order on (*R*,*R*)-P-CAP column and the (*S*,*S*)-P-CAP column under normal phase conditions. The (*R*,*R*)- and (*S*,*S*)-hydrobenzoin were chosen as example probe molecules. In order to identify the enantiomeric peaks of the probe molecules easily, the analyte sample containing (*R*,*R*)- and (*S*,*S*)-hydrobenzoin was prepared in the mole ratio of 2 to 1 respectively. Figure 6 also shows that (*R*,*R*)-P-CAP CSP retains (*R*,*R*)-hydrobenzoin longer than its (*S*,*S*)-enantiomer, and of course, the (*S*,*S*)-P-CAP CSP retains (*S*,*S*)-hydrobenzoin to a greater extent.

Interestingly, the (*R*,*R*)- and (*S*,*S*)-P-CAP columns can also separate the racemic monomers DACH-ACR very well. Figure 7 shows the chromatographic separation of DACH-ACR on both (*R*,*R*)- and (*S*,*S*)-P-CAP column. As can be seen from Figure 8, the (*R*,*R*)-P-CAP column retains (*S*,*S*)-DACH-ACR more and the (*S*,*S*)-P-CAP column favors (*R*,*R*)-DACH-ACR.

5.3.4. Interactions for chiral recognition

The P-CAP columns do not contain any aromatic moieties. Therefore, π-π interactions are not expected. Instead, the P-CAP CSPs have large numbers of amide linkages, which provide hydrogen bonding and dipolar interactions between these CSPs and chiral analytes. An examination of the compounds listed in Table 1, 2 and 3 reveals a common characteristic

for these compounds. Most of them contain a hydroxyl group, carboxylic group, carbonyl, amine, amide, urea, or fluorine group, which are capable of forming strong hydrogen bond. Thus, hydrogen bond interactions are believed to be the dominant associative interactions for chiral recognition by P-CAP CSPs [19].

Some chiral sulfoxides also were resolved on P-CAP columns. These sulfoxides include 4-chlorophenyl methyl sulfoxide and 4-bromophenhyl methyl sulfoxide, etc. These chiral sulfoxides are known to possess a strong dipole element and the amide linkage in the P-CAP CSPs also is strongly dipolar. Therefore, dipole-dipole interactions also may be important for chiral discrimination on these CSPs.

The cyclohexyl moiety (Fig. 1) is a restricted configurational nonpolar unit of the P-CAP stationary phase. It may provide solvophobic-driven attraction or steric repulsive effects. These are possible interactions for enantiomeric selectivity by these CSPs.

5.4. Conclusions

The polymeric (*R*,*R*) and (*S*,*S*) poly (*trans*-1,2-cyclohexanediyl-bis acrylamide) (known as (*R*,*R*)-P-CAP and (*S*,*S*)-P-CAP) have been used as liquid chromatographic chiral stationary phases. The branched polymer was bonded covalently to a 5 μm silica gel support and evaluated for enantiomeric separations. P-CAP CSPs can be used in the normal phase mode or the polar organic mode to produce enantiomeric separations of a variety of chiral compounds. The retention behavior, selectivity, and resolution were examined for selected compounds in each mobile phase mode. A total of 62 chiral compounds were enantioresolved on these two columns. The traditonal normal phase separation mode was the most broadly selective, but has the lowest efficiency. Halogenated mobile phases produced the highest efficiencies but separate the fewest compounds. The polar organic mode was intermediate in terms of both selectivity and efficiency to the two normal phase approaches. The elution order of enantiomers can be reversed between (*R*,*R*)- and (*S*,*S*)-P-CAP CSPs. P-CAP columns have great sample loading capacity and are therefore able to do large-scale separations. The P-CAP CSPs were chemically stable under usual separation conditions and not irreversibly damaged or modified when changing the mobile phase modes.

Acknowledgements

Support of this work by the National Institutes of Health, NIH RO1 GM53825-08, and

the Iowa Energy Center is gratefully acknowledged.

Reference

[1] D.W. Armstrong, Anal. Chem. 59 (1987) A84, A90.

[2] D.W. Armstrong, J. Liq. Chromatogr. 7 (1984) 353.

[3] E. Gil-Av, J. Mol. Evol. 6 (1975) 131.

[4] S.V. Rogozhin, V.A. Davankov, J. Chem. Soc. D-Chem. Commun. (1971) 490.

[5] D.W. Armstrong, LC–GC Curr. Issues HPLC Technol. (1997) S20.

[6] D.W. Armstrong, B. Zhang, Anal. Chem. 73 (2001) 557A.

[7] C. Yamamoto, Y. Okamoto, Bull. Chem. Soc. Jpn. 77 (2004), 227.

[8] C.A. White, G. Subramanian, in: G. Subramanian (Ed.), A Practical Approach to Chiral Separations by Liquid Chromatography, VCH, Weinheim, Germany, 1994 (Chapter 1).

[9] Y.L. Bennani, S. Hanessian, Chem. Rev. 97 (1997) 3161.

[10] J.F. Larrow, E.N. Jacobsen, Y. Gao, Y.P. Hong, X.Y. Me, C.M. Zepp, J. Organ. Chem. 59 (1994) 1939.

[11] T.A. Whitney, J. Organ. Chem. 45 (1980) 4214.

[12] R.I. Kureshy, N.H. Khan, S.H.R. Abdi, S.T. Patel, R.V. Jasra, Tetrahedron: Asymmetry 12 (2001) 433.

[13] A.M. Daly, C.T. Dalton, M.F. Renehan, D.G. Gilheany, Tetrahedron Lett. 40 (1999) 3617.

[14] C. Bied, J.J.E. Moreau, M.W.C. Man, Tetrahedron: Asymmetry 12 (2001) 329.

[15] R.I. Kureshy, N.U.H. Khan, S.H.R. Abdi, S.T. Patel, R.V. Jasra, Tetrahedron Lett. 42 (2001) 2915.

[16] Y.K. Kim, S.J. Lee, K.H. Ahn, J. Organ. Chem. 65 (2000) 7807.

[17] C. Altomare, S. Cellamare, A. Carotti, M.L. Barreca, A. Chimirri,
A.M. Monforte, F. Gasparrini, C. Villani, M. Cirilli, F. Mazza, Chirality 8 (1996) 556.

[18] A. Brandi, S. Cicchi, F. Gasparrini, F. Maggio, C. Villani, M. Koprowski, K.M. Pietrusiewicz, Tetrahedron: Asymmetry 6 (1995) 2017.

[19] B. Galli, F. Gasparrini, D. Misiti, M. Pierini, C. Villani, M. Bronzetti, Chirality 4 (1992) 384.

[20] F. Gasparrini, D. Misiti, C. Villani, Chirality 4 (1992) 447.

[21] D. Kontrec, V. Vinkovic, A. Lesac, V. Sunjia, A. Aced, Enantiomer 5 (2000) 333.

[22] B. Gallinella, F. Latorre, R. Cirilli, C. Villani, J. Chromatogr. 639 (1993) 193.

[23] D.F. Johnson, J.S. Bradshaw, M. Eguchi, B.E. Rossiter, M.L. Lee, P. Petersson, K.E. Markides, J. Chromatogr. 594 (1992) 283.

[24] Y. Okamoto, Y. Nagamura, T. Fukumoto, K. Hatada, Polym. J. 23 (1991) 1197.

[25] Z. Juvancz, K.E. Markides, P. Petersson, D.F. Johnson, J.S. Bradshaw, M.L. Lee, J. Chromatogr. A 982 (2002) 119.

[26] K. Hu, J.S. Bradshaw, N.K. Dally, K.E. Krakowiak, N. Wu, M.L. Lee, J. Heterocyclic Chem. 36 (1999) 381.

[27] T. Nakano, J. Chromatogr. A 906 (2001) 205.

[28] Y. Okamoto, E. Yashima, M. Ishikura, K. Hatada, Bull. Chem. Soc. Jpn. 61 (1988) 255.

[29] Y. Okamoto, H. Mohri, M. Ishikura, K. Hatada, H. Yuki, J. Polym. Sci. Polym. Symp. (1986) 125.

[30] F. Gasparri, D. Misiti, C. Villani, WO 2003079002, 2003.

[31] F. Gasparrini, D. Misiti, C. Villani, Trac-Trends Anal. Chem. 12 (1993) 137.

[32] F. Gasparri, D. Misiti, C. Villani, R. Rompietti, Abstracts of the 15th International Symposium on Chirality (ISCD-15), Shizuoka, Japan, 2003, 132.

[33] D.W. Armstrong, Y.B. Liu, K.H. EkborgOtt, Chirality 7 (1995) 474.

Table 1. Chromatographic data for the traditional normal-phase resolution of racemic compounds on (*R*,*R*)-P-CAP column[1]

#	Compounds	Structure	$k_1^{'}$	$k_2^{'}$	α	R_s	Mobile Phase[2]
1	Hydrobenzoin	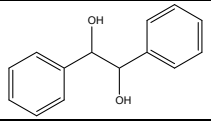	3.43	3.97	1.16	1.91	Heptane/IPA/TFA 80/20/0.1
2	Warfarin	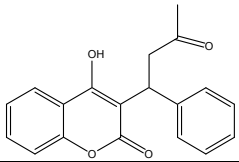	11.21	12.65	1.13	1.58	Heptane/IPA/TFA 90/10/0.1
3	1,1'-Bi-2-Naphthol	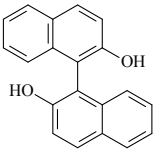	2.49	3.36	1.35	2.84	Heptane/EtOH/TFA 50/50/0.1
4	Di-6,6'-methoxy-bi-2-naphthol	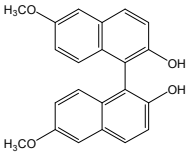	2.69	3.41	1.27	2.7	EtOH/Heptane 50/50
5	Dioxibrassinin	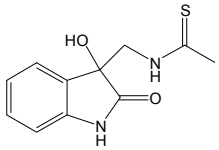	7.67	8.81	1.15	1.4	EtOH/Heptane 30/70 (v/v)
6	Indapamide	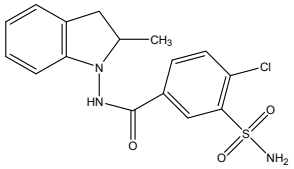	7.32	7.74	1.06	0.60	Heptane/EtOH/TFA 60/40/0.1
7	3-(α-acetonyl-4-chlorobenzyl)-4-hydroxy coumarin	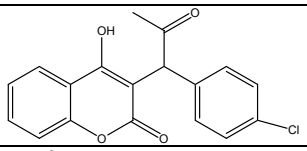	4.06	4.76	1.17	1.63	Heptane/IPA 80/20
8	Bendroflumethia-zide	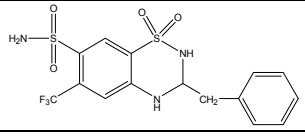	14.5	16.34	1.12	0.80	Heptane/IPA/TFA 50/50/0.1

[1] (*R*,*R*)-P-CAP was bonded to 5μm silica gel and the stationary phase was packed in a 250×4.6 mm (i.d.) stainless steel column.

[2] All samples were analyzed under the chromatographic condition: a UV detector at 254 nm, flow rate 1 ml/min, unless otherwise noted. All mobile phase ratios were volume to volume. IPA: 2-propanol. TFA: trifluoroacetic acid.

Table 1. (continued)

#	Compounds	Structure	$k_1^{'}$	$k_2^{'}$	α	R_s	Mobile Phase
10	N,N'-Bis(α-methyl benzyl)sulfamide	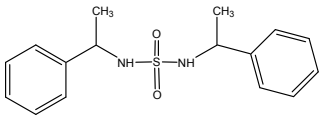	12.3	13.50	1.10	0.90	Heptane/IPA/TFA 80/20/0.1
11	2,3-O-Benzylidene-D-threitol	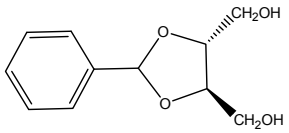	5.49	6.13	1.12	1.21	Heptane/IPA 80/20
12	α-carbethoxy- γ-phenyl-γ-butyrolactone	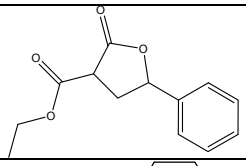	2.73	3.06	1.12	1.0	Heptane/IPA 80/20
13	Chlorthalidone	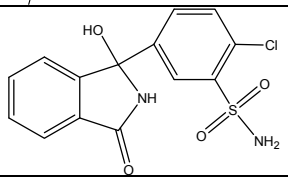	10.21	12.57	1.23	1.61	Heptane/EtOH/TFA 80/20/0.1
14	1,5-Dihydroxy-1,2,3,4-tetrahydro naphthalene	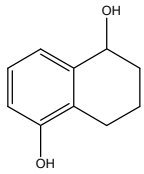	6.78	7.22	1.06	0.81	Heptane/IPA 80/20
15	DL-3,4-Dihydroxyphenyl-α-propylacetamide	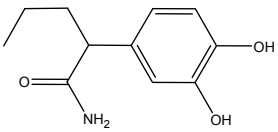	3.84	4.59	1.20	1.64	Heptane/EtOH/TFA 50/50
16	4-(Diphenylmethyl)-2-oxazolidinone	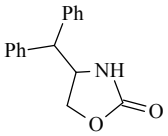	8.57	9.31	1.09	0.82	Heptane/IPA 80/20
17	1,1'-Bi- (2-naphthylamine)	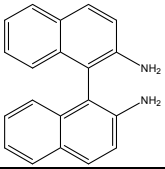	5.80	5.95	1.03	0.7	Heptane/IPA 80/20
18	cis-4,5-Diphenyl-2-oxazolidinone	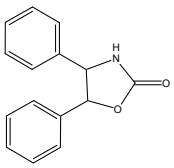	12.64	13.72	1.09	1.22	Heptane/IPA/TFA 90/10/0.1

Table 1. (continued)

#	Compounds	Structure	k_1'	k_2'	α	R_s	Mobile Phase
19	5-Ethyl-5,6-dihydro-3,8-dinitro-6-phenyl-6-phenanthridinol	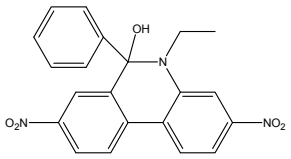	5.43	5.75	1.06	1.05	Heptane/EtOH/TFA 80/20/0.1
20	5-Fluoro-1-(tetrahydro-2-furfuryl)uracil	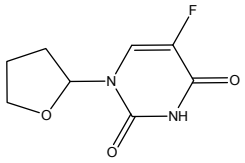	5.04	5.39	1.07	0.65	Heptane/EtOH/TFA 90/10/0.1 2ml/min
21	DL-3-(4-Hydroxyphenyl)lactic acid	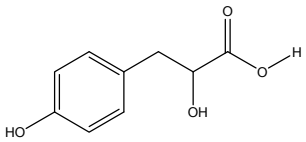	4.57	5.76	1.26	1.54	Heptane/IPA/TFA 60/40/0.1
22	Mandelamide	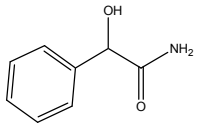	9.62	11.53	1.20	1.50	Heptane/IPA/TFA 80/20/0.1
23	5-Methyl-5-phenyl hydantoin	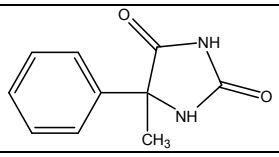	8.33	9.06	1.09	0.9	Heptane/IPA 80/20
24	cis-4-Methyl-5-phenyl-2-oxazolidinone	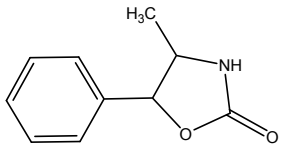	10.32	11.37	1.10	1.52	Heptane/IPA/TFA 80/20/0.1
25	N-(α-Methylbenzyl)-phthalamic acid	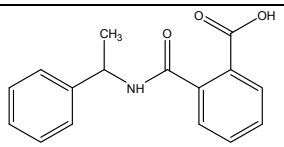	3.98	4.19	1.05	0.72	Heptane/EtOH/TFA 80/20/0.1
26	Methyl mandelate	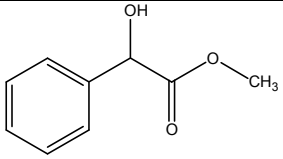	1.93	2.47	1.13	1.2	Heptane/IPA 80/20
27	Benzyl mandelate	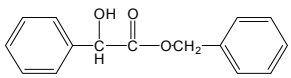	2.07	2.21	1.07	1.0	EtOH/Heptane 10/90
28	Mandelic acid	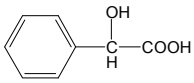	2.04	2.19	1.07	1.0	EtOH/Heptane 10/90

Table 1. (continued)

#	Compounds	Structure	k_1'	k_2'	α	R_s	Mobile Phase
29	DL-3-Phenyllactic acid	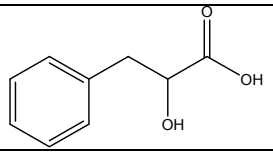	1.64	2.01	1.23	1.28	Heptane/EtOH/TFA 60/40/0.1
30	1-Phenyl-1,2-ethane diol	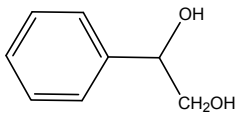	4.68	5.25	1.12	1.60	Heptane/IPA 80/20
31	γ-Phenyl-γ - butyrolactone	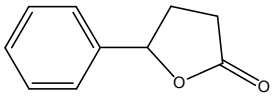	2.82	3.00	1.06	0.92	Heptane/IPA 80/20
32	Phenylsuccinic anhydride	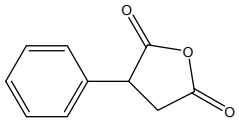	2.68	3.05	1.14	1.45	Heptane/EtOH/TFA 70/30/0.1
33	(3a(R,S)-cis)-3,3a,8,8a-Tetrahydro-2H-indeno[1,2-d]oxazol- 2-one	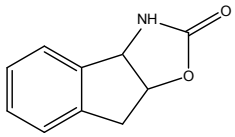	7.77	9.36	1.20	1.66	Heptane/IPA/TFA 80/20/0.1
34	Fipronil	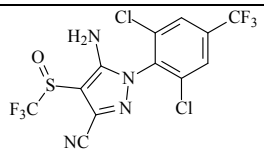	4.11	6.13	1.49	3.73	Heptane/IPA/TFA 20/80/0.1
35	*trans*-1,2-Cyclohexanediyl-bis acrylamide	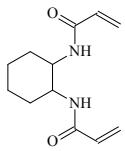	0.78	1.02	1.31	2.7	EtOH/Heptane 10/90
36	*trans*-1-(2-Amino-cyclohexyl)-3-(3,5-bis-trifluoromethyl-phenyl)-urea	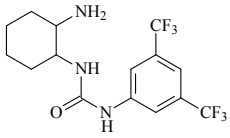	1.97	2.11	1.07	0.65	EtOH/Heptane/TFA 10/90/0.1
37	*trans*-(1,2)-Diaminocyclohexyl di(4-vinyl) benzoylamide	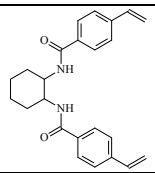	0.30	0.50	1.68	1.25	EtOH/Heptane 50/50
38	Lorazepam	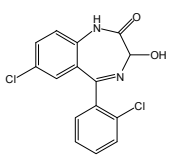	3.48	5.26	1.51	4.2	EtOH/Heptane 50/50 (v/v)

Table 1. (continued)

#	Compounds	Structure	$k_1^{'}$	$k_2^{'}$	α	R_s	Mobile Phase
39	Oxazepam	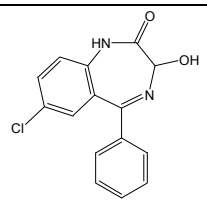	3.31	5.03	1.52	4.3	EtOH/Heptane 50/50
40	4-chlorophenyl methyl sulfoxide	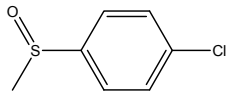	3.81	4.09	1.07	0.78	Heptane/IPA/TFA 90/10/0.1
41	Methyl 4-trifluoromethylphenyl sulfoxide	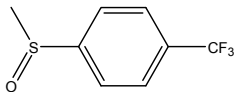	3.30	3.58	1.08	0.92	Heptane/IPA/TFA 90/10/0.1
42	4-fluorophenyl methyl sulfoxide	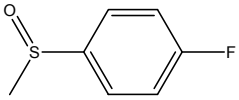	4.31	4.54	1.05	0.65	Heptane/IPA/TFA 90/10/0.1
43	4-bromophenyl methyl sulfoxide	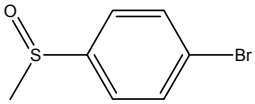	3.83	4.13	1.08	0.88	Heptane/IPA/TFA 90/10/0.1

Table 2. Chromatographic data for the polar organic mode resolution of racemic compounds on (*S*,*S*)-P-CAP column or (R,R)-P-CAP column[1]

#	Compounds	Structure	k_1'	k_2'	α	R_s	Mobile Phase[2]
1	4-Methoxy-2-phenyl-4,5,6,7-tetrahydro-benzofuran-3-carboxylic acid	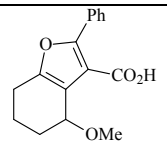	1.0	1.17	1.17	1.22	$CH_3CN/CH_3OH/TFA$ =99/1/0.1
2	Sulindac	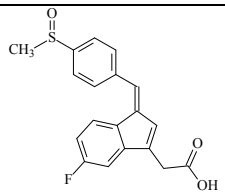	4.03	4.62	1.15	1.85	$CH_3CN/CH_3OH/TFA$ =99/1/0.1
3	Benzoin	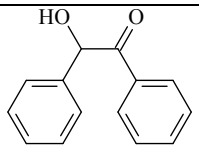	0.43	0.56	1.30	1.18	$CH_3CN/CH_3OH/$ NH_4OAc (10mM) =99/1
4	DL-β-Phenyllactic acid	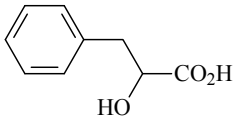	3.99	4.34	1.09	0.93	$CH_3CN/CH_3OH/TFA$ =95/5/0.1
5	(±)-1,1'-Bi-2-naphthol	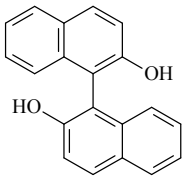	1.47	1.97	1.34	3.80	$CH_3CN/CH_3OH/$ NH_4OAc (10mM) =95/5
			1.86	2.54	1.36	3.43	$CH_3CN/CH_3OH/TFA$ =95/5/0.1
6	Althiazide	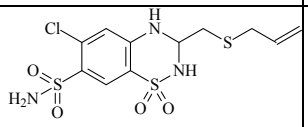	4.79	5.28	1.10	0.50	$CH_3CN/CH_3OH/$ NH_4OAc /(10mM) = 95/5
7	Benzoin methyl ether	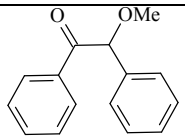	0.43	0.61	1.42	1.03	CH_3CN

[1] (*S*,*S*)-P-CAP and (*R*,*R*)-P-CAP were bonded to 5μm silica gel and the stationary phase was packed in a 250×4.6 mm (i.d.) stainless steel column. All data shown were run on SS-P-CAP column unless otherwise noted.

[2] All samples were analyzed under the chromatographic condition: a UV detector at 254nm, flow rate 1ml/min, unless otherwise noted. All mobile phase ratios were volume to volume. TEAA: triethylamino acetate. TFA: trifluoroacetic acid. ACN: acetonitrile.

Table 2. (continued)

#	Compounds	Structure	k_1'	k_2'	α	R_s	Mobile Phase
8	(±)N,N-Bis-(α-methylbenzyl) sulfamide	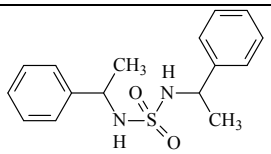	0.70	0.93	1.33	1.02	CH_3CN
9	Bendroflumethiazide	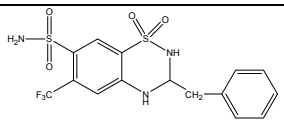	4.39	4.86	1.11	0.51	CH_3CN/CH_3OH (10mM NH_4OAc) =95/5
10	3-(4-chlorophenyl)-2-ethyl-2,3,5,6-tetrahydroimidazol [2,1-b]-thiazol-3-ol	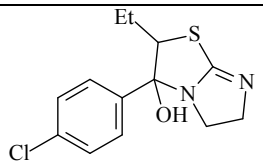	2.34	2.59	1.11	0.94	CH_3CN/HOAc/TEA =100/0.25/0.05
11	Chlothalidone	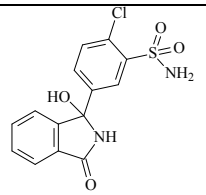	5.02	6.92	1.38	2.5	CH_3CN/CH_3OH/TFA =90/10/0.1
12	p-Chloromandelic acid	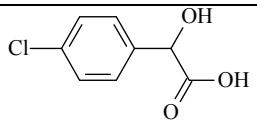	7.06	8.08	1.14	1.65	CH_3CN/CH_3OH/TFA =99/1/0.1
13	7-(2,3-Dihydroxypropyl)theophylline	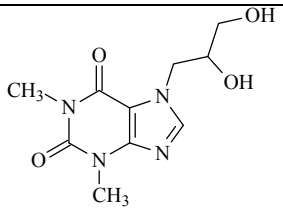	2.23	2.44	1.09	0.72	CH_3CN/HOAc/TEA =100/0.25/0.05
14	(±)-4-(Diphenylmethyl)-2-oxazolidinone	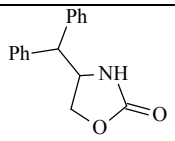	0.61	0.74	1.21	1.06	CH_3CN/CH_3OH/ (10mM NH_4OAc) = 99/1
15	(±)-2,3-Dibenzoyl-DL-tartaric acid	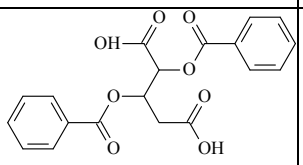	9.26	10.15	1.10	0.94	CH_3CN/CH_3OH/TFA =95/5/0.1
16	DL-p-Hydroxymandelic acid	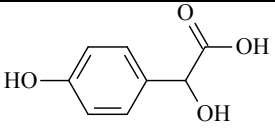	9.40	10.43	1.11	0.95	CH_3CN/CH_3OH/TFA =95/5/0.1

Table 2. (continued)

#	Compounds	Structure	k_1'	k_2'	α	R_s	Mobile Phase
17	DL-3-(4-hydroxyphenyl)lactic acid hydrate	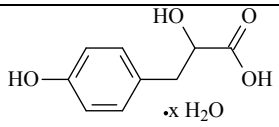	3.24	3.56	1.10	1.05	$CH_3CN/CH_3OH/TFA$ =90/10/0.1
18	3-[2-Methylphenoxy]-1,2-propanediol	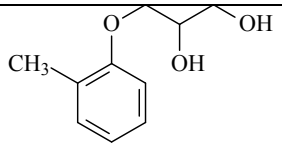	1.48	1.56	1.05	0.50	$CH_3CN/HOAc/TEAA$ =100/0.25/0.05
19	DL-Mandelic acid	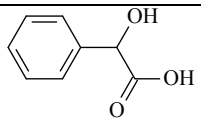	5.30	5.90	1.11	1.29	$CH_3CN/CH_3OH/TFA$ =99/1/0.1
20	DL-Mandelamide	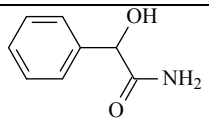	1.96	2.24	1.14	1.00	$CH_3CN/CH_3OH/TFA$ =99/1/0.1
21	(±)-N-(α-Methylbenzyl)phthalic acid monoamide	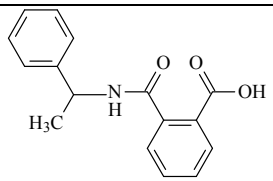	2.80	3.22	1.15	0.88	$CH_3CN/CH_3OH/TFA$ =99/1/0.1
22	(±)-Phenylsuccinic anhydride	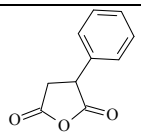	2.42	2.90	1.20	2.62	$CH_3CN/CH_3OH/TFA$ =90/10/0.1
23	3a,4,5,6-Tetrahydro-succinimido[3,4-b]acenaphthen-10-one	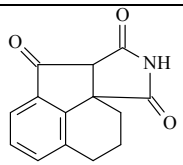	1.28	1.47	1.15	0.37	$CH_3CN/HOAc/TEA$ =100/0.25/0.05
24	DL-Tropic acid	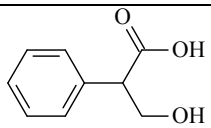	4.87	5.71	1.17	1.90	$CH_3CN/CH_3OH/TFA$ =99/1/0.1
25	(3aR,S-cis)- (±)-3,3a,8,8a-Tetrahydro-2H-indeno[1,2-d]-oxazol-2-one	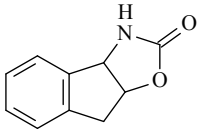	0.64	0.79	1.22	1.03	$CH_3CN/HOAc/TEA$ =100/0.25/0.05
26	(±)-1-Phenyl-1,2-ethanediol	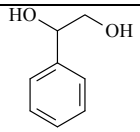	1.35	1.45	1.07	0.56	$CH_3CN/HOAc/TEA$ =100/0.25/0.05

Table 2. (continued)

#	Compounds	Structure	k_1'	k_2'	α	R_s	Mobile Phase
27	(±)-2,2,2-Trifluoro-1-(9-anthryl)ethanol	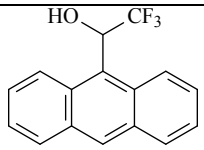	0.58	0.62	1.07	0.35	CH_3CN/HOAc/TEA= 100/0.25/0.05
28	1,1'-Binaphthyl-2,2'-diyl-H phosphate	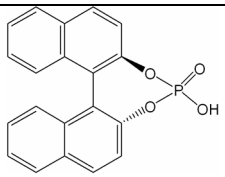	*2.00*	*2.35*	*1.17*	*1.4*	CH_3CN/CH_3OH/ (20mM NH_4OAc) = 70/30
29	Diacetyl cysteine	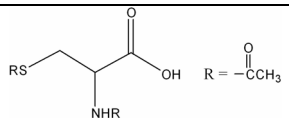	2.61	3.39	1.30	1.5	ACN/MeOH/ NH_4OAc =80/20/0.1 (v/v/w)
30	FMOC-phenylalanine	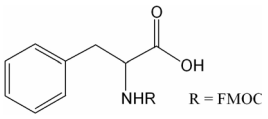	1.85	2.54	1.37	3.5	ACN/MeOH/TFA =95/5/0.1
			1.17	1.43	1.22	2.1	CH_3CN/CH_3OH/ (10mM NH_4OAc) = 70/30
31	2-Hydroxy-3-(Boc-amino)-3-phenylpropionic acid	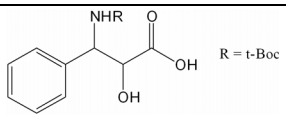	2.52	3.63	1.44	2.4	ACN/MeOH/TFA =95/5/0.1
32	Lorazepam	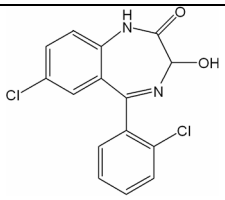	0.86	1.53	1.80	5.8	CH_3CN/CH_3OH/ (20mM NH_4OAc) = 70/30
33	Oxazepam	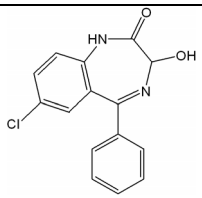	0.85	1.42	1.66	5.4	CH_3CN/CH_3OH/ (20mM NH_4OAc) = 70/30
34	*trans*-1,2-Cyclohexanediyl-bis acrylamide	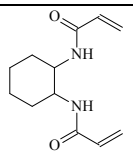	0.30	0.70	2.34	4.0	ACN/MeOH 70/30

Table 3. Chromatographic data for the normal-phase mode with halogenated solvent and other mobile phases resolution of racemic compounds on (*R*,*R*)-P-CAP column[1]

#	Compounds	Structure	k_1'	k_2'	α	R_s	Mobile Phase[2]
1	1,1'-Bi-2-naphthol	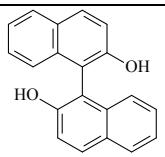	0.95	1.65	1.74	3.40	Acetone
			1.47	2.39	1.63	3.85	CH_2Cl_2/MeOH =95/5
2	Hydrobenzoin	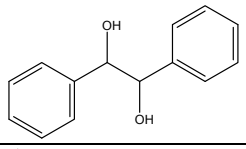	2.94	3.41	1.16	1.48	CH_2Cl_2/MeOH =99/1
3	Indapamide	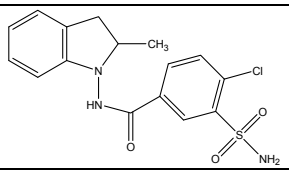	4.19	4.33	1.03	0.49	CH_2Cl_2/MeOH =95/5
4	3-(alpha-acetonyl-4-chlorobenzyl)-4-hydroxy coumarin	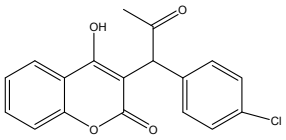	0.77	0.83	1.08	0.68	CH_2Cl_2/MeOH =95/5
5	1,5-Dihydroxy-1,2,3,4-tetrahydro-naphthalene	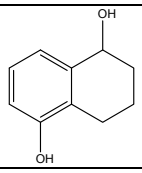	7.03	8.17	1.16	1.84	CH_2Cl_2/MeOH/TFA 98/2/0.1
6	Mephenesin	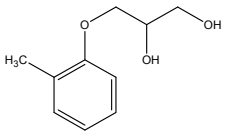	3.85	4.15	1.08	0.67	CH_2Cl_2/MeOH 9=8/2
7	Mandelamide	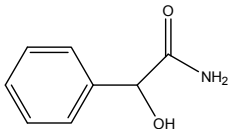	3.60	4.15	1.15	1.93	CH_2Cl_2/MeOH 95/5
8	5-Methyl-5-phenylhydantoin	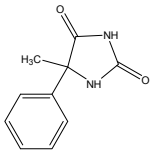	5.70	5.91	1.04	0.74	CH_2Cl_2/MeOH 95/5

[1] (*R*,*R*)-P-CAP was bonded to 5μm silica gel and the stationary phase was packed in a 250×4.6 mm (i.d.) stainless steel column.

[2] All samples were analyzed under the chromatographic condition: a UV detector at 254nm, flow rate 1ml/min, unless otherwise noted. All mobile phase ratios were volume to volume. TEAA: triethylamino acetate.

Table 3. (continued)

#	Compounds	Structure	k_1'	k_2'	α	R_s	Mobile Phase
9	3a,4,5,6-Tetrahydrosuccinimido[3,4-b]acenaphthen-10-one	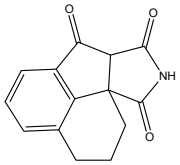	5.00	5.27	1.06	0.46	CH_2Cl_2/MeOH 99/1
10	(3a[R,S]-cis) - 3,3a,8,8a-Tetrahydro-2H-indeno[1,2-d]oxazol-2-one	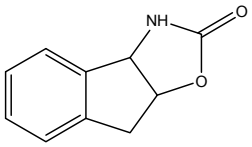	4.18	4.73	1.13	1.45	CH_2Cl_2/MeOH 99/1(v/v)

Table 4. Effect of acid additives on selectivity and resolution for the polar organic mode enantiomeric separations on (*S*,*S*)-P-CAP column

Structure	k_1	α	R_s	Mobile Phase
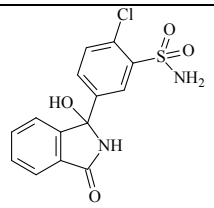	5.00	1.38	2.0	CH_3CN/CH_3OH = 90/10
	5.11	1.37	2.1	CH_3CN/CH_3OH/HOAc = 90/10/0.1
	5.02	1.38	2.5	CH_3CN/CH_3OH/TFA = 90/10/0.1
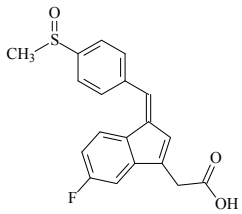	No elution			CH_3CN/CH_3OH = 95/5
	2.33	1.11	1.0	CH_3CN/CH_3OH/HOAc= 95/5/0.1
	2.16	1.12	1.0	CH_3CN/CH_3OH/TFA = 95/5/0.1
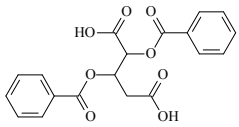	No elution			CH_3CN/CH_3OH = 95/5
	No elution			CH_3CN/CH_3OH/HOAc = 95/5/0.1
	9.26	1.10	1.0	CH_3CN/CH_3OH/TFA = 95/5/0.1

Table 5. Effect of flow rate on selectivity and resolution for the nomal-phase enantiomeric separations of fipronil on (R,R)-P-CAP column[1]

Compound	Flow rate (ml/min)	k_1'	k_2'	Selectivity (α)	Resolution (R_S)
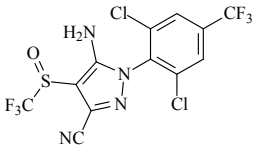	0.5	2.35	2.87	1.22	1.71
	1.0	2.30	2.80	1.22	1.57
	1.5	2.27	2.76	1.22	1.46
	2.0	2.24	2.73	1.22	1.40

[1] The mobile used to enantioseparate fipronil consisted of heptane/ethanol/TFA 80/20/0.1. The sample was analyzed with a UV detector at 254nm.

Table 6. Efficiency comparison of enantioseparation of 1.1'-bi-2-naphthol in the traditional normal-phase mode, polar organic mode and the normal phase mode with halogenated solvent system on (R,R)-P-CAP column[1]

Mobile Phase	Enantioselectivity (α)	Enantioresolution (R_S)	Number of Theoretical Plates[2] (N)
The traditonal normal-phase mode (heptane/EtOH/TFA 30/70/0.1)	1.32	1.86	1704
Polar organic mode (acetonitrile/MeOH/TFA 95/5/0.1)	1.36	3.43	3552
The normal-phase with halogenated solvent system (methylene chloride/MeOH 95/5).	1.54	4.03	6042

[1] The sample was analyzed at the flow rate of 1ml/min, with a UV detector at 254nm under room temperature (~23°C).
[2] Theoretical plates (N) are based on the second eluted enantiomer.

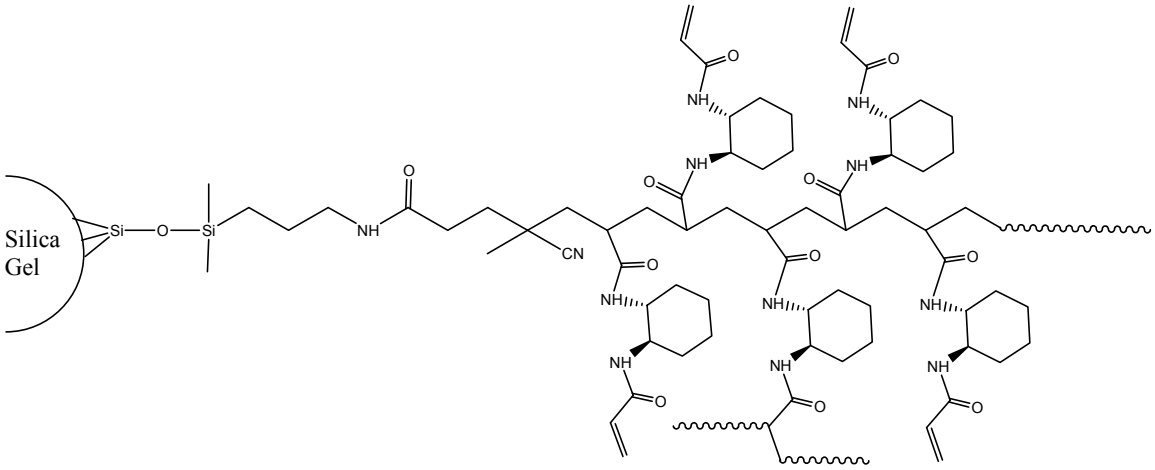

Fig. 1. The structure of (*R*,*R*)-P-CAP chiral stationary phase

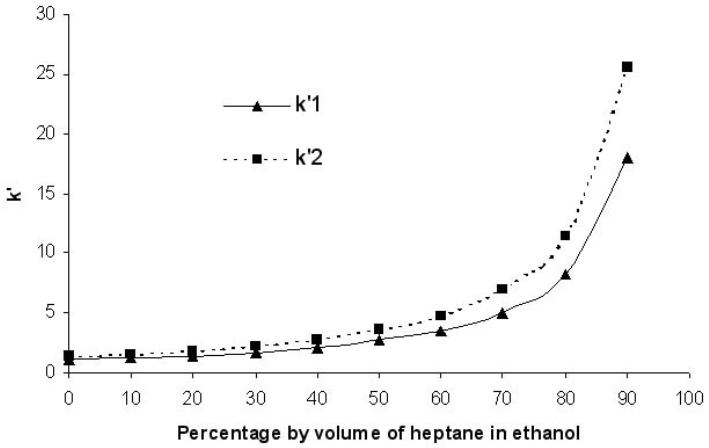

(A) 1,1'-Bi-2-naphthol

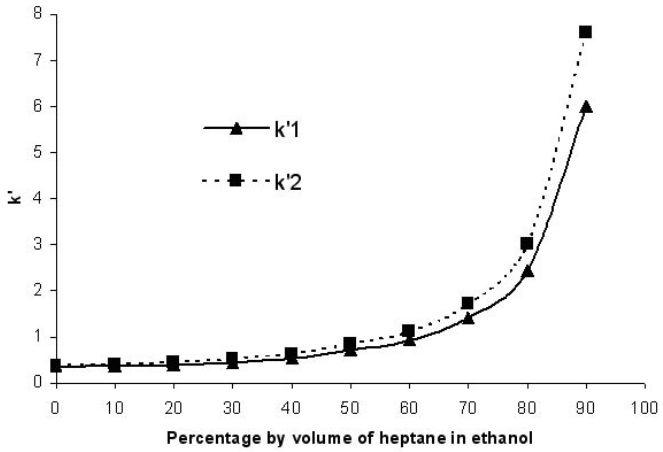

(B) Fipronil

Fig. 2. Normal-phase retention behavior of the first and second eluted enantiomers of (A) 1,1'-bi-2-naphthol, and (B) fipronil as a function of mobile phase composition. The mobile phases consisted of various ratios of ethanol and heptane. The column was a 250×4.6 mm (i.d) (R,R)-P-CAP CSP (5-µm silica gel support). Flow rate: 1.0 mL/min at ambient temperature (~23^{o}C). Detection: UV at 254nm.

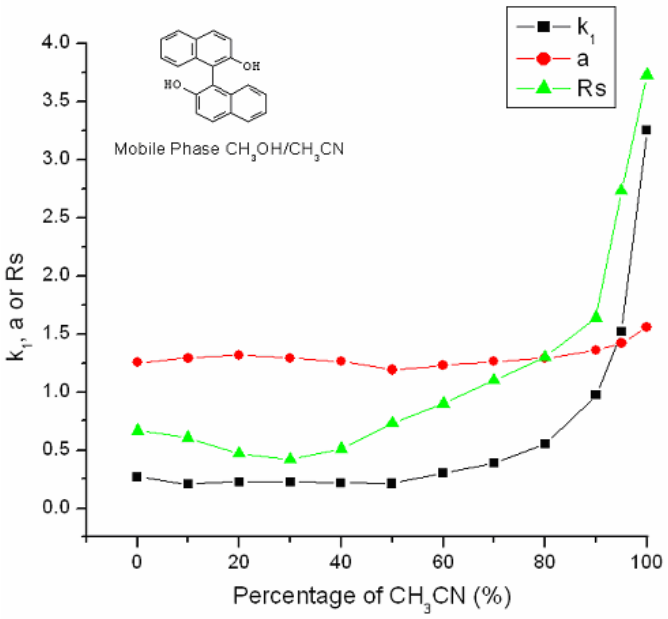

Fig. 3. Polar organic phase retention factor $k_1^{'}$ of the first eluted enantiomer, selectivity factor α, and resolution R_S of 1,1'-bi-2-naphthol as a function of mobile phase composition. The mobile phases consisted of various ratios of methanol and acetonitrile. The column was a 250×4.6 mm (i.d) (*S*,*S*)-P-CAP CSP (5-µm silica gel support). Flow rate: 1.0 mL/min at ambient temperature (~23°C). Detection: UV at 254 nm.

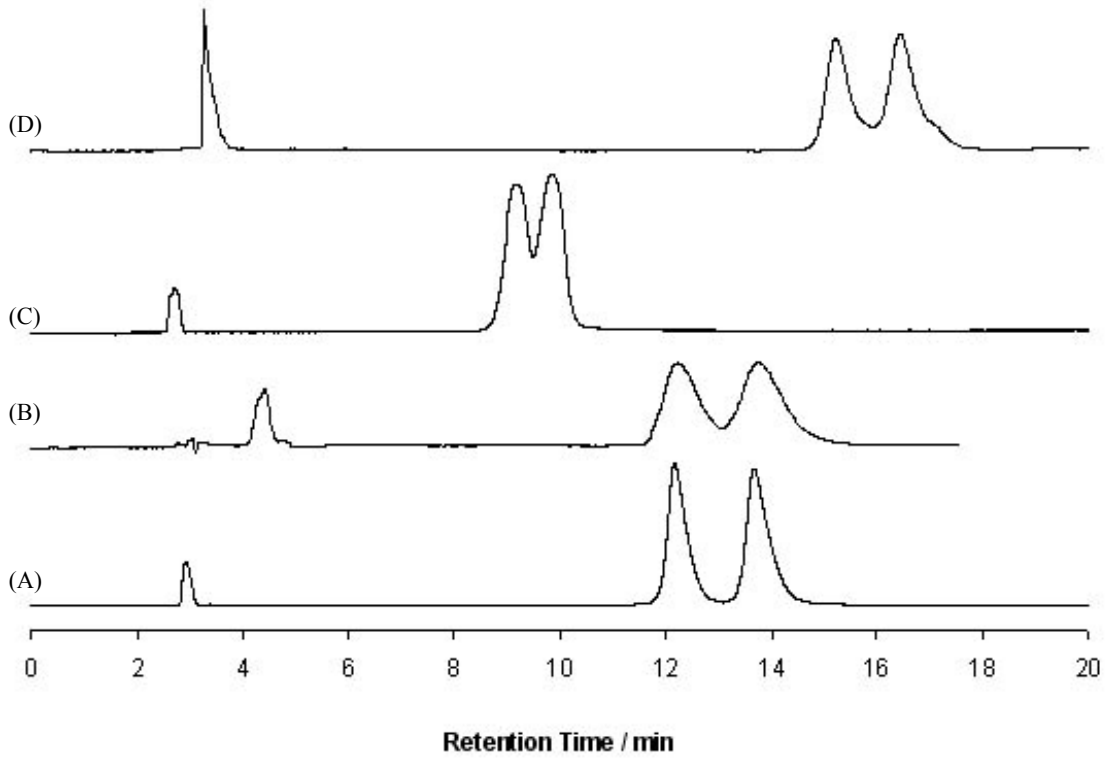

Fig. 4. Resolution of (*R*,*R*)- and (*S*,*S*)-hydrobenzoin on (*R*,*R*)-P-CAP in the normal phase: (A) heptane/2-propanol/trifluoroacetic acid 80/20/0.1 (v/v/v); (B) heptane/2-propanol 80/20 (v/v); (C) heptane/EtOH/trifluoroacetic acid 80/20/0.1 (v/v/v). (D) heptane/EtOH/trifluoroacetic acid 90/10/0.1 (v/v/v). Flow rate: 1.0 mL/min; UV detection at 254 nm, T=23^{o}C.

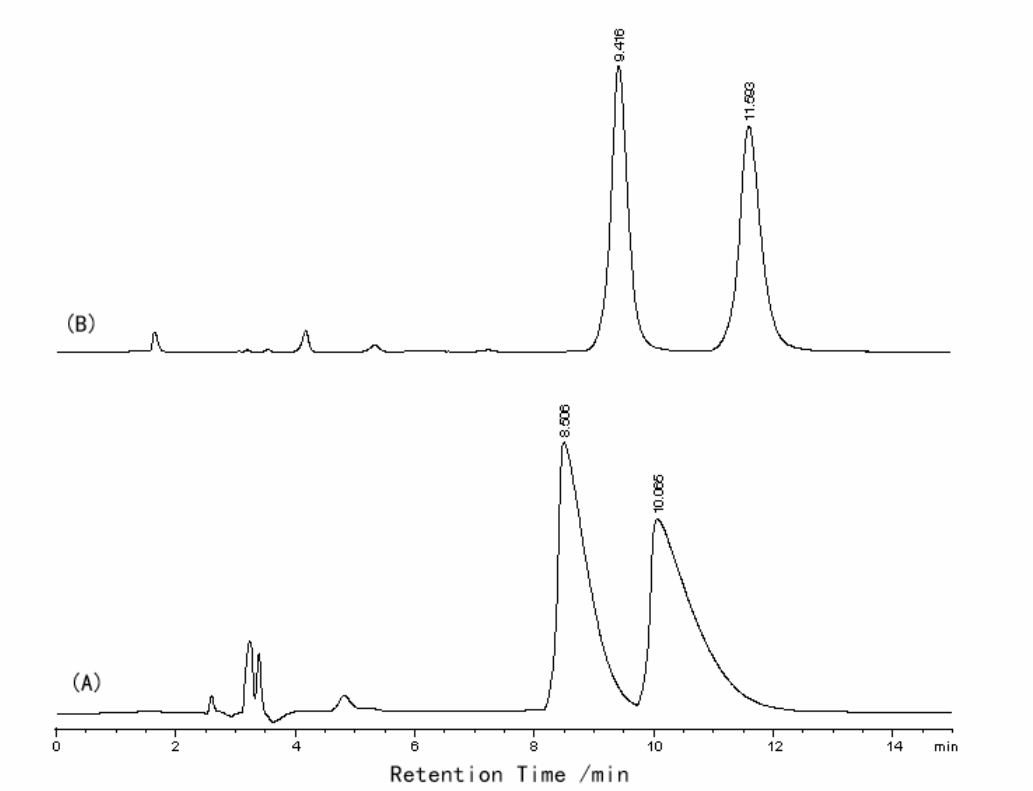

Fig. 5. Sample loading capacity test for the separation of 1,1'-bi-2-naphthol on (*R*,*R*)-P-CAP column. Sample loading (A) 1000 μg; (B) 1 μg. (*R*,*R*)-P-CAP was bonded to 5 μm silica gel and the stationary phase was packed in a 250×4.6 mm (i.d.) stainless steel column. Mobile phase: EtOH/heptane 50/50; flow rate: 1mL/min; detection: UV at 254 nm; temperature: ~23 ^{o}C.

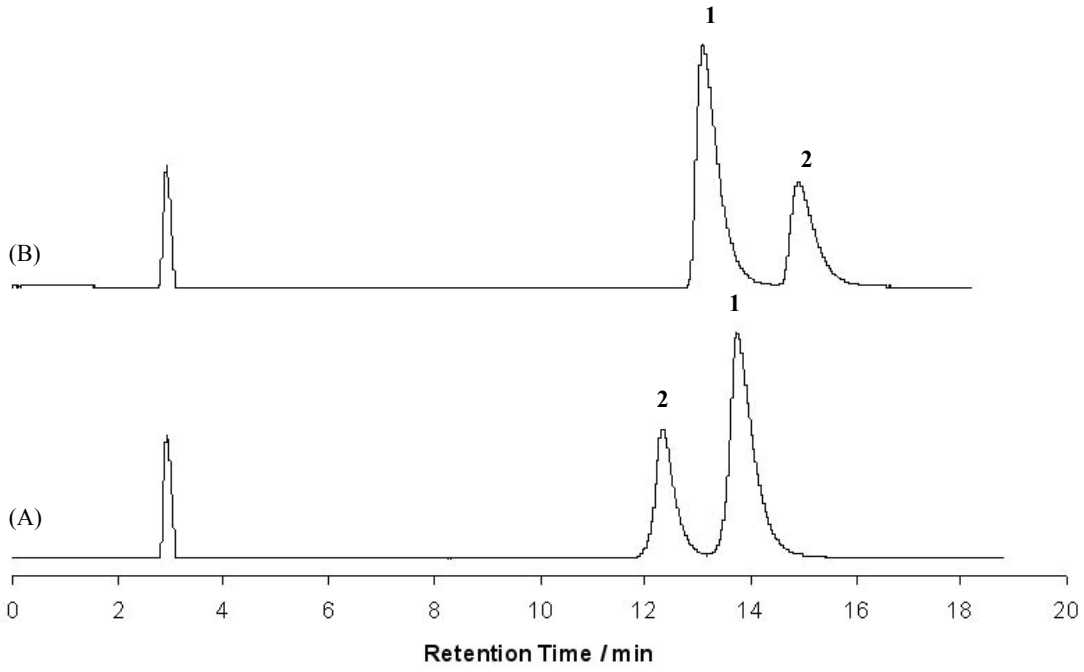

Fig. 6. Reversal of elution order on (A) (*R*,*R*)-P-CAP and (B) (*S*,*S*)-P-CAP columns under the normal phase. Peak **1** is (*R*,*R*)-hydrobenzoin and Peak **2** is (*S*,*S*)-hydrobenzoin with the mole ratio of (*R*,*R*):(*S*,*S*) = 2:1. Mobile phase: heptane/2-propanol/TFA 80/20/0.1 (v/v/v); flow rate: 1 mL/min; UV detection at 254nm; T=23 ^{o}C.

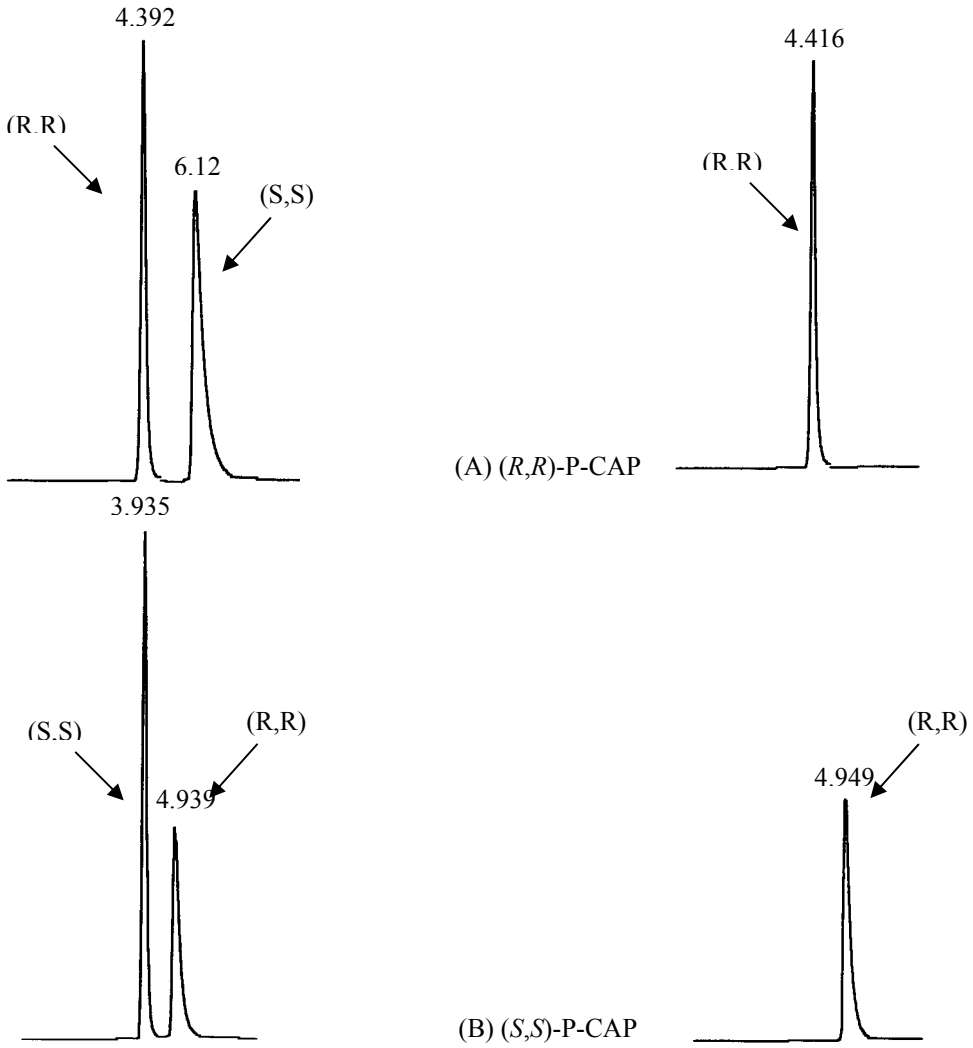

Fig. 7. Reverse elution order on (A) (*R*,*R*)-P-CAP and (B) (*S*,*S*)-P-CAP CSPs under polar organic phase. Samples are racemic mixture of (*R*,*R*) and (*S*,*S*) DACH-ACR. Mobile phase: CH_3CN/MeOH 97/3(v/v). Flow Rate: 1.0 mL/min. Detection: UV at 254 nm. Temperature: 23 °C.

Chapter 6. Synthesis and evaluation of a synthetic polymeric chiral stationary phase for HPLC based on the N, N'-[(1R,2R)-1,2-diphenyl-1,2-ethanediyl]bis-2-propenamide monomer

A paper published in *Chromatographia*[1]

X. Han, L. He, Q. Zhong, T. E. Beesley, D. W. Armstrong

Abstract

A synthetic polymeric chiral stationary phase for liquid chromatography based on *N*,*N*'-[(1R,2R)-1,2-diphenyl-1,2-ethanediyl]bis-2-propenamide monomer was prepared via a simple solution initiated radical polymerization. This stable chiral stationary phase showed enantioselectivities for a large number of racemates in polar organic and normal phase modes and high sample loading ability. However, none of the generated data has been optimized in terms of column performance. Different enantioselectivities were observed on this new chiral stationary phase compared with the commercial polymeric chiral stationary phase based on *N*-(2-acryloylamino-(1R,2R)-cyclohexyl)-acrylamine monomer. Consequently, these two chiral stationary phases are considered complementary to one another. Furthermore they utilize the same mobile phase and optimization procedures. This polymeric chiral stationary phase appears to be useful for preparative separation since high amount of analyte can be injected without loosing enantioselectivity.

Keywords: Column liquid chromatography, Chiral stationary phase (CSP), Poly-DPEDA, Enantioselectivity

6.1. Introduction

In the past two decades, research on chiral stationary phase for HPLC has advanced greatly [1-4]. Currently, more than 100 chiral stationary phases (CSPs) have been commercialized [2]. Of all the chiral stationary phases, polymeric ones (except for those based on proteins) appear to be the most suitable for preparative separations due to their potential for high sample loading. There are two classes of polymeric stationary phases. One of them uses natural polymers such as polysaccharide derivatives and proteins as chiral

[1] Reprinted with permission of C*hromatographia*, 2006, 63, 13-23.

selectors. The other group employs synthetic polymers such as polyamides, vinyl polymers, polyurethanes, and polyacetylene as chiral selectors [4]. Cellulose and amylose carbamate CSPs have been widely used for the preparative and analytical separations of racemates due to their broad enantiomeric selectivity as well as their high sample loading capacity [4-5]. Until recently, research on synthetic polymeric CSPs has not produced anything of comparable success [4]. However, the attractive characteristics of synthetic polymeric CSPs remain in the richness of the chemical structures of potential chiral selectors, the ease of chemical modification of the chiral selectors, and the possibility of obtaining polymeric CSPs with opposite absolute configuration. In addition, the covalent bonding of the chiral polymers to the supporting material increases the stability of these CSPs and they are amenable for preparative separations.

By copolymerization of chiral acrylamides with ethylene diacrylate as cross-linking agent, Blaschke and his co-workers prepared polymeric beads as CSPs [6-8]. These CSPs were not stable to high pressure and were only used for preparative purposes. This problem was circumvented through copolymerization of chiral acrylamide with methacryloyl silica gel [9]. Using a similar method, Lange and co-workers made another group of polymeric CSPs with monomers, which had amino acid and (-)-menthone or (+)-menthol units [10]. Few enantiomeric separations were reported on these polymeric CSPs [6-10]. Okamoto prepared a chiral polymer with a helical secondary structure, which was formed from a nonchiral monomer TrMA (triphenylmethyl methacrylate) via the asymmetric catalyzed anionic polymerization [11]. This polymer can be either coated [4,11] or bonded [4] to silica gel as CSP for HPLC. These CSPs showed enantiomeric selectivities for a number of racemates [4]. Saigo and his coworkers made a chiral polymer through the reaction of (-)-1,2-diphenylethylenediamine and diacid chlorides at low temperature and coated this polymer on silica gel to obtain a chiral stationary phase [12]. However, marginal separations of very few racemates were reported.

Recently, a new synthetic polymeric chiral stationary phase was developed by Gasparrini and co-workers and commercialized as the P-CAP column by Advanced Separation Technologies Inc [13-15]. More than 60 separations of racemates with various structures were reported on this CSP. The P-CAP CSP also showed high stability, high

sample loading and the ability to be used in multiple mobile phase types. Since the P-CAP CSP has no aromatic units, a polymeric CSP with such groups will show different enantioselectivities and thus be a complementary CSP. *Trans*-1,2-diphenylethylenediamine (DPEDA), a molecule with two phenyl units, has been used successfully in π-complex brush-type CSPs [16-18]. While it has been suggested that DPEDA can be used as the basis for a polymeric CSP [15], it has not yet been demonstrated to our knowledge. In this paper, a synthetic polymeric chiral stationary phase based on the *N*,*N*'-[(1R,2R)-1,2-diphenyl-1,2-ethanediyl]bis-2-propenamide is reported. Synthesis, chromatographic properties, complementarity of the normal phase and polar organic modes, and a comparison with the related P-CAP CSP are presented and discussed.

6.2. Experimental

6.2.1. Materials

Spherical silica gel (particle diameter: 5 μm, pore size: 200 Å, surface area: 213 m^2/g) was purchased from Akzo Nobel, EKA Chemicals AB, Bohus, Sweden. Acryloyl chloride, (1R,2R)-(+)-diphenylethylenediamine, 3-(trimethoxysilyl)propyl methacrylate, diisopropylethylamine, 2,2'-azobis(isobutyronitrile) (AIBN), anhydrous toluene, chloroform, acetone, and trifluoroacetic acid (TFA) were purchased from Aldrich. HPLC grade methanol, ethanol, acetonitrile, 2-propanol, hexane, and *n*-heptane were purchased from Fisher, Fairlawn, NJ.

6.2.2. Synthesis

Preparation of *N*,*N'*-[(1R,2R)-1,2-diphenyl-1,2-ethanediyl]bis-2-propenamide (DPEDA-ACR) (1)

(1R,2R)-(+)-diphenylethylenediamine (1.0g, 4.71mmol) and triethylamine (1.4 mL, 10.95 mmol) were dissolved in 20 mL anhydrous chloroform. Anhydrous chloroform (10 mL) solution of acryloyl chloride (0.8 ml, 9.85 mmol) was added dropwise into the above solution at 0 ºC under stirring and the reaction was kept at 0 ºC for 12 h. The precipitate was collected by filtration, washed with chloroform (3 x 10 mL) to get white solid 0.74 g. The filtrate was dried and the solid was crystallized with chloroform/ether. The precipitate was collected and dissolved in acetone. The acetone solution was filtered through a silica gel column to obtain 0.45 g white solid. The combined product was dried under vacuum at 25 ºC

over night to obtain 1.13 g white solid (yield: 75%). ^{1}H NMR (300 MHz, DMSO-*d*6): δ 8.74 (d, J = 8.4 Hz, 2H), 7.18-7.07 (m, 10H), 6.25 (dd, J_1 = 17.1 Hz, J_2 = 10.2 Hz, 2H), 6.02 (dd, J_1 = 17.1 Hz, J_2 = 2.1 Hz, 2H), 5.57 (dd, J_1 = 10.2 Hz, J_2 = 2.1 Hz, 2H), 5.25 (dd, J_1 = 8.4 Hz, J_2 = 6.6 Hz, 1H), 5.22 (dd, J_1 = 8.4 Hz, J_2 = 6.6 Hz, 1H). ^{13}C NMR (75 MHz, DMSO-*d*6)

Preparation of methacryl silica gel

Silica gel (8 g) and anhydrous toluene (180 mL) were added into a 500 mL round bottom flask with a Dean-Stark trap and a condenser. After removing 25 mL of distillate under reflux, the mixture was cooled down to the room temperature. 3-(trimethoxysilyl)propyl methacrylate (2 mL, 8.42 mmol) was added into the reaction medium and the reaction medium was refluxed for 4 h. The modified silic gel was collected by filtration, washed with 100 mL acetone, methanol, acetone, respectively. The methacryl silica gel was dried under vacuum at 25 ºC overnight and screened with 53 μm sieve and bottle to obtain 8.3 g. Loading: 3.8%. Elemental Analysis: C, 2.20%; H, 0.53%.

Preparation of poly-DPEDA CSP

Methacryl silica gel (3.41 g) was suspended in 70 mL anhydrous toluene in 250 mL 3-neck flask with a Dean-Stark trap and a condenser. After removing 10 mL of distillate, the reaction mixture was cooled down to room temperature and saturated with nitrogen. DPEDA-ACR (0.707g, 2.207 mmol) and AIBN (22 mg, 0.134 mmol) were put into the suspension under nitrogen protection. The suspension was kept at 80 ºC for 4 h and refluxed for 1 h. The CSP was collected by filtration, washed with 100 mL of ethanol, acetone, methanol, and chloroform respectively. The CSP was dried under vacuum at 50 ºC over night and screened with 53 μm sieve and bottle to obtain 3.82 g. Loading: 12%. Elemental Analysis: C, 10.49%; H, 1.36%; N, 1.03%. The CSP was packed into a 250 mm x 4.6 mm (i. d.) stainless steel column.

6.2.3. Equipment

Chromatographic separations were carried out using a HP 1050 HPLC system with an auto sampler, a UV VWD detector, and computer controlled Chem-station data processing software (Agilent Technologies, Palo Alto, CA, USA). The mobile phases were degassed under helium for 10 min. UV detection was carried out at 254 nm for all analytes. All separations were carried out at room temperature (~ 23˚C) and the flow rate of the mobile

phase for all separations was 1.0 mL min^{-1}.

6.2.4. Column Evaluation

The performance of poly-DPEDA chiral stationary phase was evaluated in the polar organic mode using acetonitrile/methanol and in the normal phase mode using 2-propanol/heptane, ethanol/heptane, or ethanol/hexane mobile phase. Before using a new mobile phase, ten column volumes of new mobile phase were pumped through the column prior to the injection of the analyte.

6.2.5. Calculations

The dead time (t_0) was estimated using the peak resulting from the change in refractive index from the injection solvent on the poly-DPEDA CSP. The retention factor (k) was calculated using the equation $k = (t_r-t_0) / t_0$. The enantioselectivity (α) was calculated using $\alpha = k_2 / k_1$. The resolution factor (R_S) was calculated using the equation $R_S = 2$ x $(t_{r2}-t_{r1}) / (w_1+w_2)$, where t_{r2} and t_{r1} are the retention times of the second and first enantiomers, respectively, and w_1 and w_2 are the corresponding base peak widths. The efficiency (number of theoretical plates, N) was calculated using $N = 16(t_r/w)^2$.

6.3. Results and Discussion

6.3.1. Preparation of poly-DPEDA CSP

The procedure of preparation of the new CSP is shown in Fig. 1 (see Experimental). The optically active polymers were grafted to the surface of the modified silica gel through reaction with the acryloyl group on the surface of the support. Unattached polymers in the solution can be removed by washing the CSP with various solvents. A 12% loading of the chiral selector was obtained.

6.3.2. Chromatographic performance of poly-DPEDA CSP

Two mobile phase modes were evaluated on this new polymeric chiral stationary phase. The normal phase mode is composed of nonpolar solvents such as heptane or hexane and polar modifiers such as ethanol or isopropanol. The polar organic mode is composed of acetonitrile and methanol, typically with a small amount of trifluoroacetic acid. Tables 1 and 2 list the enantiomeric separations observed on this CSP in the normal phase mode and polar organic mode, respectively. It should be noted that these results were obtained on a column in which the packing has not been optimized. Such optimization would be expected to

produce even more efficient separations, which would further improve resolution. In the normal phase mode, enantiomeric separations of 42 racemic compounds were observed and 13 of them are baseline separations. Thirty-four racemic analytes were separated in the polar organic mode and 15 baseline separations were obtained. Combined the two mobile phase modes, 56 chiral compounds were separated and 25 baseline separations were achieved (Fig. 2).

Since the polymeric chiral selector was covalently grafted to the solid support (silica gel), the new polymeric CSP shows high stability. No degradation of stationary phase or change in the enantiomeric separation performance was observed after more than 1000 injections and several mobile phase mode changes.

6.3.3. Complementary nature of the two mobile phase modes

The polar organic mode and nomal phase mode are complementary to one another for the poly-DPEDA chiral stationary phase. Fourteen of the racemic analytes separated in the polar organic mode cannot be separated in the normal phase mode. Similarly, 22 racemic compounds can only be separated in the normal phase mode. For compounds that can be separated in both the polar organic mode and normal phase mode, different enantioselectivities and resolutions were observed. For example, compound **17** can be baseline separated in the polar organic mode, while in the normal phase mode, only a partial separation was obtained (Fig. 3). Part of the contribution to the better separation in the polar organic mode for compound **17** was the increase in the enantioselectivity (α = 1.50 vs. α = 1.41), while the most contribution is from the increase in efficiency (theoretical plate number of the first peak (N_1) in the polar organic mode is 2500, while N_1 is just 310 in the normal phase mode). On the contrary, for analyte **3**, a better separation was observed in the normal phase mode, although higher enantioselectivities were obtained in the polar organic mode (Table 1 and 2). The reason is that the retention of compound **3** is so low in the polar organic mode even under the weakest mobile phase condition (100% acetonitrile) that there is not enough retention for a satisfactory enantiomeric separation to be achieved.

6.3.4. Comparison with the P-CAP CSP

The poly-DPEDA column showed different enantioselectivities as opposed to the P-CAP column (i.e., the comparable polymeric column that utilized the *trans*-1,2-

diaminocyclohexane chiral selectors) in both mobile phase modes. For the 42 separated racemates found in the normal phase mode on the poly-DPEDA column, 19 racemates can only be separated on the poly-DPEDA column, but not on the P-CAP column. Different selectivities were also observed for the analytes that can be separated on both CSPs. For example, compound **19** can be baseline separated on the poly-DPEDA CSP, while just a slightly split peak can be obtained for the same compound on the P-CAP column (Fig. 4a, 4b). In the polar organic mode, 18 of the separated analytes in this work have not been reported on the P-CAP CSP. Conversely, a much better enantiomeric selectivity was observed on the P-CAP column for compound **4** (Fig. 4c, 4d). Combining the two mobile phase modes, 20 new separations of racemates were obtained on this column compared with the analogous P-CAP column. In this respect, these two CSPs appear to be complementary to each other.

6.3.5. Sample loading study

The poly-DPEDA chiral stationary phase showed high sample loading capacity. For the enantiomeric separations of fipronil (compound **35**), excellent separation of 7.5 μg of analyte (Fig. 5a) and satisfactory separation of 500 μg of racemate (Fig. 5b) were obtained on an analytical column. Another example is the separation of fuoroin (compound **19**). Almost baseline separation was achieved for 1000 μg analyte on the same column (Fig. 5d). Thus, this column has the potential to be a good preparative LC column, which is one of the strengths of this class of CSPs.

6.4. Conclusions

A simple solution initiated radical polymeric reaction was used to produce a new polymeric chiral stationary phase based on *N*,*N*'-[(1R,2R)-1,2-diphenyl-1,2-ethanediyl] bis-2-propenamide. This CSP showed high sample loading capacity and enantioselctivities for a large variety of racemic compounds. The CSP can be used in the polar organic and normal phase modes with no degradation of stationary phase observed. Different enantiomeric selectivities and resolutions were obtained on this new CSP for the polar organic mode and normal phase mode. The new poly-DPEDA column showed different enantiomeric selectivities as opposed with the commercialized P-CAP column, thus it is complementary to the P-CAP column. High loading capacity is possible on this new CSP.

Acknowledgements

We gratefully acknowledge the support of this work by the National Institutes of Health, NIH RO1 GM53825-08.

References

1. Armstrong DW (1997) LC-GC 59 (supplemental issue): S20-S28
2. Armstrong DW, Zhang B (2001) Anal Chem 73: 557A-561A
3. Gasparrini F, Misiti D, Villani C (2001) J. Chromatogr A 906: 35-50
4. Yamamoto C, Okamoto Y (2004) Bull Chem Soc Jpn 77: 227-257
5. Okamoto Y, Yashima E (1998) Angew Chem Int Ed 37: 1020-1043
6. Blaschke G, Donow F (1975) Chem Ber 108: 1188-1197
7. Blaschke G, Donow F (1975) Chem Ber 108: 2792-2798
8. Blaschke G (1980) Angew Chem Int Ed Engl 19: 13-24
9. Blaschke G, Bröker W, Fraenkel W (1986) Angew Chem Int Ed Engl 25: 830-831
10. Arlt D, Bömer B, Grosser R, Lange W (1991) Angew Chem Int Ed Engl 30: 1662-1664
11. Okamoto Y, Honda S, Okamoto I, Yuki H, Murata S, Noyori R, Tanaka H (1981) J Am Chem Soc 103: 6971-6973
12. Saigo K, Chen Y, Kubota N, Tachibana K (1986) Chem Lett 515-518
13. Gasparrini F, Misiti D, Rompietti R, Villani C (2005) J. Chromatogr A 1064: 25-38
14. Zhong Q, Han X, He L, Beesley TE, Trahanovsky WS, Armstrong DW (2005) J. Chromatogr A 1066: 55-70
15. Gasparrini F, Misiti D, Villani C WO Patent (2003) 2003079002.
16. Uray G, Maier NM (1994) J. Chromatogr A 666: 41-53
17. Maier NM, Uray G (1996) J. Chromatogr A 732: 215-230
18. Kosjek B, Uray G (2001) Chirality 13: 657-667

Table 1. Retention factor of the first peak (k_1), enantioselectivity (α), and enantioresolution (Rs) of separated racemates on the poly-DPEDA column in the normal phase mode

#	Compound	Structure	k_1	α	R_s	Mobile Phase (v/v)[a]
1	*O*-Acetyl-mandelic acid	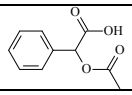	1.43	1.16	1.0	HEP/IPA/TFA = 80/20/0.1
2	Atrolactic acid	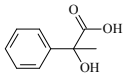	3.03	1.17	1.2	HEP/IPA/TFA = 80/20/0.1
3	Benzyl-6-oxo-2,3-diphenyl-4-morpholine carboxylate	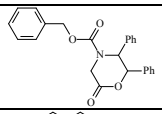	4.19	1.38	1.5	HEP/IPA = 80/20
4	1, 1'-Bi-2-naphthol		6.39	1.24	1.0	HEP/IPA = 80/20
5	1-Benzocyclobutene-carbonitrile	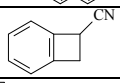	2.36	1.05	0.4	HEP/IPA = 98/2
6	3-(benzyloxycarbonyl)-4-oxazolidinecarboxylic acid	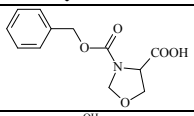	2.83	1.17	0.7	HEP/IPA = 80/20
7	6-(4-Chlorophenyl)-4,5-dihydro-2-(2-hydroxybutyl)-3(2H)-pyridazinone	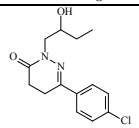	2.87	1.23	1.1	HEP/IPA = 80/20
8	2-[3-Chlorophenoxy]-propionamide	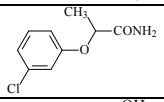	2.48	1.19	1.5	HEP/IPA = 80/20
9	*p*-Chloromandelic acid	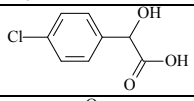	4.85	1.11	0.7	HEP/IPA/TFA = 80/20/0.1
10	α-Ethoxycarbonyl-γ- phenyl-γ-butyrolactone	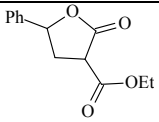	2.56	1.35	1.5	HEP/IPA = 80/20
11	1,5-dihydroxy-1,2,3,4-tetrahydronaphthalene	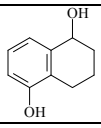	2.68	1.21	1.5	HEP/IPA = 80/20
12	*N*-(3,5-Dinitrobenzoyl)-phenylglycine	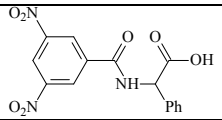	11.4	1.32	0.8	HEP/IPA/TFA = 70/30/0.1
13	2,3-dihydroxy-*N*, *N*'-bis(phenylmethyl)-butanediamide	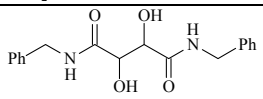	4.47	2.28	1.7	HEP/IPA/TFA = 70/30/0.1
14	*cis*-4,5-Diphenyl-2-oxazolidinone	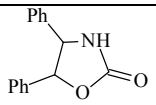	7.97	1.07	0.3	HEP/IPA = 80/20
15	1,5-Dimethyl-4-phenyl-2-imidazolidinone	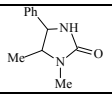	4.18	1.16	1.2	HEP/IPA/TFA = 80/20/0.1

Table 1. (continued)

#	Compound	Structure	k_1	α	R_s	Mobile Phase (v/v)[a]
16	2,3-Dibenzoyl-tartaric acid	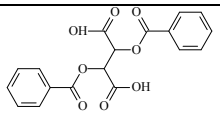	4.69	1.11	0.3	HEP/IPA/TFA = 80/20/0.1
17	*N*-(3,5-Dinitrobenzoyl)-leucine	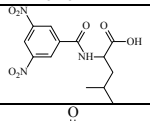	4.35	1.41	1.3	HEP/IPA/TFA = 70/30/0.1
18	5,5-Dimethyl-4-phenyl-2-oxazolidinone	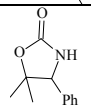	4.72	1.09	0.4	HEP/IPA/TFA = 80/20/0.1
19	Furoin	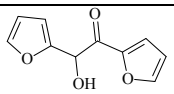	5.29	1.69	3.7	HEP/IPA/TFA = 80/20/0.1
20	Ftorafur	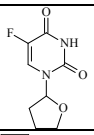	11.8	1.08	0.3	HEP/IPA/TFA = 70/30/0.1
21	3-(4-Hydroxyphenyl)-lactic acid	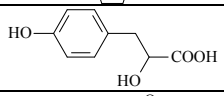	9.12	1.17	0.8	HEP/IPA/TFA = 70/30/0.1
22	5-Methyl-5-phenyl-hydantoin	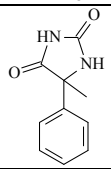	7.76	1.16	0.7	HEP/IPA = 70/30
23	Mandelamide	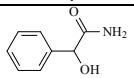	5.11	1.07	0.4	HEP/IPA = 70/30
24	Mephenesin	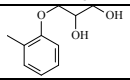	2.23	1.07	0.4	HEP/IPA = 80/20
25	Hydrobenzoin	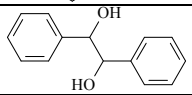	1.02	1.26	1.5	HEP/IPA = 70/30
26	Sulindac	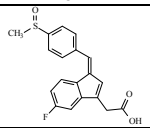	2.93	1.10	1.0	HEP/IPA = 70/30
27	*cis*-3,3a,8,8a-Tetrahydro-2H-indeno[1,2-d]oxazol-2-one	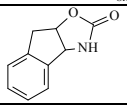	5.03	1.31	1.3	HEP/IPA = 70/30
28	1,2,3,4-Tetrahydro-1-naphthol	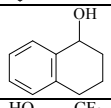	1.25	1.05	0.5	HEP/EtOH = 95/5
29	1-(9-Anthryl)-2,2,2-trifluoroethanol	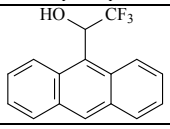	3.53	1.06	0.9	HEP/EtOH = 95/5
30	Dihydro-5-[(triphenylmethoxy)methyl]-2(3H)-Furanone	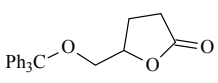	3.81	1.17	1.5	HEP/EtOH = 95/5

Table 1. (continued)

#	Compound	Structure	k_1	α	R_s	Mobile Phase (v/v)[a]
31	5-(α-phenethyl)-semioxamazide	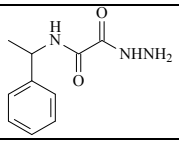	5.18	1.11	0.8	HEP/EtOH = 70/30
32	Omeprazole	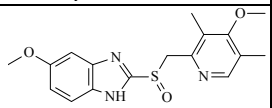	1.90	1.14	0.9	HEP/EtOH = 70/30
33	Lactamide	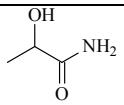	5.94	1.08	1.1	HEP/EtOH = 90/10
34	Benzoin	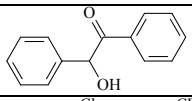	1.93	1.25	1.9	HEX/EtOH = 90/10
35	Fipronil	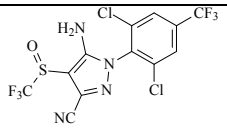	3.72	1.46	2.1	HEP/IPA = 90/10
36	Mandelic acid	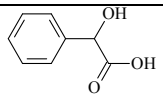	1.73	1.22	1.5	HEX/EtOH = 90/10
37	Methyl mandelate	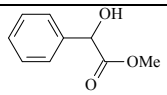	1.68	1.21	1.5	HEX/EtOH = 90/10
38	Mandelic benzylate	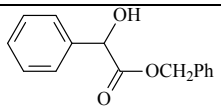	1.69	1.21	1.5	HEX/EtOH = 90/10
39	β-Phenyllactic acid	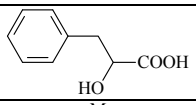	1.13	1.36	1.3	HEX/EtOH = 90/10
40	Phensuximide	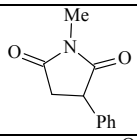	2.32	1.10	1.2	HEX/EtOH = 90/10
41	Methyl phenylsulfoxide	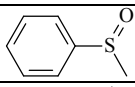	3.15	1.03	0.7	HEX/EtOH = 90/10
42	5-(4-methylphenyl)-5-phenyl-hydantoin	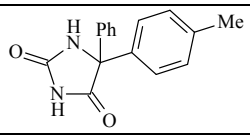	5.60	1.08	0.8	HEX/EtOH = 70/30

[a] HEP: *n*-heptane, HEX: hexane, IPA: 2-propanol, EtOH: ethanol, TFA: trifluoroacetic acid.

Table 2. Retention factor of the first peak (k_1), enantioselectivity (α), and enantioresolution (Rs) of separated racemates on the poly-DPEDA column in the polar organic mode

#	Compound	Structure	k_1	α	R_s	Mobile Phase (v/v)[a]
2	Atrolactic acid	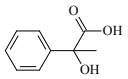	1.34	1.15	0.8	ACN/MeOH/TFA = 99/1/0.1
3	Benzyl-6-oxo-2, 3-diphenyl-4-morpholine carboxylate	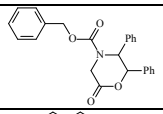	0.07	1.57	0.4	ACN/TFA =100/0.1
4	1, 1'-Bi-2-naphthol		0.61	1.11	0.5	ACN/TFA =100/0.1
6	3-(benzyloxycarbonyl)-4-oxazolidinecarboxylic acid	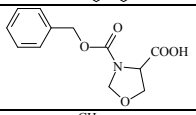	0.59	1.25	1.5	ACN/TFA =100/0.1
8	2-[3-Chlorophenoxy]-propionamide	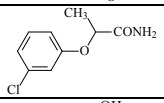	0.48	1.27	1.5	ACN
11	1,5-dihydroxy-1,2,3,4-tetrahydronaphthalene	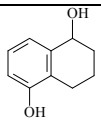	0.56	1.12	0.4	ACN/MeOH/TFA = 99/1/0.1
12	*N*-(3,5-Dinitrobenzoyl)-phenylglycine	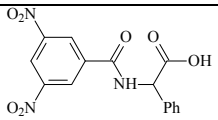	1.34	1.52	2.0	ACN/MeOH/TFA =99/1/0.1
13	2,3-dihydroxy-*N*, *N*'-bis(phenylmethyl)-butanediamide	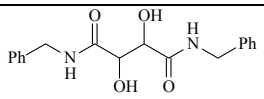	1.20	1.69	2.7	ACN/MeOH/TFA =99/1/0.1
14	*cis*-4,5-Diphenyl-2-oxazolidinone	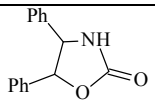	0.48	1.12	0.6	ACN/TFA =100/0.1
15	1,5-Dimethyl-4-phenyl-2-imidazolidinone	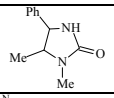	1.72	1.13	1.2	ACN/MeOH/TFA =99/1/0.1
17	*N*-(3,5-Dinitrobenzoyl)-leucine	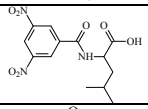	1.24	1.50	2.8	ACN/TFA=100/0.1
18	5,5-Dimethyl-4-phenyl-2-oxazolidinone	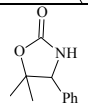	0.49	1.16	0.8	ACN/TFA =100/0.1
19	Furoin	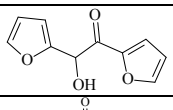	0.16	1.44	1.0	ACN/TFA =100/0.1
20	Ftorafur	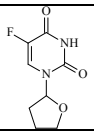	0.89	1.15	0.9	ACN/TFA =100/0.1
23	Mandelamide	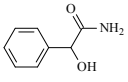	1.31	1.05	0.5	ACN/TFA =100/0.1

Table 2. (continued)

#	Compound	Structure	k_1	α	R_s	Mobile Phase (v/v)[a]
24	Mephenesin	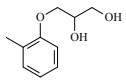	0.57	1.05	0.3	ACN/TFA =100/0.1
25	Hydrobenzoin	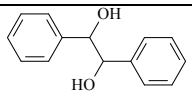	0.45	1.28	1.5	ACN
26	Sulindac	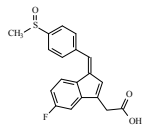	3.38	1.12	1.1	ACN/TFA =100/0.1
27	*cis*-3,3a,8,8a-Tetrahydro-2H-indeno[1,2-d]oxazol-2-one	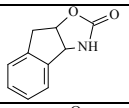	0.76	1.47	2.3	ACN/TFA =100/0.1
31	5-(α-phenethyl)-semioxamazide	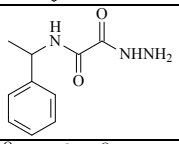	1.00	1.17	1.0	ACN/MeOH =99/1
43	Althiazide	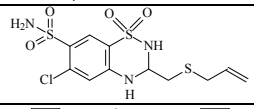	0.76	1.50	1.5	ACN/MeOH/TFA =99/1/0.1
44	*N*, *N*'-Bis(α-methylbenzyl)-sulfamide	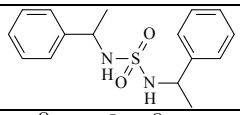	0.21	1.71	1.5	ACN/TFA =100/0.1
45	Bendroflumethiazide	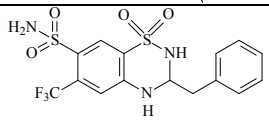	0.53	1.40	1.4	ACN/TFA =100/0.1
46	4-Benzyl-2-oxazolidinone	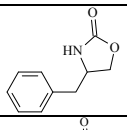	0.48	1.12	0.6	ACN/TFA =100/0.1
47	4-Benzyl-5,5-dimethyl-2-oxazolidinone	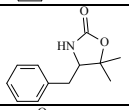	0.46	1.28	1.4	ACN/TFA =100/0.1
48	Chlorthalidone	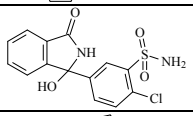	3.57	1.36	1.5	ACN/MeOH/TFA =99/1/0.1
49	4-(Diphenylmethyl)- 2-oxazolidinone	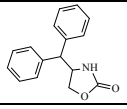	0.41	1.36	1.5	ACN/MeOH/TFA =99/1/0.1
50	3,4-dihydroxyphenyl-α-propylacetamide	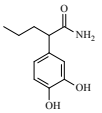	3.78	1.10	0.6	ACN/MeOH/TFA =99/1/0.1
51	7,8-benzo-1,3-diazaspiro[4,5]decane-2,4-dione	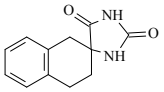	3.09	1.23	1.5	ACN/TFA =100/0.1

Table 2. (continued)

#	Compound	Structure	k_1	α	R_s	Mobile Phase (v/v)[a]
52	Phenylsuccinic anhydride	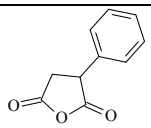	4.05	1.67	3.0	ACN/TFA =100/0.1
53	*Trans*-*N*,*N*'-1,2-cyclohexanediylbis-2-Propenamide	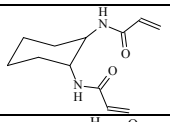	0.72	1.56	1.7	ACN/MeOH = 95/5
54	Oxazepam	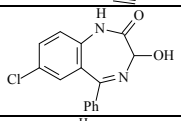	3.21	2.31	4.5	ACN/MeOH = 95/5
55	Dioxibrassinin	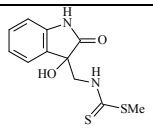	1.54	1.30	1.4	ACN/MeOH/TFA = 95/5/0.1
56	FMOC-Phenylalanine	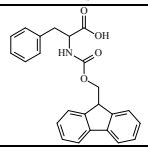	0.92	1.26	1.0	ACN/MeOH/NH_4OAc=85/15/10mM

[a] ACN: acetonitrile, MeOH: methanol, TFA: trifluoroacetic acid.

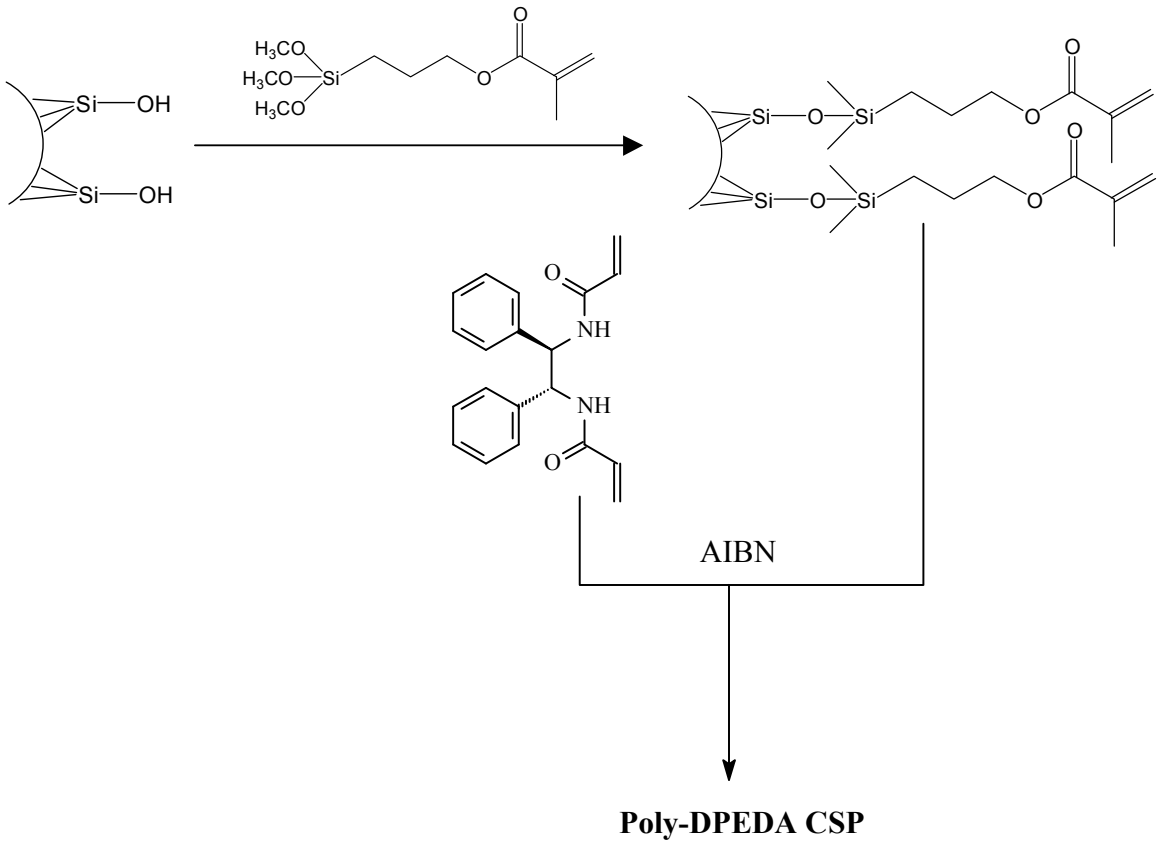

Fig. 1. Synthesis of the poly-DPEDA chiral stationary phase.

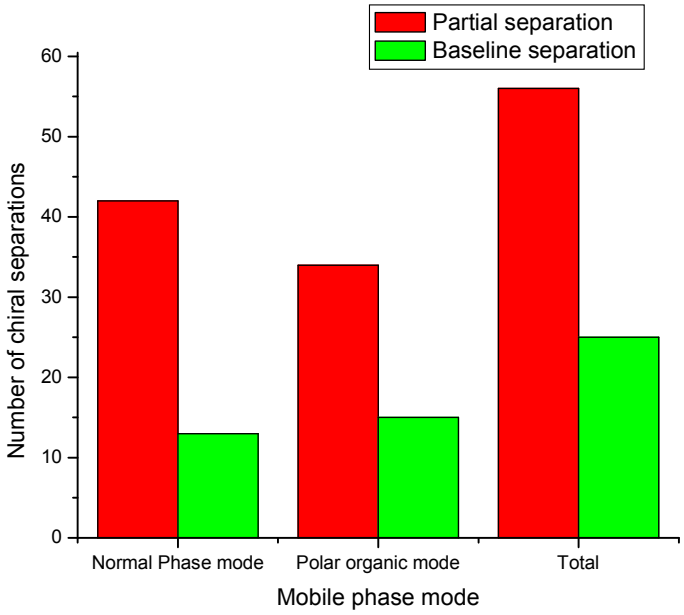

Fig. 2. Summary of the number of partial and baseline separations achieved on the poly-DPEDA CSP.

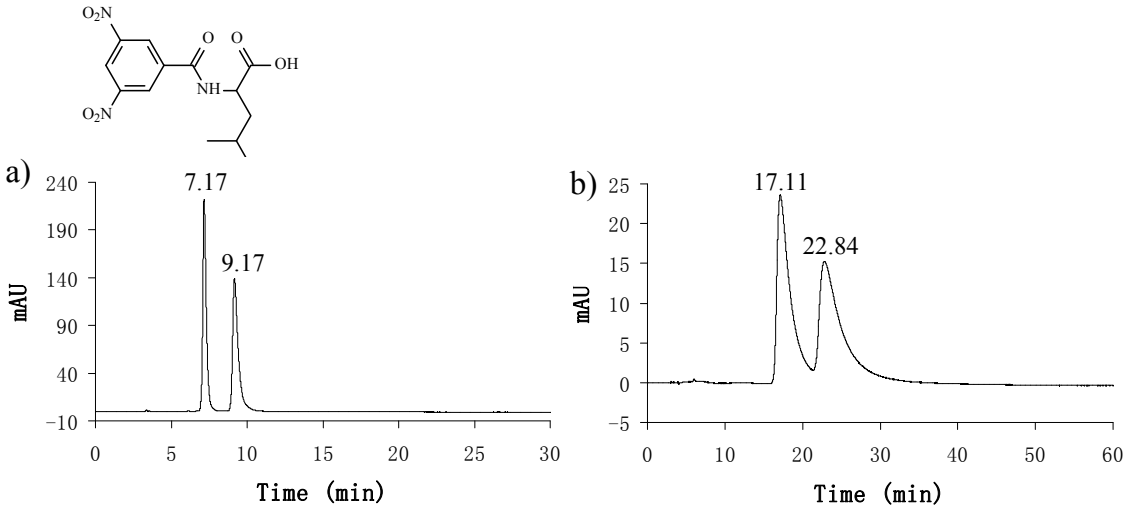

Fig. 3. Comparison of the enantiomeric separation of compound **17** in the a) polar organic mode and b) normal phase mode. Mobile phase: a) ACN/TFA = 100/0.1, b) HEP/IPA/TFA = 70/30/0.1. Enantioselectivity α: a) α = 1.50, b) α = 1.41. Resolution Rs: a) Rs = 2.8, b) Rs = 1.3. Number of theoretical plates of the first peak N_1: a) N_1 = 2500, b) N_1 = 310.

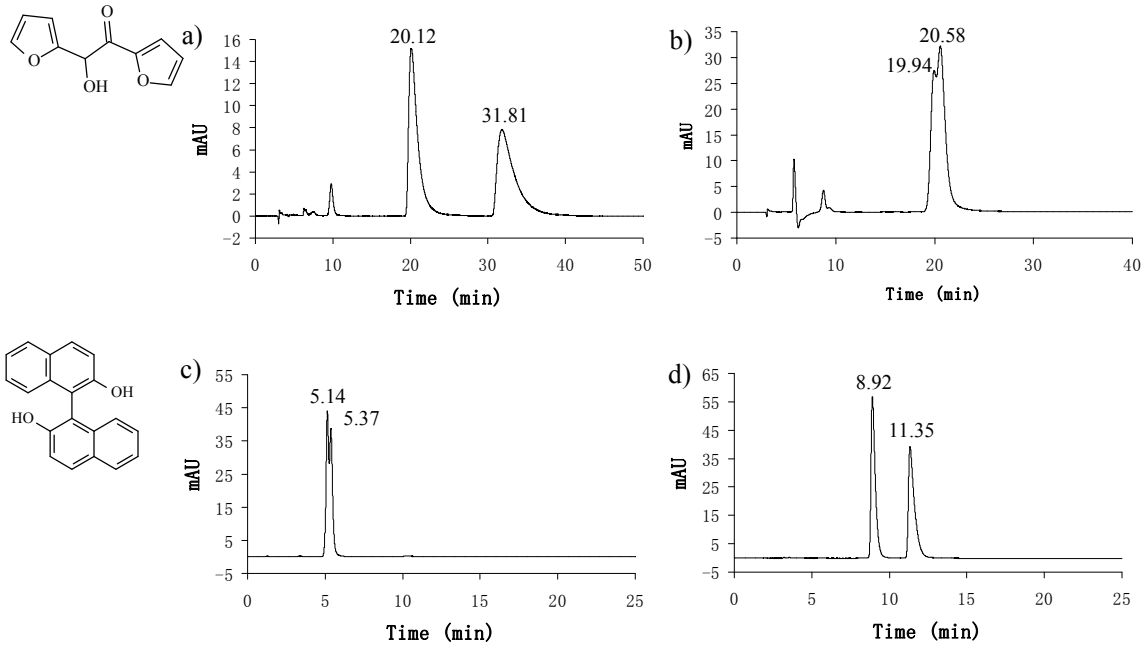

Fig. 4. Comparison of the enantiomeric separations of compound **20** (a), b)) and **4** (c), d)) on the poly DPEDA (a), c)) and P-CAP (b), d)) CSPs. Mobile phase: a) HEP/IPA/TFA = 80/20/0.1, b) HEP/IPA/TFA = 50/50/0.1, c) ACN, d) ACN/MeOH = 95/5. Enantioselectivity α: a) $\alpha = 1.69$, b) $\alpha = 1.04$, c) $\alpha = 1.11$, d) $\alpha = 1.42$.

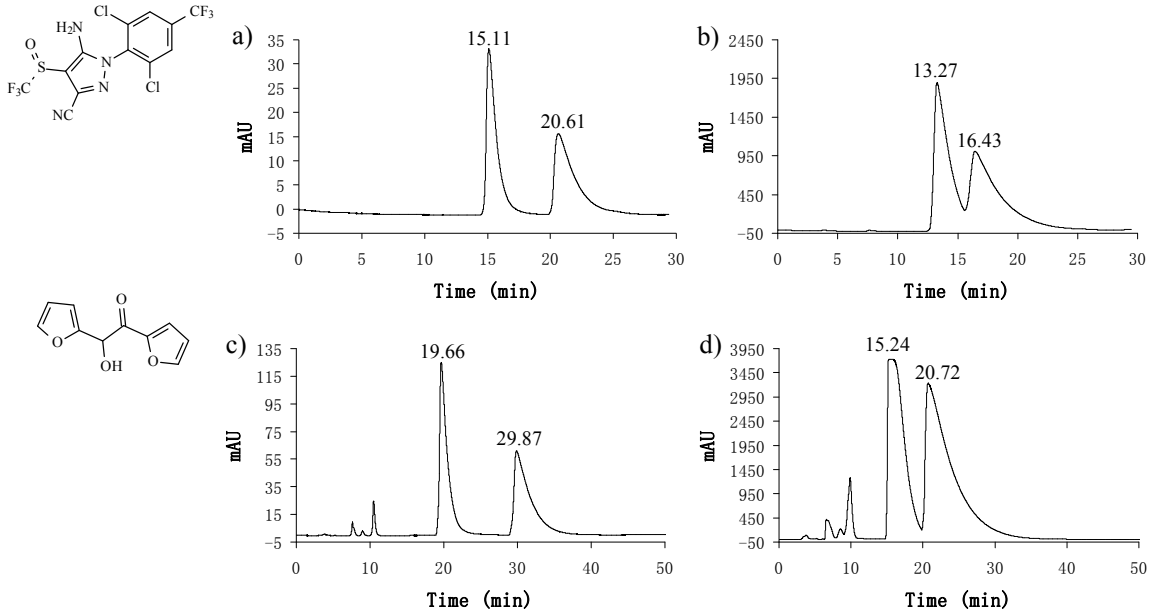

Fig. 5. The effect of sample loading on the separation of fipronil (compound **35**) with a) 7.5 µg and b) 500 µg of compound injected; and fuoroin (compound **19**) with c) 12.5 µg and d) 1000 µg of compound injected on the poly DPEDA CSP. Mobile phases: a) and b), HEP/IPA = 90/10. c) and d), HEP/IPA = 80/20.

Chpater 7. Preparation and evaluation of a new synthetic polymeric chiral stationary phase for HPLC based on the trans-9,10-dihydro-9,10-ethanoanthracene-(11S,12S)-11,12-dicarboxylic acid bis-4-vinylphenylamide monomer

A paper published in *Analytical and Bioanalytical Chemsitry*[1]

Xinxin Han, Chunlei Wang, Lingfeng He, Thomas E. Beesley,

Daniel W. Armstrong

Abstract

A new synthetic polymeric chiral stationary phase for liquid chromatography was prepared via free radical initiated polymerization of *trans*-9,10-dihydro-9,10-ethanoanthracene-(11S,12S)-11,12-dicarboxylic acid bis-4-vinylphenylamide. The new polymeric chiral stationary phase (CSP) showed enantioselectivities for many chiral compounds in multiple mobile phases. High stability and sample capacities were observed on this polymeric chiral stationary phase. Mobile phase components and additives affected chiral separation greatly. This new synthetic chiral stationary phase is complementary to two other related commercially available CSPs; the P-CAP and P-CAP-DP columns. Interactions between the chiral stationary phase and analytes that lead to retention and chiral recognition include hydrogen bonding, dipolar, and π-π interactions. Repulsive (steric) interactions also contribute to chiral recognition.

Keywords: Chiral stationary phase (CSP) · Enantioselectivity · Polymeric CSP · Preparative chromatographic separation · Normal phase LC

7.1. Introduction

HPLC on chiral stationary phases (CSPs) continues to be the most powerful and versatile method for the separation of racemates in both analytical and preparative scales [1-4]. More than 100 chiral stationary phases have been commercialized [2]. Based on the structure of the chiral selector, they can be divided into five classes: 1) polymeric, 2) macrocyclic, 3) π-π association, 4) ligand exchange, and 5) hybrid chiral stationary phases

[2]. In general, polymeric CSPs, with the exception of ones based on proteins, are highly suitable for preparative separation due to their high loading of chiral selector on the support and the fact a single bonded or adsorbed polymer molecule can interact with and separate several analyte molecules simultaneously along its length. The polymeric chiral selectors can be classified as two types by their origins [4]. One class uses natural polymers such as polysaccharides and proteins or their derivatives as chiral selectors; another class uses purely synthetic polymers as chiral selectors. Chiral stationary phases based on polysaccharide derivatives have been extensively used for the analytical and preparative separations of chiral molecules because of their broad enantioselectivities and high sample loading capacity [4-5]. Until recently, no synthetic polymeric CSP has achieved comparable success [4]. However, research on synthetic polymeric CSPs also is evolving due to a combination of attractive features such as: the richness of the possible chemical structures available, ease of their chemical modification, the possibility to obtain chiral selectors with opposite absolute configuration, and their high sample capacity [6-9].

At least four approaches have been used to make the synthetic polymeric CSPs. The first involved the co-polymerization of chiral monomers with an achiral cross-linking agent. Blaschke and his coworkers reported the first polymeric CSPs of this type [10-12]. The CSPs are polymeric beads prepared through copolymerization of chiral acrylamides or methacrylamides with ethylene diacrylate as the cross-linking agent. These CSPs could not be used under high pressure and were mainly useful for preparative purposes. A second approach used to prepare chiral polymers uses prochiral monomers via asymmetric catalyzed polymerization [4, 13]. “One-handed” helical polymers were prepared by Okamoto and co-workers from prochiral monomers such as triphenylmethyl methacrylate (TrMA) and diphenyl-2-pyridylmethyl methacrylate (D2PymA) via asymmetric catalyzed anionic polymerization [4, 13-15]. These chiral active polymers were either coated or bonded to silica gel to form CSPs. The third approach used by Allenmark and co-workers involved the catalyzed copolymerization of chiral monomers with diallyl groups with multifunctional hydrosilane molecules to form network polymeric chiral selectors [16-18]. Derivatives of *N*, *N’*-diallyl-L-tartradiamide (DATD) [16] and derivatives of *trans*-9,10-dihydro-9,10-ethanoanthracene-(11S,12S)-11,12-dicarboxylic acid [17-18] have been used as monomers.

These chiral selectors were then bonded to vinyl-functionalized silica gel to form CSPs. The separations of many compounds have been reported on these CSPs. The last approach involves the creation of a chiral linear homopolymer attached to the surface of a silica gel support. Polyacrylamide and polymethacrylamide CSPs with phenylalanine, 1-phenylethyl, 1-cyclohexylethyl [19], penicillin [20], and menthone or menthol [21] moieties were reported. These CSPs just showed enantioselectivity for a few chiral molecules. Recently, two new synthetic polymeric CSPs of this type, based on *trans*-1,2-diaminocyclohexane (commercial name = P-CAP) [6-8] and *trans*-1,2-diphenylethylenediamine (commercial name = P-CAP-DP) [9], were first developed by Gasparrini's group [6-8] and then our group [9], respectively. The "P-CAP" chiral stationary phase is prepared from radical initiated polymerization of the *N,N'*-diacryloyl derivative of *trans*-1,2-diaminocyclohexane (DACH), while the "P-CAP-DP" CSP was made from the *N,N'*-diacryloyl derivative of *trans*-1,2-diphenylethylenediamine (DPEDA). In the first case, the free radical initiator was bonded to the silica gel; while in the second case, the initiator was dissolved in the bulk reaction solution. Both CSPs were stable and can be used in multiple mobile phase modes such as the normal phase mode and the polar organic mode. Many racemates with different structures have been separated on these two synthetic polymeric CSPs. These two CSPs are known to have high sample capacities and thus have considerable potential as preparative columns; also both enantiomeric forms of these CSPs are available. Finally, these two columns are complementary to one another. Some analytes are only separated on one or the other of these two columns, and the enantioselectivities are usually different for the racemates, which can be separated on both columns.

The P-CAP CSP contains relatively rigid rings that have no aromatic moieties, while the P-CAP-DP CSP has aromatic units, and the conformation of the monomer is flexible. Another chiral monomer presented here has structural features of both of the two commercial CSPs. *trans*-9,10-Dihydro-9,10-ethanoanthracene-(11S,12S)-11,12-dicarboxylic acid provides the possibility of making a new synthetic polymeric CSP with different enantioselectivities in comparison with the P-CAP and P-CAP-DP columns. In this paper, we reported a new synthetic polymeric CSP prepared via radical initiated polymerization of the bis-4-vinylphenylamide derivative of this molecule. The synthesis of the chiral selector, its

enantiomeric resolution, bonding chemistry, and chromatographic evaluation of its enantiomeric separation abilities in the normal phase mode, and polar organic mode are presented. The effect of the polar modifier in the mobile phase, mobile phase additives, its complementary nature to related polymeric columns, and the relevant interactions that lead to chiral recognition also are discussed.

7.2. Experimental

7.2.1. Materials

Spherical silica gel (particle diameter: 5 μm, pore size: 200 Å, surface area: 213 m^2/g) functionalized with dichloride of 4,4'-azo-bis-cyanovaleric acid was obtained from Advanced Separation Technologies (Whippany, NJ, USA). Cyclobond I 2000 RSP column was also obtained from Advanced Separation Technologies. Anthracene, fumaric acid, brucine, 4-vinylaniline, triethylamine, anhydrous chloroform, anhydrous toluene, acetone, thionyl chloride, and trifluoroacetic acid (TFA) were purchased from Aldrich (Milwaukee, WI, USA). HPLC grade methylene chloride, methanol, ethanol, acetonitrile, 2-propanol, and *n*-heptane were purchased from Fisher (Fairlawn, NJ, USA).

7.2.2. Synthesis

Preparation of *trans*-9,10-dihydro-9,10-ethanoanthracene-11,12-dicarboxylic acid

The racemic dicarboxylic acid was synthesized as reported previously [18].

Anthracene (71.2 g, 0.4 mol) and fumaric acid (15.6 g, 0.134 mol) were added to 1,4-dioxane (600 mL). The solution was refluxed for 72 h. After removal of solvent under reduced pressure, 2.5% sodium carbonate solution (1 L) was added to the residue. The mixture was stirred for 24 h and filtered to remove the excessive anthracene. Hydrochloric acid (6 M) was then added to the residue until pH 1 and white precipitate appeared. The mixture was heated to reflux. After filtration of the hot mixture, 35.45 g light green solid (yield: 90%) was obtained. This product can be used directly in the next step without further purification.

Resolution of *trans*-9,10-dihydro-9,10-ethanoanthracene-11,12-dicarboxylic acid

As reported previously [18], racemic *trans*-9,10-dihydro-9,10-ethanoanthracene-11,12-dicarboxylic acid (29.4 g, 0.1 mol) and brucine (82.84g, 0.21 mol) were dissolved in 37% ethanol under reflux. After cooling the solution, the brucine salt was precipitated and

collected by filtration. After two more recrystallizations, the precipitate salts from the third recrystallization were treated with 6M HCl until pH 1 to release the (S,S)-enantiomer. Ether was added to the mixture to dissolve the diacid. The aqueous phase was extracted with ether twice. The combined ether solution was then washed with water twice. After dried over anhydrous $MgSO_4$, ether was removed under vacuum to obtain 13.17 g (S,S)-enantiomer (yield: 44.8%) in *ee* higher than 99%. (R,R)-Enantiomer 10.6 g (yield: 36.0%) in *ee* 92% were obtained via treatment of the filtrate of the first recrystallization as similar way as the precipitate. The *ee* of (R,R)-enantiomer can further increase to ≥ 95% via recrystallization of the enantiomeric enriched (R,R)-enantiomer with ether/chloroform. The enantiomeric purities were determined by HPLC on a Cyclobond I 2000 RSP column (detection wavelength: 254 nm, flow rate: 1 mL/min, mobile phase: acetoniltrile/TEAA (pH = 4.1) = 15/85). TEAA solution was prepared through addition of acetic acid to 0.1% triethylamine aqueous solution until pH 4.1. These are shown in Fig. 1.

Preparation of *trans*-9,10-dihydro-9,10-ethanoanthracene-(11S,12S)-11,12-dicarboxylic acid bis-4-vinylphenylamide (DEABV)

trans-9,10-Dihydro-9,10-ethanoanthracene-(11S,12S)-11,12-dicarboxylic acid (1.0 g, 3.40 mmol) and thionyl chloride (0.8 mL, 11.0 mmol) were added into 30 mL anhydrous toluene. The mixture was refluxed for 12 h. After removal of volatile components under vacuum, the residue was dissolved in 10 mL anhydrous chloroform. This solution was then added dropwise into the 40 mL well-stirred chloroform solution of triethylamine (1.5 mL, 11.0 mmol) and 4-vinylaniline (1.0 g, 8.40 mmol) at 0 ºC. The mixture was then raised to room temperature in 30 minutes and stirred for 12 h. The chloroform solution was washed with 1 M hydrochloric acid, 1 M sodium bicarbonate, and water twice, respectively. The organic layer was dried over sodium sulfate, filtered, and the solvent was evaporated under vacuum. The product was purified by flash chromatography on silica gel using methylene chloride as eluent to obtain 1.20 g light yellow solid (yield: 71%). ^{1}H NMR (300 MHz, $CDCl_3$): δ 8.75 (s, 2H), 7.56-7.53 (m, 2H), 7.43-7.32 (m, 10H), 7.24-7.16 (m, 4H), 6.65 (dd, J_1 = 17.4 Hz, J_2 = 11.1 Hz, 2H), 5.66 (dd, J_1 = 17.4 Hz, J_2 = 0.6 Hz, 2H), 5.18 (dd, J_1 = 11.1 Hz, J_2 = 0.6 Hz, 2H), 4.80 (s, 2H), 3.10 (s, 2H). ^{13}C NMR (75 MHz, $CDCl_3$): δ 171.6, 143.2, 140.0, 137.3, 136.2, 134.0, 127.0, 126.9, 125.7, 123.9, 120.0, 113.3, 51.0, 45.7.

Preparation of the poly-DEABV CSP

The procedure of preparation of poly-DEABV CSP is shown in Fig. 2. The silica gel functionalized with dichloride of 4,4'-azo-bis-cyanovaleric acid was synthesized as reported previously [6-7]. To 50 mL of a heated anhydrous, degassed chloroform solution of DEABV (0.7 g), silica gel functionalized with dichloride of 4,4'-azo-bis-cyanovaleric acid (3.20 g) was added under an argon atmosphere. The suspension was stirred at 60 ºC for 5 h and was heated to reflux for 1 h. The CSP was collected by filtration, washed with 100 mL of methanol, acetone, and chloroform respectively to remove the unreacted monomer. The CSP was dried under vacuum at 50 ºC over night to obtain 3.69 g. Loading: 15.30%. Elemental Analysis: C, 18.96%; H, 1.68%; N, 3.07%. The CSP was packed into a 250 mm x 4.6 mm (i. d.) stainless steel column.

7.2.3. Equipment

Chromatographic separations were carried out using a HP 1050 HPLC system with an auto sampler, a UV VWD detector, and computer controlled Chem-station data processing software (Agilent Technologies, Palo Alto, CA, USA). The mobile phases were degassed under helium for 7 min. UV detection was carried out at 254 nm for all analytes. All separations were carried out at room temperature (~ 23˚C) and the flow rate of the mobile phase for all separations was 1.0 mL min^{-1}.

7.2.4. Column evaluation

The performance of the poly-DEABV chiral stationary phase was evaluated in the polar organic mode using an acetonitrile/methanol mobile phase, and in the normal phase mode using 2-propanol/heptane, ethanol/heptane, and methylene chloride/methanol mobile phases. Before using a new mobile phase for enantiomeric separations, ten column volumes of it were pumped through the column prior to the injection of the analyte.

7.2.5. Calculations

The dead time (t_0) was estimated using the peak resulting from the change in refractive index from the injection solvent. The retention factor (k) was calculated using the equation $k = (t_r - t_0) / t_0$. The enantioselectivity (α) was calculated using $\alpha = k_2 / k_1$. The resolution factor (R_S) was calculated using the equation $R_S = 2 \times (t_{r2} - t_{r1}) / (w_1 + w_2)$, where t_{r2} and t_{r1} are the retention times of the second and first enantiomers, respectively, and w_1 and w_2 are the

corresponding base peak widths (as measured manually). The efficiency (number of theoretical plates, N) was calculated using $N = 16(t_r/w)^2$.

7.3. Results and Discussion

7.3.1. Column performance of poly-DEABV CSP

Two mobile phase modes were investigated with the new poly-DEABV CSP. They are the normal phase mode and the polar organic mode. The major solvent components for normal phase separations were heptane/isopropanol or heptane/ethanol. For the polar organic mode, the mobile phase consisted of acetonitrile with a small amount of methanol. Another combination of normal phase solvents (consisting of methylene chloride and methanol) was also evaluated. The separation factors of the separated compounds are listed in Tables 1, 2, and 3 for the three mobile phases, respectively. With the heptane/ethanol and heptane/isopropanol mobile phases, 59 enantiomeric separations and 25 baseline separations of chiral molecules were observed. The other two mobile phases were not as broadly effective as were the heptane/ethanol or heptane/isopropanol mobile phases. Only 20 enantiomeric separations and 5 baseline separations were obtained in the polar organic mode (Table 2). Nineteen separations and 7 baseline separations were acquired with the methylene chloride/methanol mobile phase (Table 3). Totally, this new polymeric CSP showed enantioselectivity for 70 chiral molecules and 28 of them were baseline separated. The number of enantiomeric separations in each mobile phase is summarized in Fig. 3. The new polymeric CSP showed enantioselectivities for 35% of all chiral molecules tested (e. g. 200 randomly chosen chiral molecules were evaluated).

The polymeric chiral selectors, which were covalently bonded to the surface of silica gel, showed exceptional stability throughout the column evaluation process. After more than 2000 injections and several mobile phase mode changes, no decrease in retention, efficiency, or enantioselectivity were observed, which indicated that no degradation of the CSP occurred.

7.3.2. Comparison of separations with the three mobile phases

Although the polar organic mode and the methylene chloride/methanol mobile phases did not produce as great a number of enantiomeric separations as the typical heptane/alcohol normal phase mobile phase, these two mobile phases have some advantages. First, 11 new separations of racemates (compounds not separated with the heptane/alcohol mobile phase)

were obtained using these two eluents (Tables 1, 2, and 3). Second, the separations with these two mobile phases are normally complete in 10 minutes or less. Finally, for some analytes such as compounds **1**, **21**, **26**, **45**, **56**, and **57**, better separations were achieved in either the polar organic mode or with the methylene chloride/methanol mobile phase compared with the same separations achieved with the heptane/alcohol mobile phase. In all cases, this improvement was due to an increase in selectivity (α) rather than in the efficiency (Tables 1, 2, and 3).

7.3.3. Effect of polar modifiers in the normal phase mode

Two polar modifiers, ethanol and isopropanol were assessed in the normal phase mode. Generally, ethanol was the better polar modifier. For most analytes, better efficiencies and resolutions were observed with the ethanol/heptane mobile phase. Typical examples are the separations of compounds **6** and **24** (Fig. 4). Although enantioselectivities of compounds **6** and **24** decreased a little bit when changing from the ethanol/heptane mobile phase to the isopropanol/heptane mobile phase, the resolutions increased greatly due to the significant improvement of peak efficiency. For compound **6**, N_1 (theoretical plate numbers of the first peak) was 2600 when ethanol was used as polar modifier, while N_1 was just 700 when isopropanol was used. For compound **2**4, N_1 also increased from 200 to 800 when the mobile phase was changed from isopropanol/heptane to ethanol/heptane. The likely reason for this is that the viscosity of ethanol is lower than that of isopropanol. The low viscosity of mobile phase improves mass transfer, thus increases efficiency and resolution. However, for a few analytes such as compounds **41** and **46**, better resolutions were achieved using the isopropanol/heptane mobile phase (data not shown). This was due to the better enantioselectivities obtained when isopropanol was used as the modifier.

7.3.4. Effect of mobile phase additive: trifluoacetic acid (TFA)

A small amount of trifluoroacetic acid (TFA) in the mobile phase plays an important role in the enantiomeric separations on this new polymeric CSP. The effect of TFA depends on the structural characteristics of the analytes. For neutral analytes without ionizable groups, addition of TFA into mobile phase has little or no effect on the enantiomeric separations. For example, no difference was observed on the retention, enantioselectivitiy, and resolution of compound **33** (Figs. 5a, 5b). However, for the separation of acidic analytes, addition of TFA

into the mobile phase can decrease the retention and increase the efficiency, selectivity and resolution in many cases. A typical example is the separation of compound **31** (Figs. 5c, 5d)). Clearly, better efficiency, enantioselectivity, and resolution were obtained when 0.1% TFA was added to the mobile phase. Another advantage of TFA is the decrease in separation time. A similar phenomenon has also been observed on the P-CAP column [8]. A small amount of TFA in the mobile phase can cover the residual amino groups on the stationary phase (Fig. 2), thus preventing strong acid-base interactions between the acidic analytes and basic sites on the stationary phase.

7.3.5. Sample loading study

This polymeric CSP showed high sample capacities and often contained high enantioselectivities, even when excess analyte was injected. For example, an excellent separation with a resolution 5.1 was achieved when 1 μg of compound **30** was injected into the column (Fig 6a). However, when 1000 μg or 5000 μg of analyte was injected into the analytical column, baseline separations still were obtained (Figs. 6b, 6c). Considering that the baseline separation of such a large amount of analyte was achieved on an analytical size column (250 x 4.6 mm), this new polymeric CSP has the potential to be an exceptional medium for preparative separations.

7.3.6. Complementary nature of the synthetic polymeric CSPs

Poly-DEABV CSP is complementary to the other two synthetic polymeric P-CAP and P-CAP-DP CSPs. For compounds that can be separated on all these three columns, different enantioselectivities were always observed [8-9]. Two examples are shown in Fig. 7. For the separation of compound **30**, the best enantioselectivity was achieved on the poly-DEABV column. However, the P-CAP column was best for the separation of compound **13**. It appears that the new polymeric CSP is particularly suitable for the separation of amino acid and oxazolidinone derivatives compared with the P-CAP and P-CAP-DP CSPs. All the amino acid derivatives (compounds **6**, **17**, **23**, **24**, **30**, **31**, **52**) and oxazolidinone derivatives (compounds **7**, **9**, **29**, **32**, **33**, **45**, **56**) tested were baseline separated, while the P-CAP and P-CAP-DP CSPs were not as effective in the separation of these compounds [8-9]. Finally, 30 enantiomeric separations of racemates were obtained that have not been reported before on either the P-CAP or the P-CAP-DP CSP.

7.3.7. Enantioselective interactions

The new DEABV CSP contains quite a number of amide linkages and aromatic groups (Fig. 2). Therefore, hydrogen bonding, dipolar, and π-π interactions likely play an important role in the chiral recognition process. Most chiral samples separated on this CSP had more than one hydrogen bonding groups such as amide, ester, carboxylic acid, and hydroxyl groups. This is similar to what was found for the P-CAP CSP [8]. However, for compounds with strong π-acid groups such as **3**, **30**, and **31**, much better enantioselectivities were observed on the new CSP than on the P-CAP CSP [8]. This indicated that π-π interactions also may affect chiral recognition. In addition, the separation of enantiomers just with one hydrogen bonding group (compounds **8** and **15**,) were found on this new CSP. This did not occur on the P-CAP CSP [8]. The only way for these separations to occur on the poly-DEABV CSP is if it can utilize one or more interactions that are not available to the related P-CAP CSP.

7.4. Conclusions

A synthetic polymeric CSP based on a new chiral monomer, *trans*-9,10-dihydro-9,10-ethanoanthracene-(11S,12S)-11,12-dicarboxylic acid bis-4-vinylphenylamide, was prepared via the surface initiated free radical polymerization method. The new CSP was stable and showed enantioselectivities for many chiral compounds in multiple mobile phases. Most enantiomeric separations were achieved with an alcohol/heptane mobile phase, while better separations for a few analytes were obtained in the polar organic mode and with a methylene chloride mobile phase. Hydrogen bonding, dipolar, and π-π interactions are important for the enantiomeric separation. In the normal phase mode, ethanol is the better polar modifier compared with isopropanol. An acidic mobile phase additive such as trifluoroacetic acid is important for the separations of many compounds with ionizable groups. This new polymeric CSP shows great potential for preparative scale applications. Furthermore, the poly-DEABV CSP is complementary to other synthetic polymeric CSPs such as the P-CAP and P-CAP-DP CSPs.

Acknowledgements

We gratefully acknowledge the support of this work by the National Institutes of Health, NIH RO1 GM53825-11.

References

[1] Armstrong DW (1997) LC-GC 59 (supplemental issue):S20-S28

[2] Armstrong DW, Zhang B (2001) Anal Chem 73:557A-561A

[3] Gasparrini F, Misiti D, Villani C (2001) J Chromatogr A 906:35-50

[4] Yamamoto C, Okamoto Y (2004) Bull Chem Soc Jpn 77:227-257

[5] Okamoto Y, Yashima E (1998) Angew Chem Int Ed 37:1020-1043

[6] Gasparrini F, Misiti D, Villani C (2003) WO Patent 2003079002

[7] Gasparrini F, Misiti D, Rompietti R, Villani C (2005) J Chromatogr A 1064:25-38

[8] Zhong Q, Han X, He L, Beesley TE, Trahanovsky WS, Armstrong DW (2005) J Chromatogr A 1066:55-70

[9] Han X, He L, Zhong Q, Beesley TE, Armstrong DW (2006) Chromatographia 63:13-23

[10] Blaschke G, Donow F (1975) Chem Ber 108:1188-1197

[11] Blaschke G, Donow F (1975) Chem Ber 108:2792-2798

[12] Blaschke G (1980) Angew Chem Int Ed 19:13-24

[13] Okamoto Y, Honda S, Okamoto I, Yuki H, Murata S, Noyori R, Tanaka H (1981) J Am Chem Soc 103:6971-6973

[14] Okamoto Y, Yashima E, Hatada K, Mislow K (1984) J Org Chem 49:557-558

[15] Okamoto Y, Mohri H, Hatada K (1989) Polym J 21:439-445

[16] Allenmark SG, Andersson S, Möller P, Sanchez D (1995) Chirality 7:248-256

[17] Thunberg L, Allenmark S, Friberg A, Ek F, Frejd T (2004) Chirality 16:614-624

[18] Thunberg L, Allenmark S (2004) J Chromatogr A 1026: 65-76

[19] Blaschke G, Bröker W, Fraenkel W (1980) Angew Chem Int Ed 25:830-831

[20] Saotome Y, Miyazawa T, Endo T (1989) Chromatographia 28:505-508

[21] Arlt D, Bömer B, Grosser R, Lang W (1991) Angew Chem Int Ed 30:1662-1664

Table 1. Retention factor of the first peak (k_1), enantioselectivity (α), and enantiomeric resolution (Rs) of the separated racemic compounds on the poly-DEABV column in the normal phase mode

#	Compound	Structure	k_1	α	R_s	Mobile Phase (v/v)[a]
1	N-Acetylhomo-cysteine thiolactone	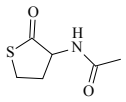	3.27	1.10	0.9	HEP/EtOH/TFA = 70/30/0.1
2	*O*-Acetyl-mandelic acid	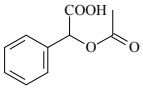	3.70	1.07	0.7	HEP/EtOH/TFA = 90/10/0.1
3	1-(2-Aminocyclohexyl)-3-(3, 5-bis-trifluoromethyl -phenyl)urea	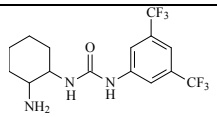	3.58	1.33	1.6	HEP/EtOH/TFA = 90/10/0.1
4	*cis*-1-Amino-2-indanol	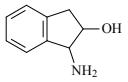	3.19	1.12	0.8	HEP/EtOH/TFA = 70/30/0.1
5	Benzoin	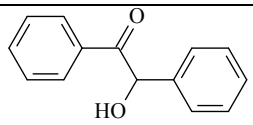	5.48	1.07	0.9	HEP/EtOH/TFA = 95/5/0.1
6	N-Benzoyl-valine	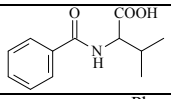	5.20	1.30	2.7	HEP/EtOH/TFA = 90/10/0.1
7	4-Benzyl-5,5-dimethyl-2-oxazolidinone	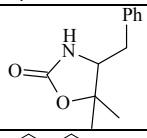	1.63	1.20	1.5	HEP/EtOH/TFA = 60/40/0.1
8	N-Benzyl-1-(1-naphthyl)-ethylamine	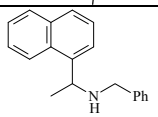	4.21	1.12	0.5	HEP/EtOH/TFA = 70/30/0.1
9	4-Benzyl-2-oxazolidinone	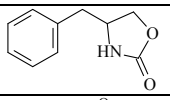	2.58	1.24	1.6	HEP/EtOH/TFA = 60/40/0.1
10	3-(Benzyloxycarbonyl)-4-oxazolidine carboxylic acid	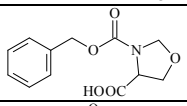	3.79	1.06	0.5	HEP/EtOH/TFA = 80/20/0.1
11	Benzylphthalide	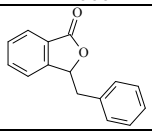	3.58	1.07	0.7	HEP/EtOH/TFA = 80/20/0.1
12	4-Benzyl-3-propoinyl-2-oxazolidinone	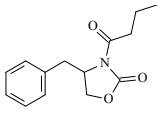	6.43	1.23	1.9	HEP/EtOH/TFA = 80/20/0.1
13	1, 1'-Bi-2-naphthol	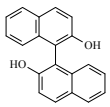	8.65	1.07	0.7	HEP/EtOH/TFA = 90/10/0.1

Table 1. (continued)

#	Compound	Structure	k_1	α	R_s	Mobile Phase (v/v)[a]
14	N,N'-Bis(α-methyl-benzyl)sulfamide	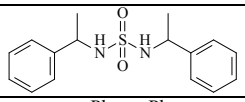	4.67	1.05	0.5	HEP/EtOH/TFA = 80/20/0.1
15	Bis[1-phenylethyl]-amine hydrochloride	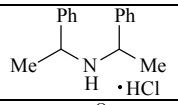	4.11	1.30	1.7	HEP/EtOH/TFA = 80/20/0.1
16	α-Carbethoxy-γ-phenyl-γ-butyrolactone	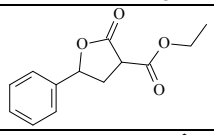	6.67	1.12	1.5	HEP/EtOH/TFA = 90/10/0.1
17	Carbobenzyloxy-alanine	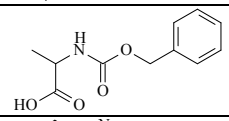	2.33	1.33	2.5	HEP/EtOH/TFA = 80/20/0.1
18	Carprofen	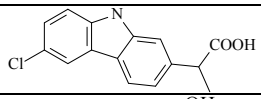	3.72	1.09	0.7	HEP/EtOH/TFA = 80/20/0.1
19	4-Chloromandelic acid	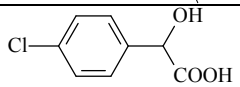	11.3	1.03	0.4	HEP/EtOH/TFA = 95/5/0.1
20	4-Chlorophenyl-2, 3-epoxypropyl ether	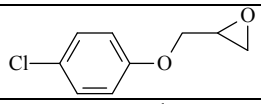	3.51	1.04	0.7	HEP/EtOH/TFA = 100/1/0.1
21	Chlorthalidone	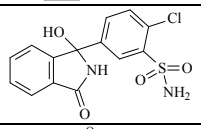	5.48	1.12	0.7	HEP/EtOH/TFA = 60/40/0.1
22	*trans*-4-Cotinine-carboxylic acid	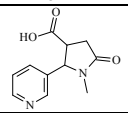	4.63	1.13	0.7	HEP/EtOH/TFA = 60/40/0.1
23	Dansyl-norleucine cyclohexylammonium salt	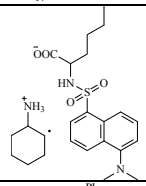	4.37	1.24	1.5	HEP/EtOH/TFA = 80/20/0.1
24	Dansyl-phenylalanine cyclohexylammonium salt	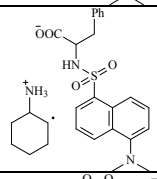	2.60	1.49	1.8	HEP/EtOH/TFA = 60/40/0.1
25	2,3-Dibenzoyl-tartaric acid	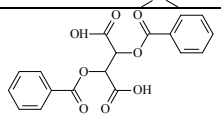	7.41	1.23	1.5	HEP/EtOH/TFA = 80/20/0.1
26	N,N'-Dibenzyl-tartramide	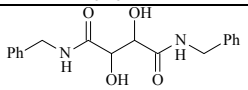	4.42	1.33	1.6	HEP/EtOH/TFA = 70/30/0.1
27	3,4-Dihydroxyphenyl-α-propylacetamide	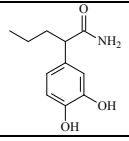	5.99	1.05	0.5	HEP/EtOH/TFA = 80/20/0.1

Table 1. (continued)

#	Compound	Structure	k_1	α	R_s	Mobile Phase (v/v)[a]
28	1,5-Dimethyl-4-phenyl-2-imidazolidinone	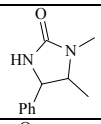	2.67	1.08	0.8	HEP/EtOH/TFA = 80/20/0.1
29	5,5-Dimethyl-4-phenyl-2-oxazolidinone	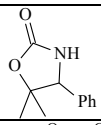	3.63	1.18	1.5	HEP/EtOH/TFA = 80/20/0.1
30	N-(3,5-Dinitrobenzoyl)-leucine	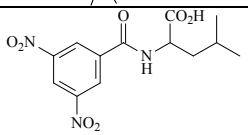	1.79	3.93	5.1	HEP/EtOH/TFA = 60/40/0.1
31	N-(3,5-Dinitrobenzoyl)- -phenylglycine	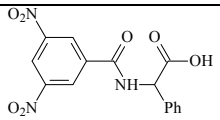	4.52	1.87	2.8	HEP/EtOH/TFA = 60/40/0.1
32	4-(Diphenylmethyl)-2-oxazolidinone	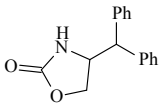	5.23	1.23	1.6	HEP/EtOH/TFA = 70/30/0.1
33	*cis*-4,5-Diphenyl-2-oxazolidinone	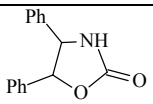	2.57	1.30	1.8	HEP/EtOH/TFA = 60/40/0.1
34	Flavanone	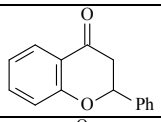	2.96	1.06	0.7	HEP/EtOH/TFA = 95/5/0.1
35	Furoin	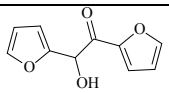	9.29	1.03	0.5	HEP/EtOH/TFA = 90/10/0.1
36	Guaiacol glyceryl ether carbamate	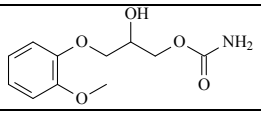	3.62	1.05	0.5	HEP/EtOH/TFA = 70/30/0.1
37	Hydrobenzoin	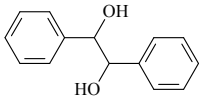	7.03	1.04	0.5	HEP/EtOH/TFA = 95/5/0.1
38	2-(4-Hydroxyphenoxy)-propionic acid	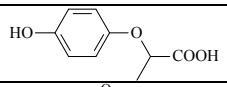	2.89	1.09	0.8	HEP/EtOH/TFA = 80/20/0.1
39	4-((1-(Isopropoxycarbonyl-4-methyl)-butyl)amino)-benzoic acid	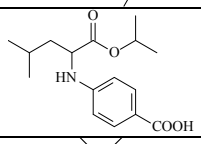	1.10	2.68	3.3	HEP/EtOH/TFA = 60/40/0.1
40	2,3-O-Isopropylidene-2,3-dihydroxy-1,4-bis-(diphenylphosphino)butane	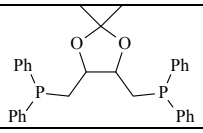	3.64	1.35	1.3	HEP/EtOH/TFA = 60/40/0.1
41	Ketamine hydrochloride	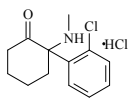	8.77	1.17	0.5	HEP/IPA/TFA = 50/50/0.1

Table 1. (continued)

#	Compound	Structure	k_1	α	R_s	Mobile Phase (v/v)[a]
42	Lormetazepam	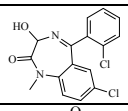	3.51	1.37	1.6	HEP/EtOH/TFA = 60/40/0.1
43	Mandelamide	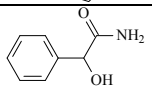	6.67	1.17	1.7	HEP/EtOH/TFA = 85/15/0.1
44	N-(α-Methylbenzyl)phthalic acid monoamide	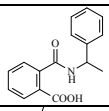	2.38	1.16	0.9	HEP/EtOH/TFA = 70/30/0.1
45	*cis*-4-Methyl-5-phenyl-2-oxazolidinone	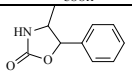	11.3	1.15	1.7	HEP/EtOH/TFA = 90/10/0.1
46	α-Methyl-α-phenyl-succinimide	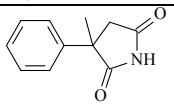	3.73	1.05	0.4	HEP/IPA/TFA = 70/30/0.1
47	Omeprazole	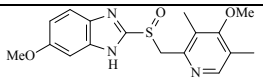	6.04	1.42	1.4	HEP/EtOH/TFA = 60/40/0.1
48	Oxazepam	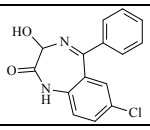	18.0	1.18	0.8	HEP/EtOH/TFA = 85/15/0.1
49	N-(α-Methylbenzyl)-phthalimide	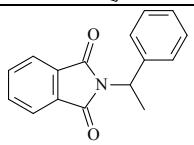	2.75	1.04	0.4	HEP/EtOH/TFA = 95/5/0.1
50	5-(α-Phenylethyl)-semioxamazide	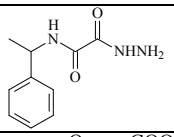	2.77	1.13	0.6	HEP/EtOH = 60/40
51	2-Phenoxypropionic acid	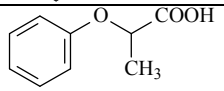	3.66	1.07	0.7	HEP/EtOH/TFA = 95/5/0.1
52	N-Carbobenzoxy-phenylalanine	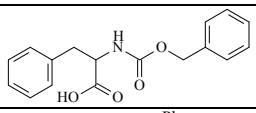	1.09	1.58	2.2	HEP/EtOH/TFA = 60/40/0.1
53	3-Phenylphthalide	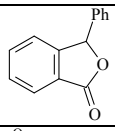	10.0	1.10	1.5	HEP/EtOH/TFA = 95/5/0.1
54	5-Phenyl-2-(2-propynylamino)-2-oxazolin-4-one	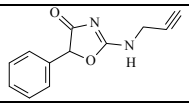	5.04	1.21	1.5	HEP/EtOH/TFA = 70/30/0.1
55	Propranolol hydrochloride	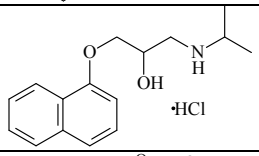	4.02	1.11	0.5	HEP/EtOH/TFA = 70/30/0.1
56	*cis*-3,3a,8,8a-Tetrahydro-2H-indeno[1,2-d]oxazol-2-one	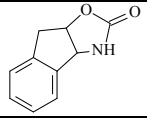	12.4	1.13	1.5	HEP/EtOH/TFA = 85/15/0.1

Table 1. (continued)

#	Compound	Structure	k_1	α	R_s	Mobile Phase (v/v)[a]
57	3a,4,5,6-Tetrahydro-succininido[3,4-b]-acenaphthen-10-one	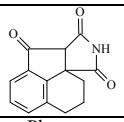	6.96	1.16	0.9	HEP/EtOH/TFA = 60/40/0.1
58	Trihexyphenidyl	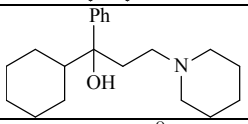	7.72	1.08	0.5	HEP/EtOH/TFA = 80/20/0.1
59	Warfarin	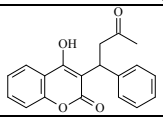	14.1	1.05	0.4	HEP/EtOH/TFA = 90/10/0.1

[a] HEP: *n*-heptane. EtOH: ethanol. IPA: isopropanol. TFA: trifluoroacetic acid.

Table 2. Retention factor of the first peak (k_1), enantioselectivity (α), and enantiomeric resolution (Rs) of the separated racemic compounds on the poly-DEABV column in the polar organic mode

#	Compound	Structure	k_1	α	R_s	Mobile Phase (v/v)[a]
1	N-Acetylhomo-cysteine thiolactone	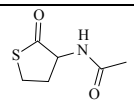	0.27	1.07	0.3	ACN/TFA=100/0.1
7	4-Benzyl-5,5-dimethyl-2-oxazolidinone	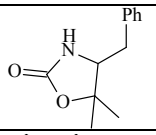	0.18	1.28	0.7	ACN/TFA =100/0.1
9	4-Benzyl-2-oxazolidinone	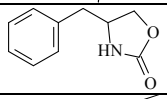	0.24	1.32	1.3	ACN/TFA =100/0.1
12	4-Benzyl-3-propoinyl-2-oxazolidinone	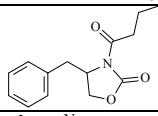	0.25	1.32	1.4	ACN/TFA =100/0.1
18	Carprofen	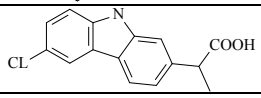	0.85	1.06	0.4	ACN/TFA =100/0.1
26	N,N'-Dibenzyl-tartramide	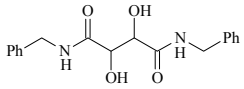	0.68	1.48	2.0	ACN/MeOH/TFA =100/1/0.1
29	5,5-Dimethyl-4-phenyl-2-oxazolidinone	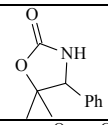	0.23	1.43	1.4	ACN/ TFA=100/0.1
30	N-(3,5-Dinitro-benzoyl)-leucine	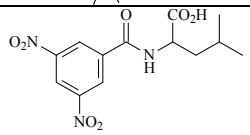	0.30	2.31	2.6	ACN/MeOH/TFA =100/1/0.1
31	N-(3,5-Dinitrobenzoyl)- -phenylglycine	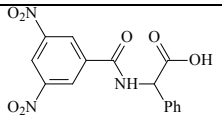	0.50	1.40	1.4	ACN/MeOH/TFA =100/1/0.1
32	4-(Diphenylmethyl)-2-oxazolidinone	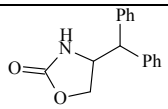	0.29	1.38	1.6	ACN/TFA =100/0.1
33	*cis*-4,5-Diphenyl-2-oxazolidinone	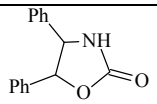	0.26	1.54	1.9	ACN/TFA =100/0.1
39	4-((1-(Isopropoxycarbonyl-4-methyl)-butyl)amino)-Benzoic acid	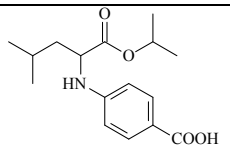	0.04	6.06	3.0	ACN/TFA =100/0.1
44	N-(α-Methylbenzyl)phthalic acid monoamide	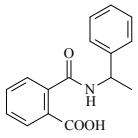	0.46	1.15	0.6	ACN/MeOH/TFA =100/1/0.1

Table 2. (continued)

#	Compound	Structure	k_1	α	R_s	Mobile Phase (v/v)[a]
45	*cis*-4-Methyl-5-phenyl-2-oxazolidinone	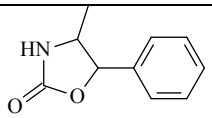	0.24	1.25	0.8	ACN/TFA =100/0.1
52	Z-Phenylalanine	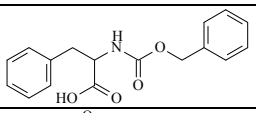	0.33	1.33	1.0	ACN/TFA =100/0.1
54	5-Phenyl-2-(2-propynylamino)-2-oxazolin-4-one	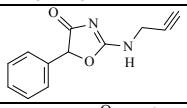	0.31	1.16	0.5	ACN/MeOH/TFA =100/1/0.1
56	*cis*-3,3a,8,8a-Tetrahydro-2H-indeno[1,2-d]oxazol-2-one	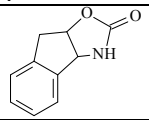	0.38	1.24	1.3	ACN/TFA =100/0.1
60	Bendroflumethiazide	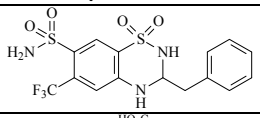	0.10	1.40	0.4	ACN/TFA =100/0.1
61	Sulindac	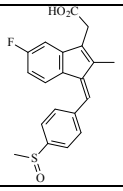	1.38	1.05	0.4	ACN/MeOH/TFA =100/1/0.1
62	1,2,3,4-Tetrahydro-1-naphthylamine	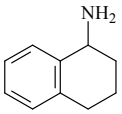	0.38	1.24	1.4	ACN/TFA =100/0.1

[a] ACN: acetonitrile. MeOH: methanol. TFA: trifluoroacetic acid.

Table 3. Retention factor of the first peak (k_1), enantioselectivity (α), and enantiomeric resolution (Rs) of the separated racemic compounds on the poly-DEABV column in the normal-phase mode with halogenated solvent

#	Compound	Structure	k_1	α	R_s	Mobile Phase (v/v)[a]
1	N-Acetylhomo-cysteine thiolactone	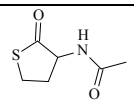	0.93	1.22	1.3	CH_2Cl_2/MeOH /TFA = 99/1/0.1
4	*Cis*-1-Amino-2-indanol	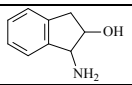	3.62	1.13	0.8	CH_2Cl_2/MeOH /TFA = 95/5/0.1
9	4-Benzyl-2-oxazolidinone	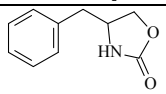	0.11	2.04	1.8	CH_2Cl_2/MeOH /TFA = 95/5/0.1
18	Carprofen	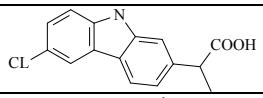	1.65	1.10	0.6	CH_2Cl_2/MeOH /TFA = 97/3/0.1
21	Chlorthalidone	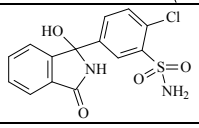	2.77	1.21	1.4	CH_2Cl_2/MeOH /TFA = 95/5/0.1
26	N,N'-Dibenzyl-tartramide	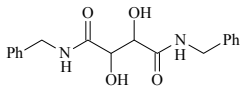	0.26	1.43	1.5	CH_2Cl_2/MeOH /TFA = 95/5/0.1
45	*cis*-4-Methyl-5-phenyl-2-oxazolidinone	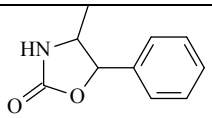	1.18	1.32	2.2	CH_2Cl_2/MeOH /TFA = 99/1/0.1
54	5-Phenyl-2-(2-propynylamino)-2-oxazolin-4-one	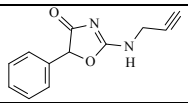	0.96	1.18	1.4	CH_2Cl_2/MeOH /TFA = 97/3/0.1
56	*cis*-3,3a,8,8a-Tetrahydro-2H-indeno[1,2-d]oxazol-2-one	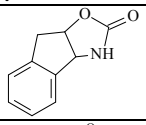	0.36	1.70	2.6	CH_2Cl_2/MeOH /TFA = 95/5/0.1
57	3a,4,5,6-Tetrahydro-succininido[3,4-b]-acenaphthen-10-one	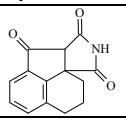	0.95	1.30	2.0	CH_2Cl_2/MeOH /TFA = 97/3/0.1
62	1,2,3,4-Tetrahydro-1-naphthylamine	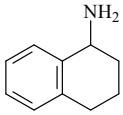	0.40	1.70	2.7	CH_2Cl_2/MeOH /TFA = 95/5/0.1
63	N-Desmethylnefopam	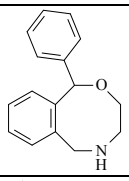	0.94	1.26	1.1	CH_2Cl_2/MeOH /TFA = 95/5/0.1
64	1,2-Diphenylethylene-diamine	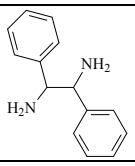	0.69	1.39	1.1	CH_2Cl_2/MeOH /TFA = 95/5/0.1

Table 3. (continued)

#	Compound	Structure	k_1	α	R_s	Mobile Phase (v/v)[a]
65	α, α-Diphenylprolinol	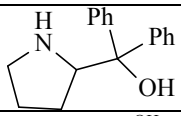	0.95	1.26	1.4	CH_2Cl_2/MeOH /TFA = 95/5/0.1
66	5-Hydroxymethyl-2(5H)-furanone	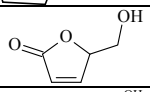	1.75	1.28	2.0	CH_2Cl_2/MeOH /TFA = 99/1/0.1
67	5-(4-Hydroxyphenyl)-5-phenylhydantoin	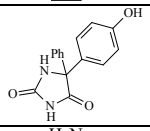	4.85	1.13	0.8	CH_2Cl_2/MeOH /TFA = 95/5/0.1
68	1-(1-Naphthyl)ethylamine	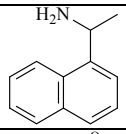	3.20	1.08	0.6	CH_2Cl_2/MeOH /TFA = 95/5/0.1
69	Ofloxacine	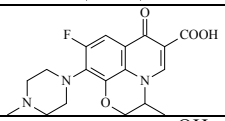	0.83	1.34	0.9	CH_2Cl_2/MeOH /TFA = 95/5/0.1
70	2-Phenylglycinol	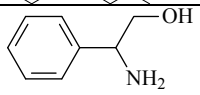	3.75	1.12	0.7	CH_2Cl_2/MeOH /TFA = 95/5/0.1

[a] MeOH: methanol. TFA: trifluoroacetic acid. CH_2Cl_2: methylene chloride.

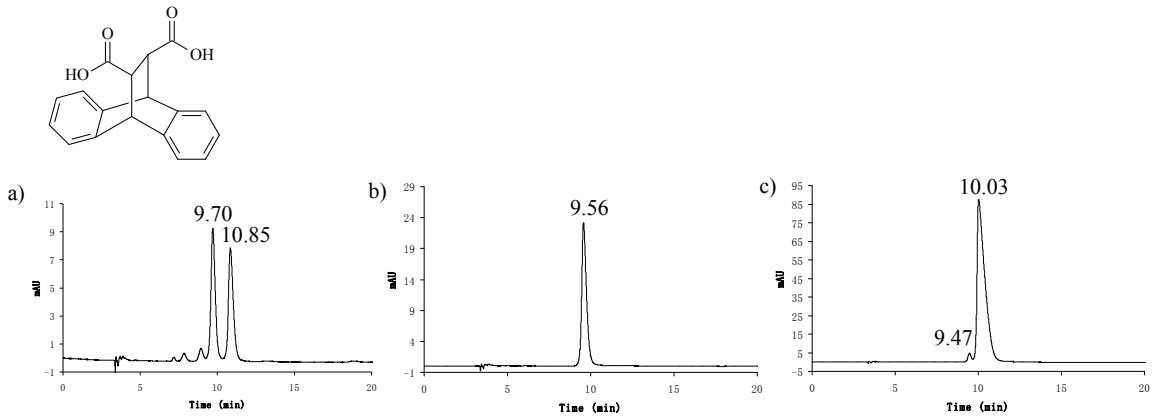

Fig. 1. Enantiomeric separation of the synthesized chiral dicarboxylic acid (*trans*-9,10-dihydro-9,10-ethanoanthracene-11,12-dicarboxylic acid) from which the new chiral selector was made. a) Racemate, b) Purified (S,S)-enantiomer, c) Purified (R,R)-enantiomer. The separations were done on a Cyclobond I 2000 RSP column. Mobile phase: Acetonitrile/TEAA buffer (pH=4.1) = 15/85. Flow rate: 1 mL/min. Detection wavelength: 254 nm.

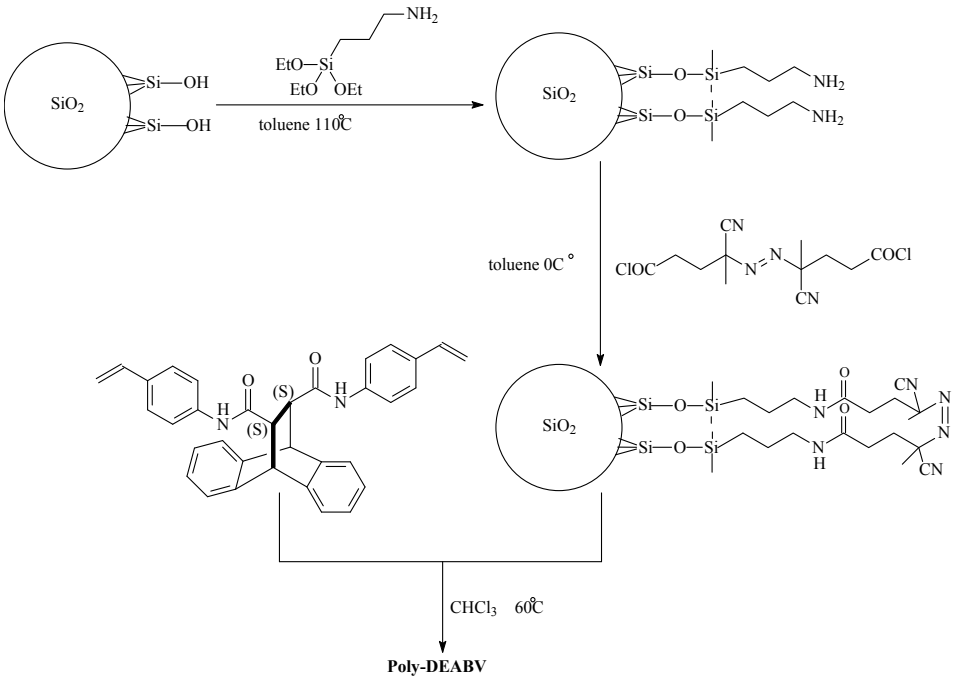

Fig. 2. Preparation of the poly-DEABV chiral stationary phase.

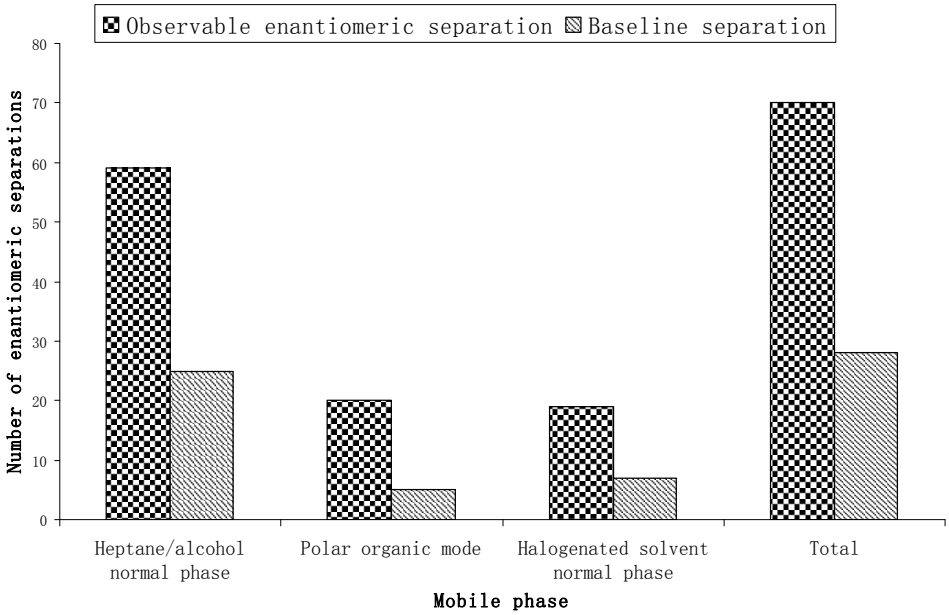

Fig. 3. Summary of the number of observable (Rs ≥ 0.4) and baseline separations (Rs ≥ 1.5) achieved on the poly-DEABV CSP.

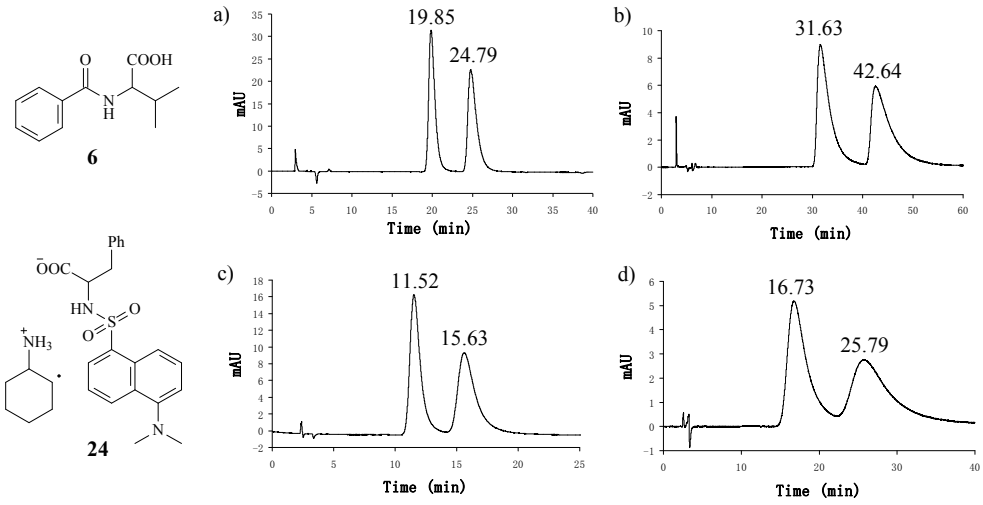

Fig. 4. The effect of polar modifier on the enantiomeric separations of compounds **6** (a), b)) and **24** (c), d)) in the normal phase mode. Mobile phase: a) Heptane/Ethanol/TFA = 90/10/0.1, b) Heptane/Isopropanol/TFA = 90/10/0.1, c) Heptane/Ethanol/TFA = 60/40/0.1, d) Heptane/Isopropanol/TFA = 50/50/0.1. Enantioselectivity, α: a) α = 1.30, b) α = 1.39, c) α = 1.49, d) α = 1.67. Resolution, Rs: a) Rs = 2.7, b) Rs = 1.8, c) Rs = 1.8, d) Rs = 1.4. Number of theoretical plates of the first peak, N_1: a) N_1 = 2600, b) N_1 = 700, c) N_1 = 800, d) N_1 = 200.

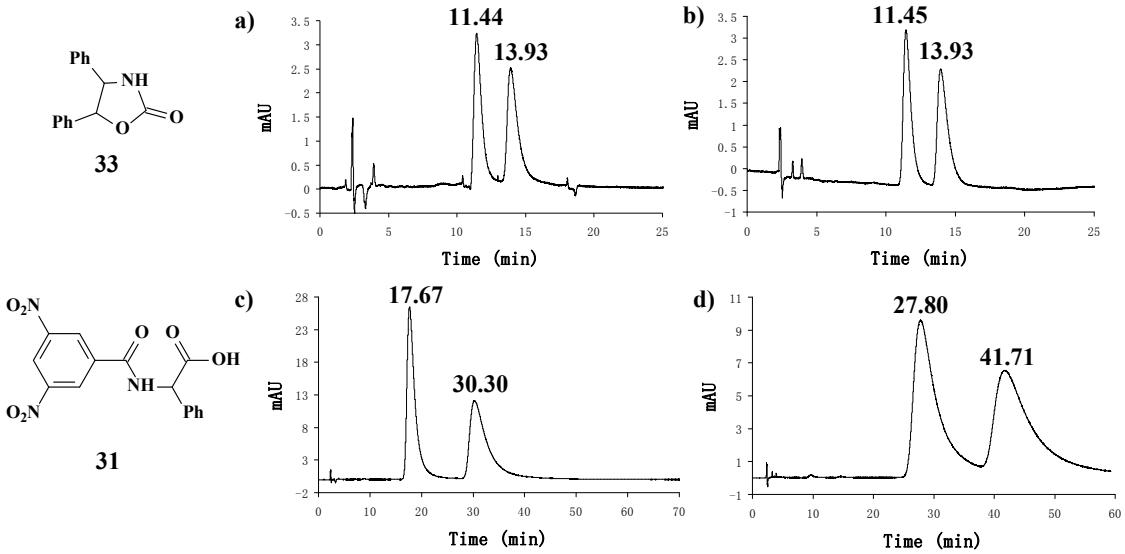

Fig. 5. The effect of the acidic additive on the enantiomeric separations of compound **33** (a), b)) and **31** (c), d)) in the normal phase mode. Mobile phase: a), c) Heptane/Ethanol/TFA = 60/40/0.1, b), d) Heptane/Isopropanol/TFA = 60/40. Enantioselectivity, α: a), b) α = 1.30, c) α = 1.87, d) α = 1.54. Resolution, Rs: a), b) Rs = 1.8, c) Rs = 2.8, d) Rs = 1.4.

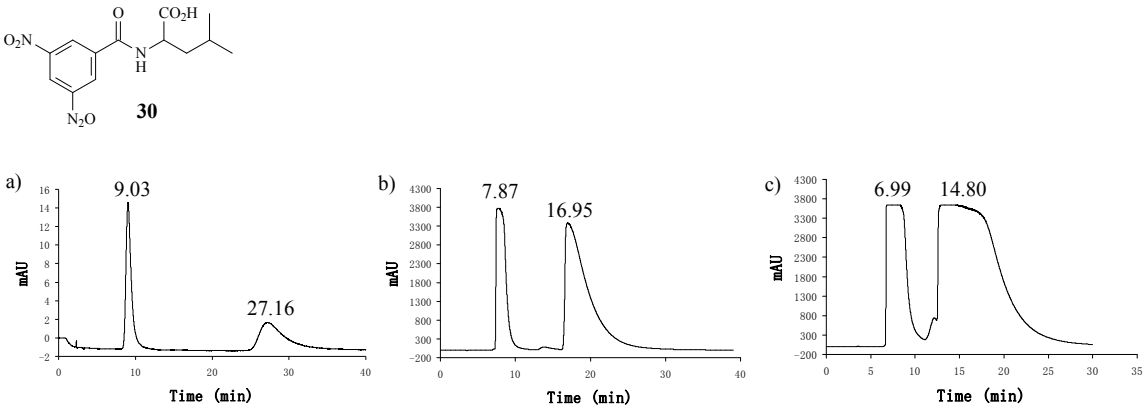

Fig. 6. The effect of sample loading on the enantiomeric separation of compound **30** with a) 1.0 μg, b) 1000 μg, and c) 5000 μg of analyte injected on the poly DEABV CSP. Mobile phases: a), b), and c) Heptane/Ethanol/TFA = 60/40/0.1.

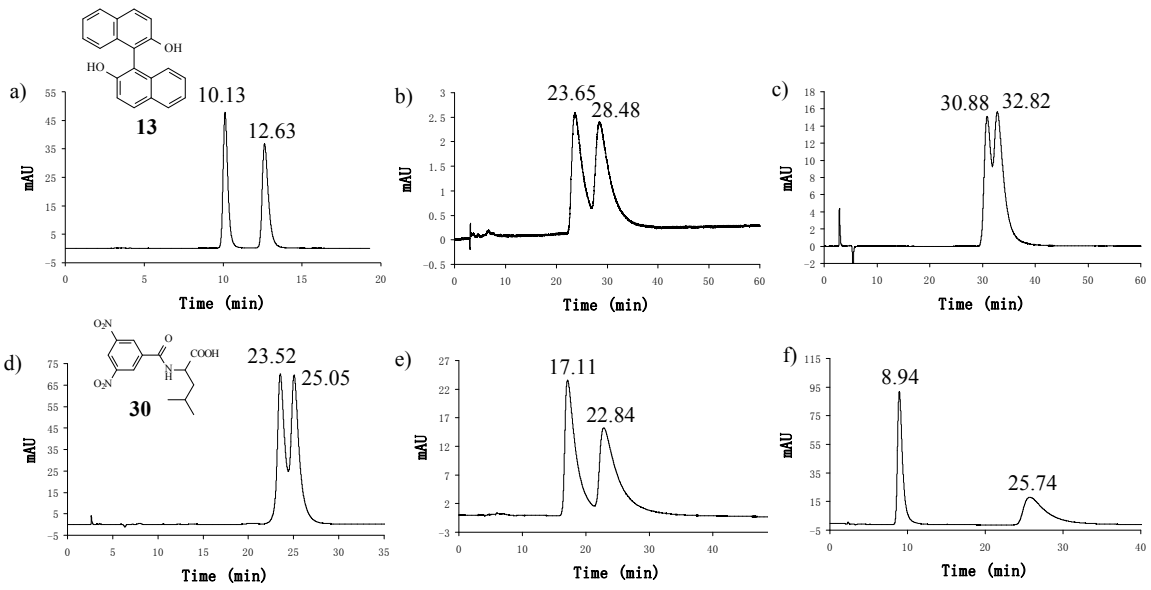

Fig. 7. Comparison of the enantiomeric separations of compound **13** (a), b), c)) and **30** (d), e), f)) on the P-CAP (a), d)), P-CAP-DP (b), e)), and poly-DEABV (c), f)) CSPs. Mobile phase: a) Heptane/Ethanol/TFA = 90/10/0.1, b) Heptane/Isopropanol = 80/20, c) Heptane/Isopropanol = 50/50, d) Heptane/Ethanol/TFA = 80/20/0.1, e) Heptane/Isopropanol/TFA = 70/30/0.1, f) Heptane/Ethanol/TFA = 60/40/0.1. Enantioselectivity, α: a) $\alpha = 1.36$, b) $\alpha = 1.23$, c) $\alpha = 1.07$, d) $\alpha = 1.07$, e) $\alpha = 1.41$, f) $\alpha = 3.93$.

Chapter 8. Super/subcritical fluid chromatography separations with four synthetic polymeric chiral stationary phases

A paper published in *Chromatographia*[1]

X. Han, A. Berthod, C. Wang, K. Huang, D. W. Armstrong

Abstract

New synthetic polymeric chiral selectors were developed recently as chiral stationary phases. They were tested with supercritical fluid mobile phases made of CO_2 plus an alcohol modifier and 0.2% v/v trifluoroacetic acid. The polymeric *N,N'*-(1S,2S)-1,2-cyclohexanediyl-bis-2-propenamide (P-CAP), the polymeric *N,N'*-[(1R,2R)]-1,2-diphenyl-1,2-ethanediyl] bis-2-propenamide (P-CAP-DP), the polymeric *trans*-9,10-dihydro-9,10-ethanoanthracene-(11S,12S)-11,12-dicarboxylic acid bis-4-vinylphenylamide (DEABV) and the polymeric *N,N'*-[(1R,2R)-1,2-diphenyl-1,2-ethanediyl] bis-4-vinylbenzamide (DPEVB) were bonded to 5 µm silica particles and used to prepare four columns that were tested with a set of 88 chiral compounds with a wide variety of chemical functionalities. All 88 test compounds were separated on one or more of these ‘‘related’’ polymeric CSPs. Forty-three enantiomeric pairs were separated in SFC conditions by only one of the CSPs. Twenty pairs were separated by two CSPs and 18 and 7 enantiomeric pairs were separated by 3 and all 4 CSPs, respectively. The three P-CAP, P-CAP-DP and DEABV CSPs have equivalent success being able to separate 49 enantiomeric pairs of the studied set with respectively 12, 14 and 20 at baseline (Rs > 1.5). The DPEVB CSP was significantly less efficient separating only 18 chiral compounds with only one at baseline. The great advantage of the SFC mobile phases is the rapid separation, which most achieved in less than 5 min.

Keywords: Supercritical fluid chromatography, Enantiomeric separations, Enantioselectivity, Synthetic polymeric chiral stationary phases

8.1. Introduction

Liquid chromatography chiral stationary phases (CSPs) can be used for analytical and preparative enantiomeric separations. However, the effectiveness of different classes of CSPs

[1] Reprinted with permission of C*hromatographia*, 2007, 65, 381-400.

at each task can vary widely. Modern chiral selectors include π-complex, ligand exchange, chiral crown ethers, cyclodextrins, polysaccharides, proteins and macrocyclic glycopeptide chiral selectors [1, 2]. All these chiral selectors were found to be very useful in separating enantiomers on an analytical scale (microgram to milligram amounts). One of the important challenges in enantiomeric separations is enhancing production, i.e. going to gram, kilogram and even to greater amounts in a facile manner. Many polymeric chiral selectors have a significant higher loading capability than smaller chiral selectors [1]. An exception to this statement is the protein CSPs which have very low capacities. Successful polymeric CSPs include natural polymers such as polysaccharide derivatives, cellulose and amylose carbamates, or synthetic polymers such as polyamides, vinyl polymers, polyurethanes and polyacetylene derivatives [3–5], polymetacrilates and polytartardiamide based CSPs [6–10]. Recent polymeric chiral selectors based on trans-1,2-diaminocyclohexane were found very useful when used to prepare CSPs for normal phase liquid chromatography (NPLC) [5, 11–13].

The need for preparative enantiomeric separations is driving the renewed interest in supercritical fluid chromatography (SFC). In the 1980s, some studies overestimated the solvent strength of supercritical CO_2 and this lead to some disappointments especially in the applicability of capillary SFC [14]. It became clear that some percentage of a more polar cosolvent, like methanol, was needed to elute most analytes. With the increased interest in high throughput separations, preparative separations and solvent disposal concerns, SFC with packed columns underwent a rebirth as a potential replacement for NPLC [15].

Enantiomeric separations using SFC with packed columns were first performed by Mourier et al. [16] separating phosphine oxide enantiomers on a π-complex based CSP. Supercritical CO_2, almost exclusively used in its subcritical state associated with significant amounts of organic modifier, was found to increase dramatically the preparative productivity of enantiomeric separations [17, 18]. Many different CSPs have been used in packed column SFC [19, 20].

The focus of this work is to evaluate the enantioselective capabilities of the recently introduced synthetic polymeric CSPs in SFC [5, 11]. Two new related polymeric CSPs will also be evaluated with the same set of solutes and SFC mobile phases. The results obtained

with the four CSPs will be discussed and compared. A set of 88 chiral compounds with a wide variety of functionalities was used to test the four CSPs. Experimental conditions were deliberately selected to favor fast rather than efficient separations. The results obtained on the four CSPs are compared and discussed in terms of enantiorecognition capabilities. The other properties that must be studied when dealing with a new CSP, such as pH and thermal stabilities and loading capability, will not be treated in this work exclusively dedicated to SFC enantioselectivity.

8.2. Experimental

8.2.1. Chemicals

Eighty-eight enantiomeric pairs with a wide variety of functionalities were evaluated on four different polymeric CSPs. All the test compounds could be placed into one of four classes: (1) compounds with a sp^2 hybridized carbon directly attached to the asymmetric center; (2) compounds whose asymmetric center is part of a ring; (3) chiral acids and derivatized amino-acids; (4) other compounds including atropoisomers, alcohols, and stereogenic phosphorous and sulfoxide compounds. All analytes were obtained from Sigma (St. Louis, MO, USA) or Aldrich (Milwaukee, WI, USA). The set of compounds contains only nine highly basic analytes that were all separated in their cationic (acidified) form. Stock solutions of 1 mg mL^{-1} of each compound were prepared and injected individually on the four polymeric CSPs.

8.2.2. Chiral Stationary Phases

Figure 1 shows the chiral monomers used to prepare the four synthetic polymeric CSPs evaluated in this work. All chiral selectors were bonded on spherical 5 µm porous silica gel (Akzo Nobel, EKA Chemicals AB, Sweden, pore size 20 nm, pore volume 0.9 mg L^{-1}, specific surface area 210 m^2 g^{-1}). The bonded particles were used to fill 250 x 4.6 mm columns. The P-CAP, from ‘‘poly Cyclic Amine Polymer’’, is actually a polymer of *trans*-1,2-cyclohexanediyl-bis-acrylamide (Fig. 1a). The P-CAP denomination comes from the Astec trade name (Astec, Whippany, NJ, USA). This stationary phase was fully described recently [5]. The P-CAP-DP, also an Astec trade name, is a polymer of *N,N*’-[(1R,2R)]-1,2-diphenyl-1,2-ethanediyl]-bis-2-propenamide (Fig. 1b). It was prepared as fully described in [11]. Figure 1c shows the monomer *trans*-9,10-dihydro-9,10-ethanoanthracene-(11S,12S)-

11,12-dicarboxylic acid bis-4-vinylphenylamide that was used to prepare the DEABV stationary phase. This molecule was synthesized in our group using a chiral dicarboxylic acid originally reported by Thunberg and Allenmark [21] and then coupled to *p*-vinylphenylamine. The chiral selector and the phase preparation were fully described in a recent article [22]. Figure 1d shows the *N,N'*-[(1R,2R)-1,2-diphenyl-1,2-ethanediyl] bis-4-vinylbenzamide monomer, a variation of b, used to prepare the DPEVB stationary phase according to the procedure described in [5] and [11]. The bonding density of the P-CAP CSP was estimated using the carbon elemental analysis to 400 μmol g^{-1} or about 2.4 μmol m^{-2} [5]. The corresponding values for the P-CAP-DP CSP were 350 μmol g^{-1} and 2.1 μmol m^{-2} [11] and 290 μmol g^{-1} and 1.7 μmol m^{-2} for the DEABV CSP and 340 μmol g^{-1} and 2.0 μmol m^{-2} for the DPEVB CSP.

8.2.3. Supercritical Fluid Chromatography

The SFC apparatus was from Thar Technologies, Inc. (Pittsburgh, PA, USA). The SFC system includes a fluid delivery module (liquid CO_2 pump and cosolvent pump), an auto sampler with a 48 sample tray, a column oven with column selection, an auto back pressure regulator, a UV VWD detector, and the SuperChrom™ software for data treatment. SFC-grade CO_2 was from Air Liquide America (Houston, TX, USA).

8.2.4. Operating Conditions

All studies of the effect of temperature in enantiomeric separations have shown that the enantioselectivity factors decrease as the temperature increases [23]. So a constant and low temperature of 32 ºC (CO_2 critical temperature is 31.3 °C) was selected for all analyses. Similarly, raising the pressure does produce faster analyses, but it is associated with a poorer enantioselectivity [24]. Consequently, a constant outlet pressure of 100 bar (1,430 p.s.i.) was used in all cases. The polarity of pure CO_2 mobile phase can be compared to that of pentane [20]. It is not high enough to perform useful separations. Therefore, significant amounts of polar organic modifier were added in all mobile phases used [20]. Trifluoroacetic acid (TFA) was also added at a concentration of 0.2% v/v in the organic modifier (unless otherwise indicated) used in all mobile phases to protonate the solutes and any stationary phase basic sites. The total flow rate (CO_2 + MeOH) was always 4 mL min^{-1} at the column inlet. The amount of methanol (MeOH) added to CO_2 was selected so that the solute peaks elute in less

than 8 min. When a particular solute was not separated on all four CSPs, another mobile phase was tested either with first another MeOH concentration and next another organic modifier (ethanol, EtOH, or isopropyl alcohol, IPA) keeping the CO_2 pressure at 100 bar and the TFA concentration at 0.2% v/v in the organic modifier until the solute's enantiomers are separated by at least one CSPs. This procedure shows that the listed results are certainly not the best results that could be obtained working with the studied polymeric CSPs. Further optimization of the mobile phase composition for each individual compounds could be done if desired. There is no objection other than silica stability to use higher pH mobile phases and/or silanol screening agents.

8.3. Results and Discussion

Table 1 gives the number code used to identify the 88 compounds; along with their names, chemical structures and chromatographic parameters obtained on the four polymeric CSPs. All blank entries correspond to non-observable enantiomeric separation (a single peak, enantioselectivity and resolution factors are respectively 1 and 0). In these cases, the retention times were deliberately omitted. With no exception, the retention times decreased dramatically when the methanol contents increased. Then, the retention values could be misleading when obtained with different mobile phase compositions. Since the retention values do not give reliable information on the retentive properties of the CSPs, they were not reported.

8.3.1. Overall CSP Effectiveness

Figure 2 (top) shows the number of enantiomeric separations obtained on each polymeric CSP. It clearly shows that the DPEVB CSP is less effective than the three other CSPs and is able to baseline separate only one compound (compound **58**, Rs = 1.6, Table 1). By chance, the other three CSPs, P-CAP, P-CAP-DP and DEABV, were able to separate exactly the same number of compounds (49). The DEABV CSP baseline separated 20 compounds (41% of the 49 separations, Table 1). Fifteen of the 49 fully or partially enantioseparated compounds were separated only on the DEABV-CSP. The number of baseline separations for the P-CAP and P-CAP-DP CSPs was, respectively, 12 and 14 compounds. The number of unique separations for the P-CAP and P-CAP-DP CSPs was 11 compounds. With the 6 compounds uniquely separated by the DPEVB CSP, a total of 43

compounds or 49% of the selected set were separated by only one CSP. Figure 2 (bottom) shows that 20 compounds were separated by 2 CSPs, 18 by 3 CSPs and 7 compounds were enantioseparated by all 4 CSPs. These later compounds are **6**, **22**, **23**, **26**, **45**, **52** and **63** (Table 1). The DEABV-CSP seems to be somewhat better than the other two P-CAP CSPs in terms of the number of baseline separations and separations of compounds which contain the stereogenic center in a ring.

8.3.2. Compound Structure and Polymer CSP Enantiorecognition

In our recent work studying the behavior of the macrocyclic glycopeptide CSPs in subcritical chromatography, strong difference in enantiorecognition was found between the different related CSPs [20]. Chiral acid and amino-acid enantiomers were significantly better separated by the teicoplanin aglycone (TAG) CSP while the chiral amino alcohols (β-blockers) were better separated on the native teicoplanin CSP [20]. The data in Fig. 3 does not indicate that there is such a profound structural selectivity difference between the polymer CSPs. The 43 compounds that are enantioseparated by a single CSP are more randomly spread among the four structural classes of compounds.

However, a closer look at solute structure and CSP enantiorecognition allows one to find some structural selectivity. More specifically, the 9 oxazolidinone derivatives (compounds **26**, **35**, **36**, **37**, **38**, **41**, **42**, **47** and **48**) with an asymmetric carbon in position 4 are all baseline separated on the DEABV CSP. Four of these compounds (**36**, **37**, **38** and **41**) are separated only on the DEABV CSP (Table 1). For the five oxazolidinone that are separated on several CSPs, the resolution factor obtained with the DEABV CSP is the highest. Clearly, there is an interaction between the oxazolidinone ring and the DEABV CSP that is very sensitive to substitution on the ring's 4-carbon.

Some general trends that have been observed with other CSPs also were observed with the polymeric CSPs studied here. First, it was observed that compounds having four very different substituents on the stereogenic center are well differentiated by many CSPs [25]. For example, the enantiomers of warfarin (**23**), with a hydrogen atom, a phenyl group, an acetonyl group and a huge hydroxylcoumarinyl group on its asymmetric center are differentiated by all four CSPs in this study. Also, it was observed that a minor change in the molecular structure of a chiral analyte can produce a dramatic change in enantioseparation

[25]. For example, compounds **39** and **40** differ only in the position of their hydroxyl group (changing from the *meta* to *para* position). Compound **39** is separated by the P-CAP CSP only and **40** is separated by the P-CAP-DP CSP only (Table 1). Such a change in enantiomeric recognition is observed only if the minor structural change occurs on an ‘‘enantiosensitive’’ part of the molecule. Considering Coumachlor (**22**) and Warfarin (**23**), they differ only by a chlorine atom, but both are equally well separated by all four CSPs indicating that the chlorine atom is not located in a part of the molecule involved in any enantioselective interactions. A similar observation can be made with Benzoin (**9**) and Hydrobenzoin (**14**) whose enantiomers are equally well separated by three polymeric CSPs (Table 1).

8.3.3. Chiral Stationary Phases and Chemical Interactions

Figure 1a shows that the P-CAP monomer does not contain any aromatic moieties. Consequently, π–π interactions cannot be important in the chiral recognition mechanism of this CSP. The P-CAP polymeric CSP has a large number of amide linkages providing a wealth of sites for hydrogen bonding and dipolar interactions [5]. The three other CSPs do have several aromatic rings in their structures (Fig. 1b–d) along with amide linkages. They should be able to combine π–π interactions with other types of interactions for chiral recognition [25].

Figure 3 shows the separation of compounds **63** (left) and **64** (right), respectively DNB-leucine and DNB-phenylglycine, on the three CSPs, PCAP, P-CAP-DP and DEABV. Pi–pi interactions are likely in the case of the DNB-leucine (**63**, Fig. 4left). The DNB derivative is a strongly π-acid substituent on the amine group of leucine. The two enantiomeric forms of DNB leucine are well (Rs = 1.6) and extremely well (Rs = 4.7) separated by the π–π capable P-CAP-DP and DEABV CSPs, respectively. They are poorly separated by the P-CAP CSP which is unable to interact through π–π interactions (Fig. 4-left). However, the P-CAP CSP separates well (Rs = 1.4) the structurally related DNB-phenylglycine (Fig. 4-right). This compound (**64**) is equally or better separated by the two other CSPs as shown. In this case, the dipolar interactions with the DNB amide group and/or the H-bond interactions with the carboxylic acid moiety are more important than the π–π interactions for enantiorecognition of DNB-phenylglycine.

The results obtained with atropoisomers suggest that π–π interactions play little or no role in their enantioseparation. Indeed, the highest enantioresolution factor of all atropoisomers is obtained with 1,1'-binaphthol (**76**) on the P-CAP CSP (no π–π interactions). All other three CSPs are able to separate partially (Rs < 0.9) the binaphthalene atropoisomers **76**, **77** and **78** (Table 1). However, the exact nature of the enantioselective interactions has not been identified.

8.3.4. Normal Phase LC versus SFC

The synthetic polymeric CSPs were shown to be highly efficient in normal phase liquid chromatography using heptane-alcohol, halogenated solvent or waterless acetonitrile-methanol mobile phases. The later mobile phase is used in the special mode called polar organic mode [5, 11, 22]. Most of the compounds whose enantiomers were successfully separated with a given polymeric phase in the normal or polar organic mode also produced successful enantioseparations with subcritical CO_2 + MeOH mobile phases. The main obvious advantage of the SFC mobile phases is their low viscosity compared to classical liquid mobile phases. The low SFC mobile phase viscosity allows for much higher flow rates allowing for faster separations at the same pressure drop.

The separations of *N*-(*α*-methylbenzyl) phthalic acid monoamide (**16**) and Furoin (**13**) respectively on the DEABV and P-CAP-DP CSPs will be used to illustrate the difference that can be observed between the normal phase mode and the subcritical fluid mode. The two enantiomers of **16** are partially separated (a = 1.13, Rs = 1.2, Fig. 4a) in the normal phase mode with an heptane/MeOH mobile phase in more than 12 min at 1 mL min^{-1}. They are separated with a similar enantioselectivity factors in less than 8 min in SFC with a CO_2/MeOH 75/25% v/v mobile phase at 4 mL min^{-1} (Fig. 4b). Raising the amount of methanol to 30% halves the separation duration without losing any enantioresolution (Fig. 4c). The two enantiomers of Furoin are very well separated (a = 1.69, Rs = 3.7, Fig. 4d) in the normal phase mode with a heptane-IPA mobile phase in about 32 min at 1 mL min^{-1}. Table 1 and Fig. 4e shows the separation obtained with a SFC mobile phase, also baseline and obtained in less than 3 min at 4 mL min^{-1}. Better resolution factors were obtained in the normal phase mode compared to the Table 1 results in SFC for many compounds. It is recalled that the SFC separations were not optimized and all Rs-factors listed in Table 1

could likely be increased. However, the solute retention times were always significantly lower in the SFC mode than in both the normal phase and polar organic modes of classical liquid chromatography.

8.3.5. Efficiency

Table 1 lists the average plate number measured for the observed enantioseparated peaks. A huge plate count variation, with efficiencies that could be as low as 500 plates for a 25 cm column (hetp = 5,000 μm or 1,000 particle diameters) or reach 9,000 plates (hetp = 270 μm or 50 particle diameters), could be observed on the four CSPs studied. Of course, a low efficiency is not favorable for an acceptable resolution factor as illustrated by Fig. 5. The enantiomers of **27** are separated with a measured plate number of about 7,000 plates and an enantioselectivity factor of 1.08 producing an almost baseline resolution factor (Rs = 1.3). With the same retention times and selectivity factor, the enantiomers of Chlorthalidone (compound **45**) are separated with a low resolution factor of 0.4 because the observed efficiency is very low (600 plates) for this compound (Fig. 5, bottom).

The observed efficiency is a measure of the kinetics of the solute exchange between the mobile phase and the stationary phase. This parameter is difficult to predict. It is known that strong interactions between a solute and the stationary phase may be linked to a slow adsorption–desorption process being associated with a low efficiency. In the case illustrated by Fig. 5, Chlorthalidone has a plethora of functionality including a sulfamide group, an amide, an alcohol, a chlorinated phenyl and another aromatic ring. These numerous functionalities are subject to a variety of different interactions with the polymeric P-CAP-DP stationary phase. At least one of these possible interactions is slow, producing the observed poor peak shape. Compound **28** has less functionalities (only phenol and alcohol) that interact rapidly with the CSP producing sharper peaks. The kinetics of a particular solute-stationary phase interaction can be completely independent of the solute's chiral recognition interactions. In some cases, a strong interaction with slow adsorption/desorption kinetic may be critical for enantiorecognition. In other cases, the strong interaction may play no role [25].

The observed peak efficiency of a particular solute separated on a given CSP is very dependent on the experimental conditions. The nature of the alcohol modifier used is especially important. However quantitative comparison is difficult because most often the

retention times and enantioselectivity factors are also changed when the organic modifier is changed. As a general trend, ethanol produced better efficiencies than methanol and isopropyl alcohol. The TFA additive has also a critical influence on efficiencies since it reduces the strong (and slow) charge–charge interactions that occur with acidic analytes.

8.4. Conclusions

The synthetic polymeric P-CAP, P-CAP-DP, DEABV and DPEVB CSPs are all capable of producing effective enantioseparations with supercritical fluid mobile phases. The DPEVB CSP is significantly less successful than the three other CSPs in separating a large number of compounds with a variety of functionalities. The DEABV CSP seems to be the most broadly applicable and useful of these CSPs. The biggest advantage of the SFC mobile phase is the short separation times observed compared to those in the normal phase mode due to the high flow rates possible thanks to the low SFC mobile phase viscosity. Retention times lower than 5 min, with 25 cm columns, were obtained for 90% of the separations presented in this work. The second advantage of SFC mobile phases is the easy recovery of the separated solutes. There is no hindrance to injecting large amounts of sample on these columns and maintaining the enantiomeric separations as was demonstrated in the normal phase mode [5, 11, 22], however the SFC loading capability was not evaluated in this study.

Acknowledgments

The support of this work by the National Institute of Health, NIH RO1 GM53825-11 is gratefully acknowledged.

References

1. Armstrong DW, Zhang B (2001) Anal Chem 73:557A–562A

2. Mitchell CR, Armstrong DW (2004) Chiral Separations. Humana Press, Totowa, chap. 3, pp 61–112

3. Yamamoto C, Okamoto I (2004) Bull Chem Soc Jpn 77:227–257

4. Okamoto Y, Yashima E (1998) Angew Chem Int Ed 37:1020–1043

5. Zhong Q, Han X, He L, Beesley TE, Trahanovsky WS, Armstrong DW (2005) J Chromatogr A 1066:55–70

6. Okamoto Y, Yashima E, Yamamoto C (2003) Top Stereochem 24:157–208

7. Preinerstorfer B, Lindner W, Lammerhofer M (2005) Electrophoresis 26:2005–2018

8. Aboul-Enein HY (2003) J Sep Sci 26:521–524
9. Lindholm J, Fornstedt T (2005) J Chromatogr A 1095:50–59
10. Allenmark SG, Andersson S, Moeller P, Sancher D (1995) Chirality 7:248–256
11. Han X, He L, Zhong Q, Beesley TE, Armstrong DW (2006) Chromatographia 63:13–23
12. Gasparrini F, Misiti D, Villani C (2003) WO Patent 2003079002
13. Gasparrini F, Misiti D, Rompietti R, Villani C (2005) J Chromatogr A 1064:25–38
14. Phinney KW (2000) Anal Chem 72:204A–211A
15. Berger TA (1995) Packed Column Supercritical Fluid Chromatography. Royal Society of Chemistry, Cambridge
16. Mourier PA, Eliot E, Caude M, Rosset R, Tambute A (1985) Anal Chem 57:2819–2823
17. Terfloth G (2001) J Chromatogr A 906:301–307
18. Schurig V, Fluck M (2000) J Biochem Biophys Methods 43:223–250
19. Villeneuve MS, Anderegg RJ (1998) J Chromatogr A 826:217–225
20. Liu Y, Berthod A, Mitchell CR, Xiao TL, Zhang B, Armstrong DW (2002) J Chromatogr A 978:185–204
21. Thunberg I, Allenmark S (2003) Chirality 15:400–408
22. Han X, Wang C, He L, Beesley TE, Armstrong DW (2007) Anal Bioanal Chem Submitted
23. Berthod A, He L, Beesley TE (2004) J Chromatogr A 1060:205–214
24. Toribio L, David F, Sandra P (1999) Quim Anal 18:269–276
25. Berthod A (2006) Anal Chem 78:2093–2099

Table 1. Enantiomeric separations on four polymeric CSPs by SFC.

#	Compound name and formula	CSP	t_1 min	α	Rs	Additive MeOH/TFA*	N plates
Compounds with sp^2 hybridized carbon on the asymmetric center							
1	1-(9-Anthryl)-2,2,2-trifluoroethanol 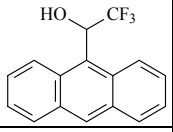	P-CAP P-CAP-DP DEABV DPEVB	2.64 3.54	1.07 1.07	0.7 0.7	30%/0.2% 15%/0.2%	4900 3700
2	2-(4-Nitrophenyl)-propionic acid 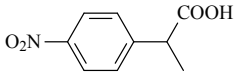	P-CAP P-CAP-DP DEABV DPEVB	7.62	1.05	0.8	5%EtOH/0.2%	7200
3	3,4-Dihydroxy-phenyl-2-propylacetamide 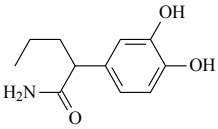	P-CAP P-CAP-DP DEABV DPEVB	7.27 7.31 6.18	1.16 1.03 1.04	1.6 0.3 0.3	25%/0.2% 20%/0.2% 20%/0.2%	2900 2200 2100
4	4-Chloromandelic acid 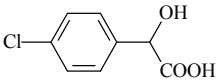	P-CAP P-CAP-DP DEABV DPEVB	2.96	1.08	0.3	20%/0.2%	600
5	4-Isobutyl-α-methyl-phenylacetic acid 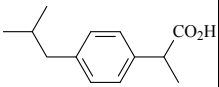	P-CAP P-CAP-DP DEABV DPEVB	4.75	1.05	0.5	5%/0.2%	3400
6	5-(α-Phenethyl)-semioxamazide 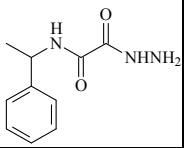	P-CAP P-CAP-DP DEABV DPEVB	2.19 3.58 1.73 3.69	1.13 1.05 1.21 1.22	0.8 0.4 1.1 1.1	30%/0.2% 15%/0.2% 40%/0.2% 10%/0.2%	2200 2400 3000 1000
7	1-Phenyl-1,2-ethanediol 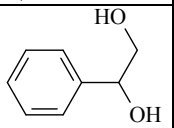	P-CAP P-CAP-DP DEABV DPEVB	6.63 11.2	1.16 1.06	1.8 1.4	15% IPA/0.2% 5%/0.2%	3500 9000
8	Atrolactic acid 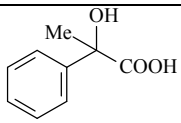	P-CAP P-CAP-DP DEABV DPEVB	4.02	1.05	0.6	10%/0.2%	3900
9	Benzoin 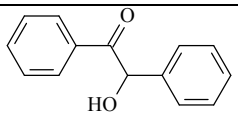	P-CAP P-CAP-DP DEABV DPEVB	3.31 3.81 4.93	1.07 1.18 1.07	0.9 2.0 1.1	10%/0.2% 5%/0.2% 10%/0.2%	6900 4700 7700
10	Bis[1-phenylethyl]-Amine hydrochloride 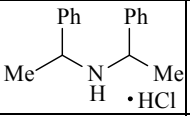	P-CAP P-CAP-DP DEABV DPEVB	7.34 3.02 4.30	1.09 1.16 1.28	1.1 0.9 2.0	5%/0.2% 15%/0.2% 20%/0.2%	4000 1400 2000
11	Carprofen 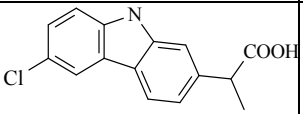	P-CAP P-CAP-DP DEABV DPEVB	4.54 4.19 4.81	1.07 1.08 1.08	0.8 0.5 0.7	25%/0.2% 40%/0.2% 30%/0.2%	4400 1300 2400
12	Doxylamine 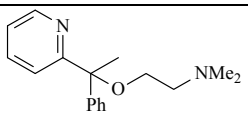	P-CAP P-CAP-DP DEABV DPEVB	3.06	1.07	0.3	15%/0.2%	700

Table 1. (continued)

#	Compound name and formula	CSP	t_1 min	α	Rs	Additive MeOH/TFA*	N plates
13	Furoin 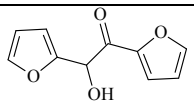	P-CAP					
		P-CAP-DP	2.48	1.25	2.0	10%/0.2%	3800
		DEABV	4.15	1.04	0.4	10%/0.2%	2800
		DPEVB	3.91	1.03	0.5	5%/0.2%	8000
14	Hydrobenzoin 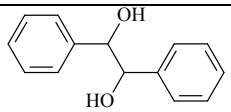	P-CAP	5.12	1.12	1.8	15%EtOH/0.5%	6500
		P-CAP-DP	5.23	1.06	0.9	10%/0.5%	5400
		DEABV	7.18	1.03	0.5	10%/0.5%	5000
		DPEVB					
15	Mandelamide 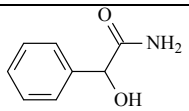	P-CAP					
		P-CAP-DP					
		DEABV	3.25	1.13	1.5	20%/0.5%	5300
		DPEVB					
16	N-(α-Methylbenzyl) phthalic acid monoamide 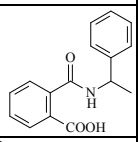	P-CAP	6.29	1.08	0.8	15%/0.2%	2800
		P-CAP-DP					
		DEABV	7.06	1.14	1.4	25%/0.2%	2800
		DPEVB					
17	N,N'-Bis(2-methyl-benzyl) sulfamide 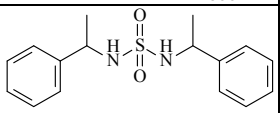	P-CAP	6.92	1.06	0.7	15%/0.2%	3800
		P-CAP-DP	3.01	1.70	3.4	20%/0.2%	1800
		DEABV	3.31	1.09	0.7	30%/0.2%	2200
		DPEVB					
18	N-Benzyl-1-(1-naphthyl)-ethylamine 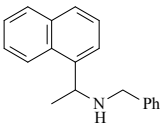	P-CAP					
		P-CAP-DP					
		DEABV	5.31	1.12	0.6	35%EtOH/0.2%	700
		DPEVB					
19	*O*-Acetyl mandelic acid 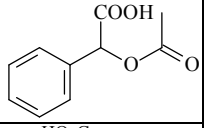	P-CAP					
		P-CAP-DP	5.33	1.06	0.7	5%/0.2%	3300
		DEABV	3.75	1.04	0.3	10%/0.2%	1500
		DPEVB					
20	Tropic acid 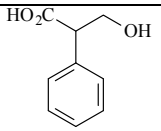	P-CAP					
		P-CAP-DP	4.44	1.15	1.6	15%EtOH/0.2%	3700
		DEABV					
		DPEVB					
21	Verapamil 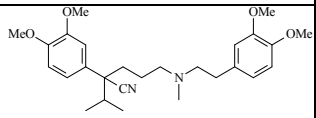	P-CAP	4.10	1.06	0.4	10%/0.2%	1300
		P-CAP-DP					
		DEABV					
		DPEVB					
22	Coumachlor 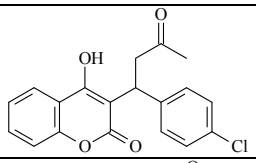	P-CAP	5.48	1.12	1.4	15%/0.2%	3600
		P-CAP-DP	4.66	1.06	0.6	15%/0.2%	2600
		DEABV	5.96	1.06	0.4	30%/0.2%	1000
		DPEVB	5.10	1.07	0.7	20%/0.2%	2100
23	Warfarin 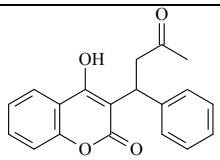	P-CAP	4.50	1.11	1.3	15%/0.2%	4500
		P-CAP-DP	4.08	1.07	0.8	15%/0.2%	4200
		DEABV	4.89	1.07	0.5	30%/0.2%	1400
		DPEVB	4.30	1.11	1.1	20%/0.2%	3100
Compounds whose asymmetric center is part of a ring							
24	Althiazide 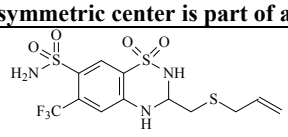	P-CAP					
		P-CAP-DP	4.00	1.31	1.4	40%/0.2%	900
		DEABV					
		DPEVB					

Table 1. (continued)

#	Compound name and formula	CSP	t_1 min	α	Rs	Additive MeOH/TFA*	N plates
25	2-Azabicyclo[2.2.1]-hept-5-en-3-one 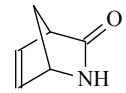	P-CAP P-CAP-DP DEABV DPEVB	5.17	1.10	1.4	3%/0.2%	5300
26	(3a-cis)-3,3a,8,8a-Tetrahydro-2H-indenol[1,2-d] oxazol-2-one 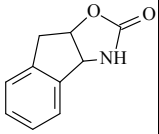	P-CAP P-CAP-DP DEABV DPEVB	4.31 4.35 5.8 2.95	1.16 1.12 1.13 1.06	1.5 1.1 1.5 0.8	20%/0.2% 15%/0.2% 20%/0.5% 20%/0.2%	2900 2700 4100 5700
27	1,2,3,4-Tetrahydro-1-naphthol 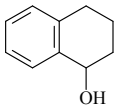	P-CAP P-CAP-DP DEABV DPEVB	4.25	1.05	0.9	5%EtOH/0.2%	8000
28	1,5-Dihydroxy-1,2,3,4-tetrahydronaphthalene 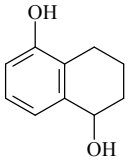	P-CAP P-CAP-DP DEABV DPEVB	4.6	1.08	1.3	15%/0.2%	7000
29	1,5-Dimethyl-4-phenyl-2-imidazolidinone 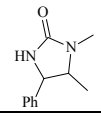	P-CAP P-CAP-DP DEABV DPEVB	3.40 2.94 6.15	1.08 1.07 1.09	1.0 0.8 1.2	10%/0.2% 20%/0.2% 5% EtOH/0.2%	5100 5000 5000
30	2-Carbethoxy-γ-phenyl-γ-butyrolactone 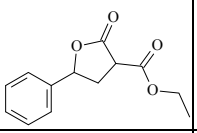	P-CAP P-CAP-DP DEABV DPEVB	3.59	1.07	0.9	10%/0.2%	5100
31	3-(Benzyloxy carbonyl)-4-oxazolidine carboxylic acid 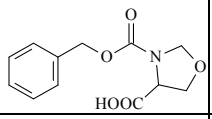	P-CAP P-CAP-DP DEABV DPEVB	7.07	1.05	0.5	10%/0.5%	2400
32	3a,4,5,6-Tetrahydro-succininido[3,4-b]-acenaphthen-10-one 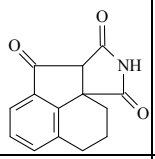	P-CAP P-CAP-DP DEABV DPEVB	6.08 5.60	1.04 1.13	0.5 1.0	15%/0.2% 35%EtOH/0.2%	3300 1800
33	3-Oxo-1-indancarboxylic acid 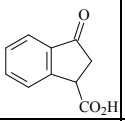	P-CAP P-CAP-DP DEABV DPEVB	4.79	1.05	0.6	10%EtOH/0.2%	4000
34	3-Phenylphthalide 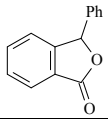	P-CAP P-CAP-DP DEABV DPEVB	6.87	1.08	1.5	10%/0.5%	8000
35	4-(Diphenylmethyl)-2-oxazolidinone 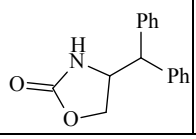	P-CAP P-CAP-DP DEABV DPEVB	6.00 6.86 2.97	1.08 1.04 1.18	1.3 0.4 1.5	10%/0.2% 10%/0.2% 40%/0.2%	6300 2400 3000

Table 1. (continued)

#	Compound name and formula	CSP	t_1 min	α	Rs	Additive MeOH/TFA*	N plates
36	4-Benzyl-2-oxazolidinone 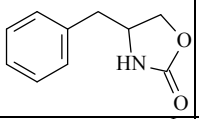	P-CAP P-CAP-DP DEABV DPEVB	2.85	1.18	1.5	30%/0.2%	3300
37	4-Benzyl-3-propionyl-2-oxazolidinone 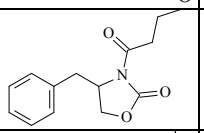	P-CAP P-CAP-DP DEABV DPEVB	4.44	1.18	2.0	20%/0.2%	4300
38	4-Benzyl-5,5-dimethyl-2-oxazolidinone 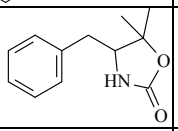	P-CAP P-CAP-DP DEABV DPEVB	3.17	1.17	1.5	25%EtOH/0.2%	3300
39	5-(3-Hydroxyphenyl)-5-phenylhydantoin 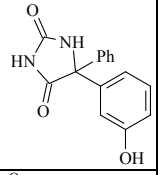	P-CAP P-CAP-DP DEABV DPEVB	7.34	1.04	0.3	40%/0.2%	1300
40	5-(4-Hydroxyphenyl)-5-phenylhydantoin 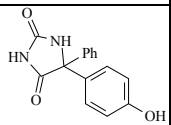	P-CAP P-CAP-DP DEABV DPEVB	4.88	1.05	0.3	40%/0.2%	900
41	5,5-Dimethyl-4-phenyl-2-oxazolidinone 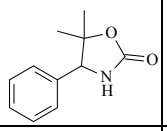	P-CAP P-CAP-DP DEABV DPEVB	3.08	1.14	1.5	20%/0.5%	4800
42	5-Phenyl-2-(2-propynylamino)-2-oxazolin-4-one 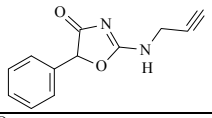	P-CAP P-CAP-DP DEABV DPEVB	4.52 4.73 3.15	1.06 1.08 1.25	0.7 0.7 1.5	15%/0.2% 15%/0.2% 35%EtOH/0.2%	4000 2400 1700
43	Bendro-flumethiazide 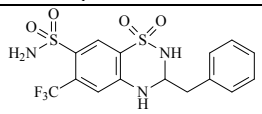	P-CAP P-CAP-DP DEABV DPEVB	8.91 3.90	1.11 1.31	0.8 1.3	40%/0.2% 35%/0.2%	1200 800
44	Benzylphthalide 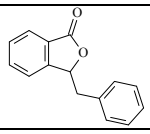	P-CAP P-CAP-DP DEABV DPEVB	3.94	1.05	0.7	20%/0.2%	5100
45	Chlorthalidone 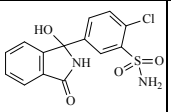	P-CAP P-CAP-DP DEABV DPEVB	7.08 4.38 3.79 5.27	1.21 1.09 1.09 1.07	1.5 0.4 0.5 0.6	40%/0.2% 40%/0.2% 40%/0.2% 30%/0.2%	1600 600 1100 2000
46	*cis*-1-Amino-2-indanol 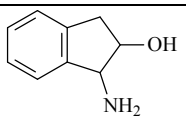	P-CAP P-CAP-DP DEABV DPEVB	6.38	1.10	1.3	20%/0.2%	4400
47	*cis*-4,5-Diphenyl-2-oxazolidinone 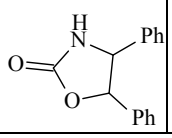	P-CAP P-CAP-DP DEABV DPEVB	7.43 4.51 3.66	1.06 1.06 1.21	1.0 0.9 1.6	10%/0.2% 15%/0.2% 30%/0.2%	6700 6600 2400

Table 1. (continued)

#	Compound name and formula	CSP	t_1 min	α	Rs	Additive MeOH/TFA*	N plates
48	*cis*-4-Methyl-5-phenyl-2-oxazolidinone 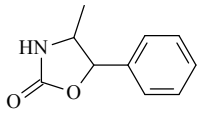	P-CAP P-CAP-DP DEABV DPEVB	4.15 4.94 3.76	1.07 1.08 1.16	0.9 1.0 1.5	15%EtOH/0.2% 10%/0.2% 25%EtOH/0.2%	5100 4600 3300
49	Flavanone 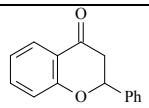	P-CAP P-CAP-DP DEABV DPEVB	5.11	1.31	0.4	10%/0.2%	100
50	Ketamine (hydrochloride) 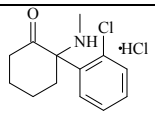	P-CAP P-CAP-DP DEABV DPEVB	5.79	1.05	0.5	10%/0.2%	2300
51	Lormetazepam 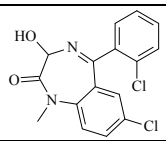	P-CAP P-CAP-DP DEABV DPEVB	4.79 3.00	1.15 1.31	2.0 1.8	15%/0.2% 40%/0.2%	5800 1800
52	Oxazepam 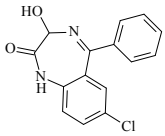	P-CAP P-CAP-DP DEABV DPEVB	3.43 3.18 3.62 3.32	1.37 1.36 1.34 1.08	2.2 2.5 1.0 0.5	40%/0.2% 40%/0.2% 40%/0.2% 30%/0.2%	1800 2600 400 1400
53	N-(α-Methylbenzyl)-phthalimide 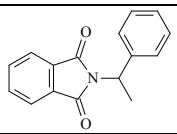	P-CAP P-CAP-DP DEABV DPEVB	4.48	1.02	0.3	10%/0.2%	4600
54	Phensuximide 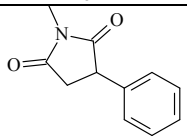	P-CAP P-CAP-DP DEABV DPEVB	6.25	1.11	1.5	1%/0.2%	4700
55	*t*-Butyl-6-oxo-2,3-diphenyl-4-morpholine carboxylate 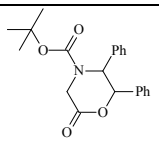	P-CAP P-CAP-DP DEABV DPEVB	3.66 4.85	1.04 1.16	0.3 1.5	5%/0.2% 5%EtOH/0.2%	1700 3000
56	Thioridazine 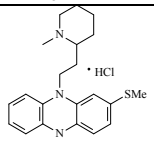	P-CAP P-CAP-DP DEABV DPEVB	3.9	1.09	0.4	15%/0.2%	700
57	*trans*-4-Cotinine-carboxylic acid 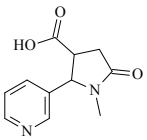	P-CAP P-CAP-DP DEABV DPEVB	5.25 4.27	1.06 1.02	0.6 0.3	10%/0.2% 20%/0.2%	2800 4300
Chiral acids and amino-acid derivatives							
58	4-((1-(Isopropoxy-carbonyl-4-methyl)-butyl) amino) -benzoic acid 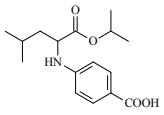	P-CAP P-CAP-DP DEABV DPEVB	2.64 2.22 3.46	1.28 1.93 1.21	1.6 4.0 1.6	10%/0.2% 30%/0.2% 10%/0.2%	1800 2200 2500

Table 1. (continued)

#	Compound name and formula	CSP	t_1 min	α	Rs	Additive MeOH/TFA*	N plates
59	4-Chlorophenyl-alanine ethyl ester hydrochloride 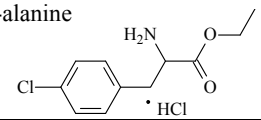	P-CAP P-CAP-DP DEABV DPEVB	4.08	1.10	0.7	15%/0.2%	1700
60	Carbobenzyloxy-alanine 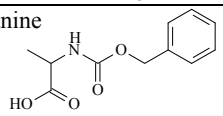	P-CAP P-CAP-DP DEABV DPEVB	4.44 3.68 2.79	1.07 1.06 1.21	0.9 0.7 1.5	15%EtOH/0.2% 10%/0.2% 20%/0.2%	5300 5100 2500
61	Dansyl-norleucine cyclohexylammonium salt 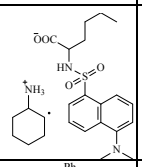	P-CAP P-CAP-DP DEABV DPEVB	4.08 3.96	1.08 1.16	1.0 1.4	30%/0.2% 30%/0.2%	5600 2900
62	Dansyl-phenylalanine cyclohexylammonium salt 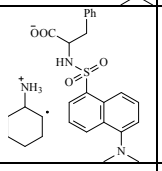	P-CAP P-CAP-DP DEABV DPEVB	 3.81 3.90	 1.09 1.29	 0.5 1.7	 30%/0.2% 40%/0.2%	 1000 1400
63	N-(3,5-Dinitro-benzoyl)-leucine 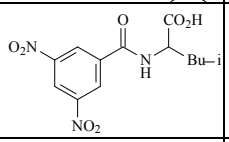	P-CAP P-CAP-DP DEABV DPEVB	7.17 2.35 1.97 3.74	1.04 1.30 3.14 1.10	0.4 1.6 4.5 1.2	15%/0.2% 20%/0.2% 40%/0.2% 20%/0.2%	2600 1900 1200 4400
64	N-(3,5-Dinitro-benzoyl)-phenyl glycine 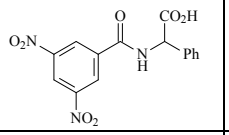	P-CAP P-CAP-DP DEABV DPEVB	3.75 3.94 3.70	1.19 1.23 1.58	1.4 1.8 2.7	30%/0.2% 20%/0.2% 40%/0.2%	3100 2400 1300
65	N-Acetylhomo-cysteine thiolactone 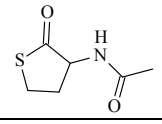	P-CAP P-CAP-DP DEABV DPEVB	7.36 4.73 3.55	1.06 1.11 1.06	0.9 1.3 0.7	5%/0.2% 10%/0.2% 20%/0.2%	5600 4600 4700
66	N-Benzoyl-valine 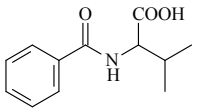	P-CAP P-CAP-DP DEABV DPEVB	4.85 3.58	1.11 1.07	1.3 0.7	15%EtOH/0.2% 10%/0.2%	4200 3800
67	N-carbobenzoxy-Phenylalanine 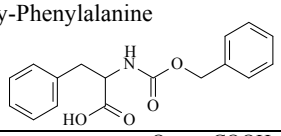	P-CAP P-CAP-DP DEABV DPEVB	5.13 4.38 2.04	1.04 1.09 1.35	0.5 0.9 1.5	15%/0.2% 15%EtOH/0.2% 40%/0.2%	4300 3000 1600
68	2-Phenoxy propionic acid 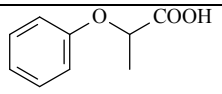	P-CAP P-CAP-DP DEABV DPEVB	 3.49	 1.03	 0.4	 10%/0.2%	 5100
69	2-(3-Chlorophenoxy) propionamide 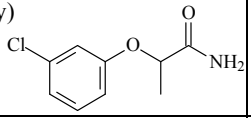	P-CAP P-CAP-DP DEABV DPEVB	 6.73	 1.06	 0.9	 5%/0.2%	 5300
70	2-(4-Chloro-2-methyl-phenoxy) propionic acid 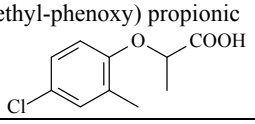	P-CAP P-CAP-DP DEABV DPEVB	 4.81	 1.09	 1.1	 5%EtOH/0.2%	 4700

Table 1 (continued)

#	Compound name and formula	CSP	t_1 min	α	Rs	Additive MeOH/TFA*	N plates
71	2,3-Dibenzoyl-tartaric acid 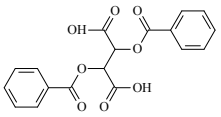	P-CAP P-CAP-DP DEABV DPEVB	 3.80 4.61	 1.15 1.03	 1.3 0.3	 30%/0.2% 20%/0.2%	 2700 2200
72	2-Bromo-3-methylbutyric acid 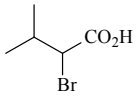	P-CAP P-CAP-DP DEABV DPEVB	4.02	1.08	0.9	5%/0.2%	4400
73	Bromosuccinic acid 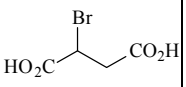	P-CAP P-CAP-DP DEABV DPEVB	5.15 5.90	1.05 1.11	0.6 1.5	20%/0.2% 10%/0.2%	3100 5100
74	Iopanoic acid 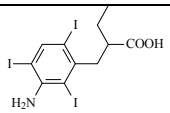	P-CAP P-CAP-DP DEABV DPEVB	 6.02	 1.13	 1.0	 30%/0.2%	 1600
75	Iophenoxic acid 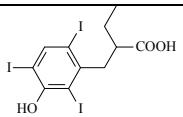	P-CAP P-CAP-DP DEABV DPEVB	 5.75	 1.12	 0.7	 30%/0.2%	 1000
Atropoisomerism and miscellaneous chemical functionalities on the asymmetric center							
76	1,1'-Bi-2-naphthol 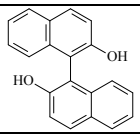	P-CAP P-CAP-DP DEABV DPEVB	4.17 7.96	1.32 1.04	2.7 0.3	40%/0.2% 30%/0.2%	3100 1500
77	1,1'-Bi-2-naphthol bis(trifluoromethane sulfonate) 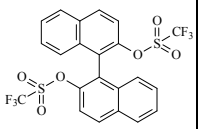	P-CAP P-CAP-DP DEABV DPEVB	 5.18	 1.08	 0.9	 5%EtOH/0.2 %	 3200
78	2,2'-Diamino-1,1'-binaphthalene 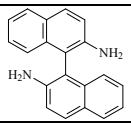	P-CAP P-CAP-DP DEABV DPEVB	 6.54	 1.08	 0.8	 20%/0.2%	 2800
79	6-(4-Chlorophenyl)-4,5-dihydro-2-(2-hydroxybutyl)-3-(2H)-pyridazinone 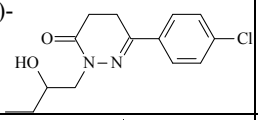	P-CAP P-CAP-DP DEABV DPEVB	6.65 11.6	1.22 1.06	2.4 1.0	10% IPA/0.2% 5%/0.2%	3800 6800
80	7-(2,3-Dihydroxy-propyl) theophyline 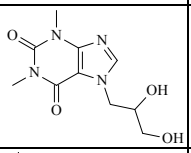	P-CAP P-CAP-DP DEABV DPEVB	6.08	1.03	0.4	10%/0.2%	3900
81	Baytan) 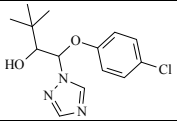	P-CAP P-CAP-DP DEABV DPEVB	3.94	1.20	1.6	10% IPA/0.2%	2500
82	N,N'-Dibenzyl-tartramide 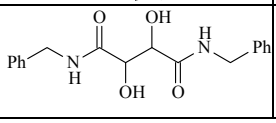	P-CAP P-CAP-DP DEABV DPEVB	2.60 3.44 2.73	1.46 1.45 1.36	2.5 2.2 1.5	30%/0.2% 20%/0.2% 40%/0.2%	2100 1300 1100

Table 1. (continued)

#	Compound name and formula	CSP	t_1 min	α	Rs	Additive MeOH/TFA*	N plates
83	2-Amino-3-phenyl-1-propanol 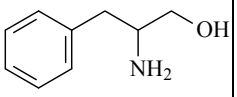	P-CAP P-CAP-DP DEABV DPEVB	4.61 2.90	1.09 1.07	1.3 0.4	15%/0.2% 20%/0.2%	6000 1400
84	Propranolol 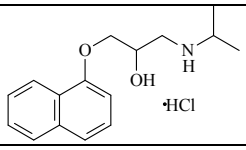	P-CAP P-CAP-DP DEABV DPEVB	7.12	1.10	0.4	20%/0.2%	400
85	3-(4-Nitrophenyl) glycidol 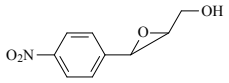	P-CAP P-CAP-DP DEABV DPEVB	9.4	1.07	0.9	5%EtOH/0.2 %	4200
86	Crufomate (Ruelene) 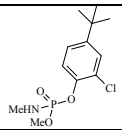	P-CAP P-CAP-DP DEABV DPEVB	3.27 5.72	1.06 1.14	0.5 1.7	5%/0.2% 5%EtOH/0.2 %	2700 4300
87	Fipronil 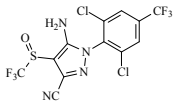	P-CAP P-CAP-DP DEABV DPEVB	3.10 5.54	1.25 1.21	2.1 1.9	10%/0.2% 5%/0.2%	
88	Omeprazole 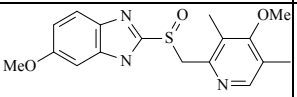	P-CAP P-CAP-DP DEABV DPEVB	5.44 5.04	1.09 1.05	0.9 0.7	15%/0.2% 20%/0.2%	2700 700

*The TFA is added to the alcohol modifier.

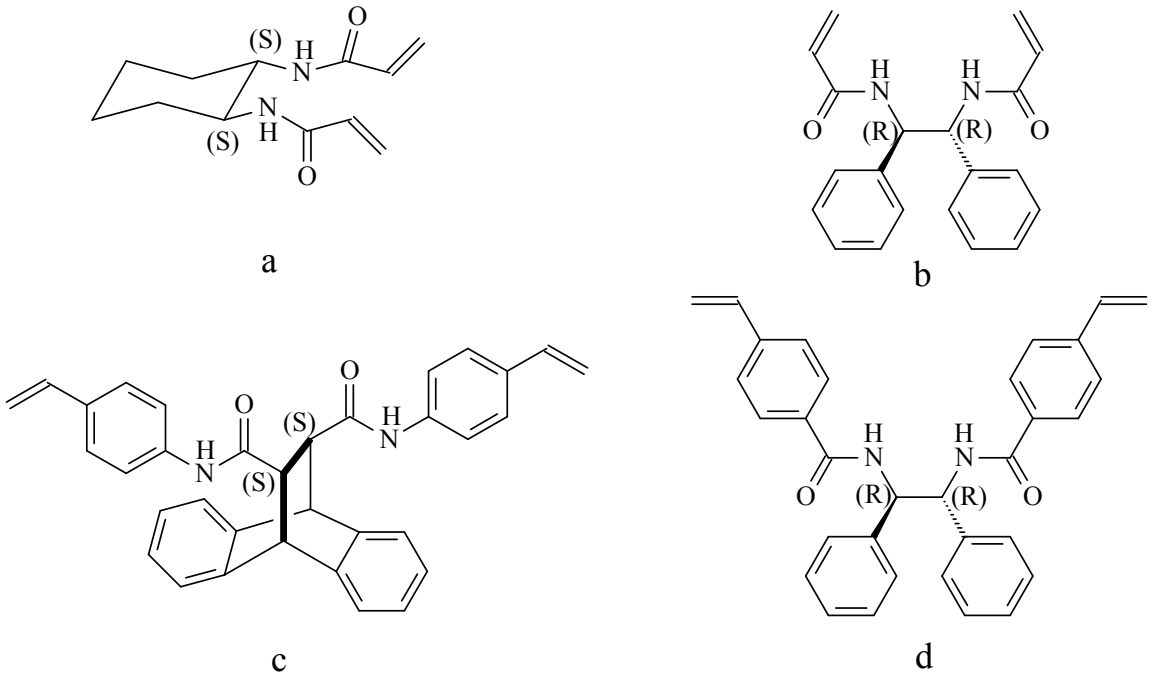

Fig. 1. The monomer of the polymeric chiral stationary phases used. **a)** P-CAP (*trans*-1,2-cyclohexanediyl-bis acrylamide) , **b)** P-CAP-DP (N,N'-[(1R,2R)]-1,2-diphenyl-1,2-ethanediyl] bis-2-propenamide), **c)** DEABV (*trans*-9,10-dihydro-9,10-ethanoanthracene-(11S,12S)-11,12-dicarboxylic acid bis-4-vinylphenylamide), **d)** DPEVB (N,N'-[(1R,2R)-1,2-diphenyl-1,2-ethanediyl] bis[4-vinylbenzamide]).

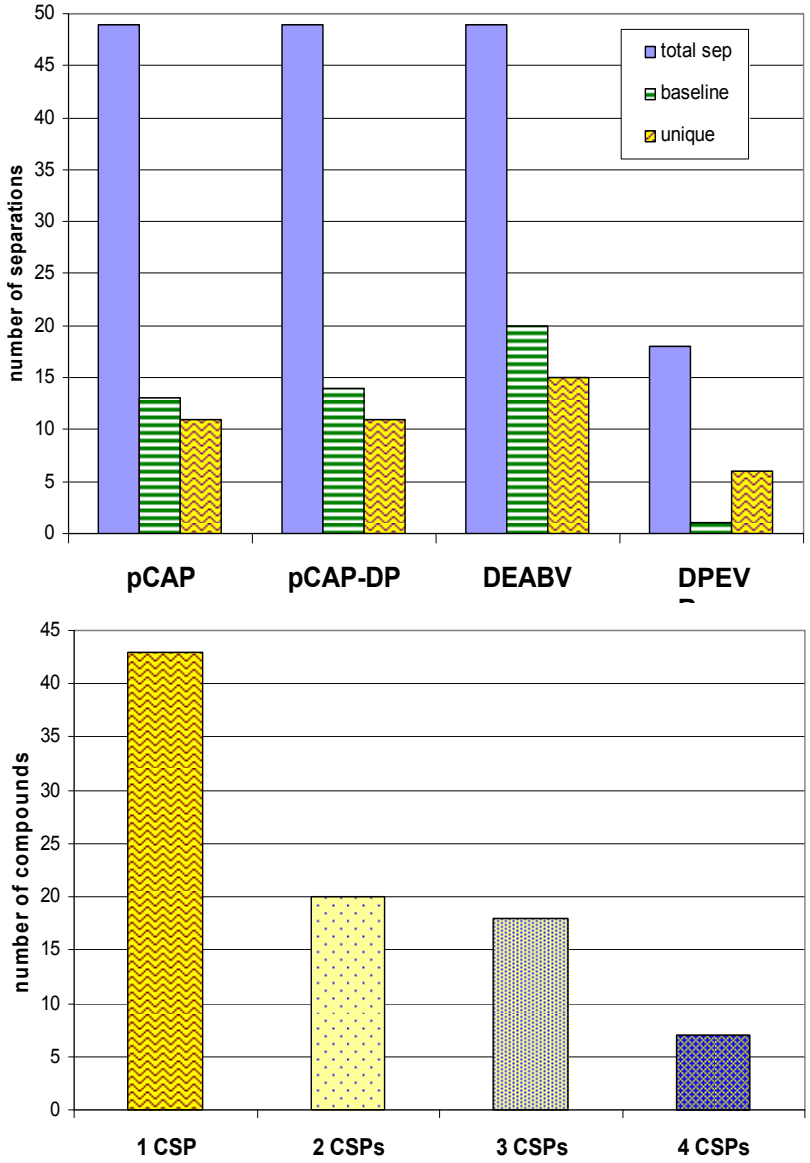

Fig. 2. Overall results obtained with the four synthetic polymeric chiral stationary phases in subcritical mode. Top diagram: number of separations obtained on each CSPs. Bottom diagram: the number of compounds that were separated only by one single CSP or 2 or 3 or all 4 CSPs. The percentages refer to the number of compounds from the 88 compound set shown in Table 1.

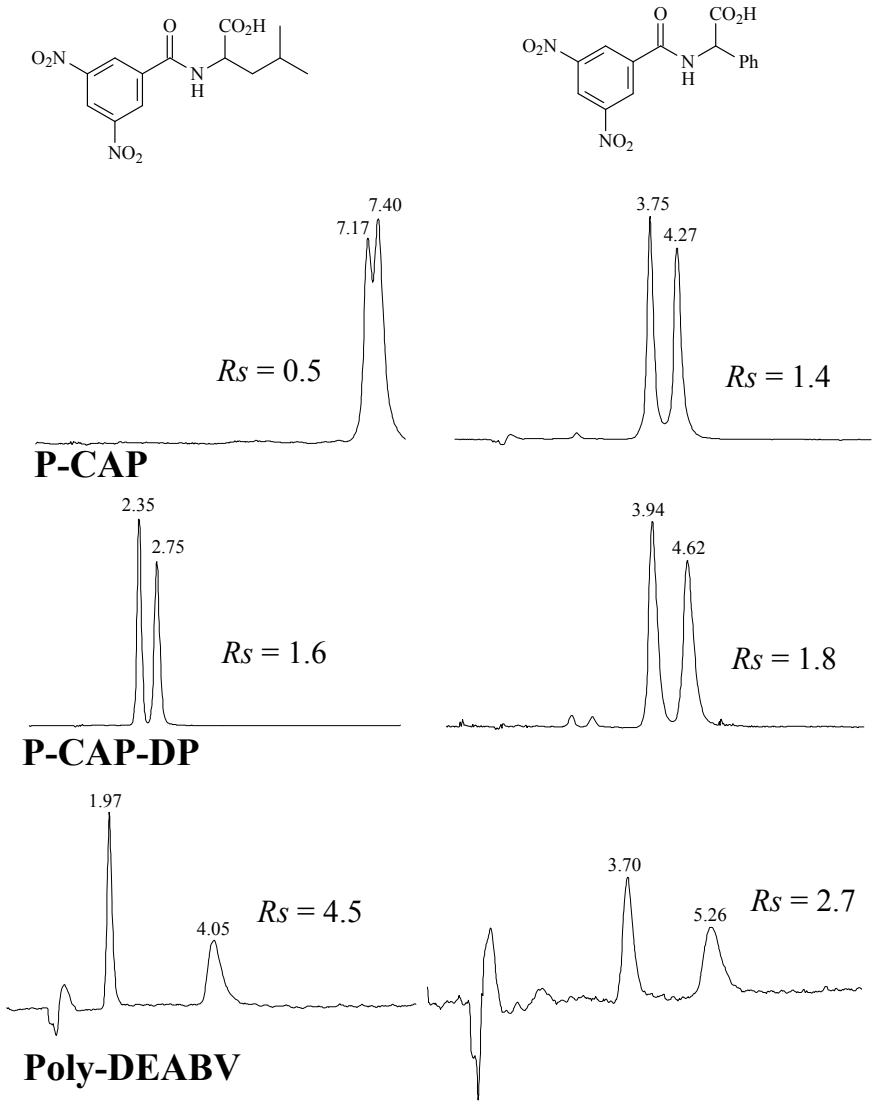

Fig. 3. Enantioseparation of DNB-leucine (3 left chromatograms) and DNB-phenylglycine (3 right chromatograms on the indicated polymeric chiral stationary phases. Column 250 x 4.6 mm with 5 µm silica particles bonded by the indicated selector, subcritical mobile phase with CO_2 + methanol (+ 0.2% v/v TFA) (proportion for DNB-leucine: p-CAP 15%, p-CAP-DP 20%, Poly-DEABV 40%; proportion for DNB-phenylglycine: p-CAP 30%, p-CAP-DP 20%, Poly-DEABV 40%, Compounds **63** and **64**), 100 bar, 4 mL min^{-1}, 32°C, UV detection 254 nm.

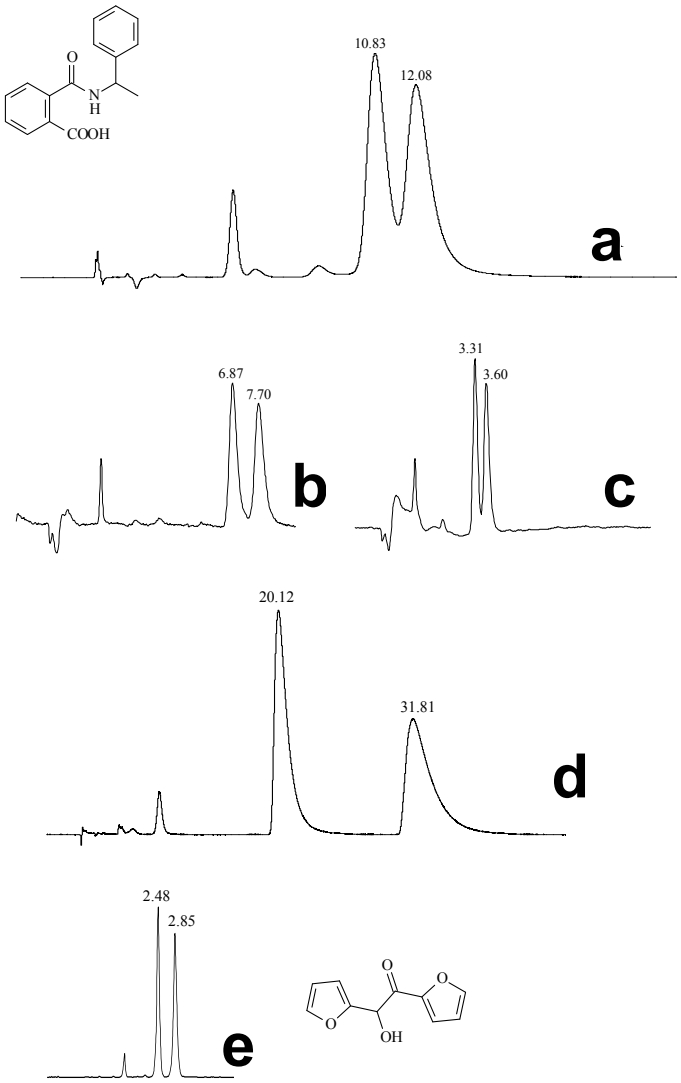

Fig. 4. Separation of the enantiomers of N-(α-methylbenzyl) phthalic acid monoamide (**16**) on the DEABV CSP. **a**: normal phase heptane/EtOH 70%/30% (+0.1% v/v TFA), 1 ml/min, α = 1.13, *Rs* = 1.2; **b**: SFC CO_2/MeOH 75/25% v/v (+0.2% v/v TFA), 100 bar, 4 ml/min, 32°C, α = 1.14, *Rs* = 1.4; **c**: SFC CO_2/MeOH 70/30% v/v (+0.2% v/v TFA), 100 bar, 4 ml/min, 32°C, α = 1.12, *Rs* = 1.3. Separation of the enantiomers of Furoin (**13**) on the polymeric P-CAP-DP CSP. **d:** normal phase mode, mobile phase heptane/IPA 80/20 %v/v (with 0.1% TFA), 1 ml/min, α = 1.69, *Rs* = 3.7; **e**: SFC CO_2/MeOH 90/10% v/v (+0.2% v/v TFA), 100 bar, 4 ml/min, 32°C, α = 1.25, *Rs* = 2.0, detection UV 254 nm.

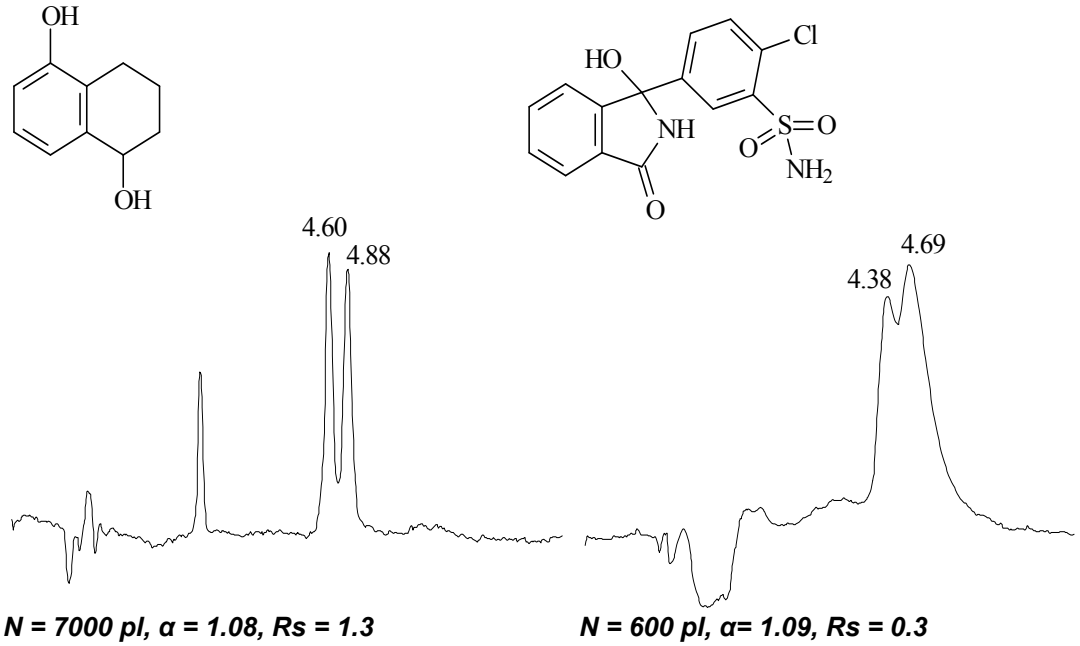

Fig. 5. Efficiency variations on the P-CAP-DP chiral stationary phase. Left: separation of the enantiomers of 1,5-dihydroxy-1,2,3,4-tetrahydronaphthalene (**28**), mobile phase, CO_2 + 15% v/v (MeOH + 0.2% v/v TFA); right: enantioseparation of Chlorthalidone (**45**), mobile phase, CO_2 + 40% v/v (MeOH + 0.2% v/v TFA). Total flow rate 4 mL min^{-1}, 32°C, 100 bar, UV detection 254 nm.

Chapter 9. General conclusions

In the first part (chapters 2-4) of the dissertation, the enantiomeric separation of three groups of new synthesized racemates: racemic furans, racemic isochromenes, and racemic chiral polycycles, was investigated on cyclodextrin based chiral stationary phases. Cyclodextrin-based CSPs are effective for separation of these new relatively hydrophobic, often neutral racemates in the reverse phase mode. Enantioselective separations for 93%, 85%, and 100% of the racemic furans, racemic isochromenes and racemic polycycles, respectively, were observed on cyclodextrin-based CSPs in the reverse phase mode. Very few enantiomeric separations were observed in the normal phase mode or polar organic mode. The hydroxypropyl-β-cyclodextrin (Cyclobond RSP) and the 2,3-dimethyl-β-cyclodextrin (Cyclobond DM) CSPs are the most effective for the separation of all three groups of analytes in comparison to other cyclodextrin-based columns. Eighty three percent of chiral furans, 60% of chiral isochromenes, and 100% of chiral polycycles were separated on either the Cyclobond RSP or DM columns or both. In the reverse phase mode, the pH of the buffered mobile phase only showed significant effect on the separation of compounds with ionizable groups such as carboxylic acid or amino groups. Increases in the separation efficiency and decreases in separation time were observed in the buffered mobile phase for these analytes with ionizable groups at appropriate pHs. For the separation of chiral furans, a small amount of methyl *t*-butyl ether in the mobile phase can decrease the retention and improve peak efficiency for some of the more strongly retained analytes. Better efficiencies were obtained in the separation of polycycles, when acetonitrile was used as organic modifier, compared to methanol. The structural features of the analytes affect the enantiomeric separations greatly. A small change in the structure of the analytes can result in a substantial change in the enantioselectivities on any given CSP.

The second part (chapters 5-7) of this thesis focuses on the evaluation and development of new synthetic polymeric CSPs. P-CAP CSP is prepared with a radical initiated polymerization of *N,N'*-diacryloyl derivative of *trans*-1,2-diaminocyclohexane. The polymeric process begins from the surface of the azo-activated silica support. This CSP showed enantioselectivities for many racemates in the normal phase mode and polar organic mode. The two mobile phase modes are complementary to each other. For the separation of

organic acids, 0.1% trifluoacetic acid in the mobile phase can decrease the retention and increase the peak efficiency in both mobile phase modes. More racemates were separated in the normal phase mode than in the polar organic mode, while faster separations and higher efficiency were obtained in the polar organic mode. The elution order of two enantiomers can be easily reversed by use the two CSPs in which the chiral center of the monomer has the opposite absolute configuration. The P-CAP CSP showed high sample loading capacity and was a promising semi-preparative or preparative CSP. Two new synthetic polymeric CSPs based on *N*,*N'*-[(1R,2R)]-1,2-diphenyl-1,2-ethanediyl] bis-2-propenamide (commercial name = P-CAP-DP), and *trans*-9,10-dihydro-9,10-ethanoanthracene-(11S,12S)-11,12-dicarboxylic acid bis-4-vinylphenylamide (Poly-DEABV) were developed. The P-CAP-DP CSP was prepared by a different polymeric method, in which both the monomer and radical initiator are dissolved in a suspension of the silica gel derivatized with an acryloyl functional group. The polymeric process begins from solution. Poly-DEABV CSP was prepared using a method similar to the one used for the P-CAP CSP. Both CSPs showed similar enantioseparation abilities compared to the P-CAP CSP. However, these two columns provide complementary results to the P-CAP column. Similar to the P-CAP CSP, a small amount of TFA in the mobile phase helps the enantioselective separation of the analytes with ionizable groups. These columns also showed high sample loading capacity.

The third part (chapters 8) of this dissertation involves the application of the above three synthetic polymeric CSPs and another new synthetic polymeric CSP in SFC. The four tested columns showed enantioselectivities for many racemates and high stability in supercritical fluid chromatography. The enantiomeric separations obtained in SFC are much faster than those obtained in HPLC due to the high flow rate (4 mL/min for SFC vs. 1 mL/min for HPLC). Most separations in SFC were done in 5 minutes. Due to the better separation efficiency in SFC, better enantiomeric resolutions for some analytes were observed in SFC than HPLC.

Acknowledgements

It is my great honor and pleasure to carry out my Ph.D study in Professor Daniel W. Armstrong's research group at Iowa State University and the University of Texas at Arlington. Professor Armstrong is a great scientist! His interest in and devotion to science, broad knowledge, great patience with students, and excellent presentation skills will benefit me the rest of my life. Without his kind help, I may mot have had a chance to enjoy such stimulating research.

I would like to acknowledge Dr. Robert S. Houk, Dr. Jacob W. Petrich, Dr. Klaus Schmidt-Rohr, and Dr. George A. Kraus for their serving in my POS committee. I would also like to thank all the visiting scientists, postdocs, and graduate students in Dr. Armstrong's group for their help in my research, English, and living in both Ames and Arlington. The friendship with them will be in my mind forever.

I would especially thank for my wife, Yuhua Cheng, for her encouragement to overcome the difficulties I met. I am perpetually indebted to my parents and my-parents-in-law for their emotional and financially support. I hope they will be proud of their son's achievement.

Finally, thanks for everyone who have helped me.